Founders Award Introduction

Mark S. Humayun, MD, PhD

Symposium 1: Awards Ceremony – 8:20-8:25 am

Founders Award Introduction

Innovations in Retina Tumors 2016

Mark S. Humayun, MD, PhD

Carol L. Shields, MD

Symposium 1: Awards Ceremony – 8:20-8:25 am

Financial Disclosure

- I have no financial interests or relationships to disclose.

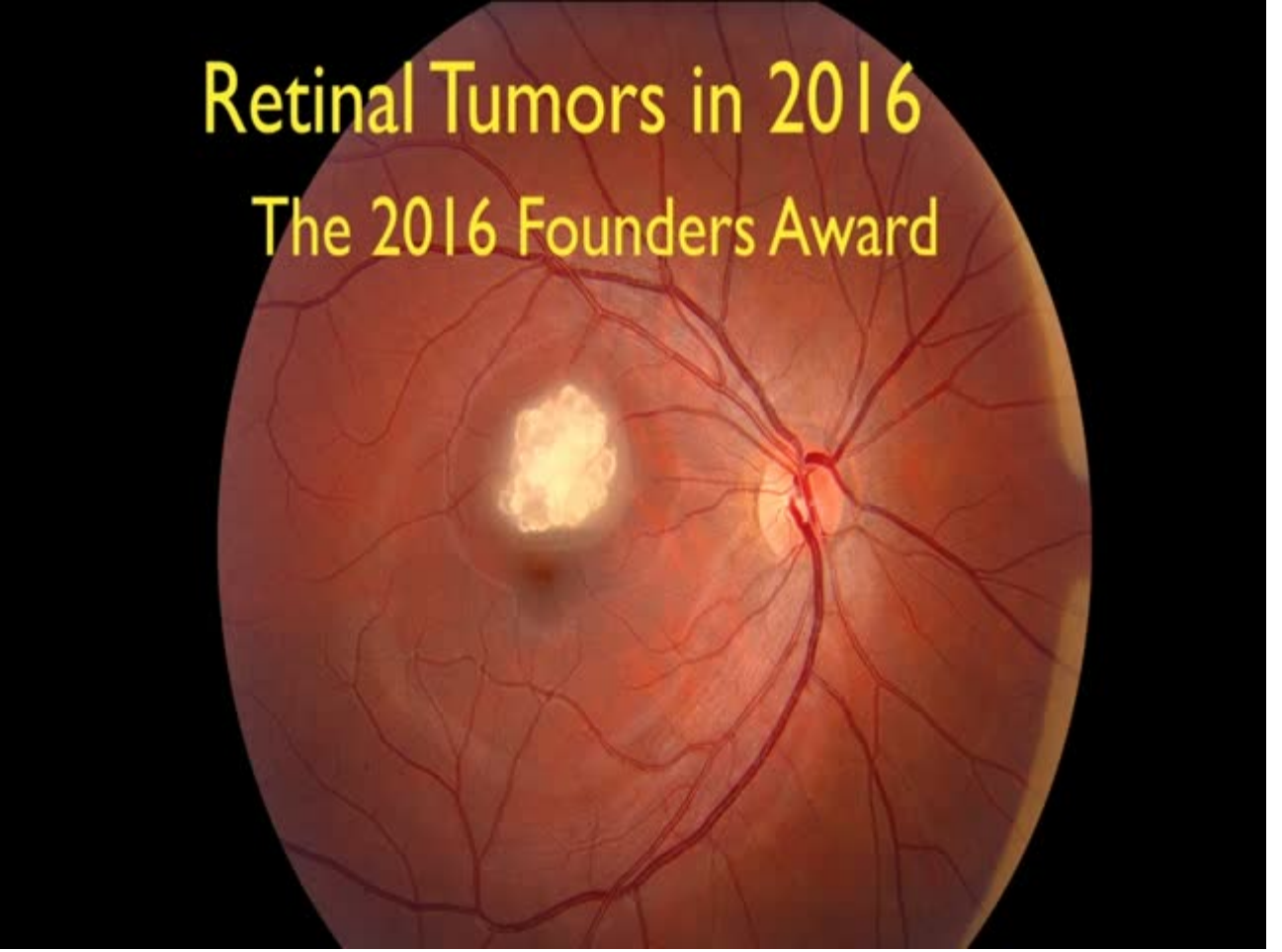
Retinal Tumors in 2016
The 2016 Founders Award

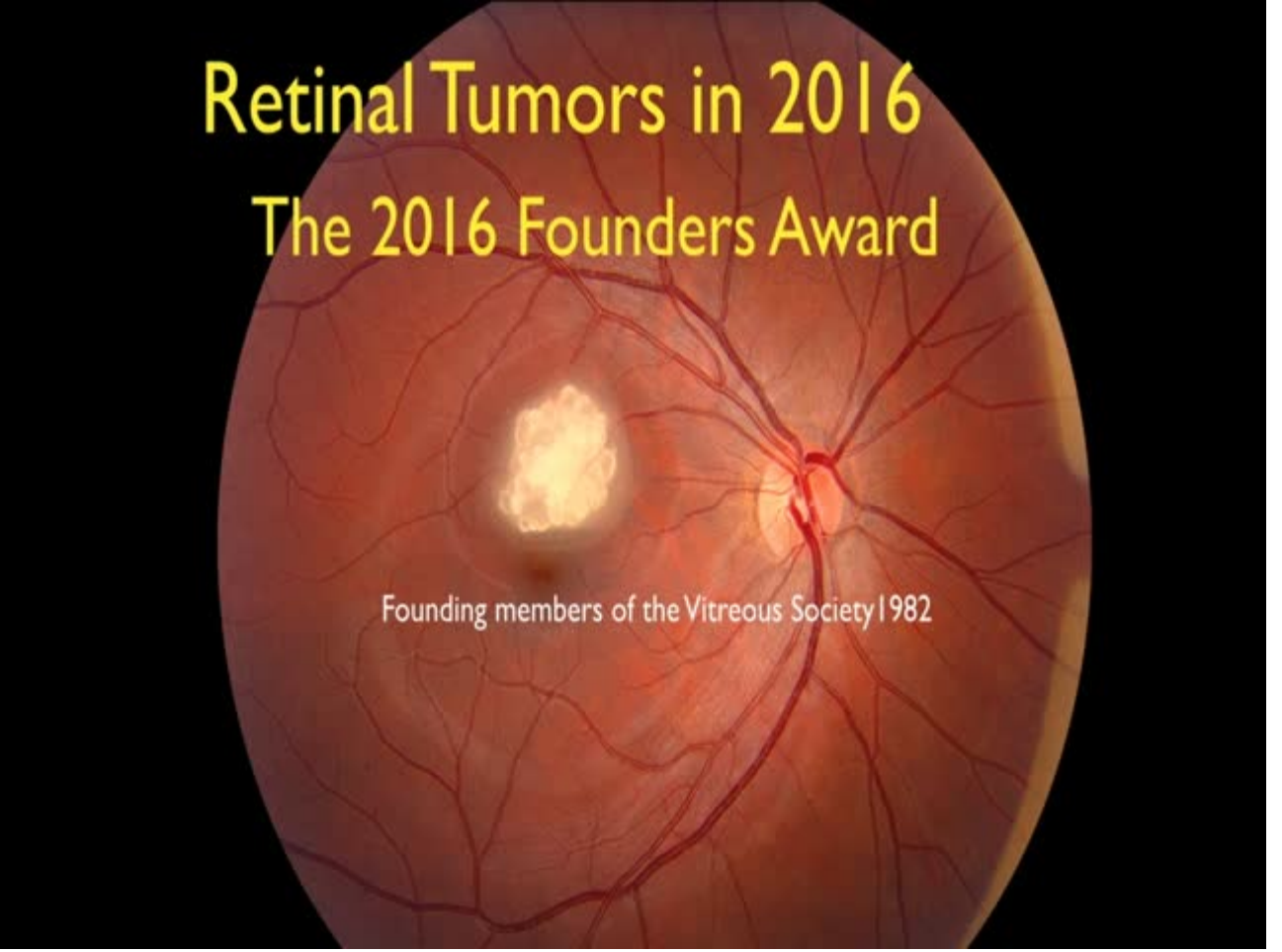
Retinal Tumors in 2016
The 2016 Founders Award
Founding members of the Vitreous Society 1982

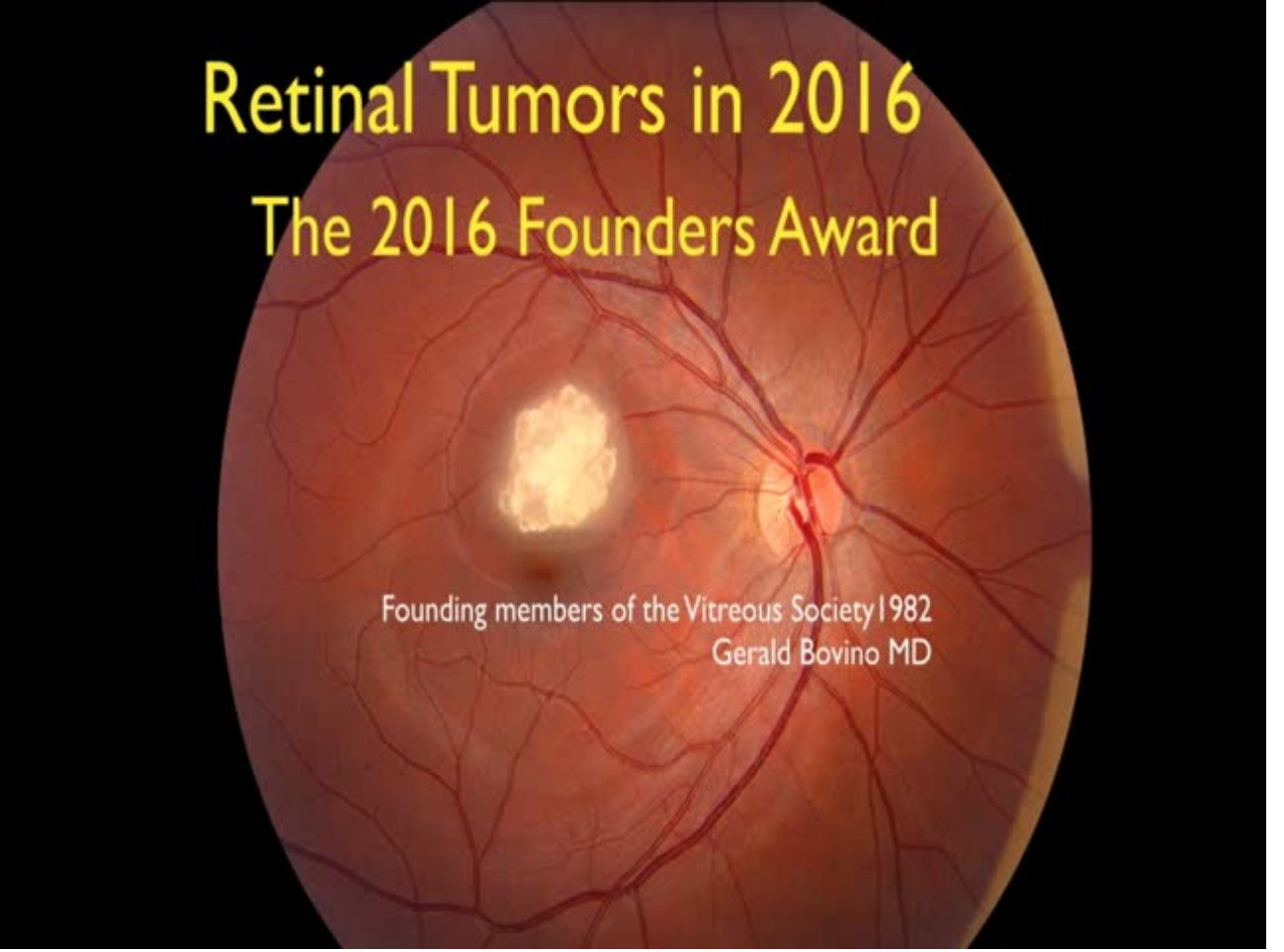
Retinal Tumors in 2016
The 2016 Founders Award
Founding members of the Vitreous Society 1982
Gerald Bovino MD

Retinal Tumors in 2016

The 2016 Founders Award

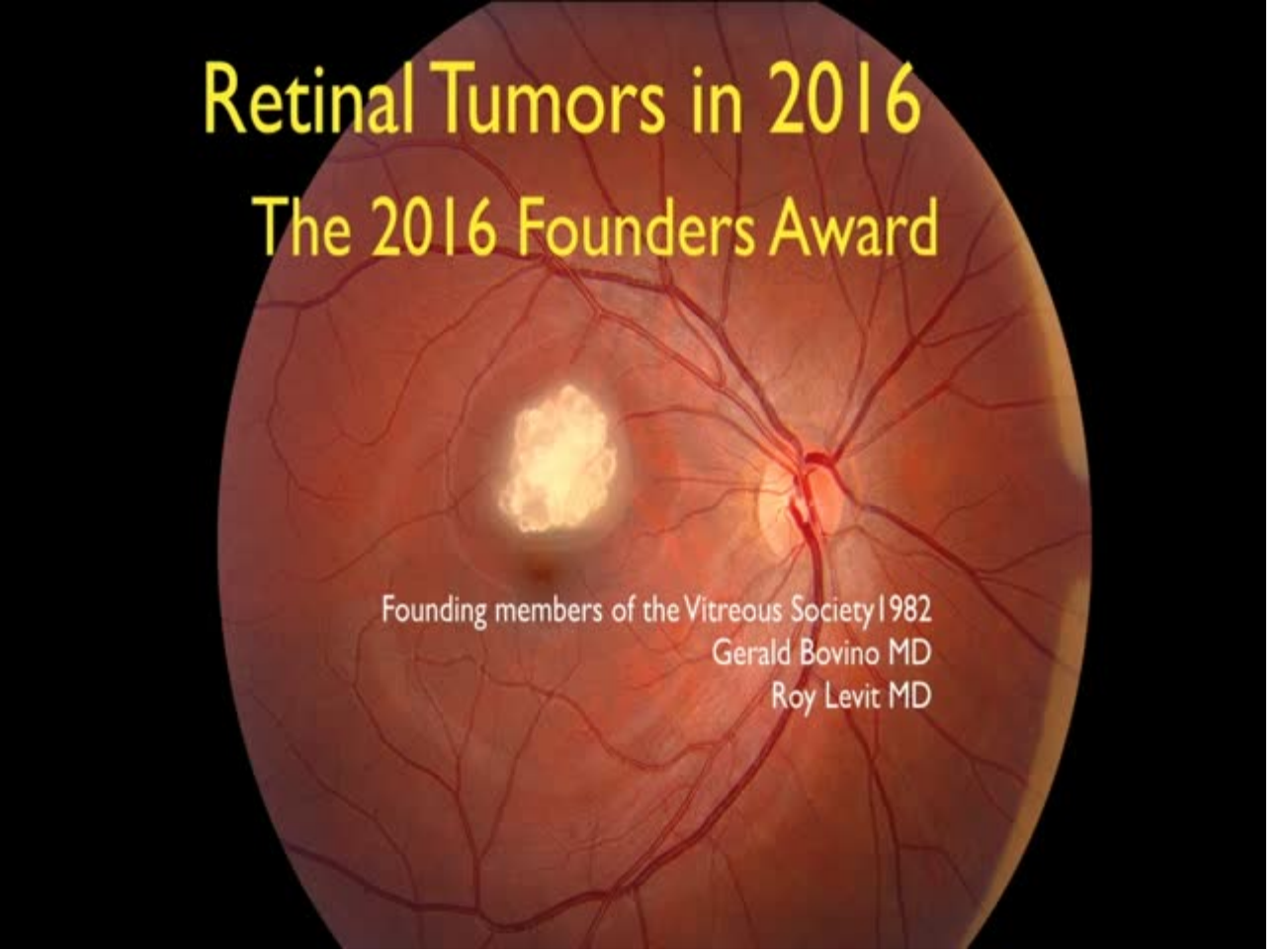

Founding members of the Vitreous Society 1982

Gerald Bovino MD
Roy Levit MD

Retinal Tumors in 2016

The 2016 Founders Award

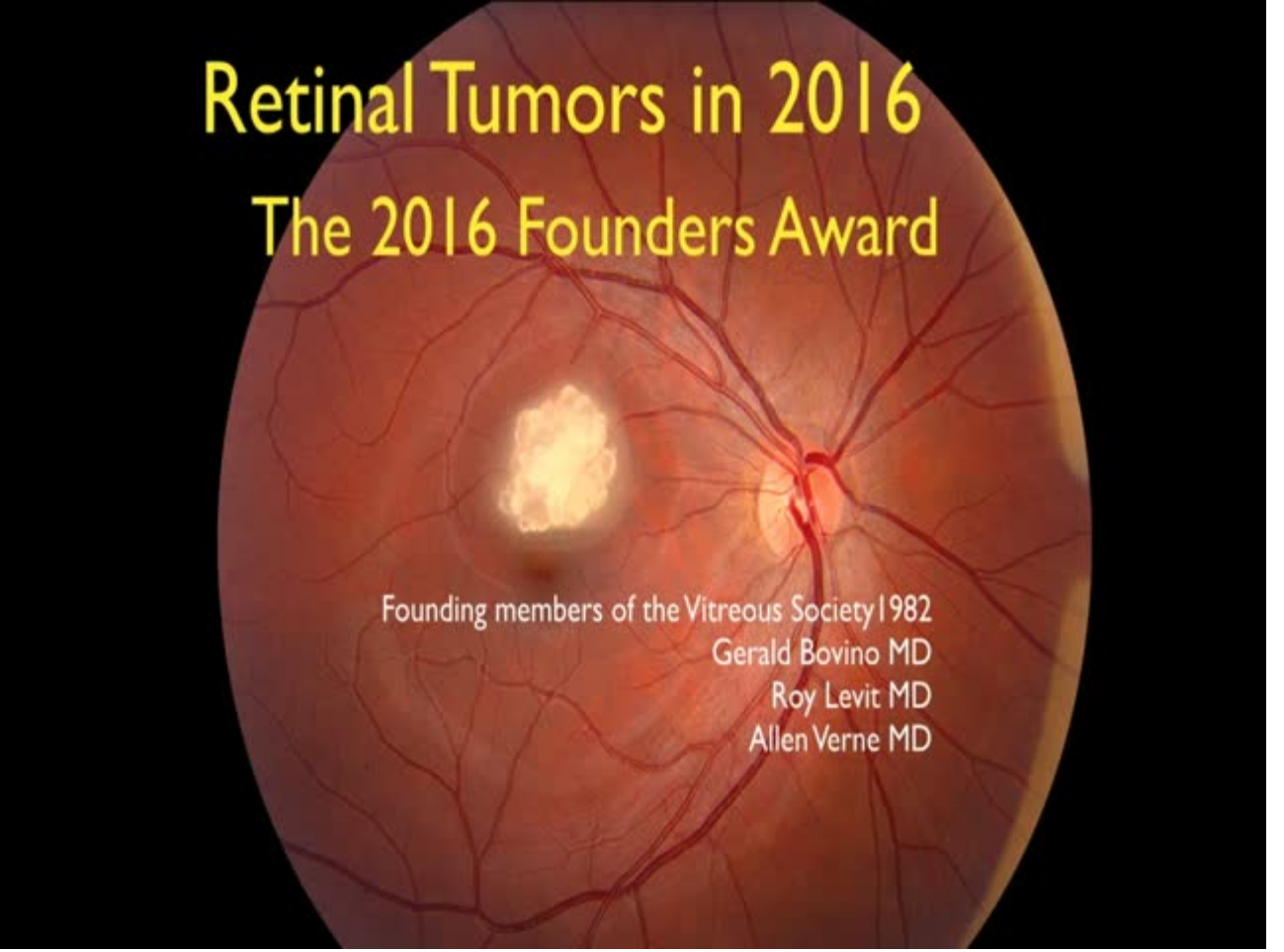

Founding members of the Vitreous Society 1982

Gerald Bovino MD

Roy Levit MD

Allen Verne MD

Retinal Tumors in 2016

The 2016 Founders Award

Founding members of the Vitreous Society 1982
Gerald Bovino MD
Roy Levit MD
Allen Verne MD
Later to become American Society of Retina Specialists

Retinal Tumors in 2016

The 2016 Founders Award

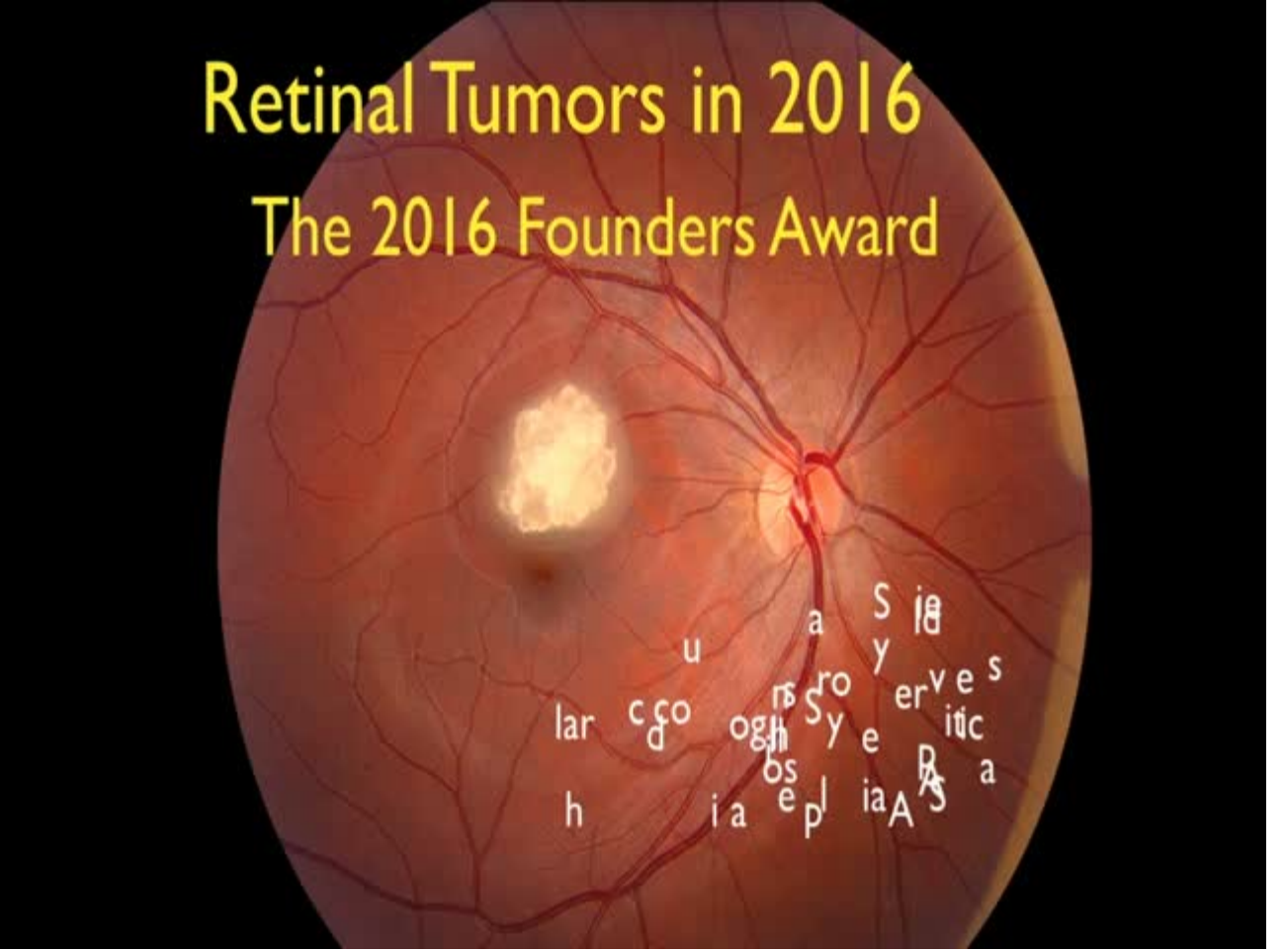

Rhegmatogenous Retinal Detachment after Intra-Arterial Chemotherapy for Retinoblastoma.

The 2016 Founders Award Lecture

Carol L. Shields, M.D.

Emil Anthony T. Say, M.D.

Maria Pefkianaki, M.D., M.Sc., Ph.D.

Carl D. Regillo, M.D.

Emi H. Caywood, M.D.

Pascal M. Jabbour, M.D.

Jerry A. Shields, M.D.

From the Ocular Oncology Service (CLS, EATS, MP, JAS) and the Retina Service (CDR), Wills Eye

Rhegmatogenous Retinal Detachment after Intra-Arterial Chemotherapy for Retinoblastoma.

The 2016 Founders Award Lecture

n=10/157 (6%)

at risk	p value
older children	0.05
more extensive vitreous seeding	0.02
diffuse infiltrating without srf	0.02

cause	
atrophic hole after rb regression	n=7
cryotherapy hole	n=2
flap tear pvd	n=1

pattern (1/24 (4 ... t RRD (n=157)

found significan ... nths, p=0.0522),

greater 4-quadra ... f subretinal fluid

(3/10, 30% vs ... atrophic retinal

hole(s) in 7 (7/10, 70%) (unifocal (1/10, 10%) or multifocal (6/10, 60%) holes), cryotherapy-induced single

atrophic hole in 2 (2/10, 20%), and single flap-tear from posterior vitreous detachment in 1 (1/10, 10%). In

Rhegmatogenous Retinal Detachment after Intra-Arterial Chemotherapy for Retinoblastoma.

The 2016 Founders Award Lecture

Carol L. Shields, M.D.

Emil Anthony T. Say, M.D.

Maria Pefkianaki, M.D., M.Sc., Ph.D.

Carl D. Regillo, M.D.

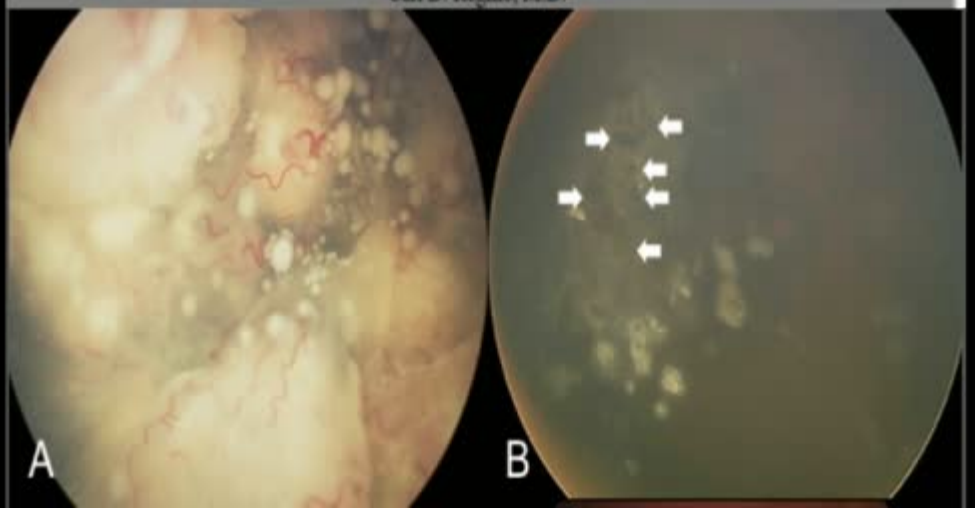

Rhegmatogenous Retinal Detachment after Intra-Arterial Chemotherapy for Retinoblastoma.

The 2016 Founders Award Lecture

Carol L. Shields, M.D.

Emil Anthony T. Say, M.D.

Maria Pefkianaki, M.D., M.Sc., Ph.D.

Carl D. Regillo, M.D.

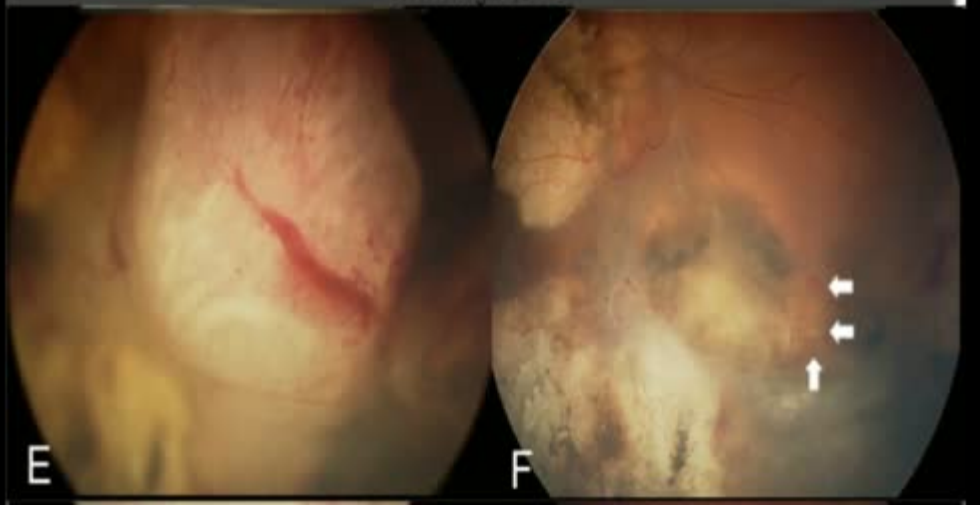

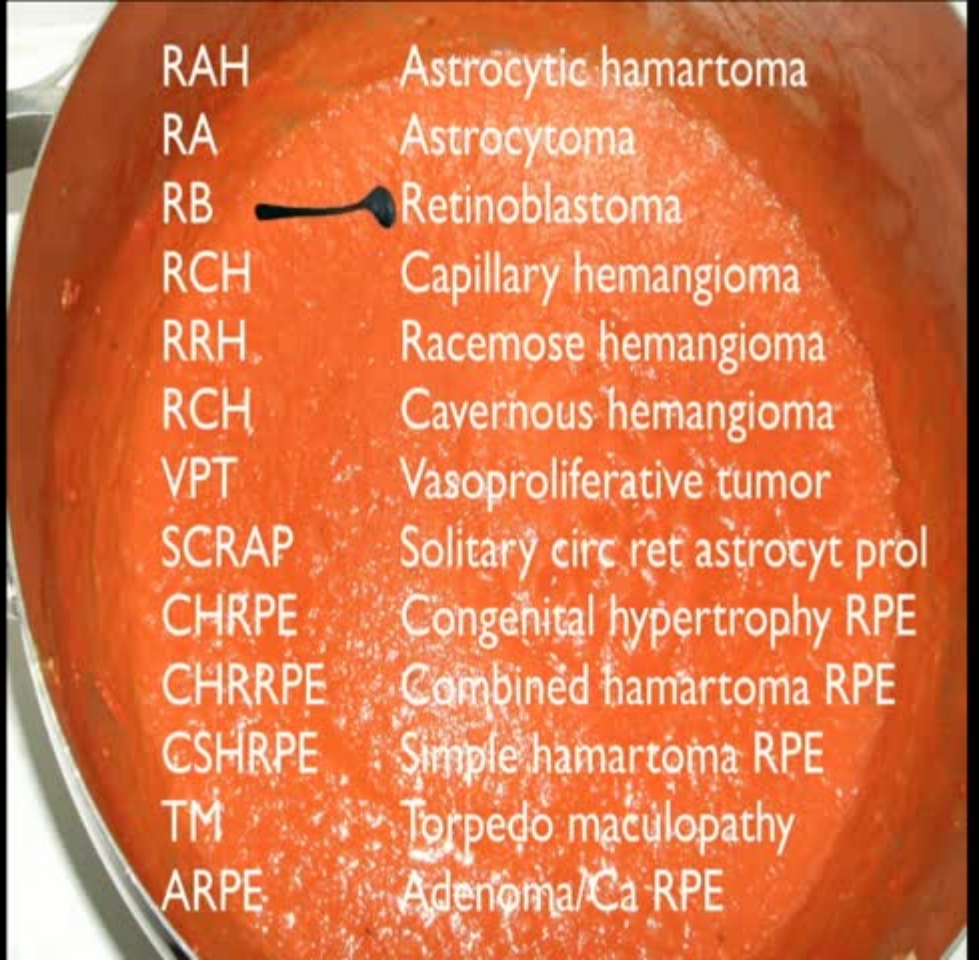
RAH Astrocytic hamartoma
RA Astrocytoma
RB Retinoblastoma
RCH Capillary hemangioma
RRH Racemose hemangioma
RCH Cavernous hemangioma
VPT Vasoproliferative tumor
SCRAP Solitary circ ret astrocyt prol
CHRPE Congenital hypertrophy RPE
CHRRPE Combined hamartoma RPE
CSHRPE Simple hamartoma RPE
TM Torpedo maculopathy
ARPE Adenoma/Ca RPE

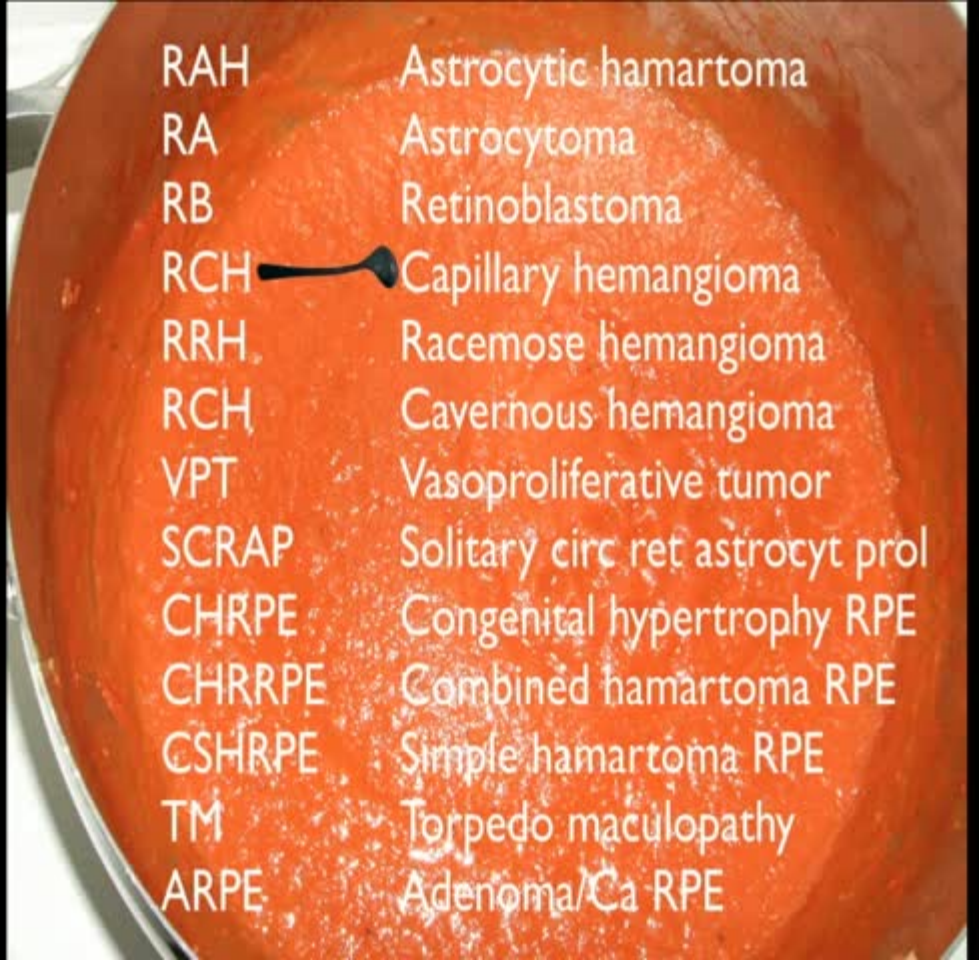
RAH Astrocytic hamartoma
RA Astrocytoma
RB Retinoblastoma
RCH Capillary hemangioma
RRH Racemose hemangioma
RCH Cavernous hemangioma
VPT Vasoproliferative tumor
SCRAP Solitary circ ret astrocyt prol
CHRPE Congenital hypertrophy RPE
CHRRPE Combined hamartoma RPE
CSHRPE Simple hamartoma RPE
TM Torpedo maculopathy
ARPE Adenoma/Ca RPE

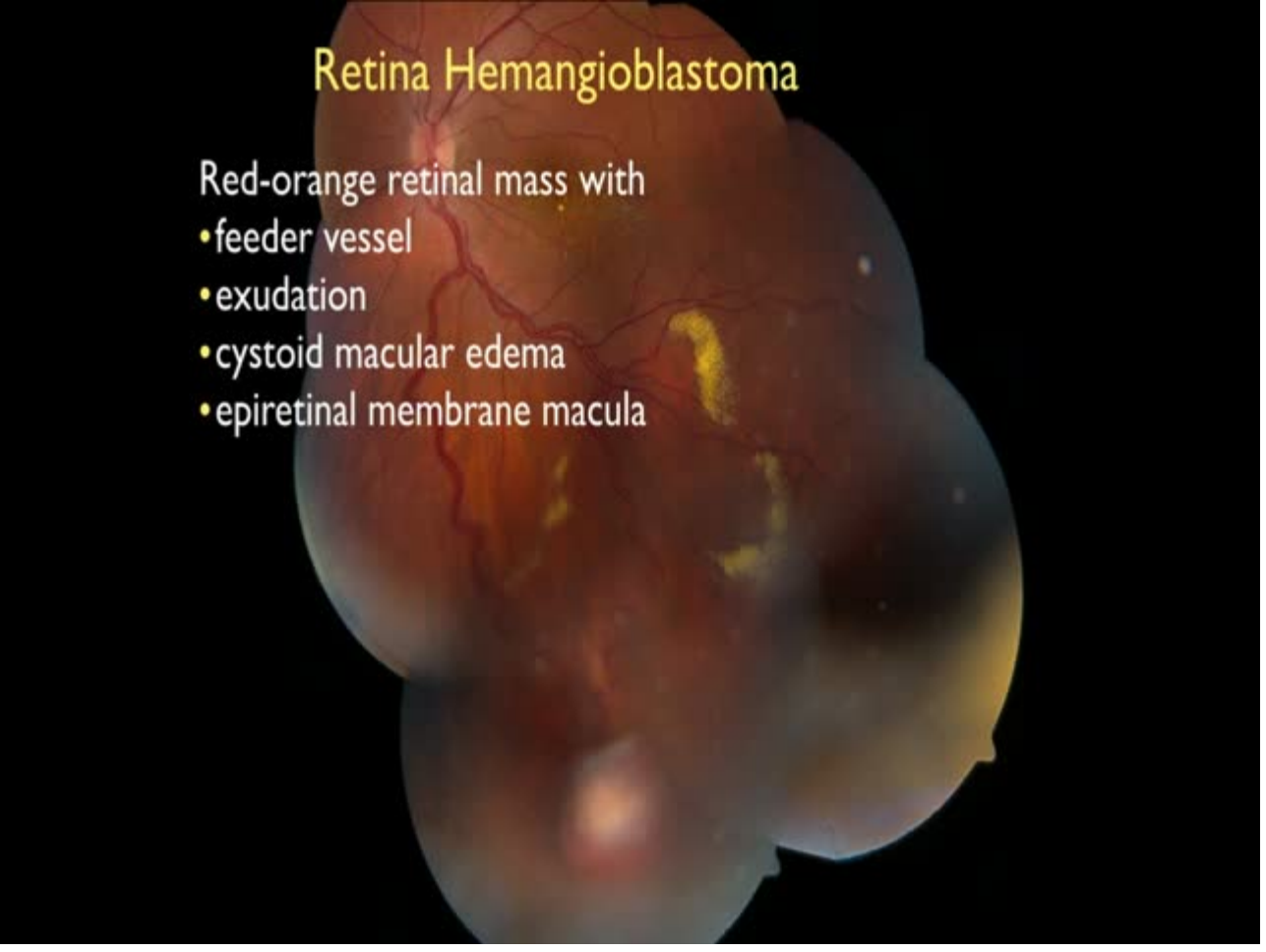
Retina Hemangioblastoma
Red-orange retinal mass with
•feeder vessel
•exudation
•cystoid macular edema
•epiretinal membrane macula

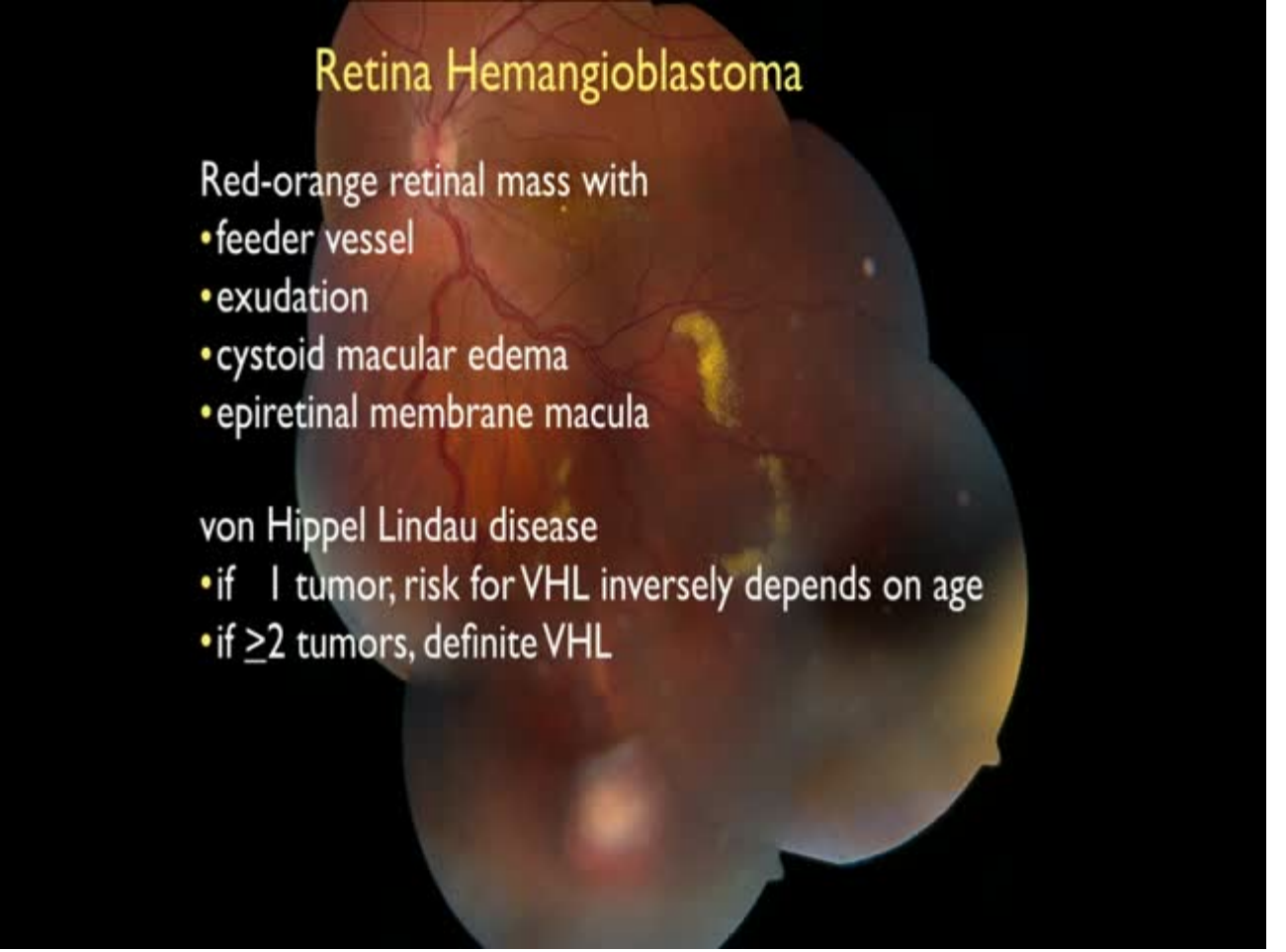
Retina Hemangioblastoma
Red-orange retinal mass with
•feeder vessel
•exudation
•cystoid macular edema
•epiretinal membrane macula
von Hippel Lindau disease
•if 1 tumor, risk for VHL inversely depends on age
•if ≥2 tumors, definite VHL

Clinical Characterization of Retinal Capillary Hemangioblastomas in a Large Population of Patients with von Hippel–Lindau Disease

Wai T. Wong, MD, PhD,[1] Elvira Agrón, MS,[1] Hanna R. Coleman, MD,[1] Tam Tran, BS,[1]
George F. Reed, PhD,[1] Karl Csaky, MD,[2] Emily Y. Chew, MD[1]

Objective: To report the epidemiology and ocular phenotype of retinal capillary hemangioblastomas associated with von Hippel–Lindau (VHL) disease in a large cohort of patients and to correlate patient and ocular characteristics to visual morbidity in this population.

Design: Cross-sectional study.

Participants: In 220 unrelated pedigrees, 335 patients affected with VHL disease and retinal capillary hemangioblastomas (RCHs) in at least 1 eye.

Methods: Demographics of the patient population were recorded and the ocular phenotype of each patient was obtained with a comprehensive ocular examination.

Main Outcome Measures: The patient population was characterized and the ocular phenotype described in relationship to tumor location, number, and extent of retinal involvement. Correlations between patient demographics, ocular phenotype, and visual function were analyzed.

Results: We detected RCHs unilaterally in 42.1% and bilaterally in 57.9% of patients. No correlation was detected between the age, gender, or laterality of involvement. Of involved eyes, 86.6% had tumors that could be individually visualized; of these, tumors were commonly found in the peripheral retina (84.7%) only, and less commonly in the juxtapapillary area (15.3%). The tumor count in the periphery averaged 2.5±1.8 per eye, with 25.2% of eyes having >1 quadrant of retinal involvement. Of involved eyes, 13.4% were enucleated or prephthsical; approximately 1 in 5 patients had ≥1 eyes so affected. Severe visual impairment (visual acuity ≤20/160) in affected eyes were more likely to be associated with increasing age, the presence of juxtapapillary lesions, and an increasing number and extent of peripheral lesions.

Conclusions: This large cohort of VHL patients with RCHs has enabled a systematic and quantitative characterization of the demographics, ocular features, and visual function in VHL disease. Clinical correlations between the visual morbidity and ocular features of the disease were also performed, producing measures that can help clinicians to estimate visual prognoses better based on the ocular phenotype of the disease.
Ophthalmology 2008;115:181–188

Clinical Characterization of Retinal Capillary Hemangiobl
Population of Patients
Hippel–Lindau Diseas

Wai T. Wong, MD, PhD,[1] Elvira Agrón, MS,[1] Hann
George F. Reed, PhD,[1] Karl Csaky, MD,[2] Emily Y. C

Objective: To report the epidemiology and ocula
ciated with von Hippel–Lindau (VHL) disease in a la
characteristics to visual morbidity in this population.
Design: Cross-sectional study.
Participants: In 220 unrelated pedigrees, 335
hemangioblastomas (RCHs) in at least 1 eye.
Methods: Demographics of the patient populatio
was obtained with a comprehensive ocular examinati
Main Outcome Measures: The patient populatio
in relationship to tumor location, number, and ext
demographics, ocular phenotype, and visual function
Results: We detected RCHs unilaterally in 42.1
detected between the age, gender, or laterality of in
be individually visualized; of these, tumors were com
commonly in the juxtapapillary area (15.3%). The tu
25.2% of eyes having >1 quadrant of retinal inv
prephthsical; approximately 1 in 5 patients had ≥1
≤20/160) in affected eyes were more likely to be ass
lesions, and an increasing number and extent of per
Conclusions: This large cohort of VHL patient
characterization of the demographics, ocular feature
between the visual morbidity and ocular features of the
can help clinicians to estimate visual prognoses better based on the ocular phenotype of the disease.
Ophthalmology 2008;115:181–188 © 2008 by the American Academy of Ophthalmology.

von Hippel Lindau disease
n=335 patients
Retinal hemangioblastoma
- unilateral 42%
- bilateral 58%
- peripheral 85%
- juxtapapillary 15%

Va ≤20/160
- older age
- juxtapapillary location
- increasing # tumors
- increasing size tumors

Enucleation 13%

Retinal Tumors in 2016

An ae ou

Carol Shields
Ocular Oncology Service
Wills Eye Hospital
Philadlephia PA USA

Table 3. Impact of Features of Ocular Angiomatosis on Visual Acuity in Eyes with Retinal Capillary Hemangiomas that Can Be Individually Characterized

	Odds Ratio* (95% Wald Confidence Limits)
Fundus location of retinal capillary hemangiomas	
Juxtapapillary tumor only versus peripheral tumor/s only	2.88 (1.12–7.41)
Juxtapapillary + peripheral tumors versus peripheral tumor/s only	6.38 (2.12–19.18)
Number of retinal capillary hemangiomas	
≥3 Peripheral tumors vs. <3 peripheral tumors	4.18 (2.15–8.12)
≥5 Peripheral tumors vs. <5 peripheral tumors	8.27 (3.78–18.10)
Extent of peripheral retinal involvement	
≥1 quadrant of involvement vs. <1 quadrant of involvement	26.58 (11.93–59.25)

*Of eyes having a visual acuity <20/160 (letter score 0–38) versus a visual acuity of >20/20 (letter score ≥84).

features predictive of poor vision (<20/160) compared to good vision (20/20)

Table 3. Impact of Features of Ocular Angiomatosis on Visual Acuity in Eyes with Retinal Capillary Hemangiomas that Can Be Individually Characterized

	Odds Ratio* (95% Wald Confidence Limits)
Fundus location of retinal capillary hemangiomas	
Juxtapapillary tumor only versus peripheral tumor/s only	2.88 (1.12–7.41)
Juxtapapillary + peripheral tumors versus peripheral tumor/s only	6.38 (2.12–19.18)
Number of retinal capillary hemangiomas	
≥3 Peripheral tumors vs. <3 peripheral tumors	4.18 (2.15–8.12)
≥5 Peripheral tumors vs. <5 peripheral tumors	8.27 (3.78–18.10)
Extent of peripheral retinal involvement	
≥1 quadrant of involvement vs. <1 quadrant of involvement	26.58 (11.93–59.25)

*Of eyes having a visual acuity <20/160 (letter score 0–38) versus a visual acuity of >20/20 (letter score ≥84).

features predictive of poor vision (<20/160) compared to good vision (20/20)

Table 3. Impact of Features of Ocular Angiomatosis on Visual Acuity in Eyes with Retinal Capillary Hemangiomas that Can Be Individually Characterized

	Odds Ratio* (95% Wald Confidence Limits)
Fundus location of retinal capillary hemangiomas	
Juxtapapillary tumor only versus peripheral tumor/s only	2.88 (1.12–7.41)
Juxtapapillary + peripheral tumors versus peripheral tumor/s only	6.38 (2.12–19.18)
Number of retinal capillary hemangiomas	
≥3 Peripheral tumors vs. <3 peripheral tumors	4.18 (2.15–8.12)
≥5 Peripheral tumors vs. <5 peripheral tumors	8.27 (3.78–18.10)
Extent of peripheral retinal involvement	
≥1 quadrant of involvement vs. <1 quadrant of involvement	26.58 (11.93–59.25)

*Of eyes having a visual acuity <20/160 (letter score 0–38) versus a visual acuity of >20/20 (letter score ≥84).

features predictive of poor vision (<20/160) compared to good vision (20/20)

Table 3. Impact of Features of Ocular Angiomatosis on Visual Acuity in Eyes with Retinal Capillary Hemangiomas that Can Be Individually Characterized

	Odds Ratio* (95% Wald Confidence Limits)
Fundus location of retinal capillary hemangiomas	
Juxtapapillary tumor only versus peripheral tumor/s only	2.88 (1.12–7.41)
Juxtapapillary + peripheral tumors versus peripheral tumor/s only	6.38 (2.12–19.18)
Number of retinal capillary hemangiomas	
≥3 Peripheral tumors vs. <3 peripheral tumors	4.18 (2.15–8.12)
≥5 Peripheral tumors vs. <5 peripheral tumors	8.27 (3.78–18.10)
Extent of peripheral retinal involvement	
≥1 quadrant of involvement vs. <1 quadrant of involvement	26.58 (11.93–59.25)

*Of eyes having a visual acuity <20/160 (letter score 0–38) versus a visual acuity of >20/20 (letter score ≥84).

features predictive of poor vision (<20/160) compared to good vision (20/20)

Table 3. Impact of Features of Ocular Angiomatosis on Visual Acuity in Eyes with Retinal Capillary Hemangiomas that Can Be Individually Characterized

	Odds Ratio* (95% Wald Confidence Limits)
Fundus location of retinal capillary hemangiomas	
Juxtapapillary tumor only versus peripheral tumor/s only	2.88 (1.12–7.41)
Juxtapapillary + peripheral tumors versus peripheral tumor/s only	6.38 (2.12–19.18)
Number of retinal capillary hemangiomas	
≥3 Peripheral tumors vs. <3 peripheral tumors	4.18 (2.15–8.12)
≥5 Peripheral tumors vs. <5 peripheral tumors	8.27 (3.78–18.10)
Extent of peripheral retinal involvement	
≥1 quadrant of involvement vs. <1 quadrant of involvement	26.58 (11.93–59.25)

*Of eyes having a visual acuity <20/160 (letter score 0–38) versus a visual acuity of >20/20 (letter score ≥84).

features predictive of poor vision (<20/160) compared to good vision (20/20)

Table 3. Impact of Features of Ocular Angiomatosis on Visual Acuity in Eyes with Retinal Capillary Hemangiomas that Can Be Individually Characterized

	Odds Ratio* (95% Wald Confidence Limits)
Fundus location of retinal capillary hemangiomas	
Juxtapapillary tumor only versus peripheral tumor/s only	2.88 (1.12–7.41)
Juxtapapillary + peripheral tumors versus peripheral tumor/s only	6.38 (2.12–19.18)
Number of retinal capillary hemangiomas	
≥3 Peripheral tumors vs. <3 peripheral tumors	4.18 (2.15–8.12)
≥5 Peripheral tumors vs. <5 peripheral tumors	8.27 (3.78–18.10)
Extent of peripheral retinal involvement	
≥1 quadrant of involvement vs. <1 quadrant of involvement	26.58 (11.93–59.25)

*Of eyes having a visual acuity <20/160 (letter score 0–38) versus a visual acuity of >20/20 (letter score ≥84).

features predictive of poor vision (<20/160) compared to good vision (20/20)

Table 3. Impact of Features of Ocular Angiomatosis on Visual Acuity in Eyes with Retinal Capillary Hemangiomas that Can Be Individually Characterized

	Odds Ratio* (95% Wald Confidence Limits)
Fundus location of retinal capillary hemangiomas	
Juxtapapillary tumor only versus peripheral tumor/s only	2.88 (1.12–7.41)
Juxtapapillary + peripheral tumors versus peripheral tumor/s only	6.38 (2.12–19.18)
Number of retinal capillary hemangiomas	
≥3 Peripheral tumors vs. <3 peripheral tumors	4.18 (2.15–8.12)
≥5 Peripheral tumors vs. <5 peripheral tumors	8.27 (3.78–18.10)
Extent of peripheral retinal involvement	
≥1 quadrant of involvement vs. <1 quadrant of involvement	26.58 (11.93–59.25)

*Of eyes having a visual acuity <20/160 (letter score 0–38) versus a visual acuity of >20/20 (letter score ≥84).

features predictive of poor vision (<20/160) compared to good vision (20/20)

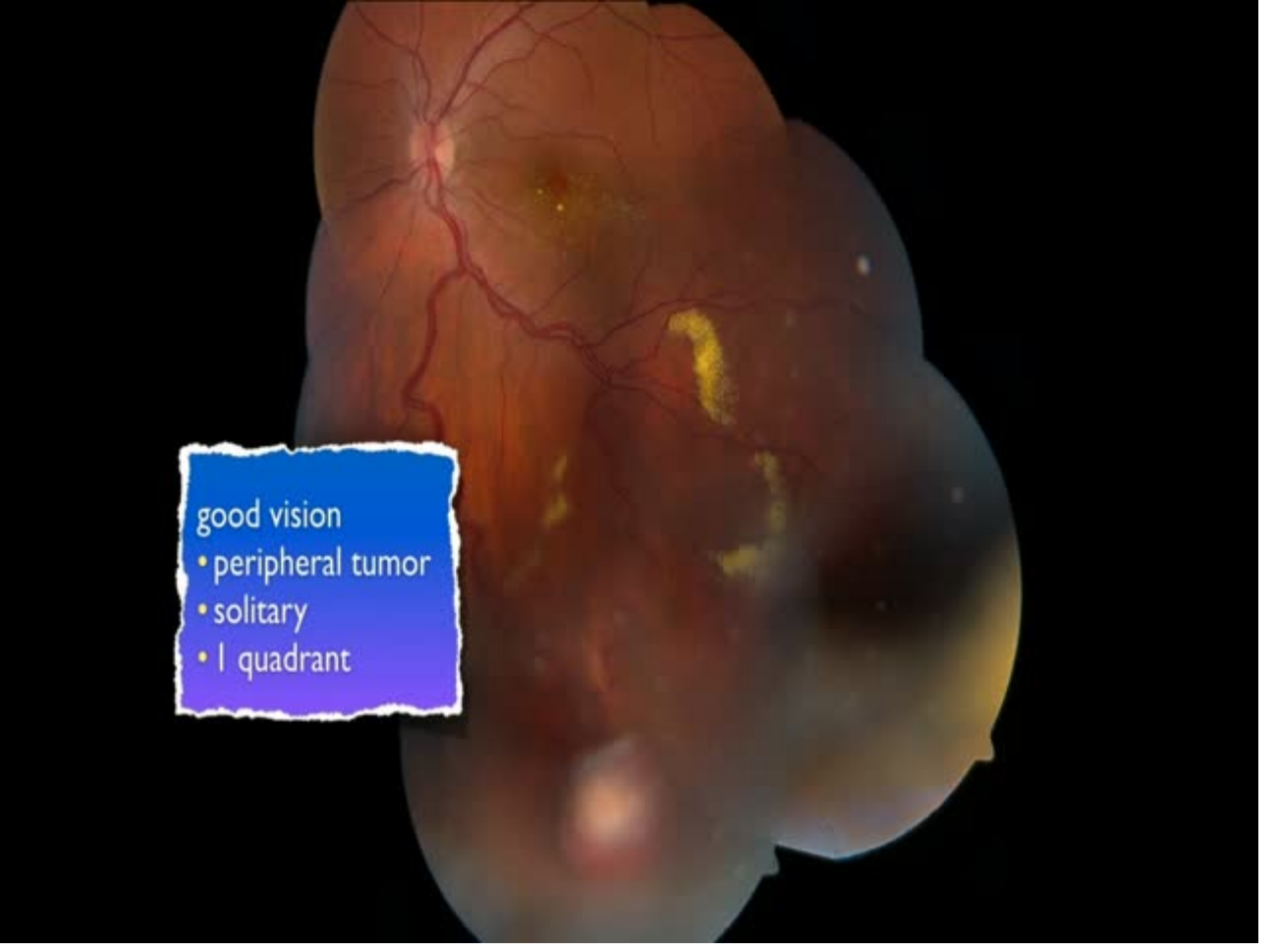
good vision
• peripheral tumor
• solitary
• 1 quadrant

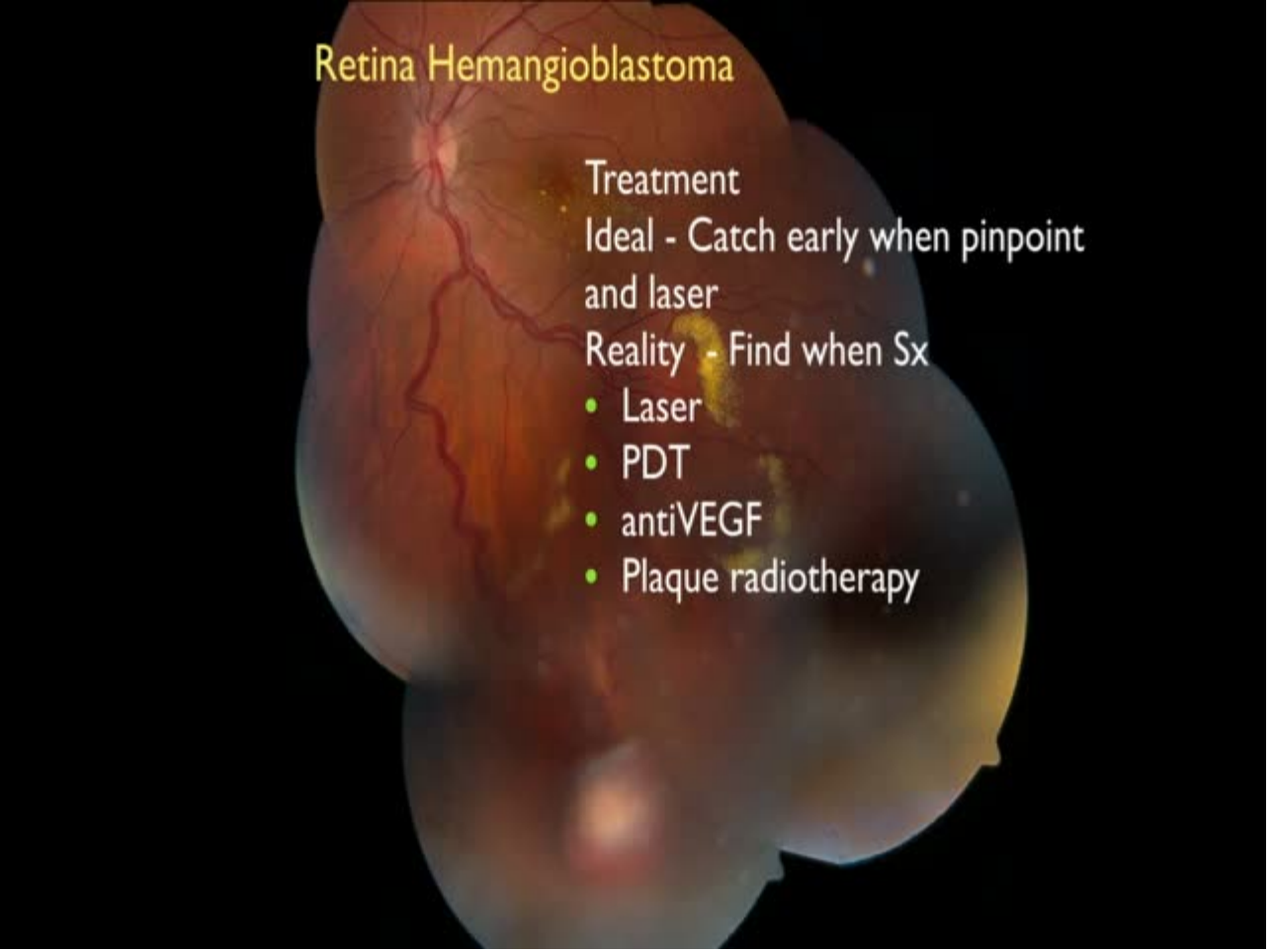
Retina Hemangioblastoma
Treatment
Ideal - Catch early when pinpoint and laser
Reality - Find when Sx
• Laser
• PDT
• antiVEGF
• Plaque radiotherapy

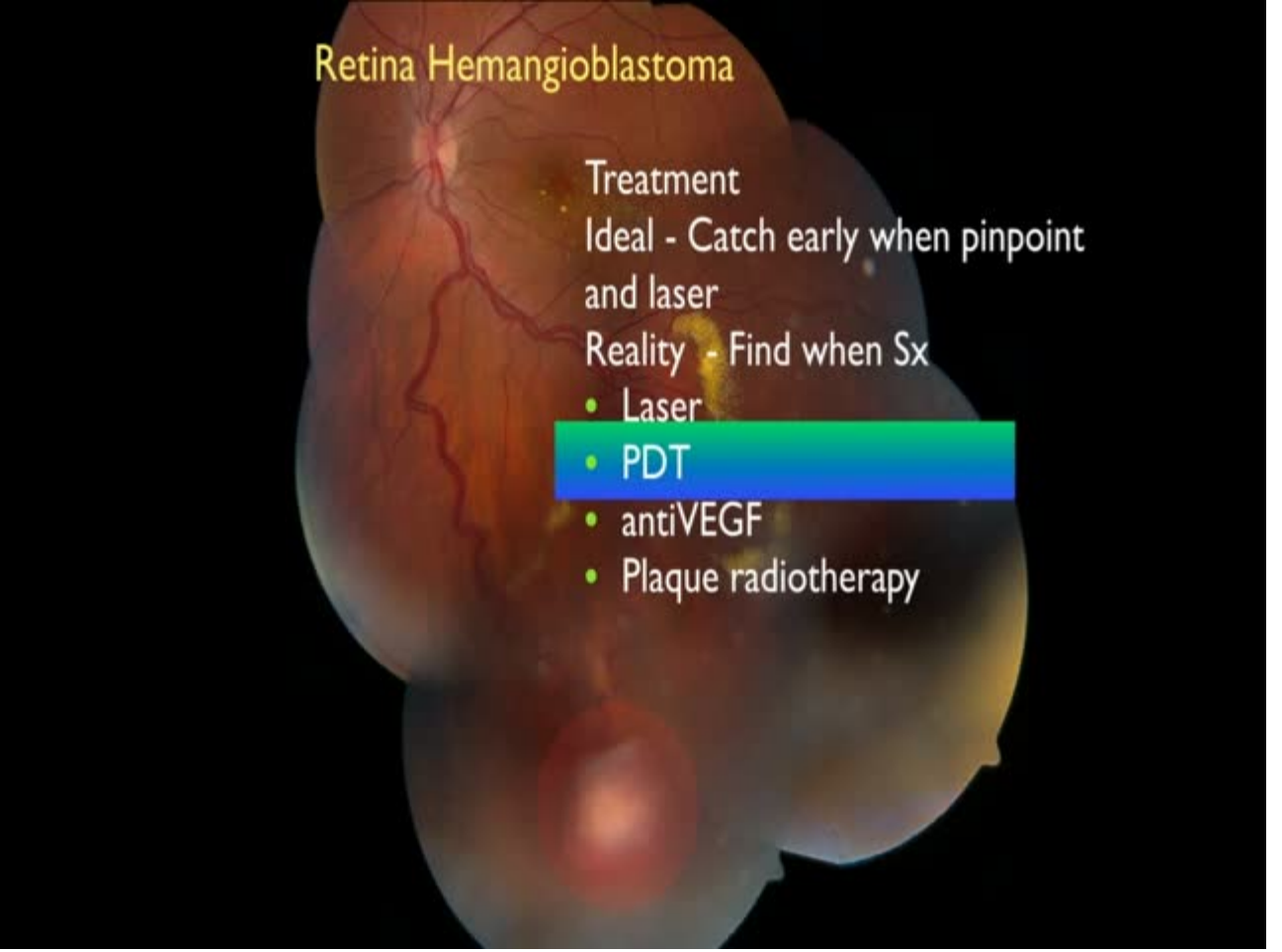
Retina Hemangioblastoma
Treatment
Ideal - Catch early when pinpoint and laser
Reality - Find when Sx
• Laser
• PDT
• antiVEGF
• Plaque radiotherapy

Retinal Tumors in 2016
Alphabet Soup

Carol Shields
Ocular Oncology Service
Wills Eye Hospital
Philadlephia PA USA

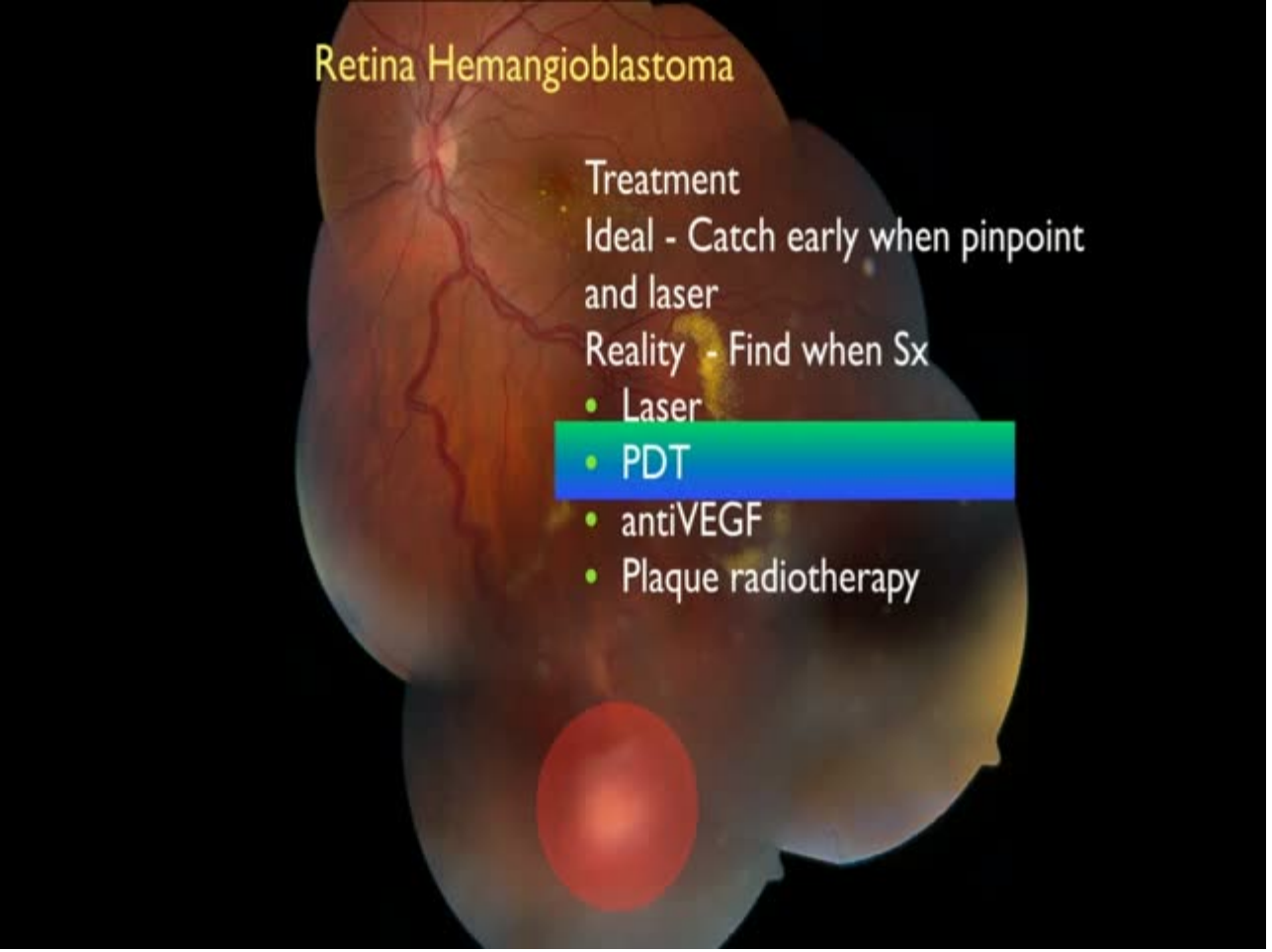
Retina Hemangioblastoma
Treatment
Ideal - Catch early when pinpoint and laser
Reality - Find when Sx
• Laser
• PDT
• antiVEGF
• Plaque radiotherapy

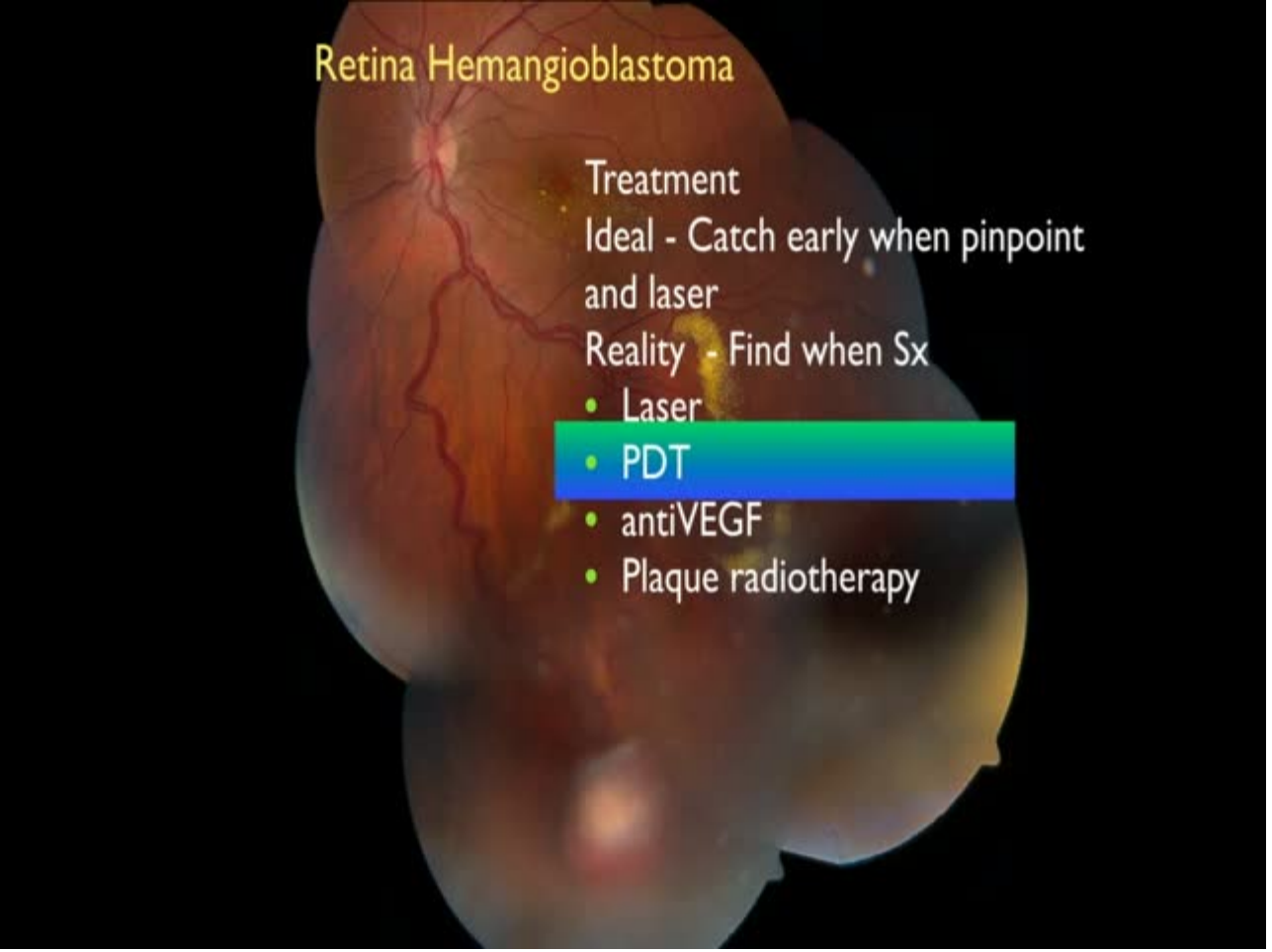
Retina Hemangioblastoma
Treatment
Ideal - Catch early when pinpoint and laser
Reality - Find when Sx
• Laser
• PDT
• antiVEGF
• Plaque radiotherapy

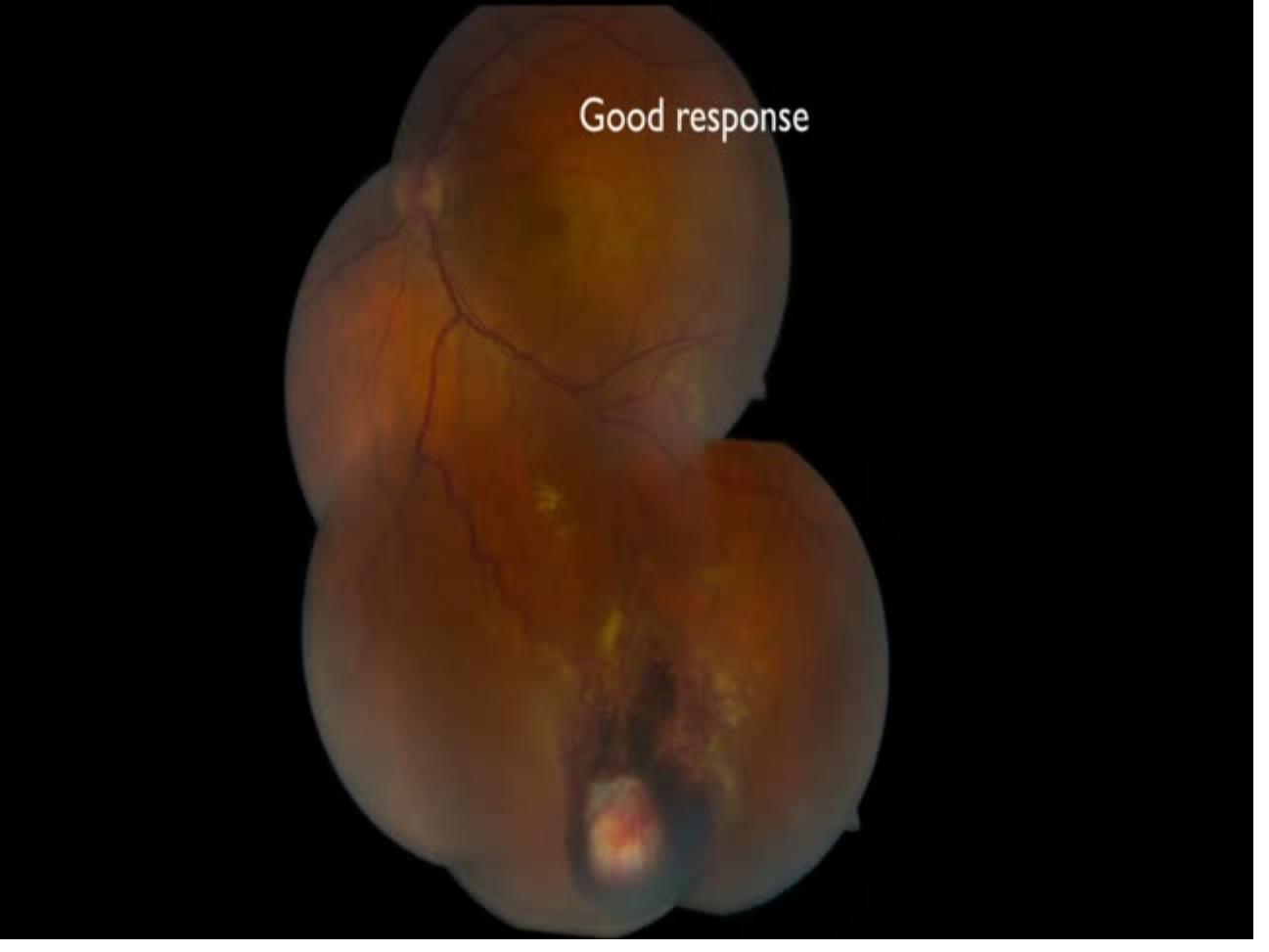
Good response

Retina Hemangioblastoma Plaque Radiotherapy

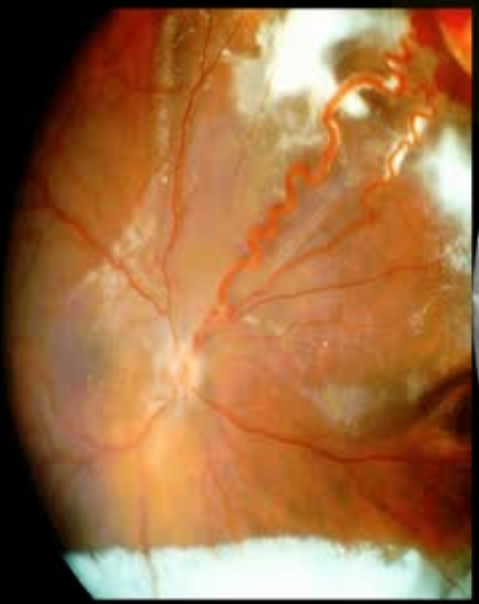

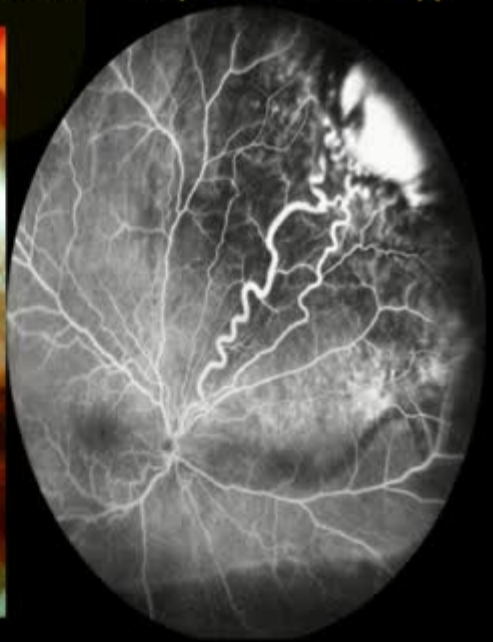

Retina Hemangioblastoma Plaque Radiotherapy

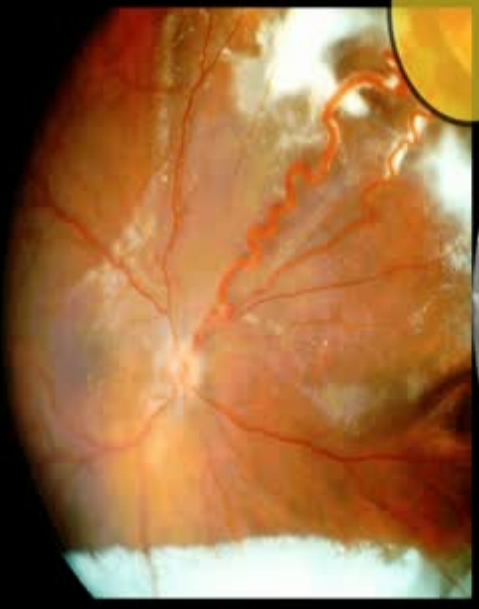

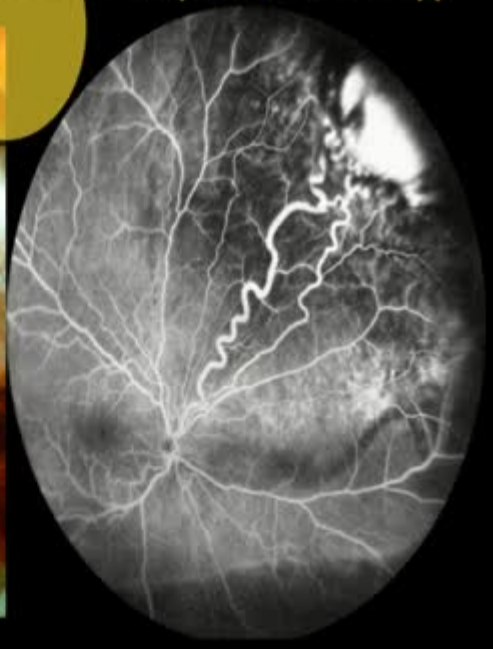

Retina Hemangioblastoma Plaque Radiotherapy

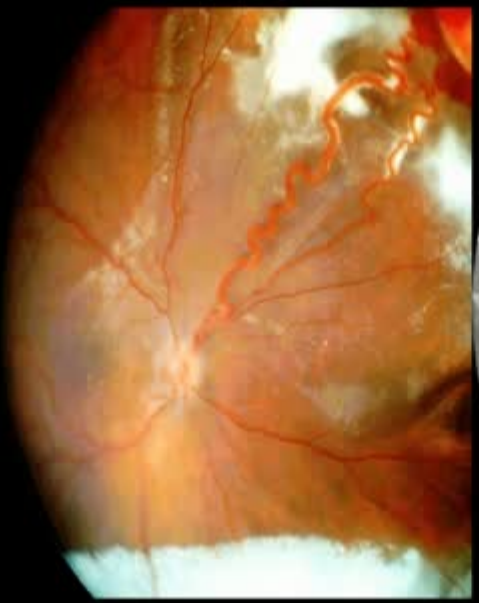

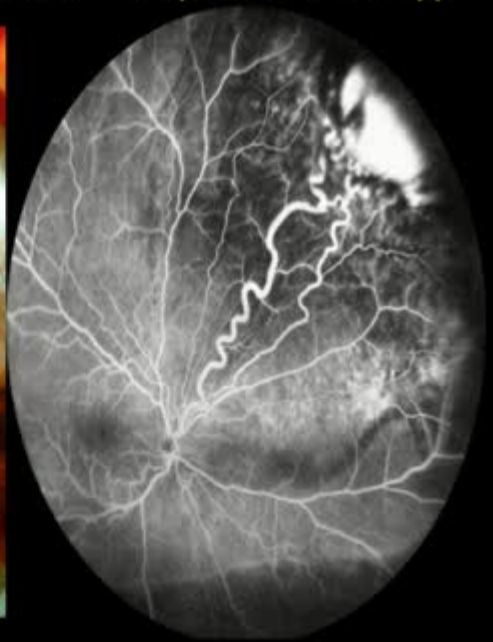

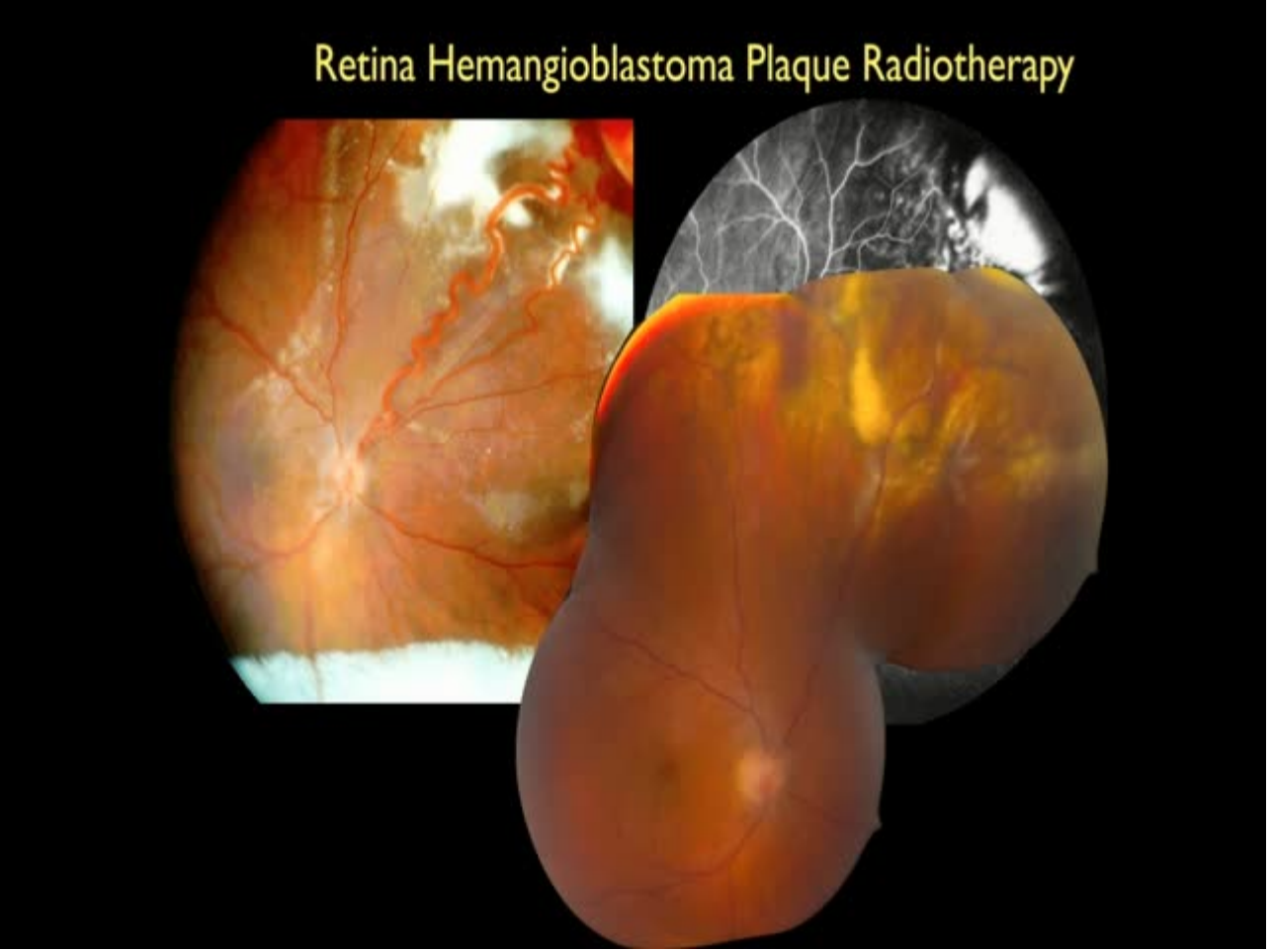
Retina Hemangioblastoma Plaque Radiotherapy

Invisible Retina Hemangioblastoma

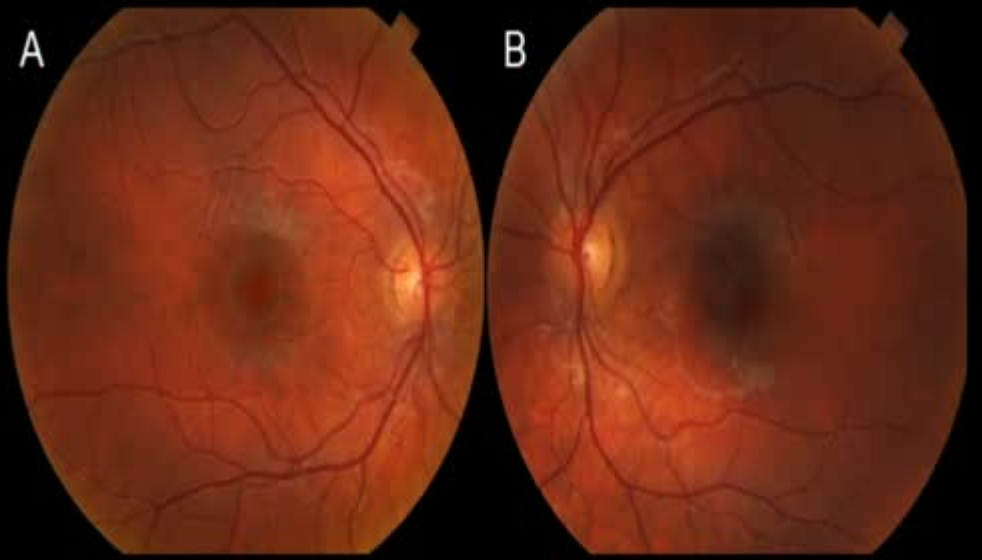

Schoen M, Shields CL, Say EAT, Douglass A, Shields JA, Jampol L. Invisible retinal hemangioblastoma detected by spectral domain optical coherence tomography. Ret Cases & Brief Rep 2016; in press.

Invisible Retina Hemangioblastoma

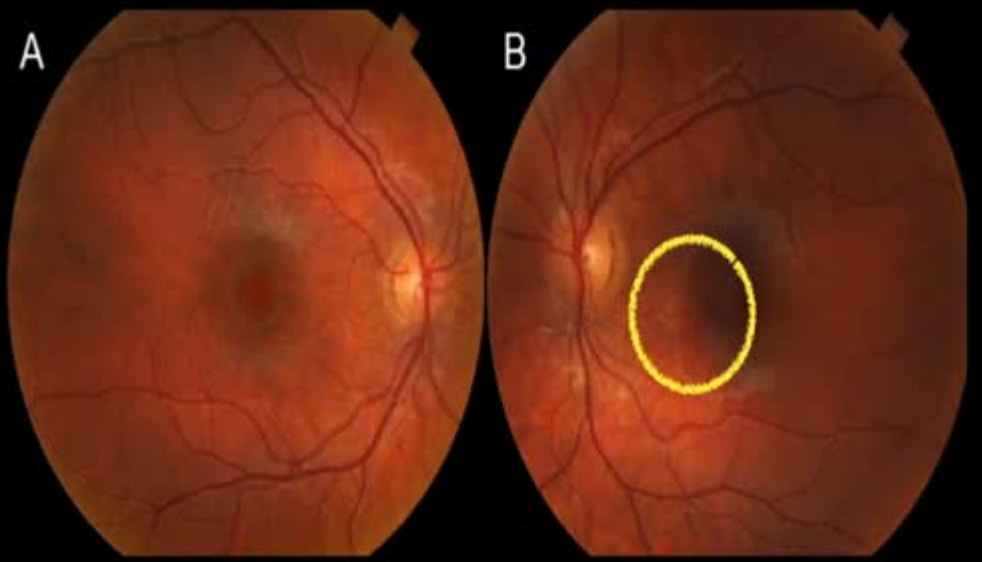

Schoen M, Shields CL, Say EAT, Douglass A, Shields JA, Jampol L. Invisible retinal hemangioblastoma detected by spectral domain optical coherence tomography. Ret Cases & Brief Rep 2016; in press.

Invisible Retina Hemangioblastoma

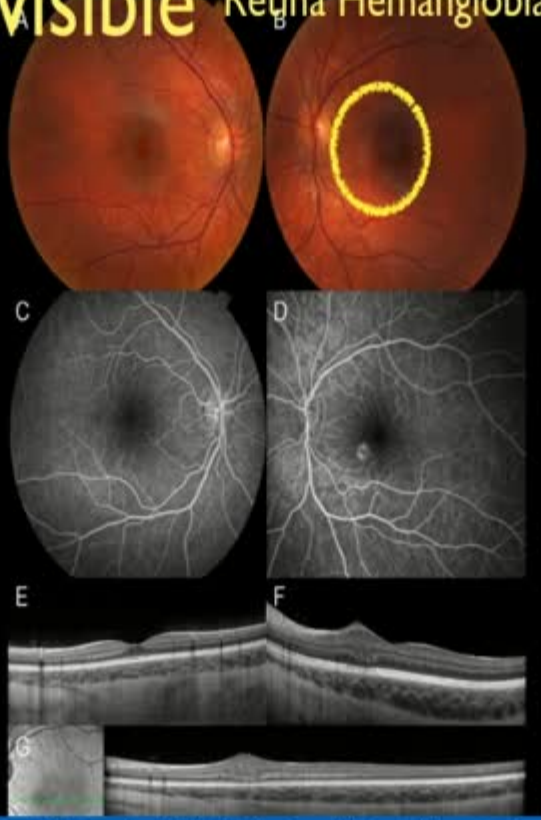

Schoen M, Shields CL, Say EAT, Douglass A, Shields JA, Jampol L. Invisible retinal hemangioblastoma detected by spectral domain optical coherence tomography. Ret Cases & Brief Rep 2016; in press.

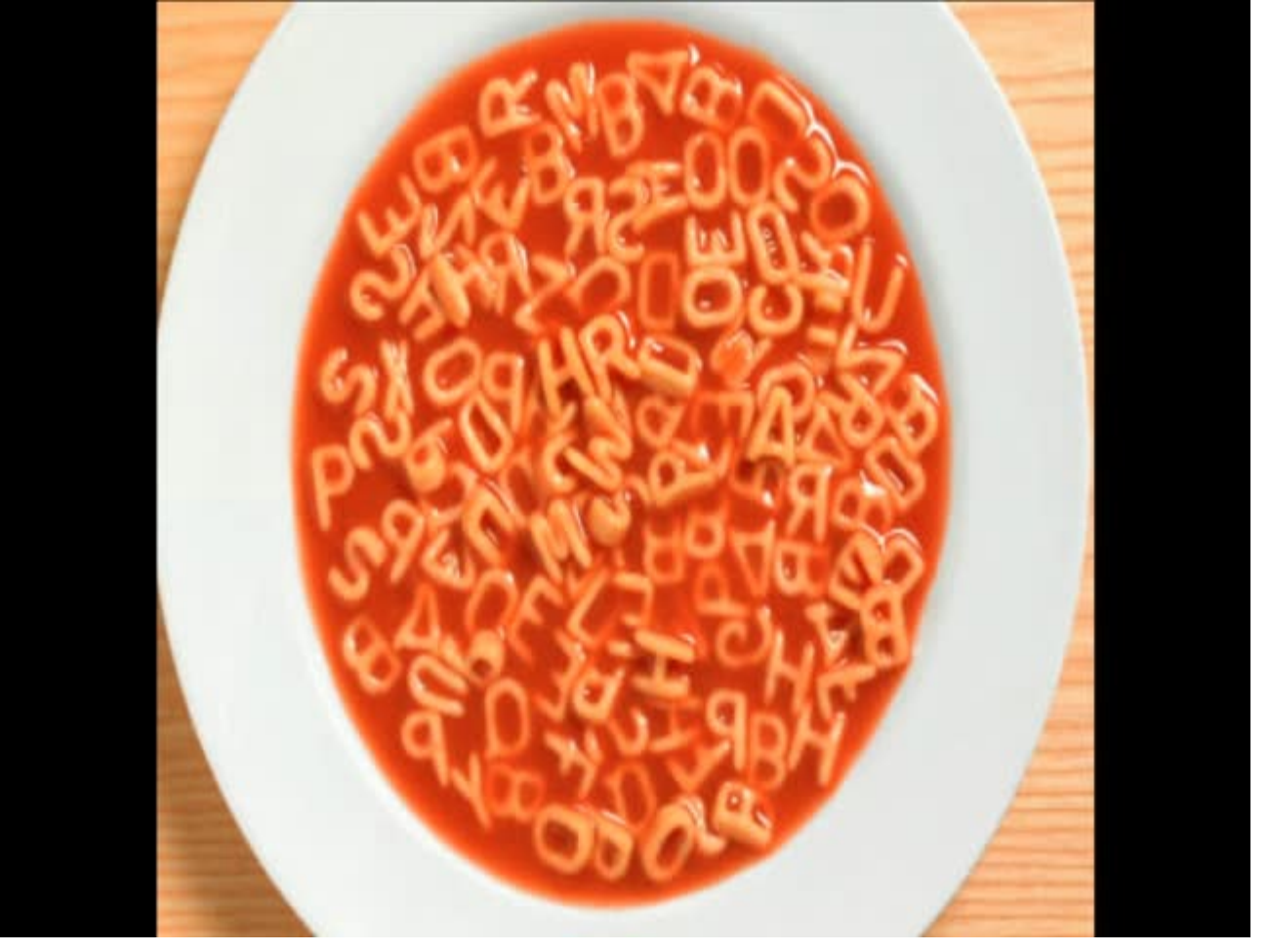

Invisible Retina Hemangioblastoma

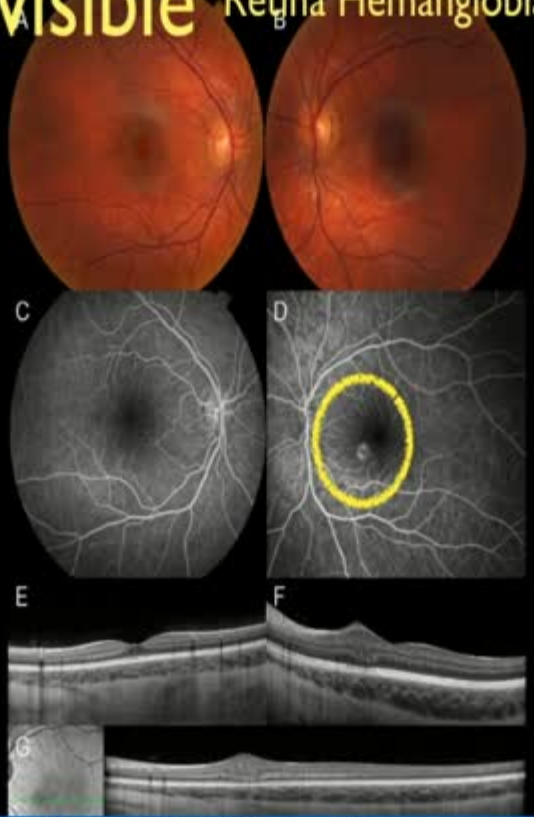

Schoen M, Shields CL, Say EAT, Douglass A, Shields JA, Jampol L. Invisible retinal hemangioblastoma detected by spectral domain optical coherence tomography. Ret Cases & Brief Rep 2016; in press.

Invisible Retina Hemangioblastoma

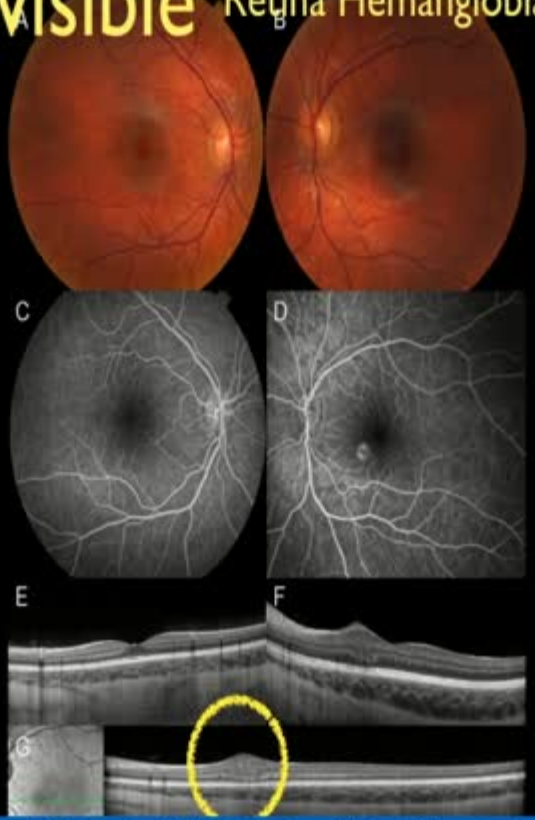

Schoen M, Shields CL, Say EAT, Douglass A, Shields JA, Jampol L. Invisible retinal hemangioblastoma detected by spectral domain optical coherence tomography. Ret Cases & Brief Rep 2016; in press.

CLINICALLY INVISIBLE RETINAL HEMANGIOBLASTOMAS DETECTED BY SPECTRAL DOMAIN OPTICAL COHERENCE TOMOGRAPHY AND FLUORESCEIN ANGIOGRAPHY IN TWINS

Marisa A. Schoen, BA,* Carol L. Shields, MD,* Emil Anthony T. Say, MD,*
Alexzandra M. Douglass, BS,* Jerry A. Shields, MD,* Lee M. Jampol, MD†

RETINAL CASES & BRIEF REPORTS

Purpose: To report subclinical retinal hemangioblastoma detected by enhanced depth imaging optical coherence tomography and fluorescein angiography in at-risk twins.

Methods: Case report.

Results: A set of twins, age 7 years, (Twin A and Twin B) with known family history of von Hippel–Lindau disease (gene test positive) and no systemic manifestations were evaluated. [illegible] tumor in the right eye, and a clinically evident 4-mm hemangioblastoma in the superior retina of the left eye. The enhanced depth imaging optical coherence tomography demonstrated normal fovea in both eyes. However, imaging at the inferonasal juxtapapillary region in the right eye documented an intraretinal mass from nerve fiber layer to outer plexiform layer on enhanced depth imaging optical coherence tomography and with hyperfluorescence on fluorescein angiography, consistent with retinal hemangioblastoma. Twin B demonstrated no clinically visible tumors in both eyes, but the left eye showed a small hyperreflective lesion in

super-early detection is key

CLINICALLY INVISIBLE RETINAL HEMANGIOBLASTOMAS DETECTED BY SPECTRAL DOMAIN OPTICAL COHERENCE TOMOGRAPHY AND FLUORESCEIN ANGIOGRAPHY IN TWINS

Marisa A. Schoen, BA,* Carol L. Shields, MD,* Emil Anthony T. Say, MD,*
Alexzandra M. Douglass, BS,* Jerry A. Shields, MD,* Lee M. Jampol, MD†

RETINAL CASES & BRIEF REPORTS

Purpose: To report subclinical retinal hemangioblastoma detected by enhanced depth imaging optical coherence tomography and fluorescein angiography in at-risk twins.

Methods: Case report.

Results: A set of twins, age 7 years, (Twin A and Twin B) with known family history of von

super-early detection is key

tumor in the right eye, and a clinically invisible 4-mm hemangioblastoma in the superior retina of the left eye. The enhanced depth imaging optical coherence tomography demonstrated normal fovea in both eyes. However, imaging at the inferonasal juxtapapillary region in the right eye documented an intraretinal mass from nerve fiber layer to outer plexiform layer on enhanced depth imaging optical coherence tomography and with hyperfluorescence on fluorescein angiography, consistent with retinal hemangioblastoma. Twin B demonstrated no clinically visible tumors in both eyes, but the left eye showed a small hyperreflective lesion in


Retinal hemangioblastoma
In addition to the eye, …
keep in mind the systemic associations

von Hippel Lindau

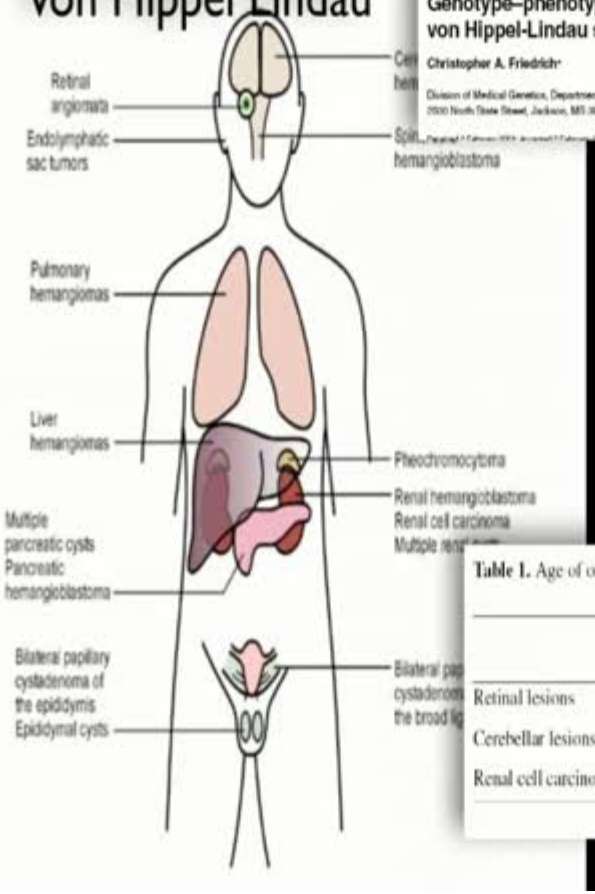

© 2001 Oxford University Press Human Molecular Genetics, 2001, Vol. 10, No. 7 763–767

Genotype–phenotype correlation in von Hippel-Lindau syndrome

Christopher A. Friedrich*

Division of Medical Genetics, Department of Preventive Medicine, University of Mississippi School of Medicine, 2500 North State Street, Jackson, MS 39216-4505, USA

Table 1. Age of onset of characteristic tumors

	Mean age (years)	Age range (years)	Patients (%)
Retinal lesions	25	1–67	45–59
Cerebellar lesions	30	11–78	44–72
Renal cell carcinoma	37	16–67	40–70

von Hippel Lindau

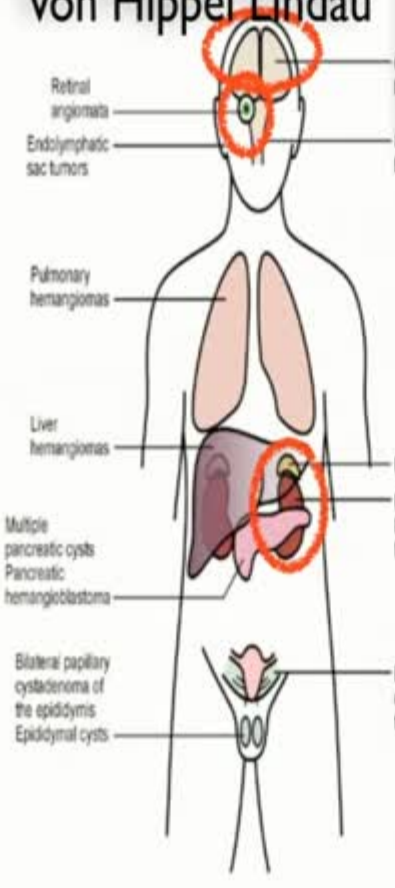

© 2002 Oxford University Press Human Molecular Genetics, 2002, Vol. 10, No. 7 763–767

Genotype–phenotype correlation in von Hippel-Lindau syndrome

Christopher A. Friedrich*

Division of Medical Genetics, Department of Preventive Medicine, University of Mississippi School of Medicine, 2500 North State Street, Jackson, MS 39216-4505, USA

Table 1. Age of onset of characteristic tumors

	Mean age (years)	Age range (years)	Patients (%)
Retinal lesions	25	1–67	45–59
Cerebellar lesions	30	11–78	44–72
Renal cell carcinoma	37	16–67	40–70

von Hippel Lindau

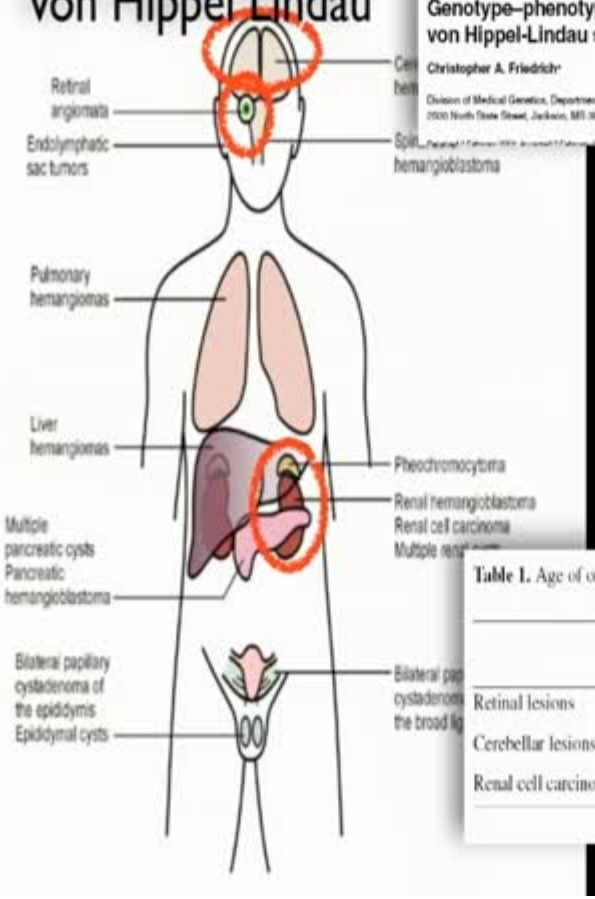

© 2001 Oxford University Press Human Molecular Genetics, 2001, Vol. 10, No. 7 763–767

Genotype–phenotype correlation in von Hippel-Lindau syndrome

Christopher A. Friedrich*

Division of Medical Genetics, Department of Preventive Medicine, University of Mississippi School of Medicine, 2500 North State Street, Jackson, MS 39216-4505, USA

Table 1. Age of onset of characteristic tumors

	Mean age (years)	Age range (years)	Patients (%)
Retinal lesions	25	1–67	45–59
Cerebellar lesions	30	11–78	44–72
Renal cell carcinoma	37	16–67	40–70

von Hippel Lindau

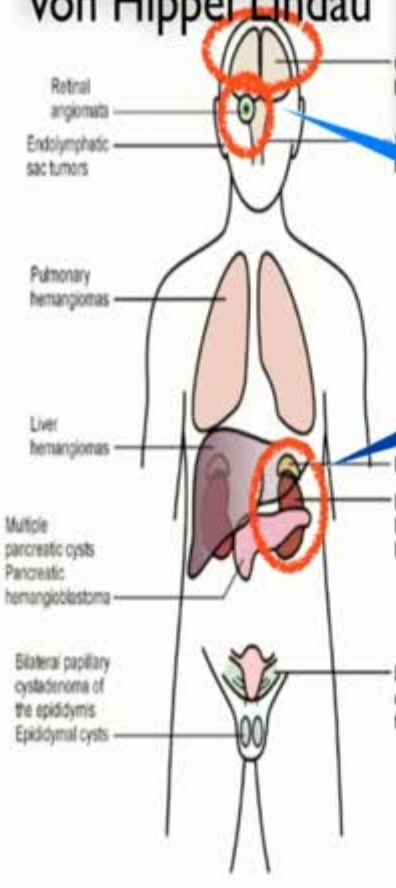

© 2002 Oxford University Press
Human Molecular Genetics, 2002, Vol. 10, No. 7 763–767

Genotype–phenotype correlation in von Hippel-Lindau syndrome

Christopher A. Friedrich*

Division of Medical Genetics, Department of Preventive Medicine, University of Mississippi School of Medicine, 2500 North State Street, Jackson, MS 39216-4505, USA

mean survival 50 years
death from
- brain hemangioblastoma
- renal cell carcinoma

Table 1. Age of onset of characteristic tumors

	Mean age (years)	Age range (years)	Patients (%)
Retinal lesions	25	1–67	45–59
Cerebellar lesions	30	11–78	44–72
Renal cell carcinoma	37	16–67	40–70

von Hippel Lindau

Genotype phenotype correlation

Type 1 80%

- Pheochromocytoma absent
- Deletion
- Premature termination mutation

Type 2 20%

- Pheochromocytoma present
- Missense mutation

Human Molecular Genetics, 2001, Vol. 10, No. 7 N1–N7

Genotype–phenotype correlation in von Hippel-Lindau syndrome

Christopher A. Friedrich*

Division of Medical Genetics, Department of Preventive Medicine, University of Mississippi School of Medicine, 1930 North State Street, Jackson, MS 39210-4505, USA

Received 12 February 2001, Accepted 27 February 2001

The von Hippel Lindau (VHL) syndrome (OMIM 193300) is an autosomal dominant disorder caused by deletions or mutations in a tumor suppressor gene on human chromosome 3p25. It is characterized clinically by vascular tumors (to include hemangioblastomas of the cerebellum, spine, brain stem and retina. Clear-cell renal cell carcinoma is a frequent cause of death, occurring in up to 70% of patients with VHL. Pheochromocytomas occur in association with specific alleles (usually mutations as opposed to deletions), therefore a family history of pheochromocytoma in association with VHL is an indication for thorough surveillance for pheochromocytoma in affected family members.The VHL gene coding sequence contains three exons. Two isoforms of mRNA exist, reflecting the presence or absence of exon 2. Tumors arise following the loss or inactivation of the wild-type allele in a cell. In initial studies 20% of patients had large germline mutations detectable by Southern blot analysis, 21% had missense mutations and 27% had nonsense or frameshift mutations. Advances in mutation analysis now allow for a 100% mutation detection rate in families with definite VHL. Families may be characterized by the presence (type 2 (1–20% of families)) or absence (type 1) of pheochromocytomas. Most type 2 families are affected by missense mutations, whereas most type 1 families have deletions or premature termination mutations. The prognosis for the lifetime risk of pheochromocytoma can be estimated by determination of the underlying mutation even if there is no family history of VHL.

INTRODUCTION

The von Hippel Lindau (VHL) syndrome is a rare autosomal dominant condition characterized by the development of specific benign and malignant tumors. It is caused by point mutations or deletions in a tumor suppressor gene. Although there is great variation in the clinical presentation, those who have a mutated gene are at greatly increased risk of developing spinal hemangioblastoma, renal cell carcinoma (RCC), retinal hemangioblastoma, cerebellar hemangioblastoma, pheochromocytoma, pancreatic and renal cysts, endolymphatic sac tumors, hemangiomas of the adrenals, liver and lungs, and papillary cystadenoma of the epididymis or broad ligament, as illustrated in the Figure 1 (1–3). As many as 10% of patients in VHL families may show only rare manifestation of the syndrome (3,5). Although there is variable expressivity among families, some clinical features are similar within families. Clear-cell renal RCC occurs in up to 70% of patients (5). In early studies death was often due to complications of cerebellar hemangioblastoma (75%) or metastatic RCC (22%) (5,6). The retinal lesions can cause retinal detachment or hemorrhage which lead to blindness, but usually respond to treatment with laser therapy or cryotherapy if detected early.

Table 1 lists the age of onset of typical findings (7,9). Pheochromocytoma may be the initial presentation. A registry of 63 patients in northwest England was started in 1989 (10). Their mean age of onset (the first sign or symptom was 26.27 years, with a mean age at diagnosis of 30.67 years. Cerebellar hemangioblastoma was the most common initial manifestation (34.9%). The most common cause of death was complications of cerebellar hemangioblastoma (47.7%), and the mean age at death was 40.9 years. The cumulative occurrence of cerebellar hemangioblastoma was 68.2%, retinal hemangioblastoma (50%), RCC (39.3%), spinal hemangioblastoma (23.9%) and pheochromocytoma (13.5%).

Family studies have shown reduced penetrance of the clinical phenotype. Three obligate carriers without lesions were found in the northwest England registry (10). The prevalence of VHL disease was estimated at 1 in 53 000 in East Anglia, with an incidence of 1 in 36 000 (2), and the prevalence was 1 in 38 000 in Freiburg (4). The northwest England VHL registry estimated the prevalence at 1 in 41 000 with an incidence of 1 in 61 000 (10).

The life expectancy of those affected has been <30 years. Earlier diagnosis and the recent development of surveillance protocols emphasizing regular monitoring for predictable complications, followed by early intervention, may have improved the prognosis.

CLINICAL MANIFESTATIONS

The diagnosis is usually made on clinical grounds. In a patient with a family history of VHL, the finding of a single retinal or cerebellar hemangioblastoma, pheochromocytoma or RCC is

Tel: +1 601 984 1490; Fax: +1 601 984 1515; Email: cfriedrich@mcsnet.umsmed.edu


ABC

Targeting von Hippel-Lindau Pathway in Renal Cell Carcinoma

Premal H. Patel,[1,2] Rajendrakumar S.V. Chadalavada,[2] R.S.K. Chaganti,[1,2] and Robert J. Motzer[1]

Abstract Inheritance of a defective copy of the von Hippel-Lindau (*VHL*) gene leads to the most common cause of inherited renal cell carcinoma (RCC). In addition, most patients with sporadic RCC have aberrant *VHL*. In the absence of VHL, hypoxia-inducible factor α accumulates, leading to production of several growth factors, including vascular endothelial growth factor and platelet-derived growth factor. We review here the biology of RCC and how a combination of proximal and distal block of VHL/hypoxia-inducible factor α pathway by novel targeted agents, including sunitinib, sorafenib, bevacizumab, everolimus, and temsirolimus, has led to significant improvements in progression-free survival.

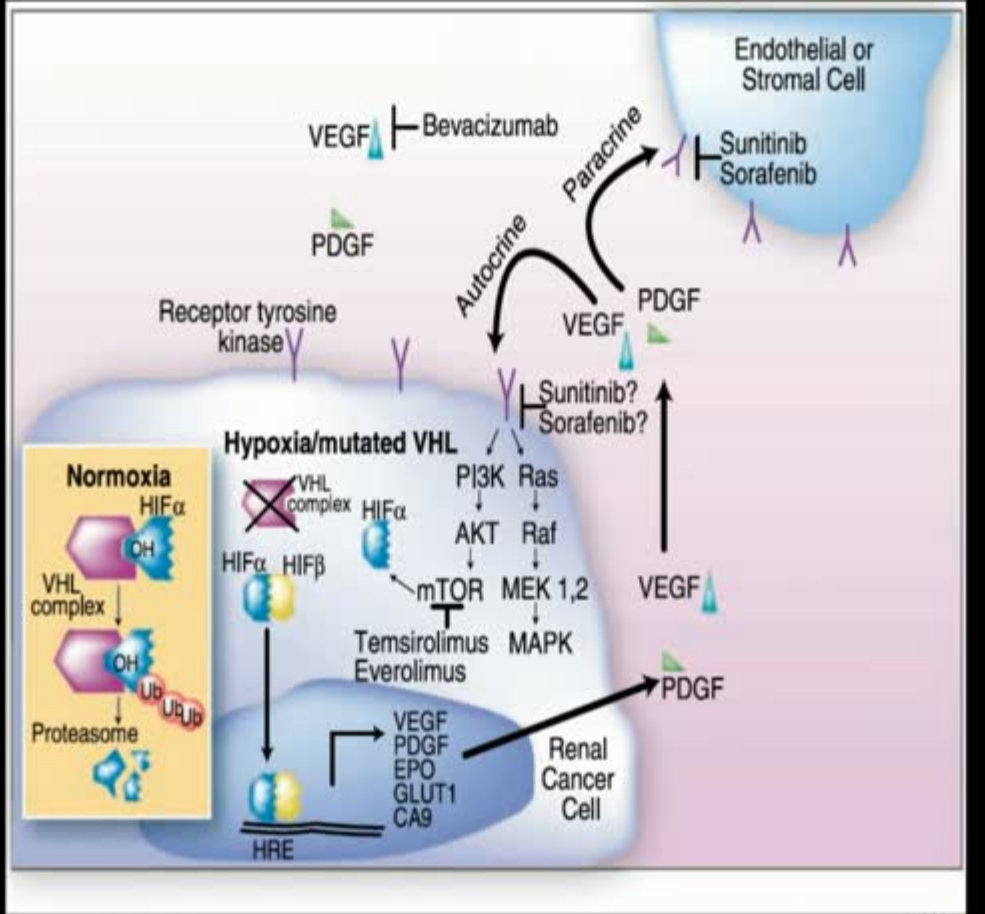

CCR Molecular Pathways

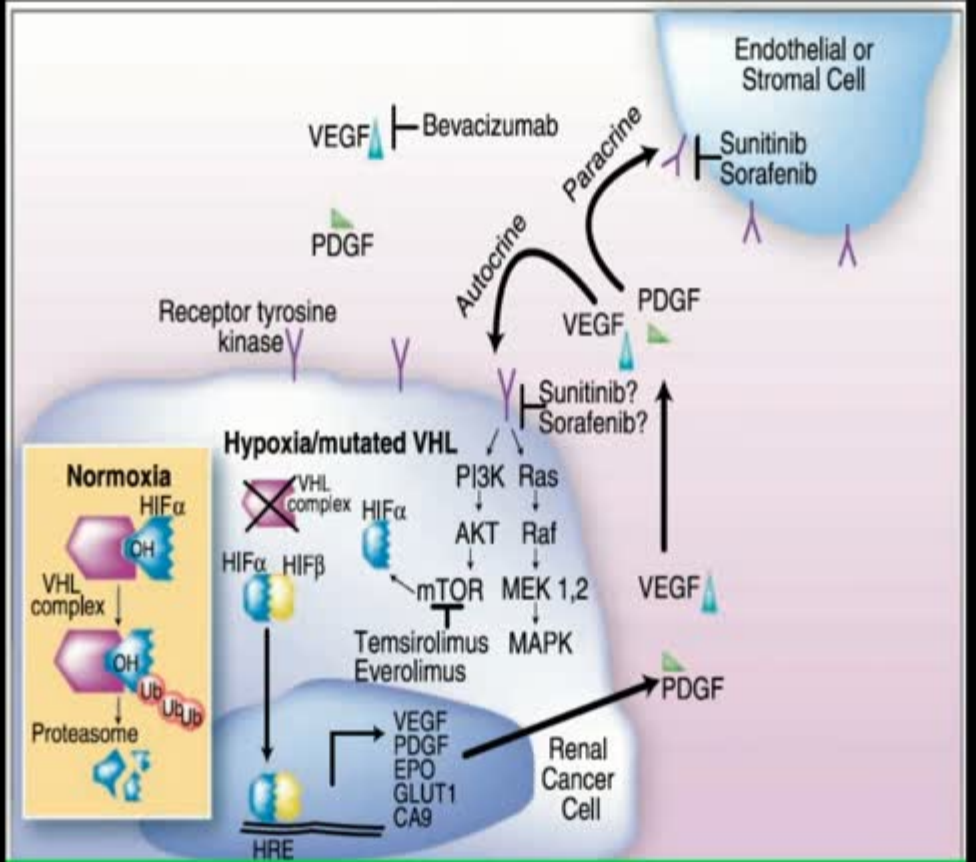

HIF hypoxia inducible factor

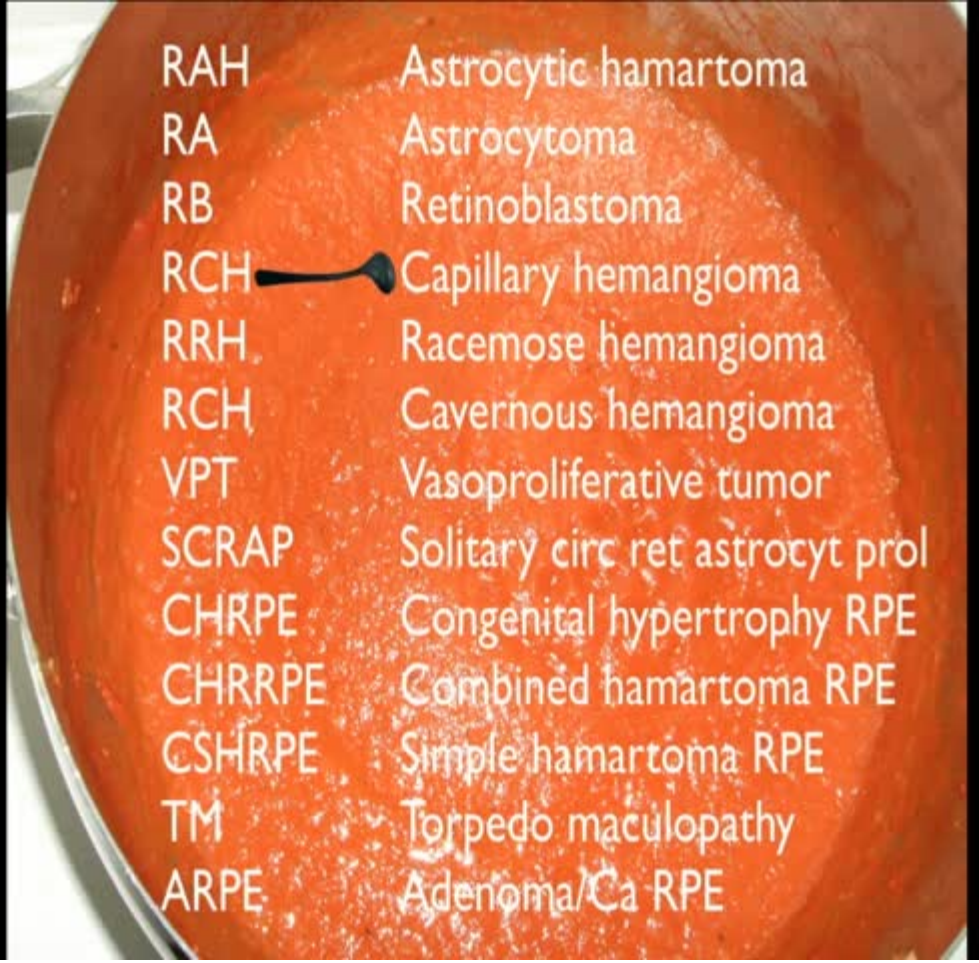
RAH Astrocytic hamartoma
RA Astrocytoma
RB Retinoblastoma
RCH Capillary hemangioma
RRH Racemose hemangioma
RCH Cavernous hemangioma
VPT Vasoproliferative tumor
SCRAP Solitary circ ret astrocyt prol
CHRPE Congenital hypertrophy RPE
CHRRPE Combined hamartoma RPE
CSHRPE Simple hamartoma RPE
TM Torpedo maculopathy
ARPE Adenoma/Ca RPE

RAH	Astrocytic hamartoma
RA	Astrocytoma
RB	Retinoblastoma
RCH	Capillary hemangioma
RRH	Racemose hemangioma
RCH	Cavernous hemangioma
VPT	Vasoproliferative tumor
SCRAP	Solitary circ ret astrocyt prol
CHRPE	Congenital hypertrophy RPE
CHRRPE	Combined hamartoma RPE
CSHRPE	Simple hamartoma RPE
TM	Torpedo maculopathy
ARPE	Adenoma/Ca RPE

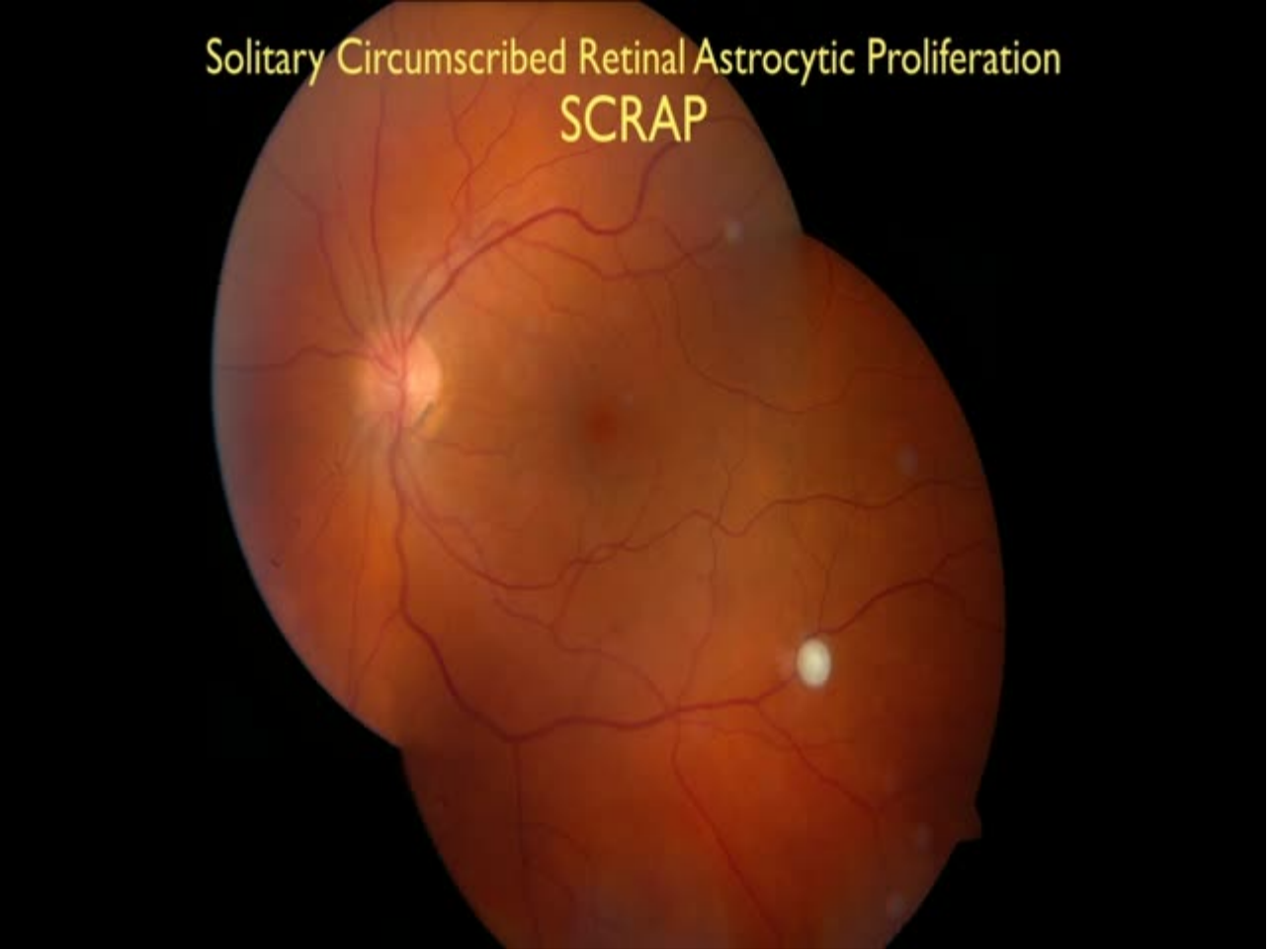
Solitary Circumscribed Retinal Astrocytic Proliferation
SCRAP

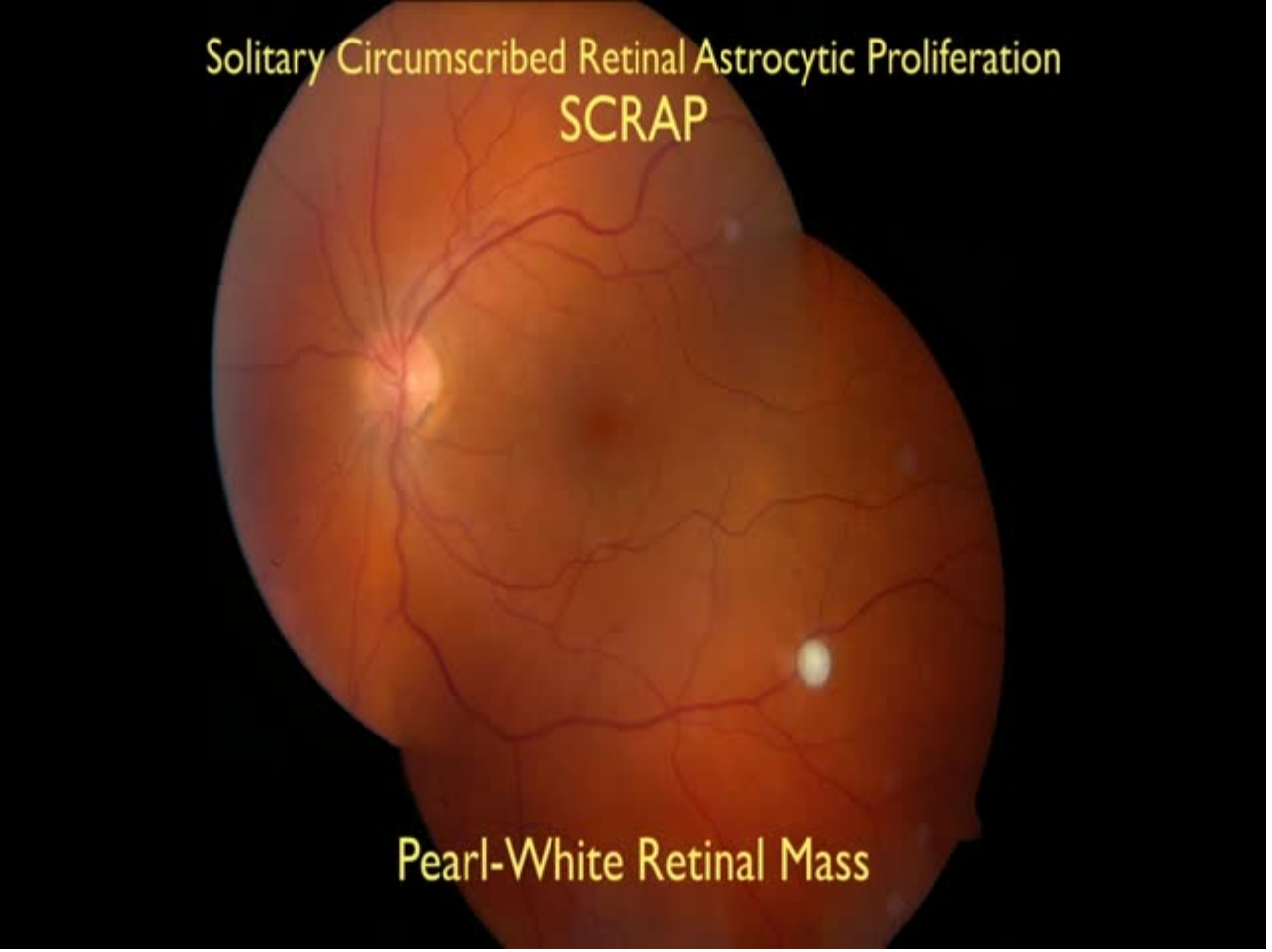
Solitary Circumscribed Retinal Astrocytic Proliferation
SCRAP
Pearl-White Retinal Mass

Presumed Solitary Circumscribed Retinal Astrocytic Proliferation

The 2010 Jonathan W. Wirtschafter Lecture

Jerry A. Shields, MD; Carlos G. Bianciotto, MD; Tero Kivela, MD; Carol L. Shields, MD

Objective: To report the clinical features and differential diagnosis of an unusual entity termed *presumed solitary circumscribed retinal astrocytic proliferation* (PSCRAP).

Methods: Retrospective review of medical records.

Results: All patients with PSCRAP were asymptomatic, and the lesion was found during routine examination. There were 5 men and 2 women with a median age of 53 years. No patient had a history or clinical findings of tuberous sclerosis complex. Each PSCRAP lesion was circumscribed, abruptly elevated, and opaque white to yellow and mostly obscured the underlying retinal vessels. The lesions had no associated subretinal fluid, hemorrhage, calcification, or retinal traction. Fluorescein angiography disclosed mild hyperfluorescence in the venous phase and moderate late staining of the lesions. Autofluorescence showed mild hyperautofluorescence of the lesions. Ultrasonography revealed no calcification. Optical coherence tomography showed an abruptly elevated retinal mass with optical shadowing posterior to the lesion. Six lesions were stable after a median follow-up of 6 years, and 1 lesion gradually disappeared. The pathogenesis and pathologic features of PSCRAP are unknown.

Conclusion: Presumed solitary circumscribed retinal astrocytic proliferation appears to be a unique retinal lesion of adulthood that resembles astrocytic hamartoma or retinoblastoma but displays distinctive ophthalmoscopic features.

Arch Ophthalmol. 2011;129(9):1189-1194

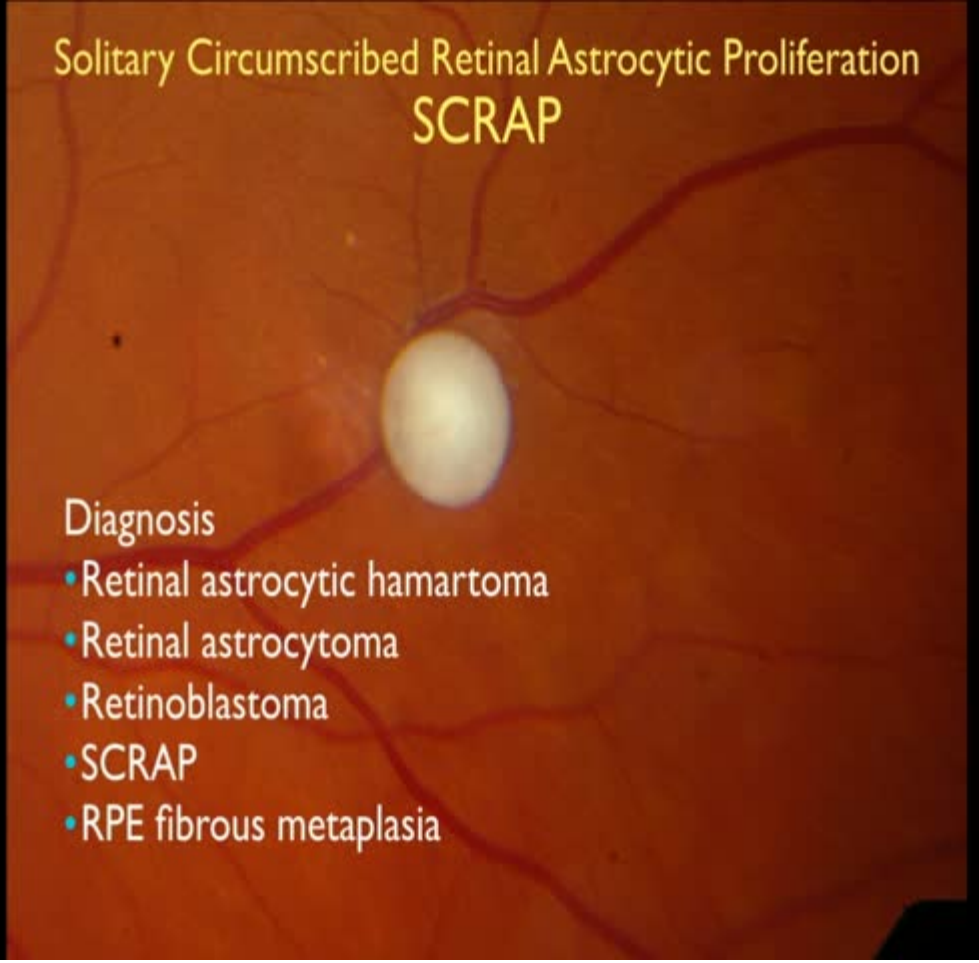
Solitary Circumscribed Retinal Astrocytic Proliferation
SCRAP
Diagnosis
•Retinal astrocytic hamartoma
•Retinal astrocytoma
•Retinoblastoma
•SCRAP
•RPE fibrous metaplasia

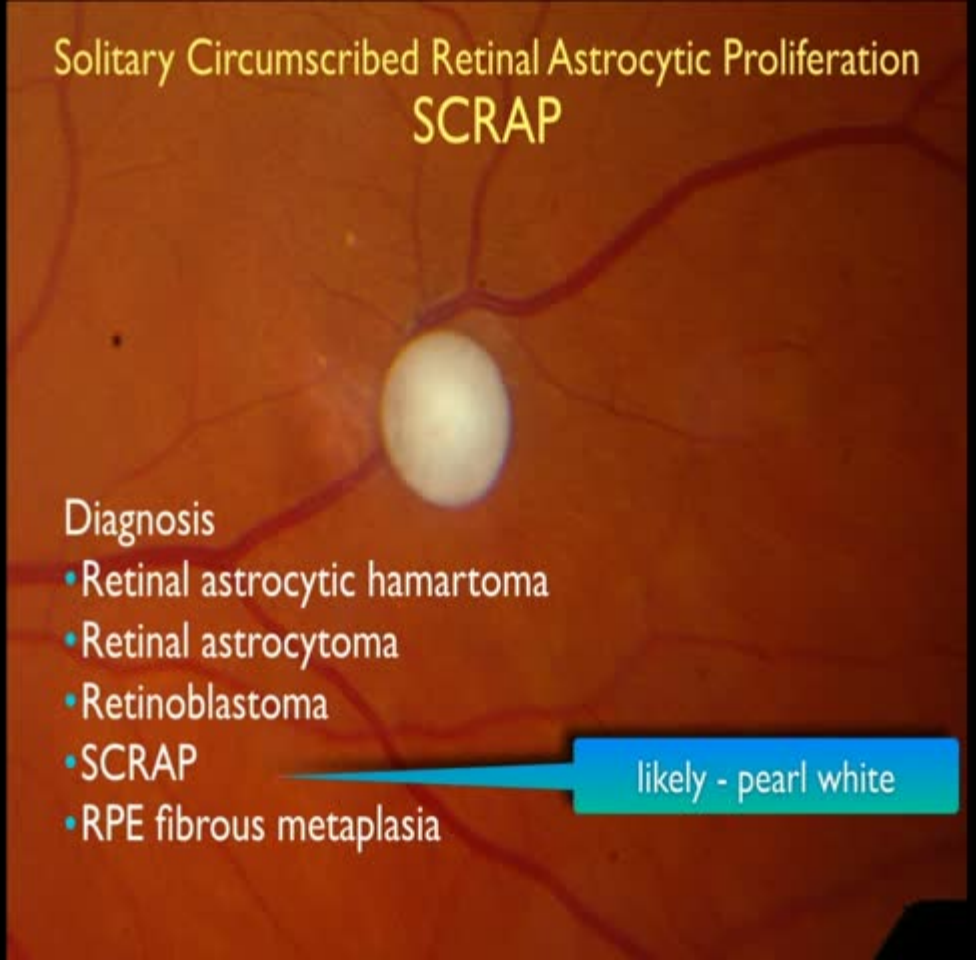
Solitary Circumscribed Retinal Astrocytic Proliferation
SCRAP
Diagnosis
•Retinal astrocytic hamartoma
•Retinal astrocytoma
•Retinoblastoma
•SCRAP
•RPE fibrous metaplasia
likely - pearl white


ABC
HELP

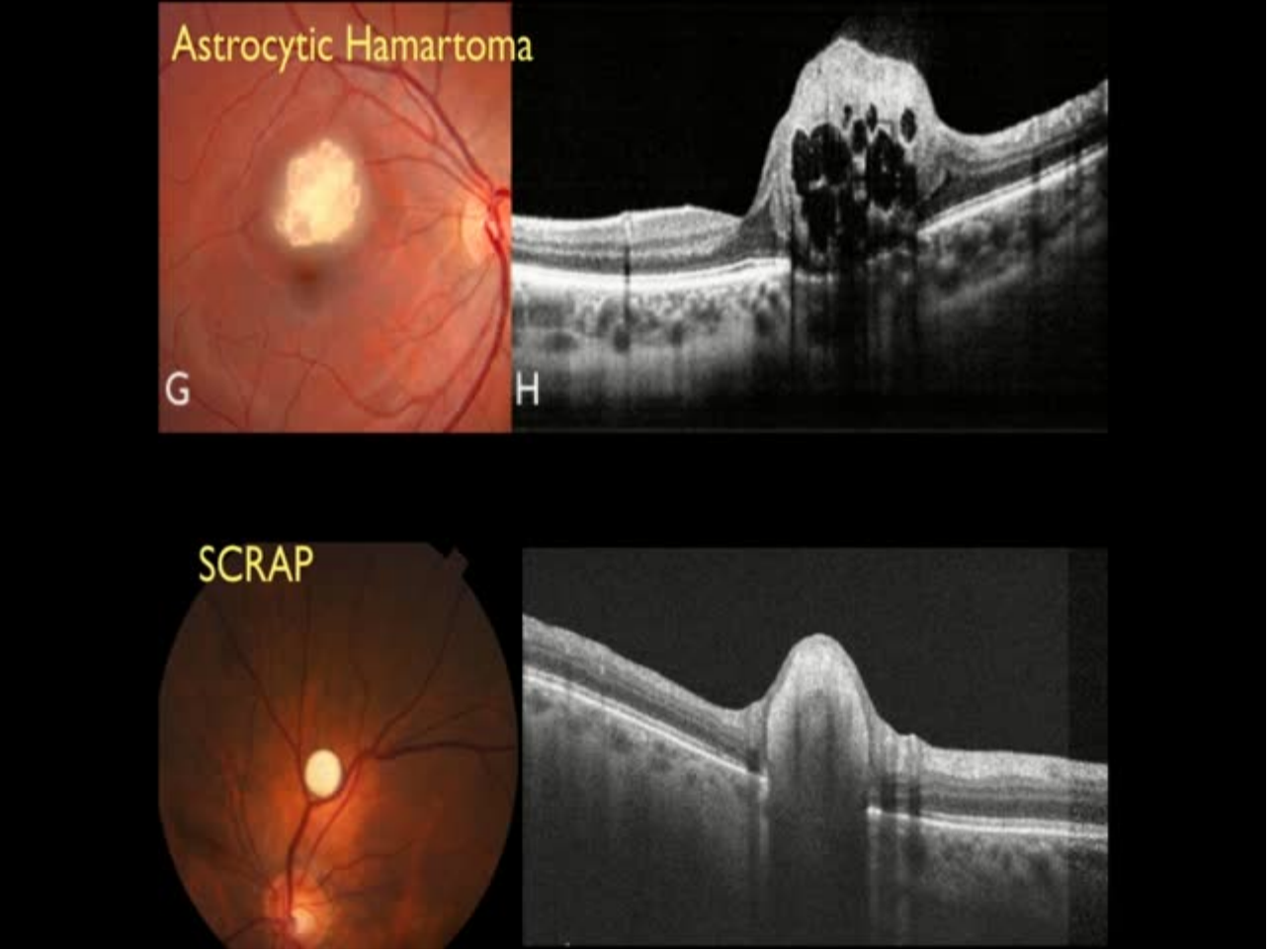
Astrocytic Hamartoma
G
H
SCRAP

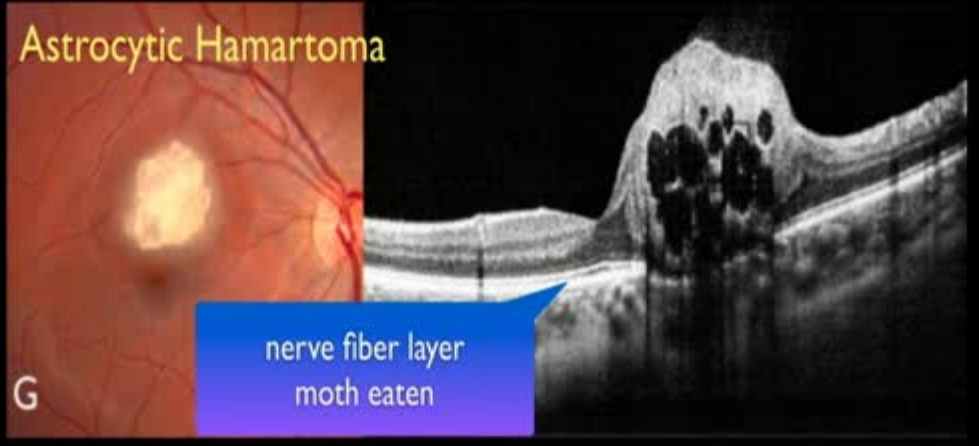
Astrocytic Hamartoma
nerve fiber layer
moth eaten
G

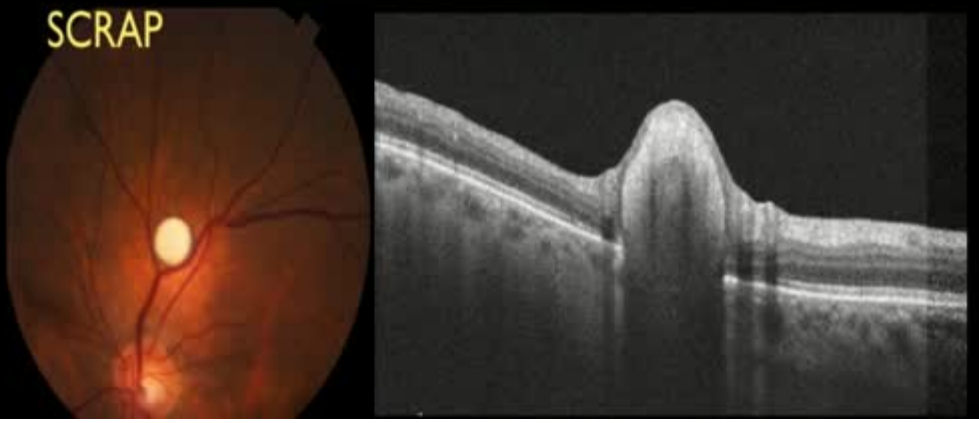
SCRAP

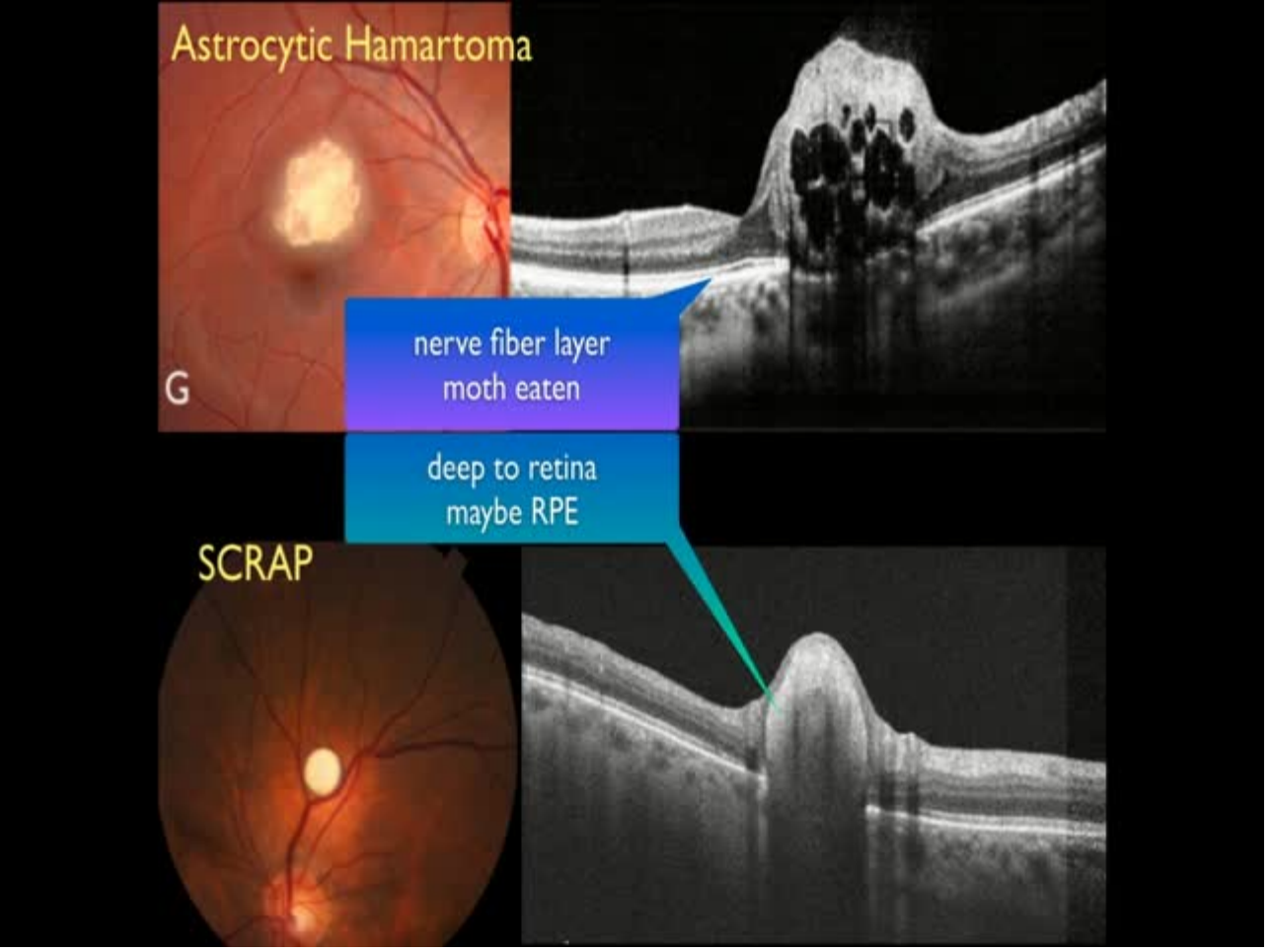
Astrocytic Hamartoma
G
nerve fiber layer
moth eaten
deep to retina
maybe RPE
SCRAP

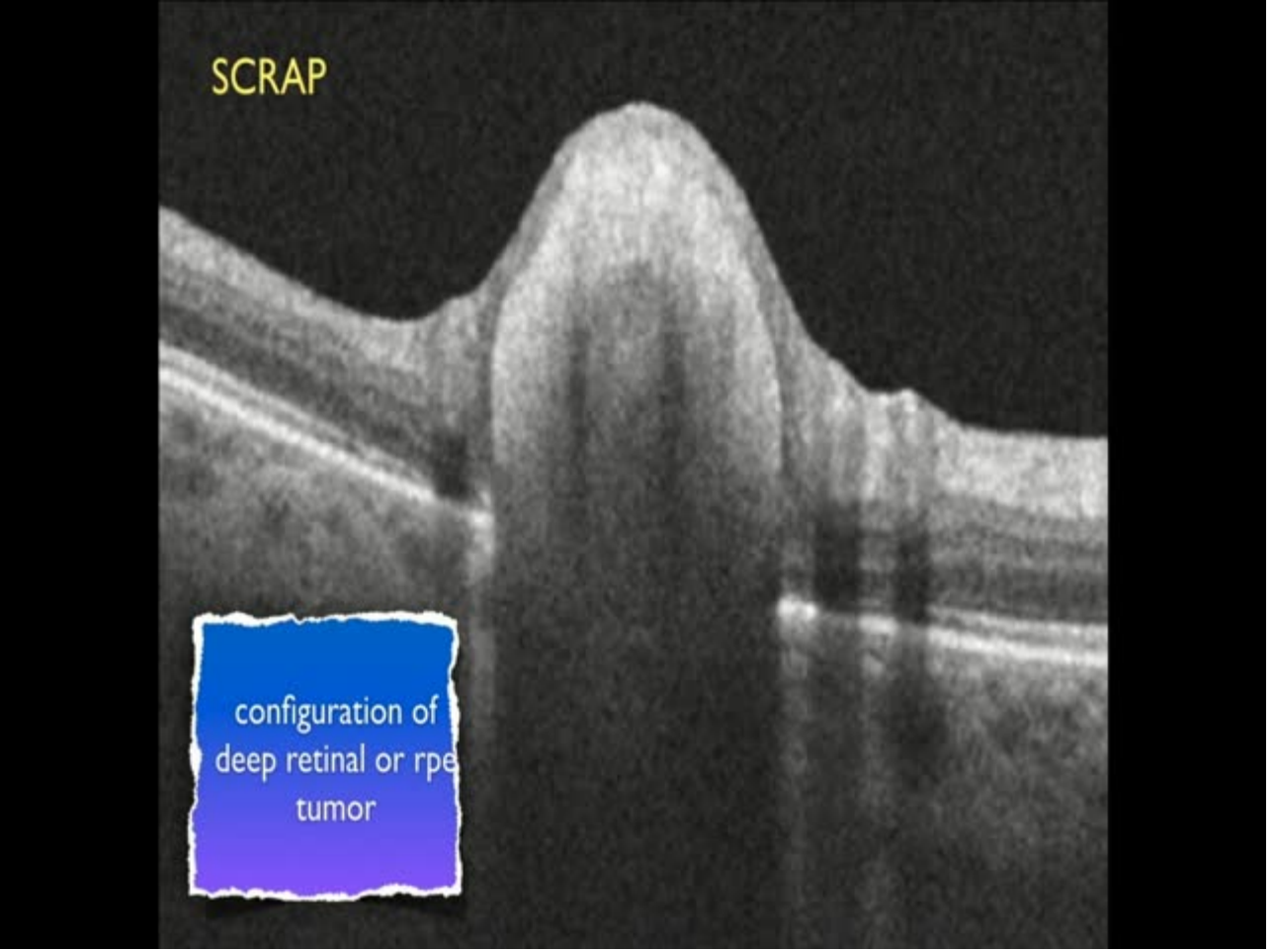
SCRAP
configuration of
deep retinal or rpe
tumor

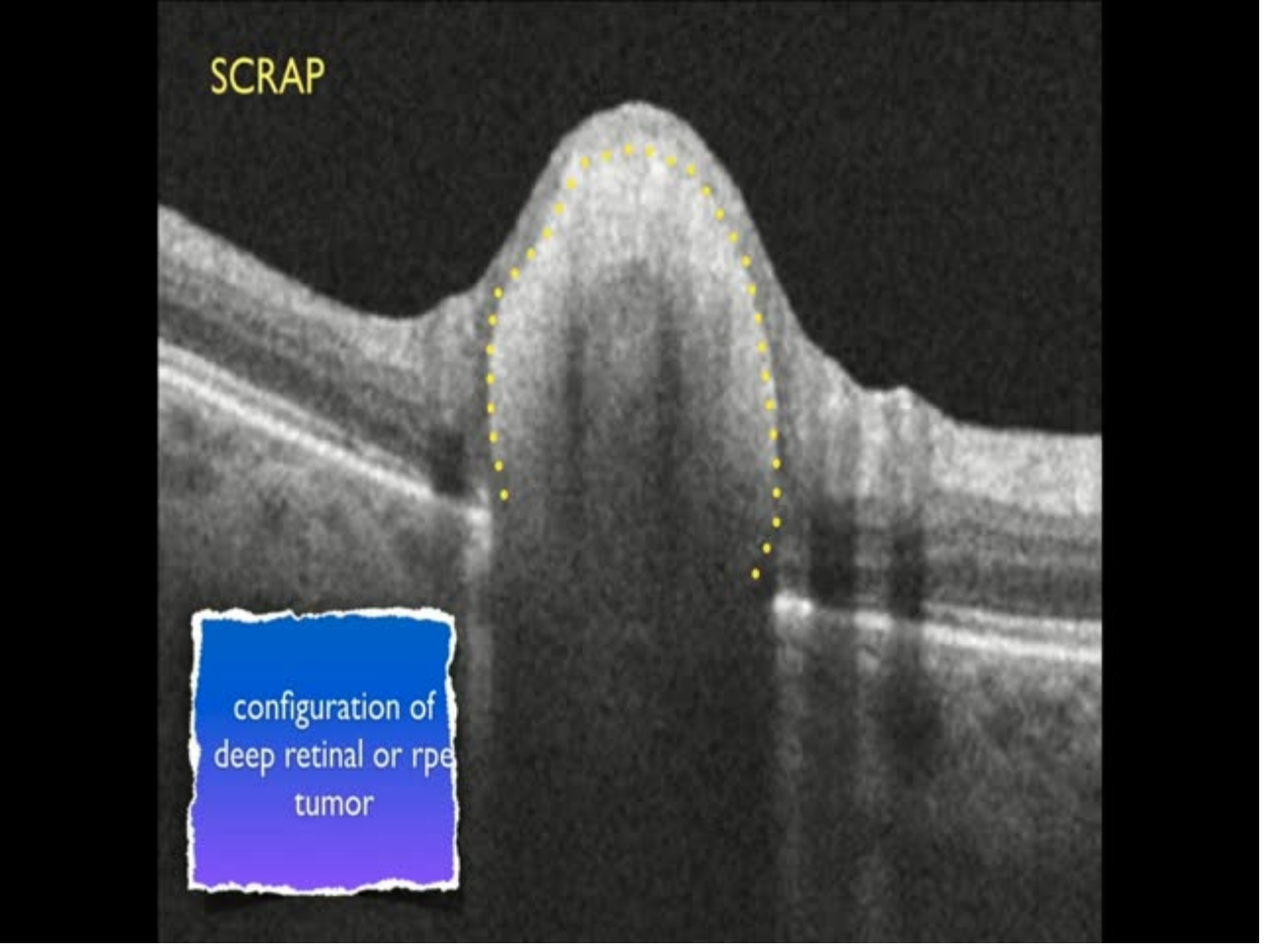
SCRAP
configuration of
deep retinal or rpe
tumor

SOLITARY CIRCUMSCRIBED "PEARL WHITE" RETINAL MASS (SO-CALLED RETINAL ASTROCYTIC PROLIFERATION) RESIDES IN DEEP RETINA OR BENEATH RETINA: FINDINGS ON MULTIMODAL IMAGING IN 4 CASES

Carol L. Shields, MD,* Richard Roe, MD, MHS,† Lawrence A. Yannuzzi, MD,‡
Jerry A. Shields, MD*

RETINA

Purpose: To report novel observations of previously described solitary circumscribed retinal astrocytic proliferation using spectral domain optical coherence tomography that suggests this tumor does not arise in the nerve fiber layer as initially believed, but arises within deep retinal or retinal pigment epithelial structures.

Methods: Retrospective review of four cases.

Results: Patient age ranged from 46 to 75 years. The tumor was pearl white or yellow-white (n = 4, 100%), located in the macula (n = 1, 25%) or macula to equator (n = 3, 75%) regions, and with mean tumor base of 1.2 mm and thickness of 0.8 mm. There were no feeding vessels, intrinsic vessels, subretinal fluid, or vitreoretinal traction. Mild surrounding retinal pigment epithelial hyperplasia and atrophy rimmed each tumor (n = 4, 100%). Fluorescein angiography depicted the mass with early hypofluorescence (n = 3/3, 100%) and late hypofluorescence (n = 2/3, 67%). Spectral domain optical coherence tomography demonstrated the mass with an abruptly elevated "snowball" configuration (n = 4, 100%), with smooth or slightly irregular surface (n = 4, 100%), and originating from deep retina or retinal pigment epithelial (n = 4, 100%), with overlying compression and draping of retinal tissue (n = 4, 100%).

Conclusion: This previously described small yellow-white retinal tumor appears to arise in the outer retinal layers and not from the inner retinal layers as formerly believed. This tumor may not be astrocytic as initially believed since it arises deep within the retina, but it could represent a deep glial or pigment epithelial fibrous mass. The pathogenesis and pathology of this rare lesion remain unknown.

RETINAL CASES & BRIEF REPORTS 00:1–6, 2015

RAH	Astrocytic hamartoma
RA	Astrocytoma
RB	Retinoblastoma
RCH	Capillary hemangioma
RRH	Racemose hemangioma
RCH	Cavernous hemangioma
VPT	Vasoproliferative tumor
SCRAP	Solitary circ ret astrocyt prol
CHRPE	Congenital hypertrophy RPE
CHRRPE	Combined hamartoma RPE
CSHRPE	Simple hamartoma RPE
TM	Torpedo maculopathy
ARPE	Adenoma/Ca RPE

RAH	Astrocytic hamartoma
RA	Astrocytoma
RB	Retinoblastoma
RCH	Capillary hemangioma
RRH	Racemose hemangioma
RCH	Cavernous hemangioma
VPT	Vasoproliferative tumor
SCRAP	Solitary circ ret astrocyt prol
CHRPE	Congenital hypertrophy RPE
CHRRPE	Combined hamartoma RPE
CSHRPE	Simple hamartoma RPE
TM	Torpedo maculopathy
ARPE	Adenoma/Ca RPE

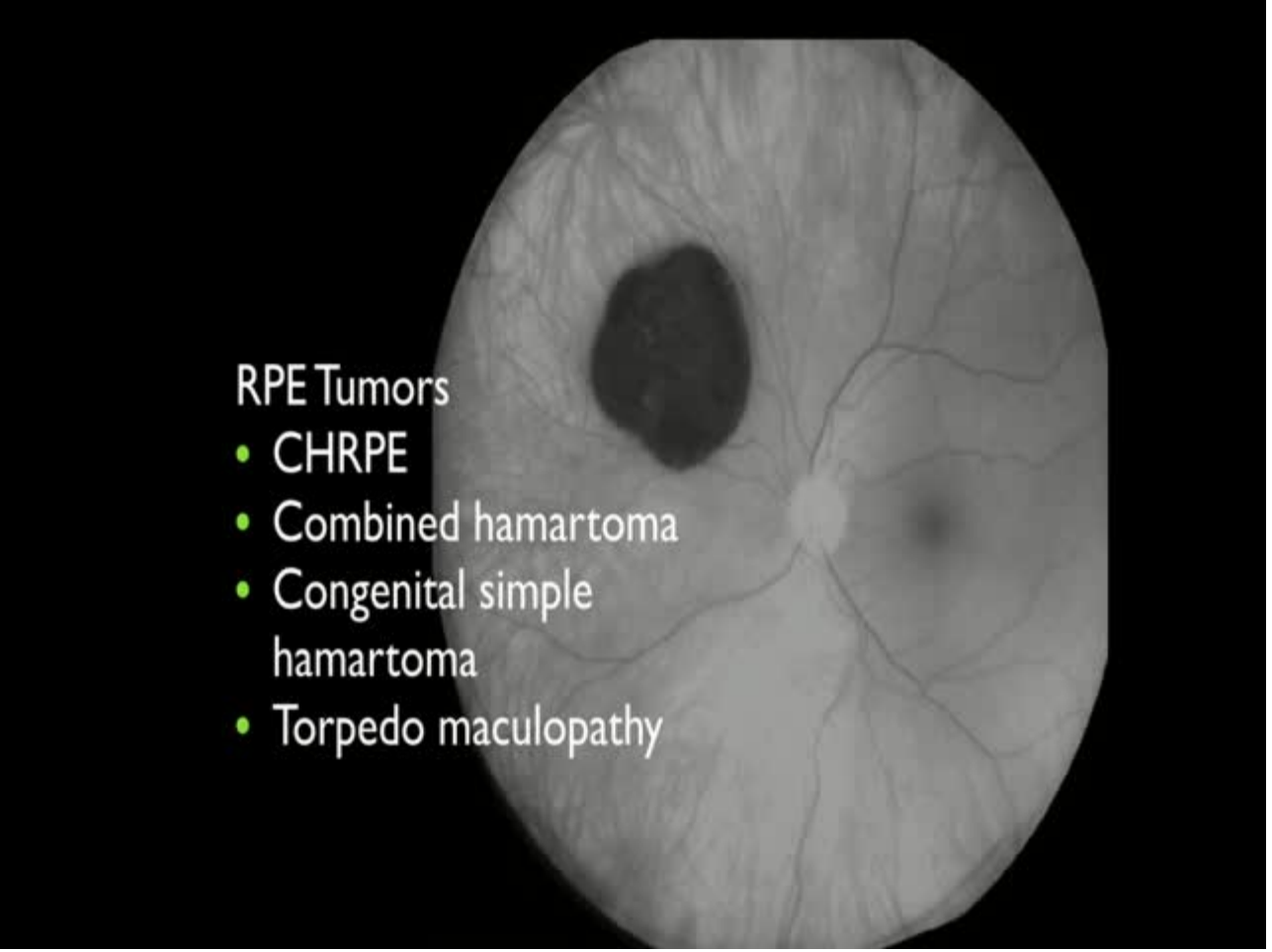
RPE Tumors
• CHRPE
• Combined hamartoma
• Congenital simple hamartoma
• Torpedo maculopathy

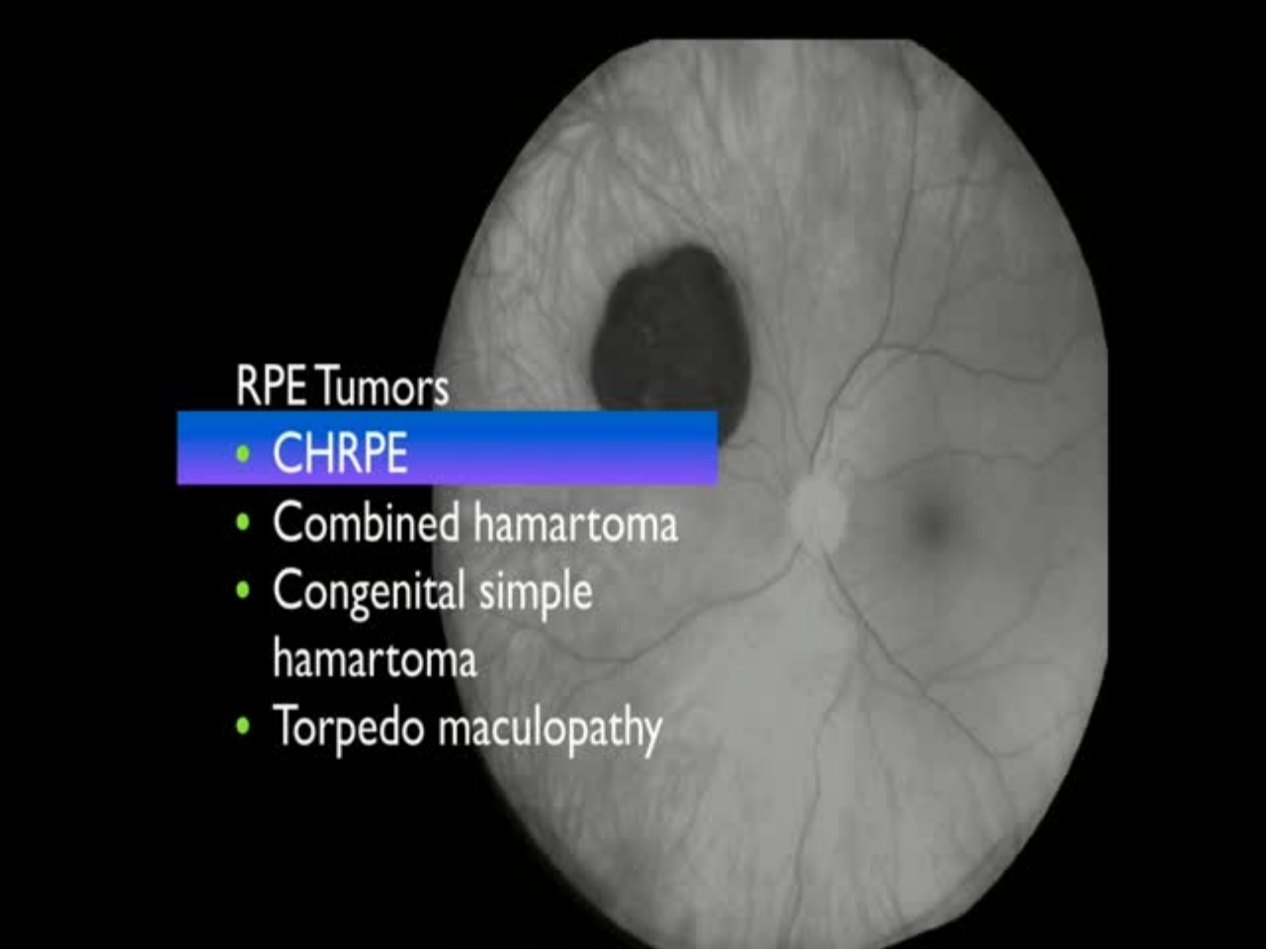
RPE Tumors
• CHRPE
• Combined hamartoma
• Congenital simple hamartoma
• Torpedo maculopathy


ABC
HELP
SWAG
WIN

Solitary Congenital Hypertrophy of the Retinal Pigment Epithelium

Clinical Features and Frequency of Enlargement in 330 Patients

Carol L. Shields, MD, Arman Mashayekhi, MD, Thucanh Ho, MD, Jacqueline Cater, PhD, Jerry A. Shields, MD

Objective: To describe the clinical features of solitary congenital hypertrophy of the retinal pigment epithelium (CHRPE) and to determine the frequency of enlargement of this lesion

Design: Retrospective, observational, noncomparative case series.

Participants: Three hundred thirty consecutive patients with solitary CHRPE.

Main Outcome Measures: The 3 main outcome measures included flat lesion enlargement, intralesional lacunae enlargement, and development of an elevated nodule within the lesion. The clinical features at the time of presentation were analyzed for their impact on the main outcomes using a series of Cox proportional hazards regressions.

Results: The most common referring diagnosis included choroidal nevus (26%), choroidal melanoma (15%), CHRPE (9%), and unspecified lesion (48%). The median age at diagnosis was 45 years (range, 1–80 years), and there were no patients with familial adenomatous polyposis or related colon cancer, although a history of cancer was noted in 8% of patients, most commonly breast cancer (3%). The lesion most frequently was located inferotemporally (31%) and at the equatorial region (45%). Rarely, it was located in the macula (1%) or peripapillary region (1%). The median largest basal diameter was 4.5 mm, and the lesion was flat in all cases except in 5 (1.5%), in which there was an intralesional lesion nodule. The lesion was pigmented in 88% of cases and nonpigmented in 12%. Lacunae were noted in 43% of the pigmented CHRPE, and the lacunae showed gradual enlargement in 32%. Factors related to lacunae enlargement included number and relative size of lacunae. Flat enlargement of the lesion was documented in 46% of patients with comparative photographic follow-up and in 83% of those followed up for more than 3 years. The median rate of enlargement was 10 μm per month. The most important factor associated with flat lesion enlargement was relative size of the lacunae within CHRPE. There were no cases of CHRPE in which a nodule developed while the patient was being followed up. Of the 5 lesions that had a nodule, progressive enlargement of the nodule was found in 3.

Conclusions: Congenital hypertrophy of the retinal pigment epithelium generally has been regarded as a benign, stable lesion, but subtle, flat enlargement was noted in most patients (83%) followed up for 3 or more years using meticulous photographic comparison. Flat enlargement of the lesion appeared to be related to percentage of the mass occupied by lacunae. *Ophthalmology 2003;110:1968–1976 © 2003 by the American Academy of Ophthalmology.*

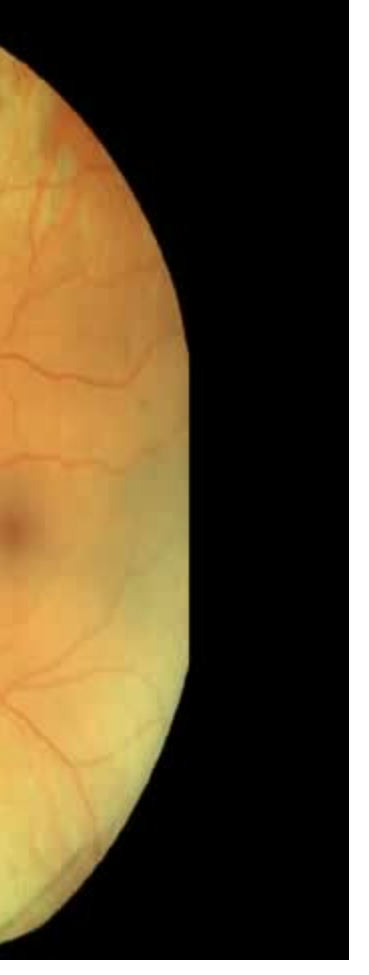

Solitary Congenital Hypertrophy of the Retinal Pigment Epithelium

Clinical Features and Frequency of Enlargement in 330 Patients

Carol L. Shields, MD, Arman Mashayekhi, MD, Thucanh Ho, MD, Jacqueline Cater, PhD, Jerry A. Shields, MD

Objective: To describe th
lium (CHRPE) and to determ
Design: Retrospective, a
Participants: Three hund
Main Outcome Measures: The 3 usual outcome measures included flat lesion enlargement, intralesional lacunae enlargement, and development of an elevated nodule within the lesion. The clinical features at the time of presentation were analyzed for their impact on the main outcomes using a series of Cox proportional hazards regressions.

Results: The most common referring diagnosis included choroidal nevus (26%), choroidal melanoma (15%), CHRPE (9%), and unspecified lesion (48%). The median age at diagnosis was 45 years (range, 1–80 years), and there were no patients with familial adenomatous polyposis or related colon cancer, although a history of cancer was noted in 8% of patients, most commonly breast cancer (3%). The lesion most frequently was located inferotemporally (31%) and at the equatorial region (45%). Rarely, it was located in the macula (1%) or peripapillary region (1%). The median largest basal diameter was 4.5 mm, and the lesion was flat in all cases except in 5 (1.5%), in which there was an intralesional lesion nodule. The lesion was pigmented in 88% of cases and nonpigmented in 12%. Lacunae were noted in 43% of the pigmented CHRPE, and the lacunae showed gradual enlargement in 32%. Factors related to lacunae enlargement included number and relative size of lacunae. Flat enlargement of the lesion was documented in 46% of patients with comparative photographic follow-up and in 83% of those followed up for more than 3 years. The median rate of enlargement was 10 μm per month. The most important factor associated with flat lesion enlargement was relative size of the lacunae within CHRPE. There were no cases of CHRPE in which a nodule developed while the patient was being followed up. Of the 5 lesions that had a nodule, progressive enlargement of the nodule was found in 3.

Conclusions: Congenital hypertrophy of the retinal pigment epithelium generally has been regarded as a benign, stable lesion, but subtle, flat enlargement was noted in most patients (83%) followed up for 3 or more years using meticulous photographic comparison. Flat enlargement of the lesion appeared to be related to percentage of the mass occupied by lacunae. *Ophthalmology 2003;110:1968–1976 © 2003 by the American Academy of Ophthalmology.*

subtle flat enlargement in 83%

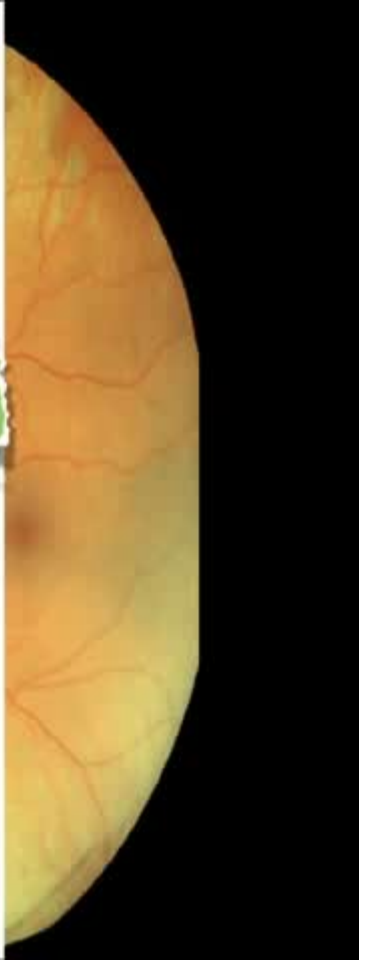

Solitary Congenital Hypertrophy of the Retinal Pigment Epithelium

Clinical Features and Frequency of Enlargement in 330 Patients

Carol L. Shields, MD, Arman Mashayekhi, MD, Thucanh Ho, MD, Jacqueline Cater, PhD, Jerry A. Shields, MD

Objective: To describe th
lium (CHRPE) and to determ
Design: Retrospective, c
Participants: Three hund
Main Outcome Measures: The 3 main outcome measures included flat lesion enlargement, intralesional lacunae enlargement, and development of an elevated nodule within the lesion. The clinical features at the time of presentation were analyzed
regressions.
Results: The most com
CHRPE (9%), and unspecifie
there were no patients with fa
was noted in 8% of patients, most commonly breast cancer (3%). The lesion most frequently was located inferotemporally (31%) and at the equatorial region (45%). Rarely, it was located in the macula (1%) or peripapillary region (1%). The median largest basal diameter was 4.5 mm, and the lesion was flat in all cases except in 5 (1.5%), in which there was an intralesional lesion nodule. The lesion was pigmented in 88% of cases and nonpigmented in 12%. Lacunae were noted in 43% of the pigmented CHRPE, and the lacunae showed gradual enlargement in 32%. Factors related to lacunae enlargement included number and relative size of lacunae. Flat enlargement of the lesion was documented in 46% of patients with comparative photographic follow-up and in 83% of those followed up for more than 3 years. The median rate of enlargement was 10 μm per month. The most important factor associated with flat lesion enlargement was relative size of the lacunae within CHRPE. There were no cases of CHRPE in which a nodule developed while the patient was being followed up. Of the 5 lesions that had a nodule, progressive enlargement of the nodule was found in 3.
Conclusions: Congenital hypertrophy of the retinal pigment epithelium generally has been regarded as a benign, stable lesion, but subtle, flat enlargement was noted in most patients (83%) followed up for 3 or more years using meticulous photographic comparison. Flat enlargement of the lesion appeared to be related to percentage of the mass occupied by lacunae. *Ophthalmology 2003;110:1968–1976 © 2003 by the American Academy of Ophthalmology.*

subtle flat enlargement in 83%

is this a low-grade neoplastic lesion

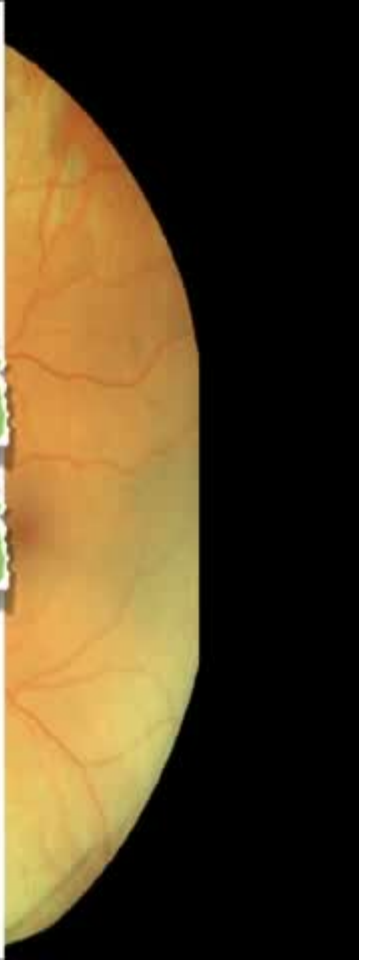

Solitary Congenital Hypertrophy of the Retinal Pigment Epithelium

Clinical Features and Frequency of Enlargement in 330 Patients

Carol L. Shields, MD, Arman Mashayekhi, MD, Thucanh Ho, MD, Jacqueline Cater, PhD, Jerry A. Shields, MD

Objective: To describe th
lium (CHRPE) and to determ
Design: Retrospective, c
Participants: Three hund
Main Outcome Measures: The 3 main outcome measures included flat lesion enlargement, intralesional lacunae enlargement, and development of an elevated nodule within the lesion. The clinical features at the time of presentation were analyzed
regressions.
Results: The most com
CHRPE (9%), and unspecifie
there were no patients with fa
was noted in 8% of patients, most commonly breast cancer (3%). The lesion most frequently was located inferotemporally (31%) and
peripapillary region (1%). Th
except in 5 (1.5%), in which th
and nonpigmented in 12%.
gradual enlargement in 32%
lacunae. Flat enlargement of the lesion was documented in 40% of patients with comparative photographic follow-up and in 83% of those followed up for more than 3 years. The median rate of enlargement was 10 μm per month. The most important factor associated with flat lesion enlargement was relative size of the lacunae within CHRPE. There were no cases of CHRPE in which a nodule developed while the patient was being followed up. Of the 5 lesions that had a nodule, progressive enlargement of the nodule was found in 3.
Conclusions: Congenital hypertrophy of the retinal pigment epithelium generally has been regarded as a benign, stable lesion, but subtle, flat enlargement was noted in most patients (83%) followed up for 3 or more years using meticulous photographic comparison. Flat enlargement of the lesion appeared to be related to percentage of the mass occupied by lacunae. *Ophthalmology 2003;110:1968–1976 © 2003 by the American Academy of Ophthalmology.*

subtle flat enlargement in 83%

is this a low-grade neoplastic lesion

adenoma development <1%

enlargement 8 years

increased lacunae 8 years

adenoma 2 years

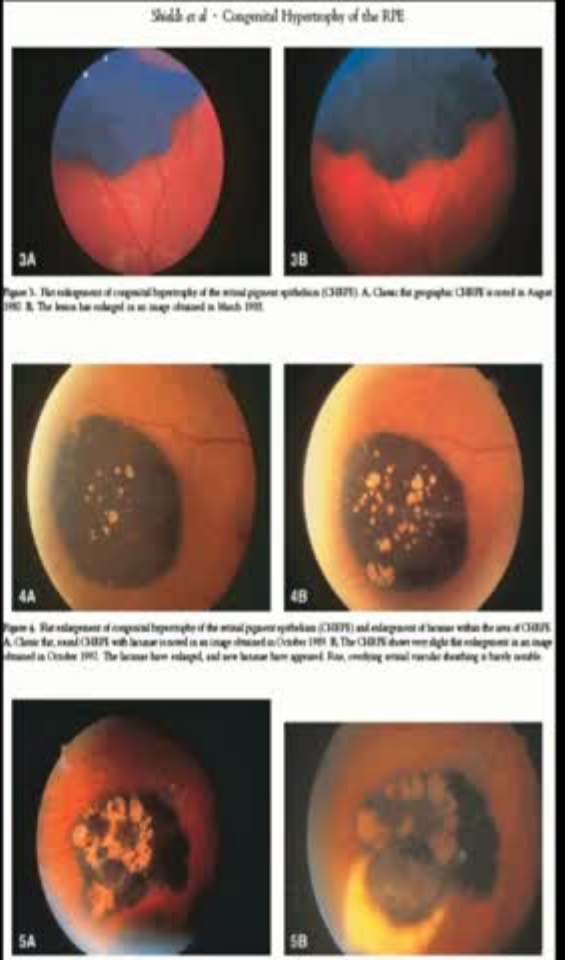

enlargement 8 years

increased lacunae 8 years

adenoma 2 years

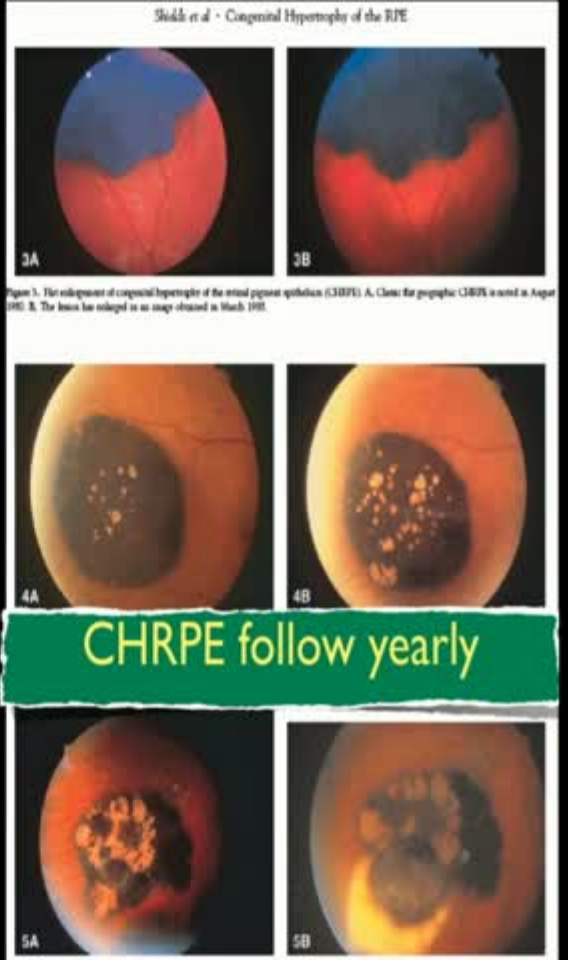

CHRPE follow yearly

Congenital Hypertrophy of the Retinal Pigment Epithelium

Enhanced-Depth Imaging Optical Coherence Tomography in 18 Cases

Adrian T. Fung, MBBS, MMed, Marco Pellegrini, MD, Carol L. Shields, MD

Objective: To describe the imaging characteristics of congenital hypertrophy of the retinal pigment epithelium (CHRPE).

Design: Retrospective, observational case series.

Participants: Eighteen eyes of 18 patients with CHRPE.

Methods: Review of chart, fundus photography, ultrasonography, fundus autofluorescence, infrared reflectance (IR) imaging, and enhanced-depth imaging optical coherence tomography (EDI-OCT).

Main Outcome Measures: Features of CHRPE as analyzed by EDI-OCT.

Results: The mean age at diagnosis was 48 years (range, 13–73 years). There were 5 males and 13 females, and 17 Caucasian and 1 African American patients. The mean best-corrected visual acuity was 20/22 (range, 20/20–20/40). The CHRPE was located in the retinal periphery (n = 16) with intralesional lacunae (n = 14) and surrounding nonpigmented (n = 4) and pigmented (n = 14) halo. By ultrasonography, the mean CHRPE thickness was 1.0 mm (range, 0.9–1.4 mm). Fundus autofluorescence disclosed hypoautofluorescence (n = 18) with lacunae (n = 14) showing isoautofluorescence (n = 10) or hypoautofluorescence (n = 4). Infrared reflectance imaging displayed hyporeflectivity in the area of pigmentation (n = 16) and hyperreflectivity within lacunae (n = 14). On EDI-OCT, all 18 lesions were flat with a mean basal diameter of 4529 μm (median, 3707 μm; range, 697–11617 μm). The mean central sublesional choroidal thickness (126.4 μm) was not different compared with thickness 50 μm outside the margin (126.8 μm; $P = 0.99$). The retinal pigment epithelium (RPE) was absent (n = 2), thickened (n = 16), or irregular (n = 15). Of 9 lesions in which lacunae were imaged, 8 showed absent RPE. The overlying retinal findings included thinning or absence of the outer retina beginning at the ganglion cell layer (n = 1), outer plexiform layer (n = 4), outer nuclear layer (n = 12), or inner segment/outer segment junction (n = 1). Additional retinal findings included hyperreflective spots (n = 11), cystoid edema (n = 5), and subretinal cleft (n = 6). Subretinal cleft specifically occurred at the site of absent photoreceptors.

Conclusions: Generally, CHRPE displays hypoautofluorescence and hyporeflectivity with hyperreflective lacunae on IR imaging. On EDI-OCT, CHRPE seems flat with thickened, irregular RPE and absent RPE within lacunae. A prominent feature is outer retinal loss, generally involving the outer nuclear layer to photoreceptors, occasionally with a characteristic subretinal cleft. *Ophthalmology 2014;121:251-256*

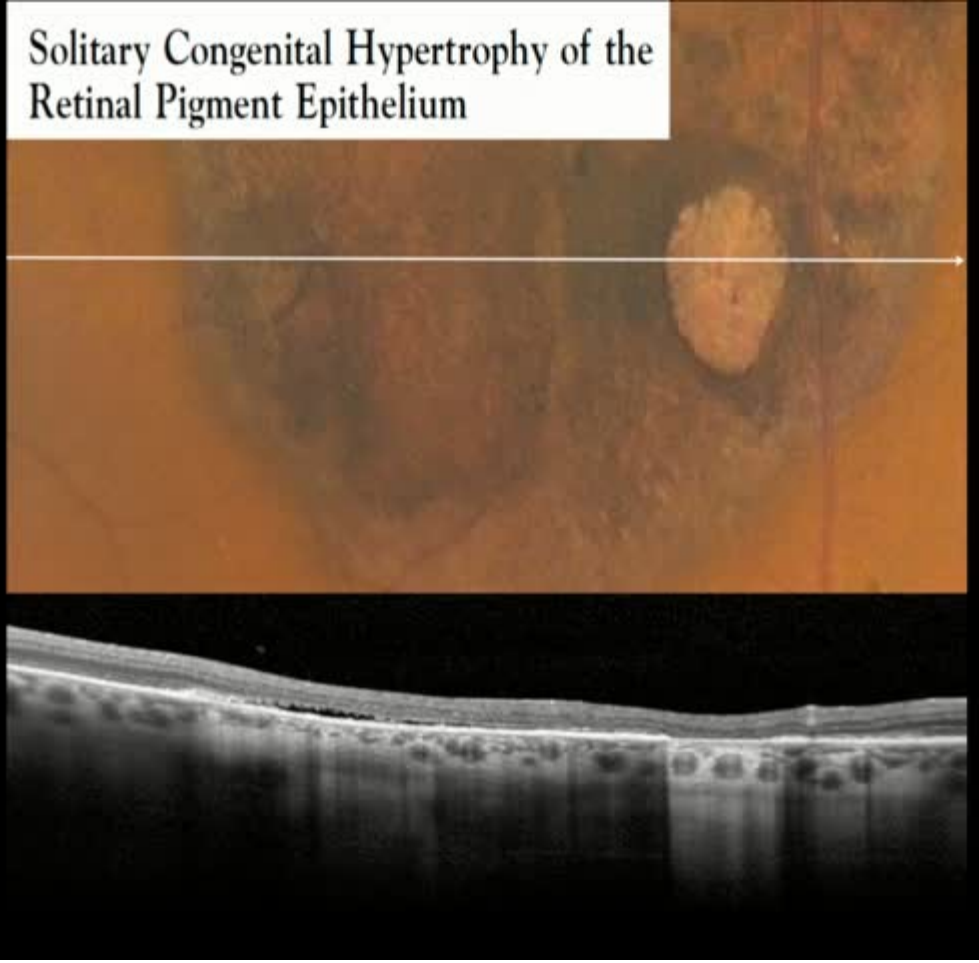
Solitary Congenital Hypertrophy of the
Retinal Pigment Epithelium

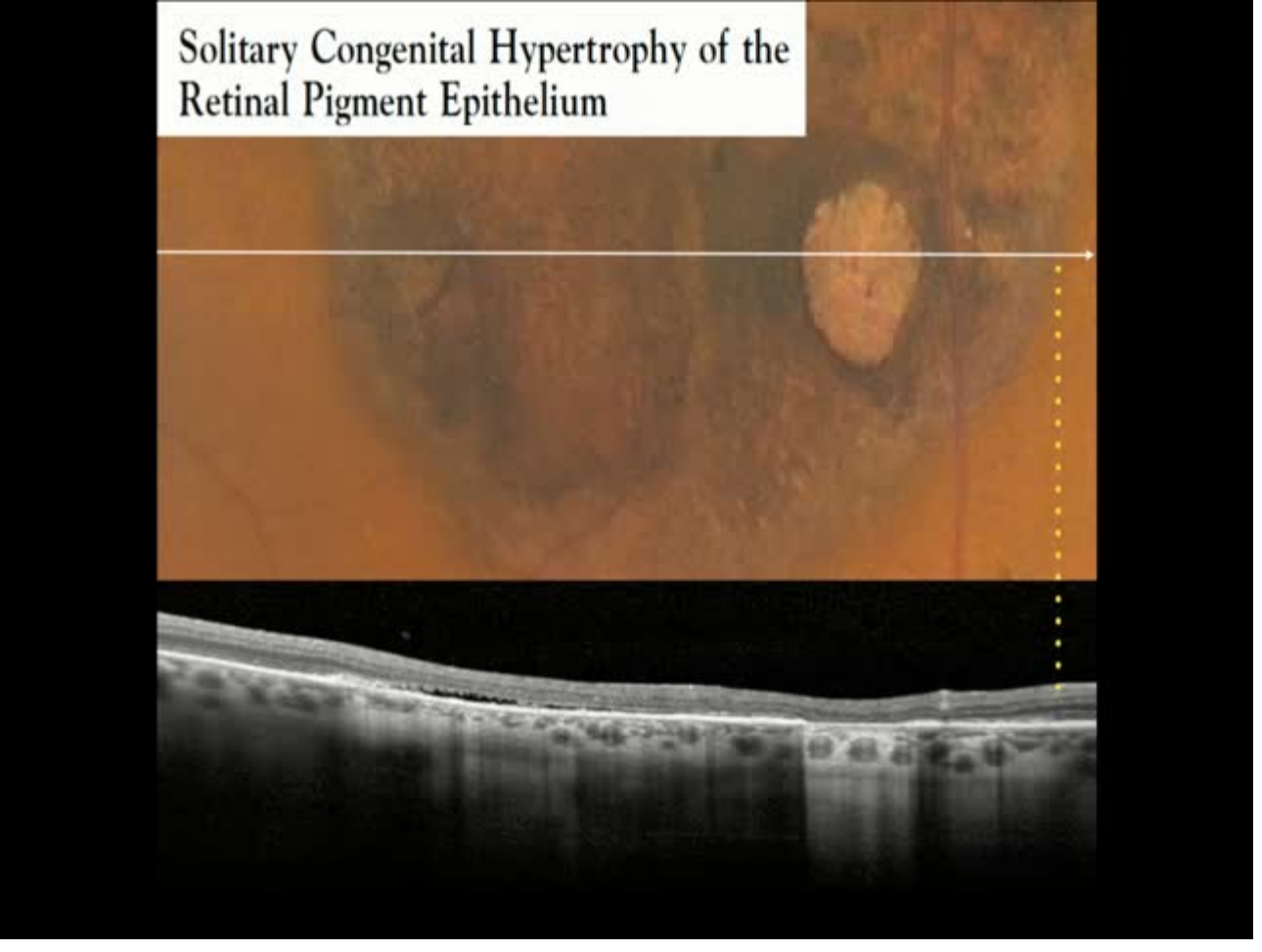
Solitary Congenital Hypertrophy of the
Retinal Pigment Epithelium

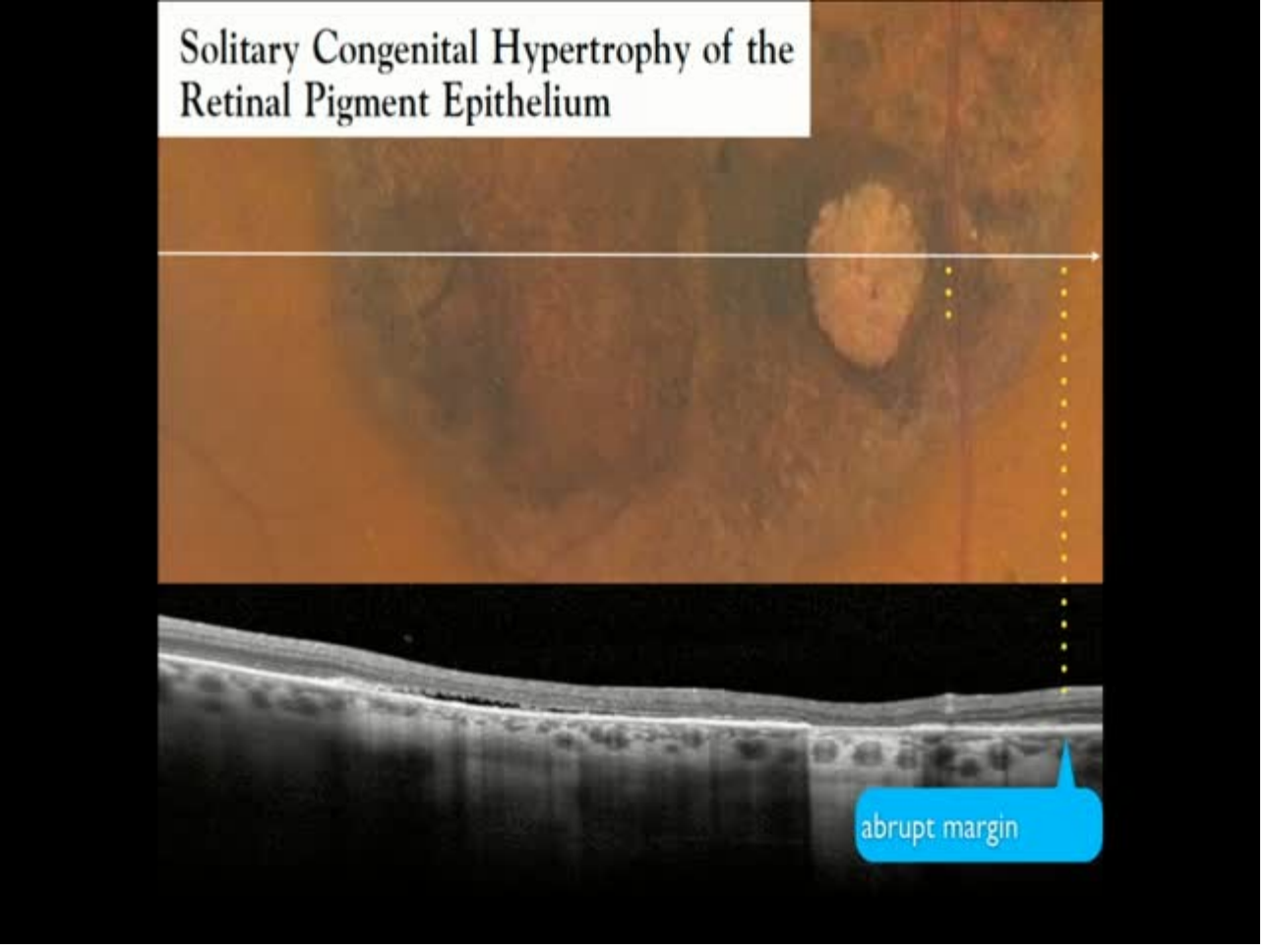
Solitary Congenital Hypertrophy of the Retinal Pigment Epithelium
abrupt margin


ABC
HELP
SWAG
WIN

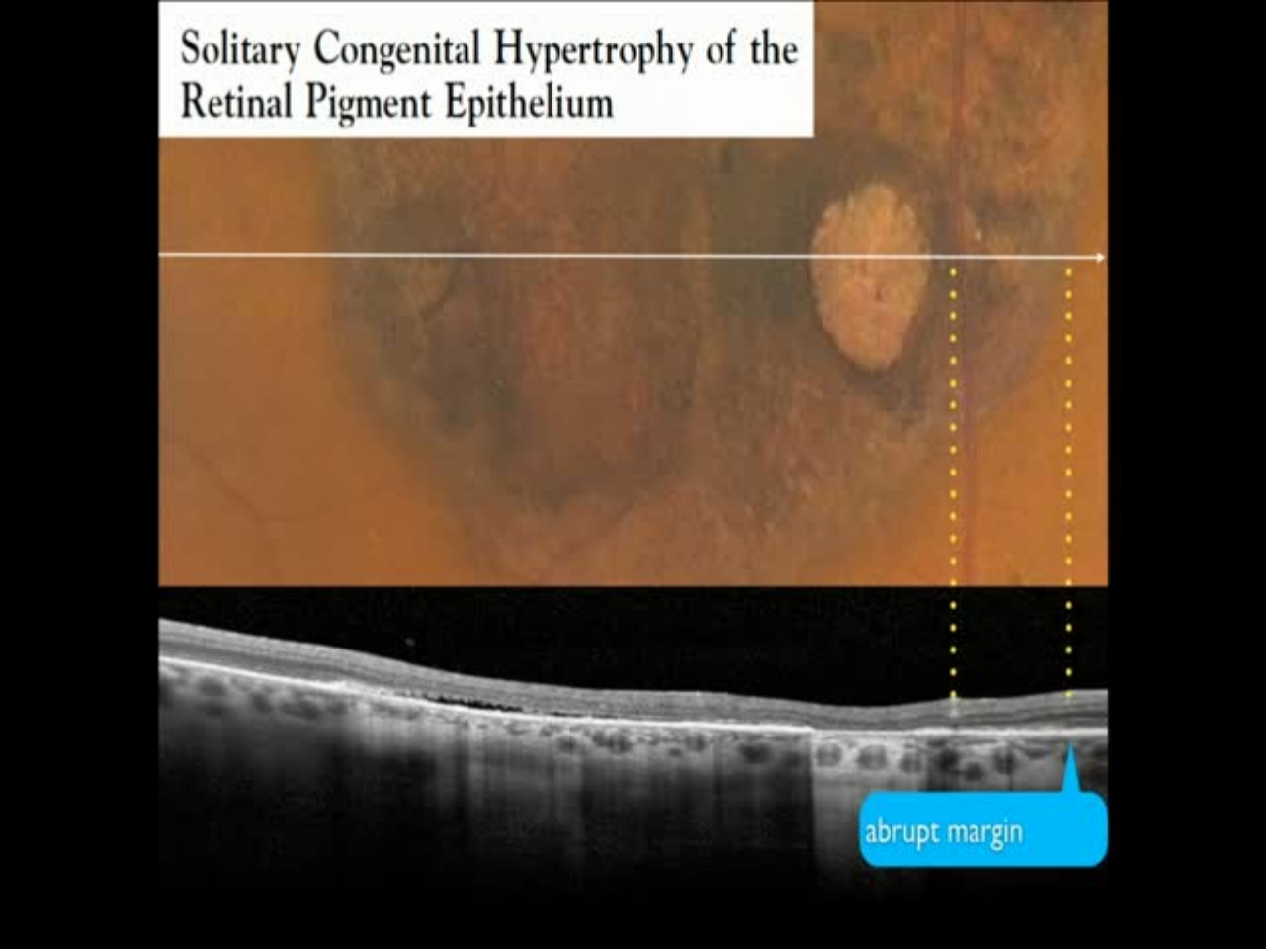
Solitary Congenital Hypertrophy of the Retinal Pigment Epithelium
abrupt margin

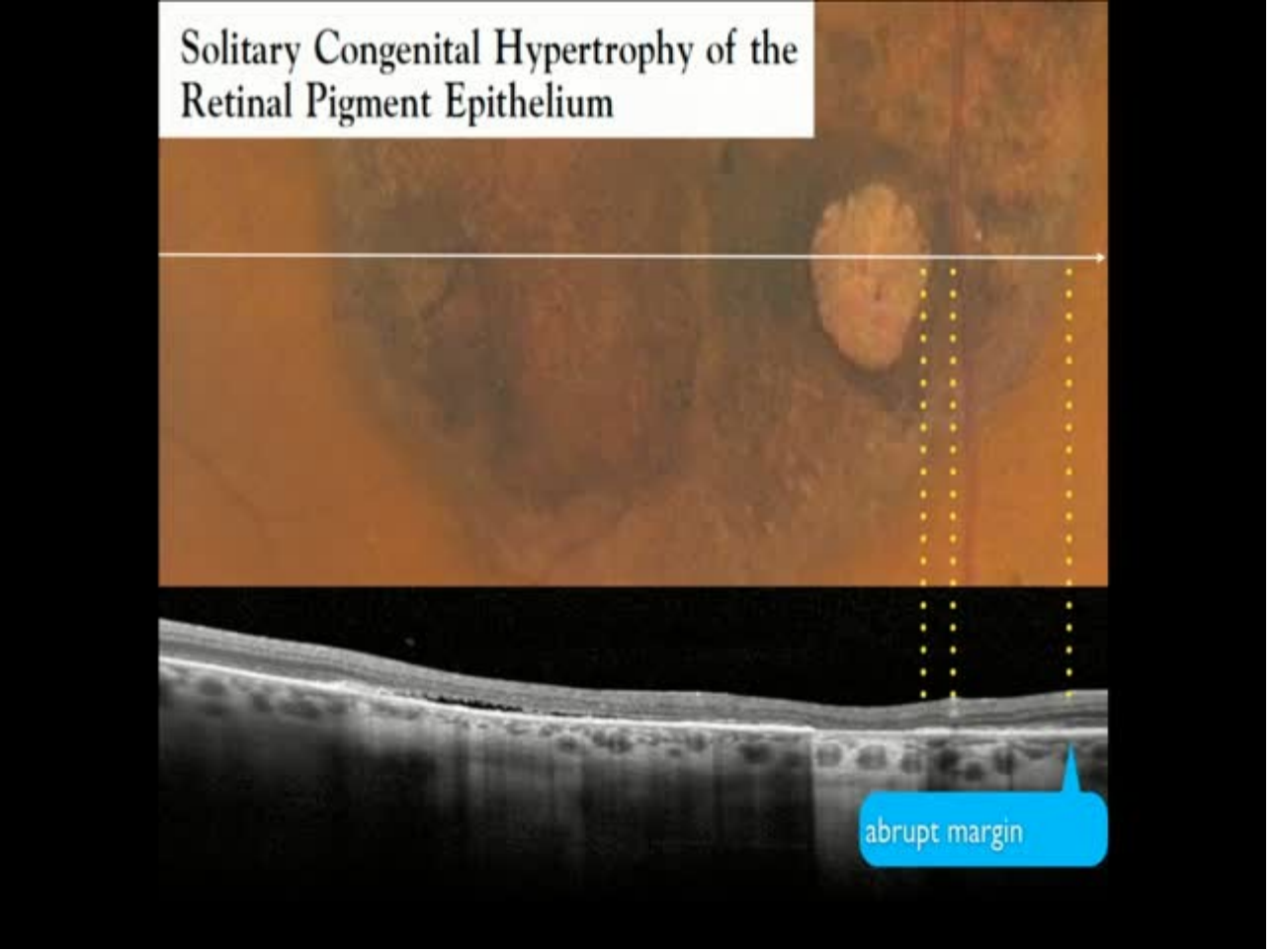
Solitary Congenital Hypertrophy of the Retinal Pigment Epithelium
abrupt margin

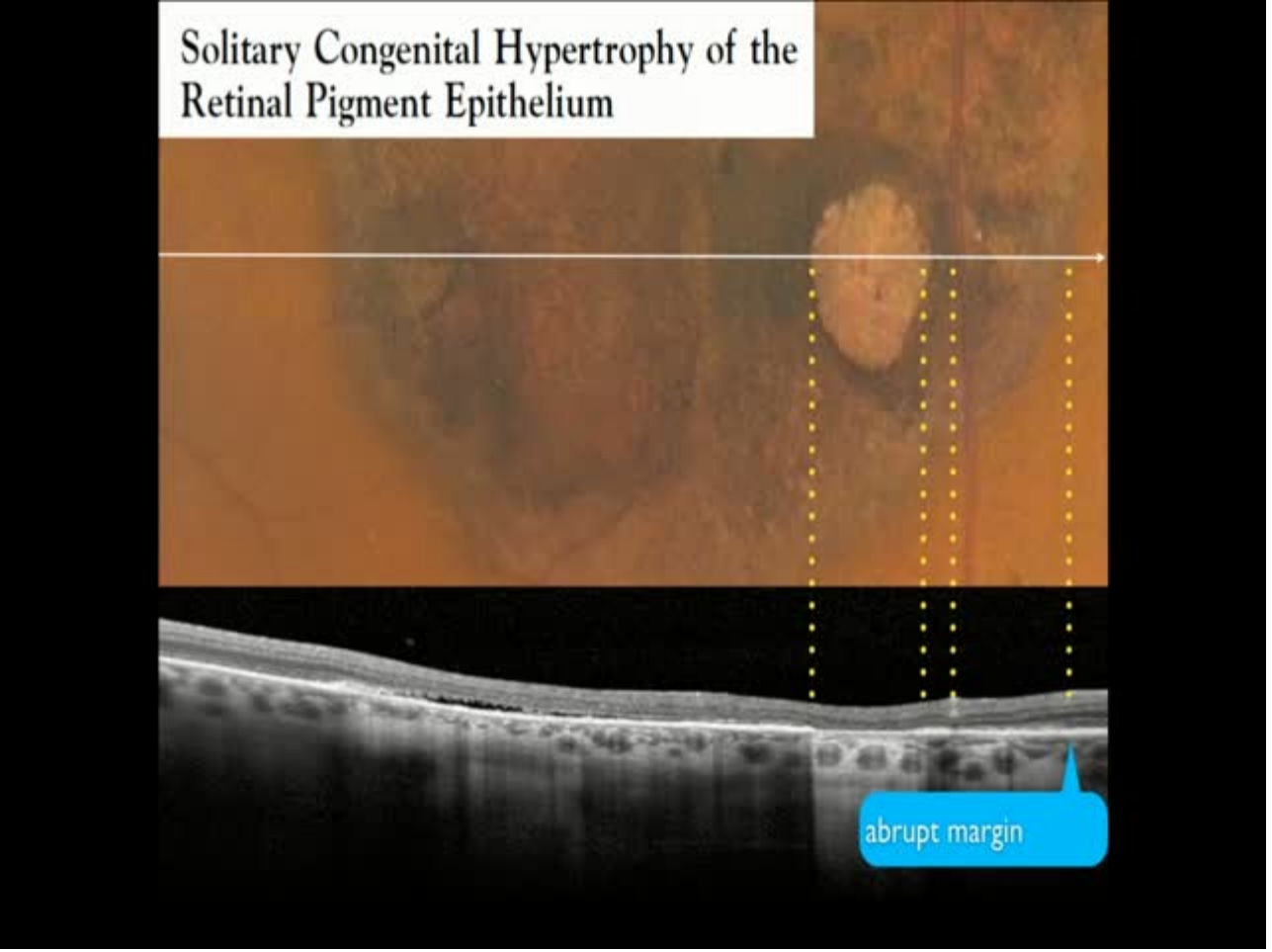
Solitary Congenital Hypertrophy of the Retinal Pigment Epithelium
abrupt margin

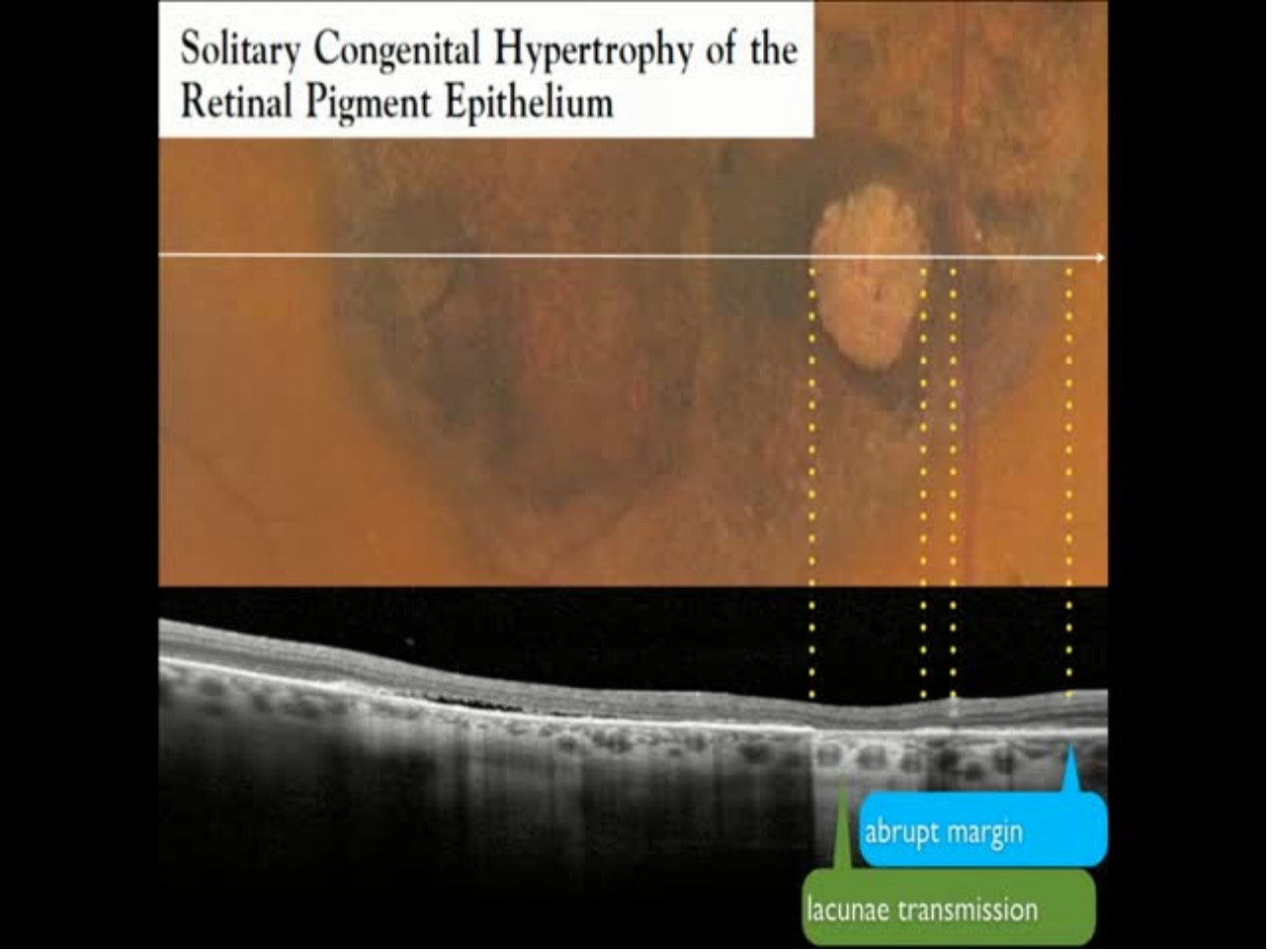
Solitary Congenital Hypertrophy of the Retinal Pigment Epithelium
abrupt margin
lacunae transmission

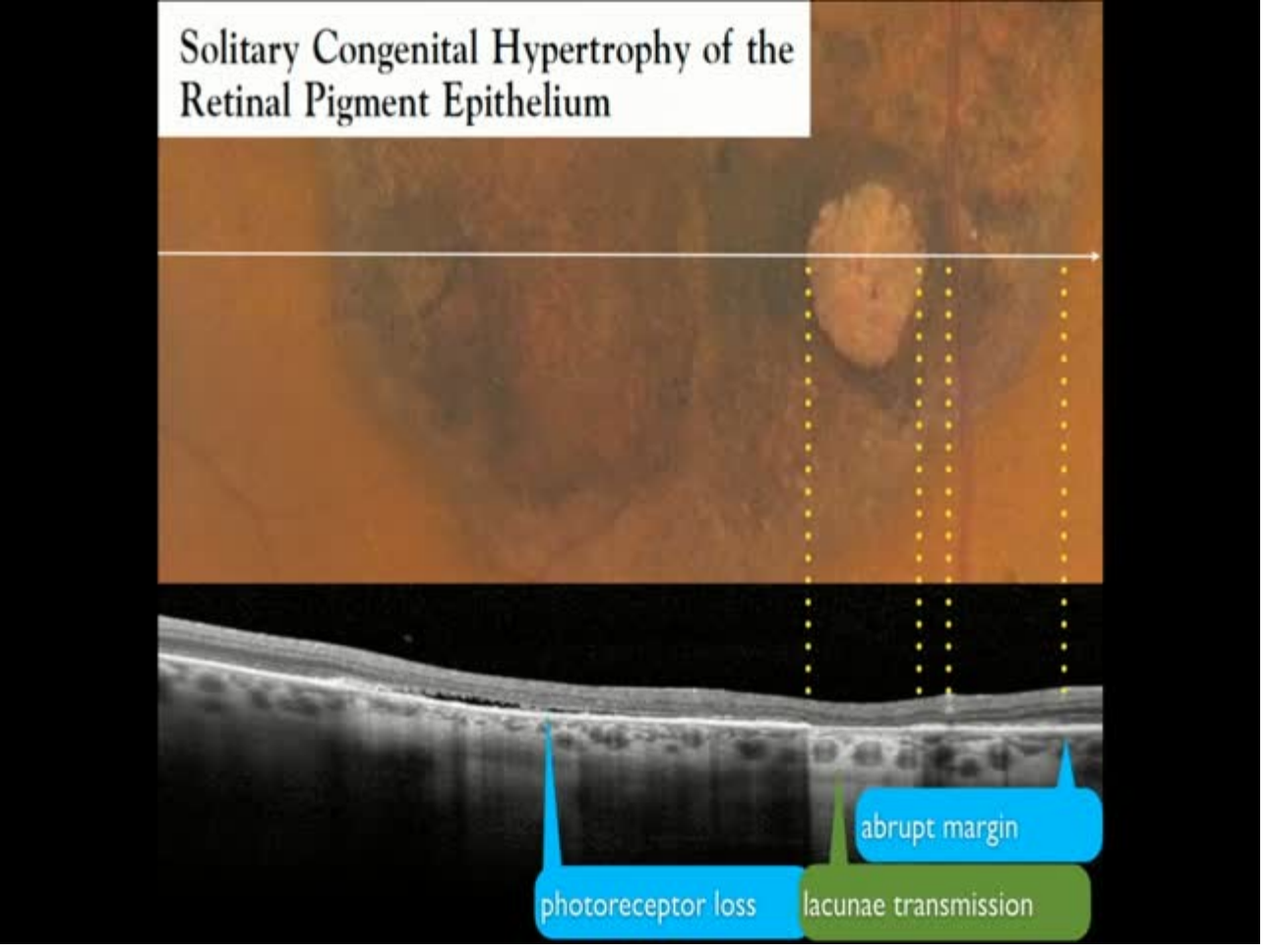
Solitary Congenital Hypertrophy of the Retinal Pigment Epithelium
abrupt margin
photoreceptor loss
lacunae transmission

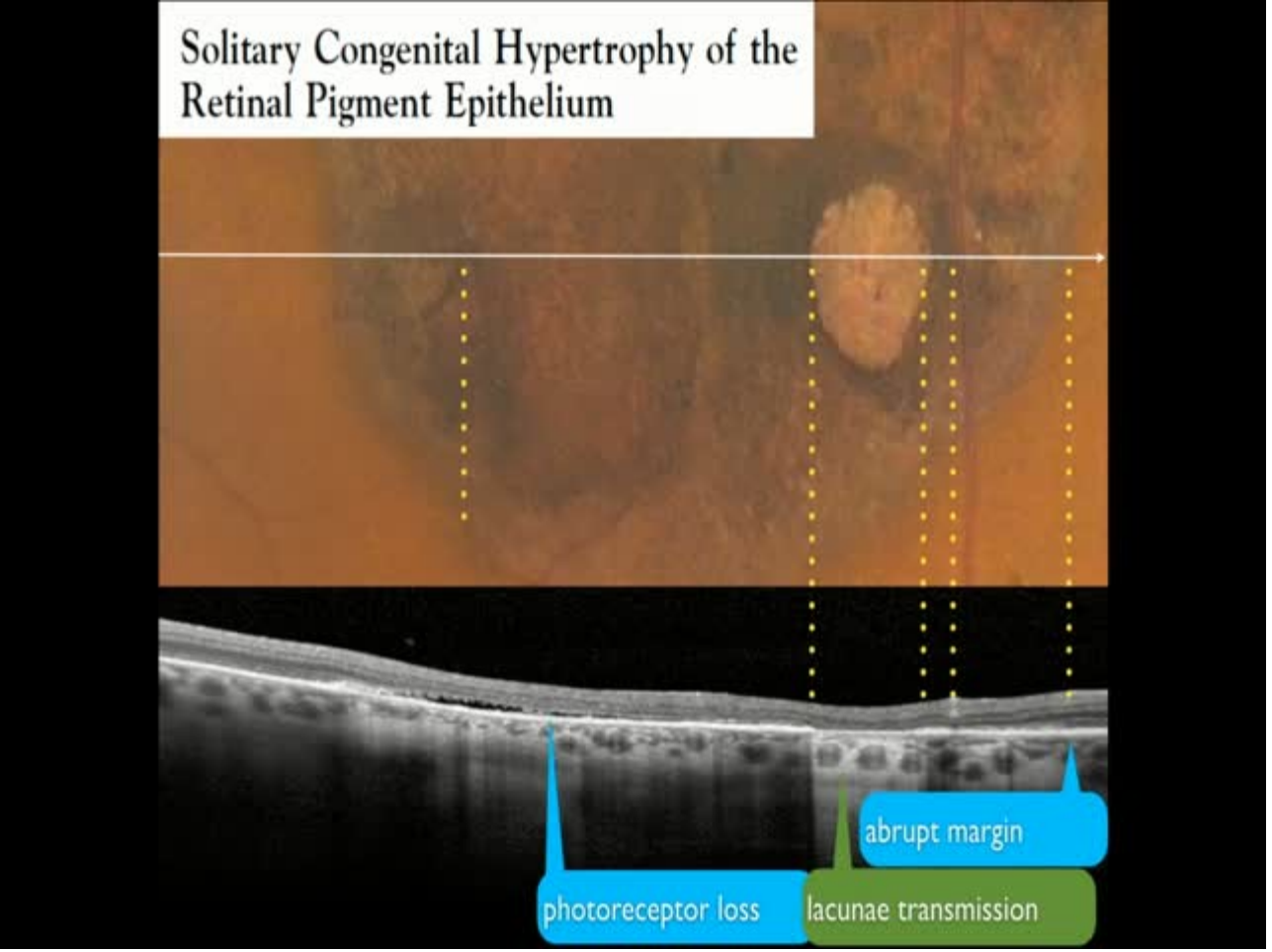
Solitary Congenital Hypertrophy of the Retinal Pigment Epithelium
abrupt margin
photoreceptor loss
lacunae transmission

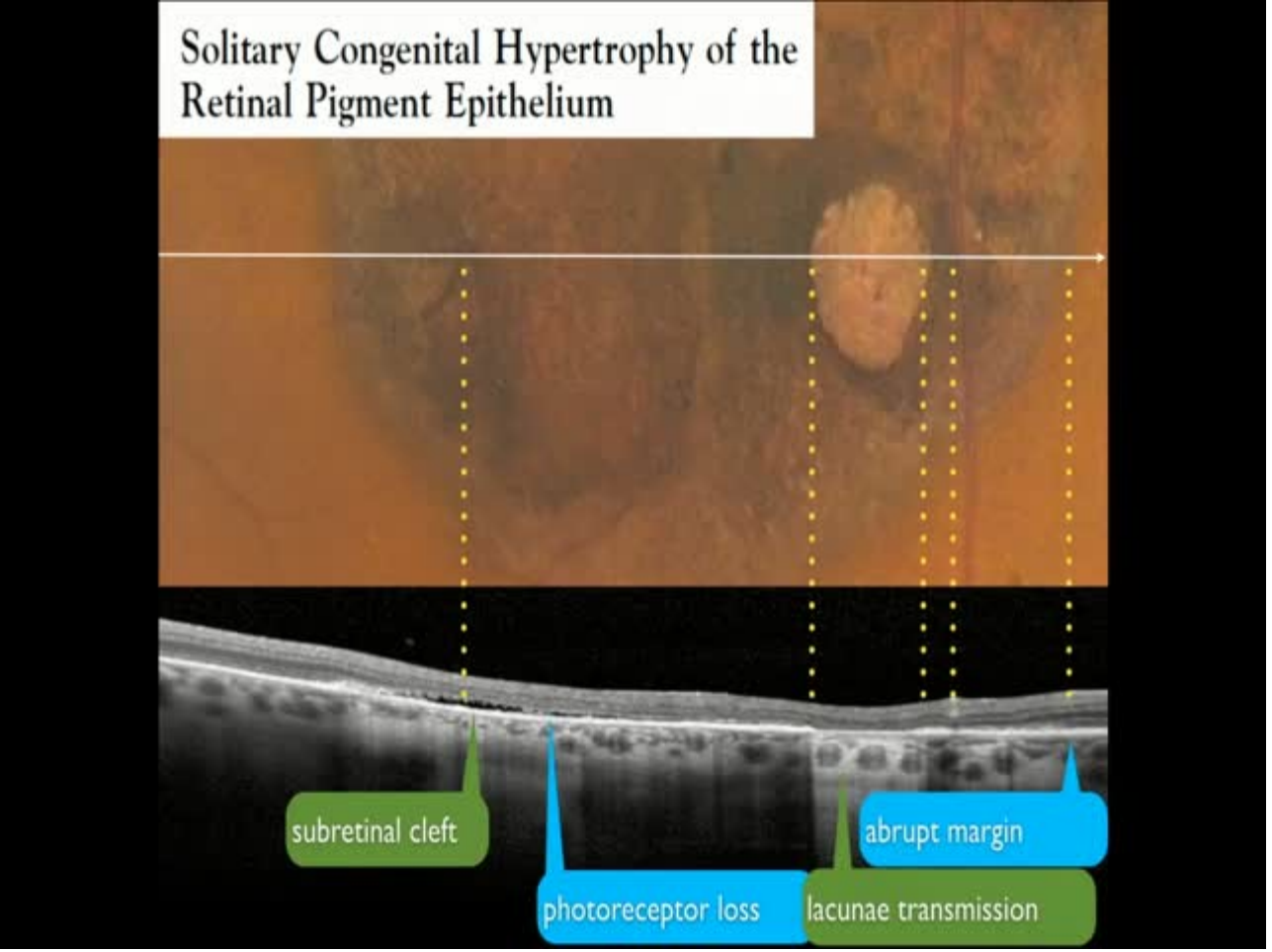
Solitary Congenital Hypertrophy of the Retinal Pigment Epithelium
subretinal cleft
photoreceptor loss
lacunae transmission
abrupt margin

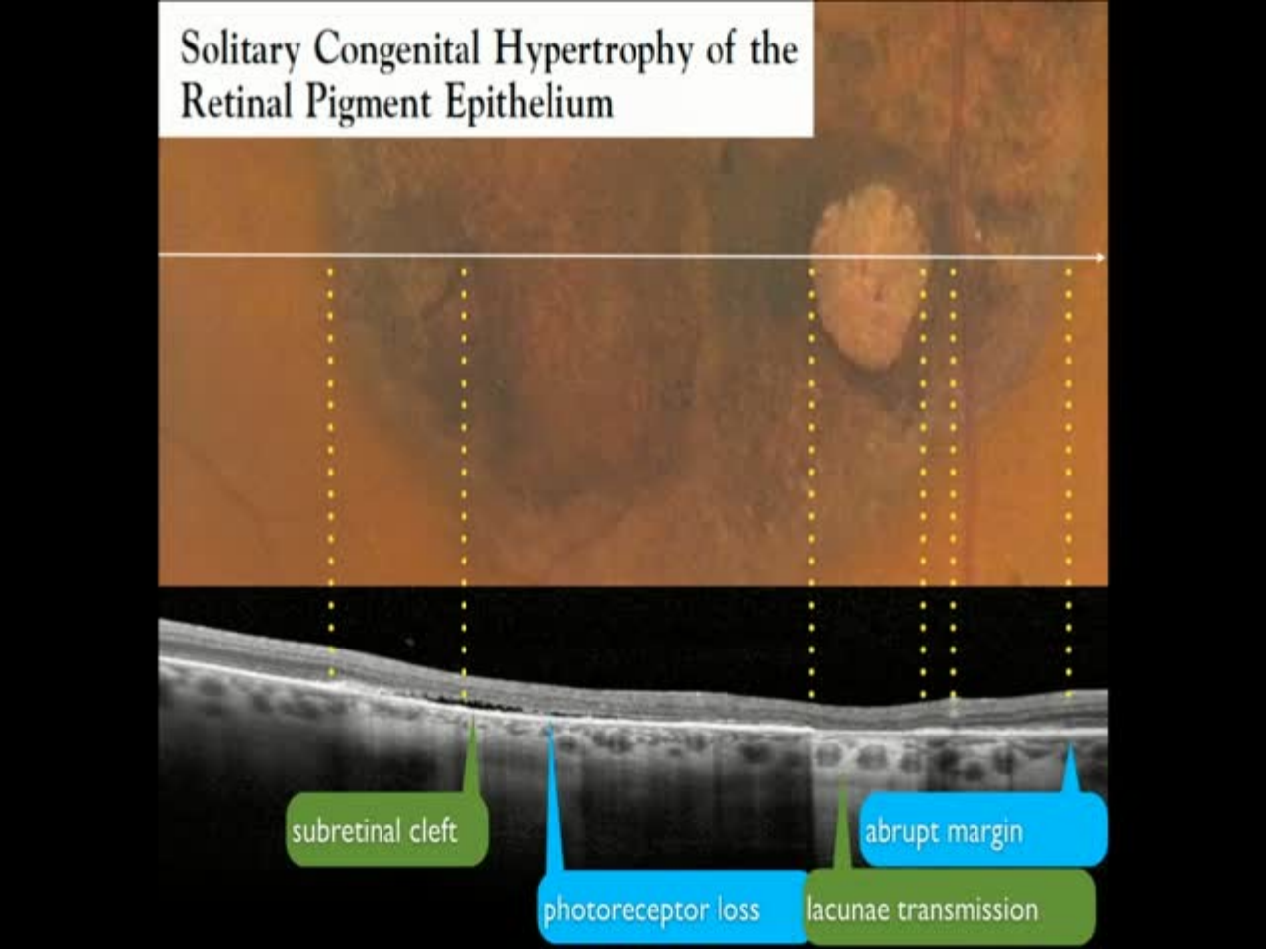
Solitary Congenital Hypertrophy of the Retinal Pigment Epithelium
subretinal cleft
photoreceptor loss
lacunae transmission
abrupt margin

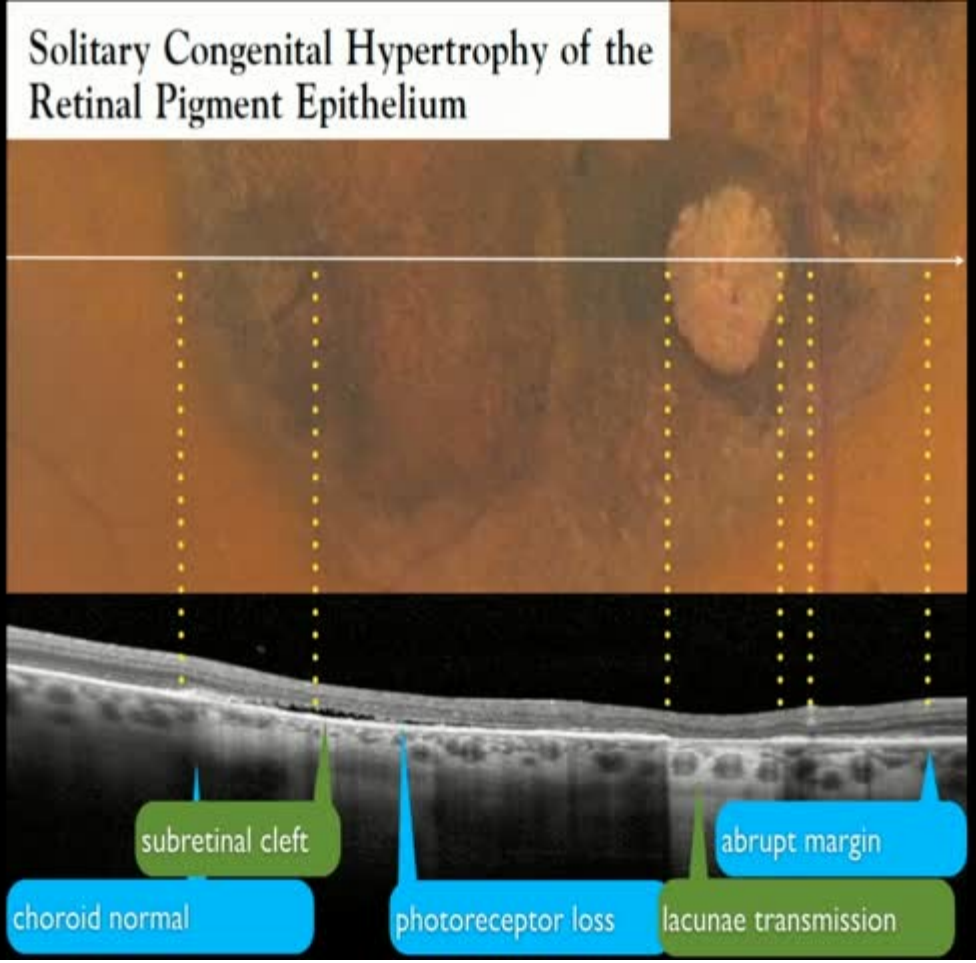
Solitary Congenital Hypertrophy of the Retinal Pigment Epithelium
subretinal cleft
abrupt margin
choroid normal
photoreceptor loss
lacunae transmission

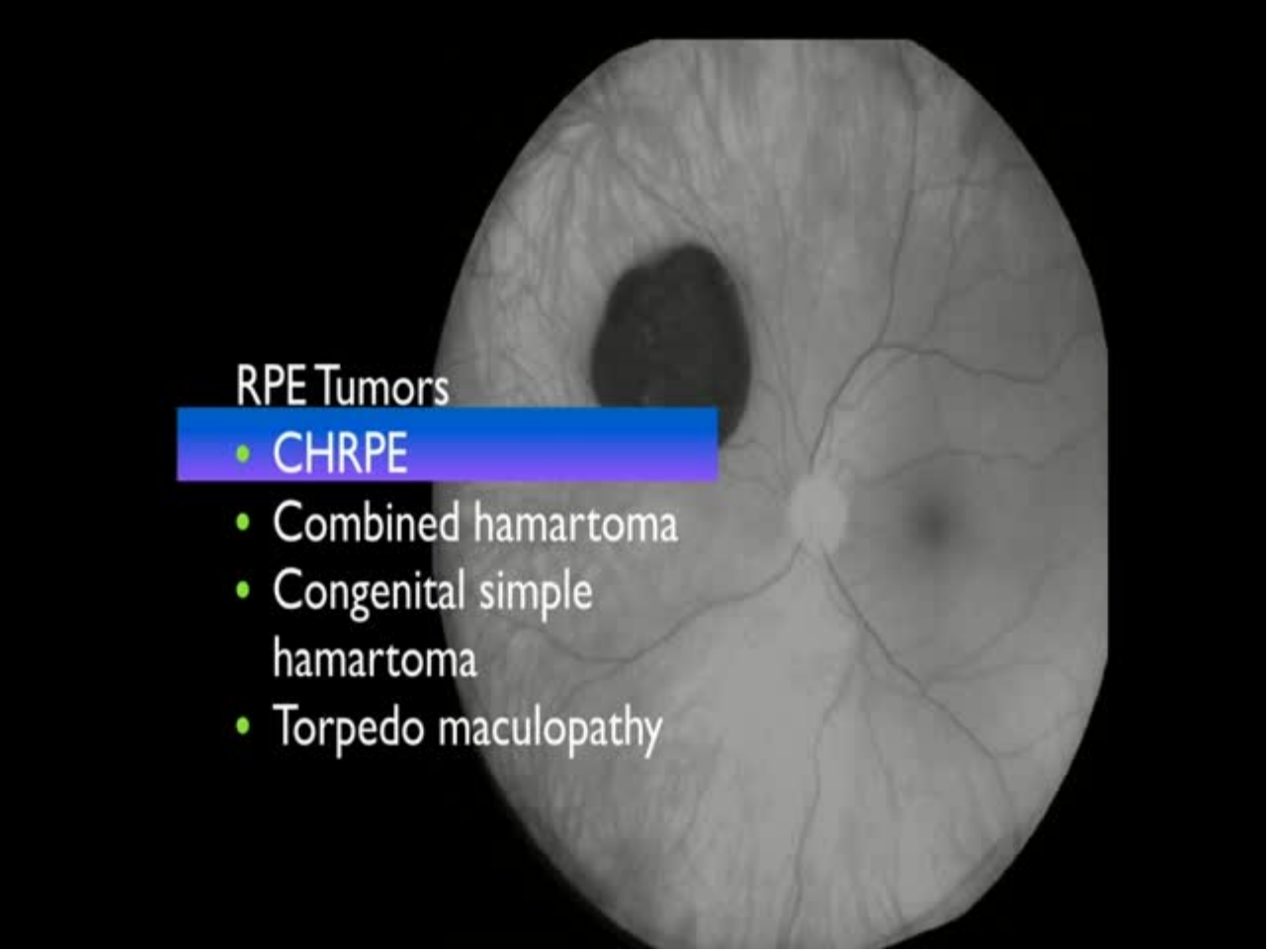
RPE Tumors
• CHRPE
• Combined hamartoma
• Congenital simple hamartoma
• Torpedo maculopathy


ABCDEFGHIJKLMNOPQRSTUVWXYZ
ABCDEFGHIJKLMNOPQRSTUVWXYZ
ABCDEFGHIJKLMNOPQRSTUVWXYZ
ABCDEFGHIJKLMNOPQRSTUVWXYZ
ABCDEFGHIJKLMNOPQRSTUVWXYZ
ABCDEFGHIJKLMNOPQRSTUVWXYZ
ABCDEFGHIJKLMNOPQRSTUVWXYZ
ABCDEFGHIJKLMNOPQRSTUVWXYZ
ABCDEFGHIJKLMNOPQRSTUVWXYZ
ABCDEFGHIJKLMNOPQRSTUVWXYZ
ABCDEFGHIJKLMNOPQRSTUVWXYZ
ABCDEFGHIJKLMNOPQRSTUVWXYZ
ABCDEFGHIJKLMNOPQRSTUVWXYZ

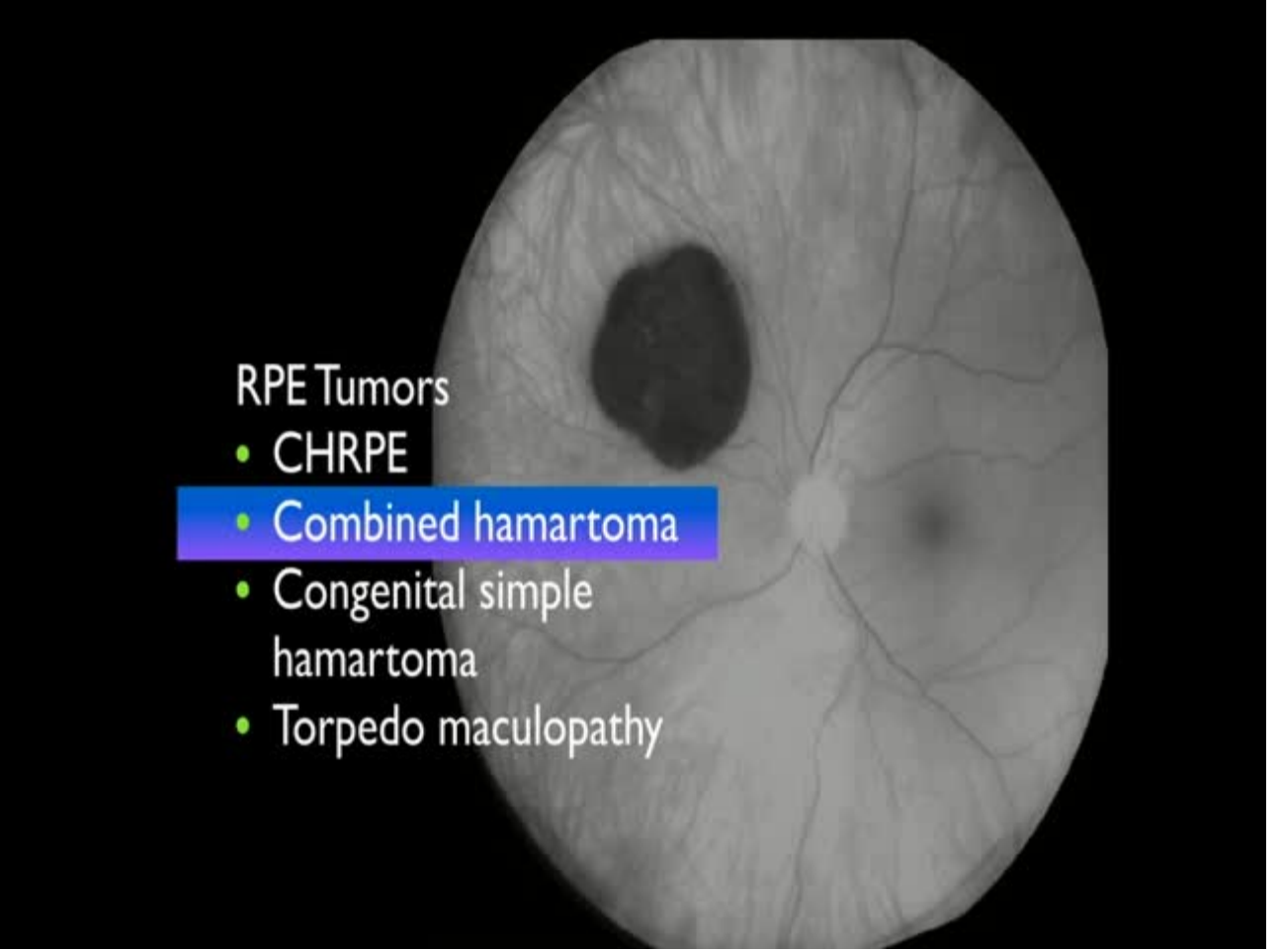
RPE Tumors
• CHRPE
• Combined hamartoma
• Congenital simple hamartoma
• Torpedo maculopathy

COMBINED HAMARTOMA OF THE RETINA AND RETINAL PIGMENT EPITHELIUM

Findings on Enhanced Depth Imaging Optical Coherence Tomography in Eight Eyes

SRUTHI AREPALLI, MD, MARCO PELLEGRINI, MD, SANDOR R. FERENCZY, CRA, OCT-C, CAROL L. SHIELDS, MD

Purpose: To assess combined hamartoma of the retina and retinal pigment epithelium with enhanced depth imaging optical coherence tomography.

Methods: Retrospective, observational cases series in eight eyes of eight patients, with comparison between affected and unaffected eyes regarding enhanced depth imaging optical coherence tomography features of tumor, fovea, and choroid.

Results: The mean age at presentation was 7 years. The tumor was macular (n = 5) or extramacular (n = 3). Enhanced depth imaging optical coherence tomography revealed irregularities in inner retina (n = 8) and/or all retinal layers (n = 3), with epiretinal membrane (n = 8), causing an inner retinal sawtooth (mini-peak) pattern (n = 2), full thickness retinal folds (maxi-peak) (n = 3), or both (n = 3). In the 5 macular tumors, foveal retinal thickness measured mean 608 μm compared with 244 μm in the unaffected eye ($P = 0.0004$). Mean tumor epicenter retinal thickness in 8 tumors measured 650 μm compared with 327 μm in a corresponding area in the unaffected eye ($P = 0.01$). In all cases, choroidal thickness beneath the tumor epicenter was decreased at mean 210 μm compared with 328 μm in the corresponding area of unaffected eye ($P = 0.009$).

Conclusion: Enhanced depth imaging optical coherence tomography of combined hamartoma revealed epiretinal membrane with vitreoretinal traction in a sawtooth (mini-peak) or folded (maxi-peak) pattern. Combined hamartoma seems to be a thickened retinal mass secondary to focal vitreoretinal traction.

RETINA 0:1–6, 2014

COMBINED HAMARTOMA OF THE RETINA AND RETINAL PIGMENT EPITHELIUM

Findings on Enhanced Depth Imaging Optical Coherence Tomography in Eight Eyes

SRUTHI AREPALLI, MD, MARCO PELLEGRINI, MD, SANDOR R. FERENCZY, CRA, OCT-C, CAROL L. SHIELDS, MD

Purpose: To assess comb
with enhanced depth imagin
Methods: Retrospective, c
comparison between affecte
optical coherence tomograp
Results: The mean age at
extramacular (n = 3). Enhan
irregularities in inner retina (n
(n = 8), causing an inner ret
folds (maxi-peak) (n = 3), or
measured mean 608 μm cor
tumor epicenter retinal thickr
a corresponding area in the
beneath the tumor epicenter was decreased at mean 210 μm compared with 328 μm in the corresponding area of unaffected eye (P = 0.009).
Conclusion: Enhanced depth imaging optical coherence tomography of combined hamartoma revealed epiretinal membrane with vitreoretinal traction in a sawtooth (mini-peak) or folded (maxi-peak) pattern. Combined hamartoma seems to be a thickened retinal mass secondary to focal vitreoretinal traction.

RETINA 0:1–6, 2014

Associated with
NF2
Brachiocephalic cleft
Potters syndrome

Retina RPE Combined Hamartoma

Like a mountain mini peak
maxi peak

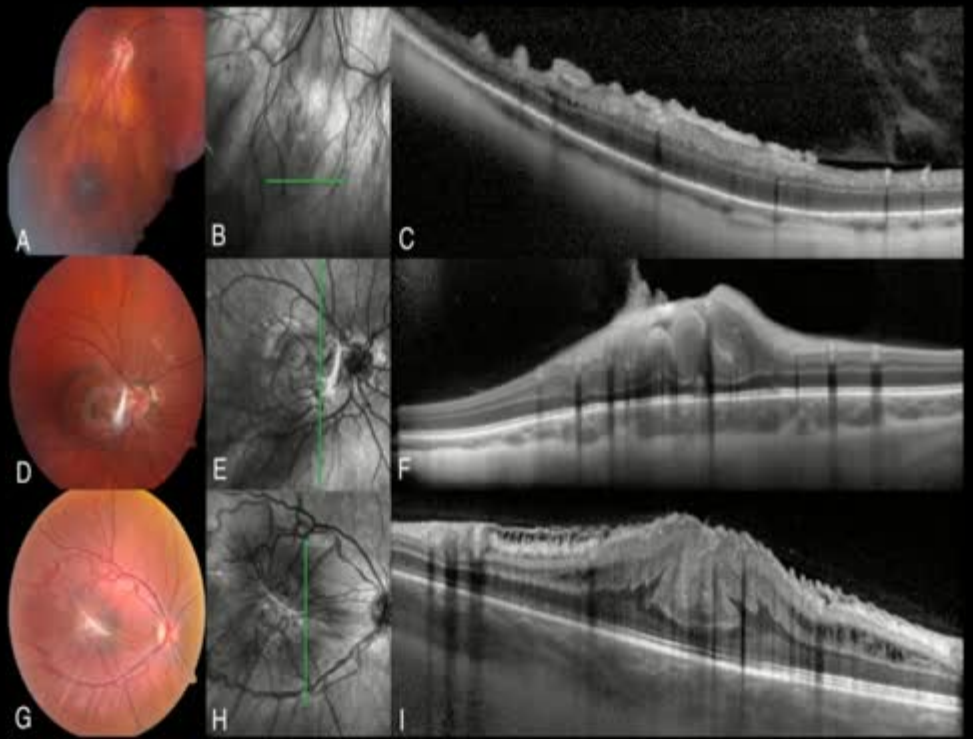

Retina RPE Combined Hamartoma

Like a mountain

maxi peak

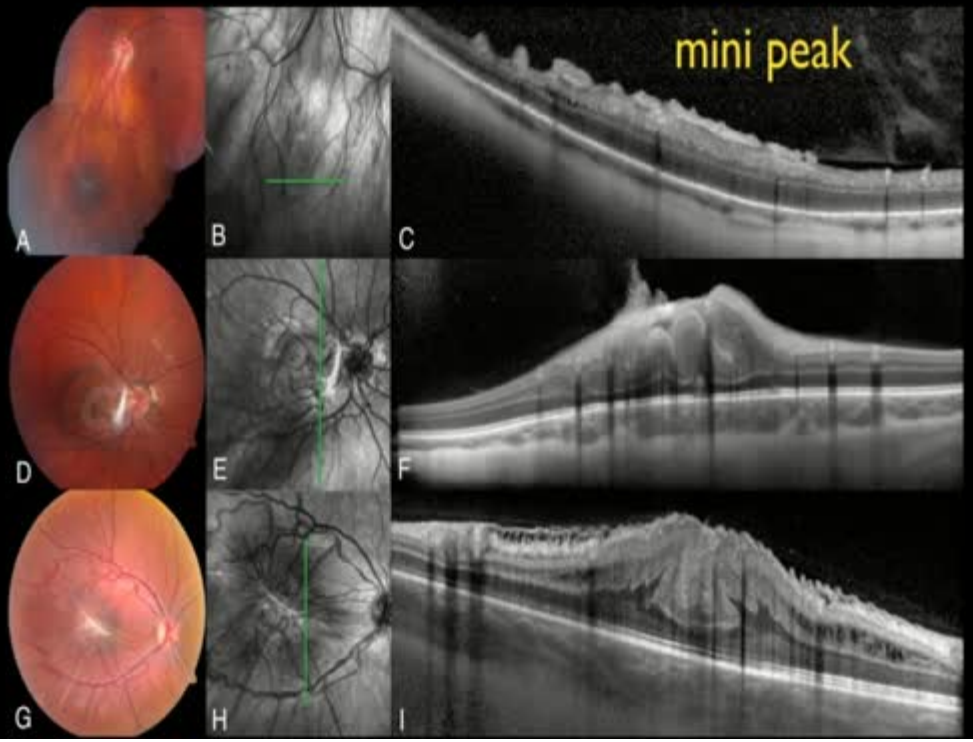

Retina RPE Combined Hamartoma

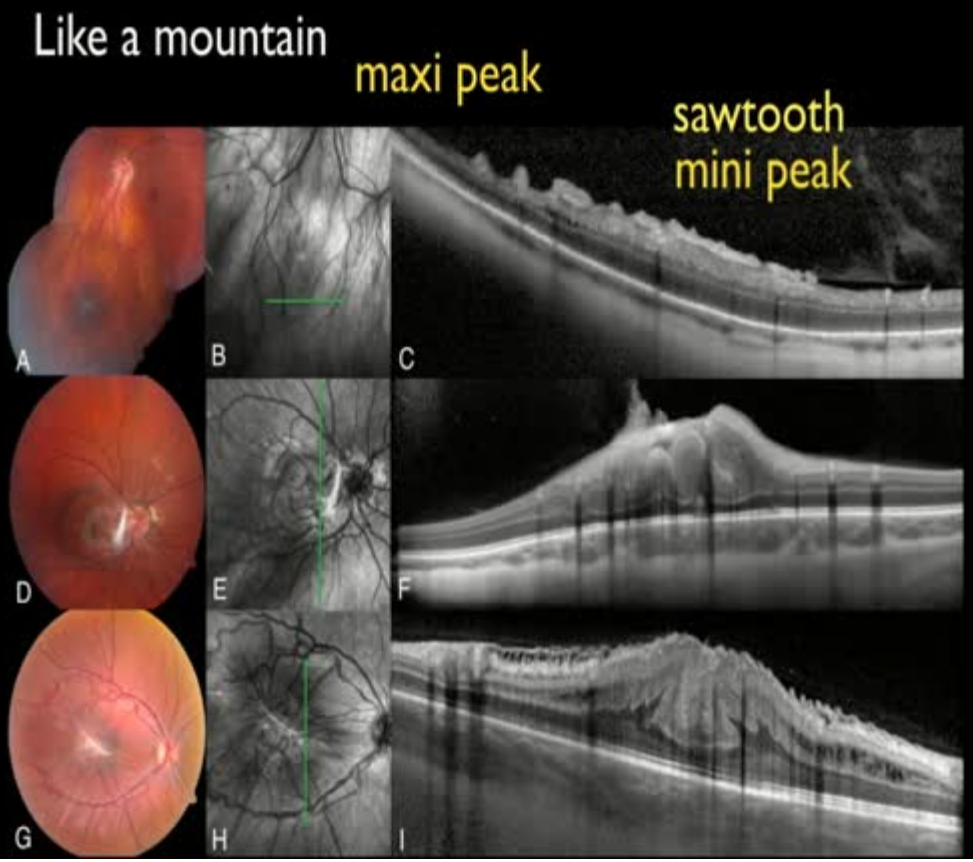

Retina RPE Combined Hamartoma

Like a mountain

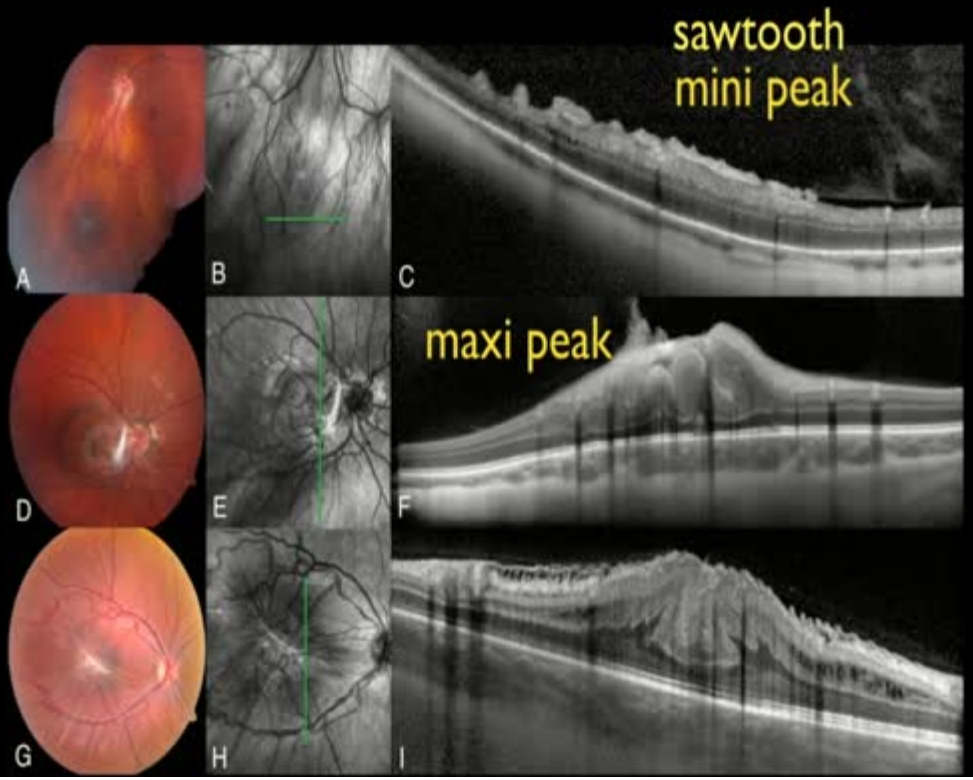

Retina RPE Combined Hamartoma

Like a mountain

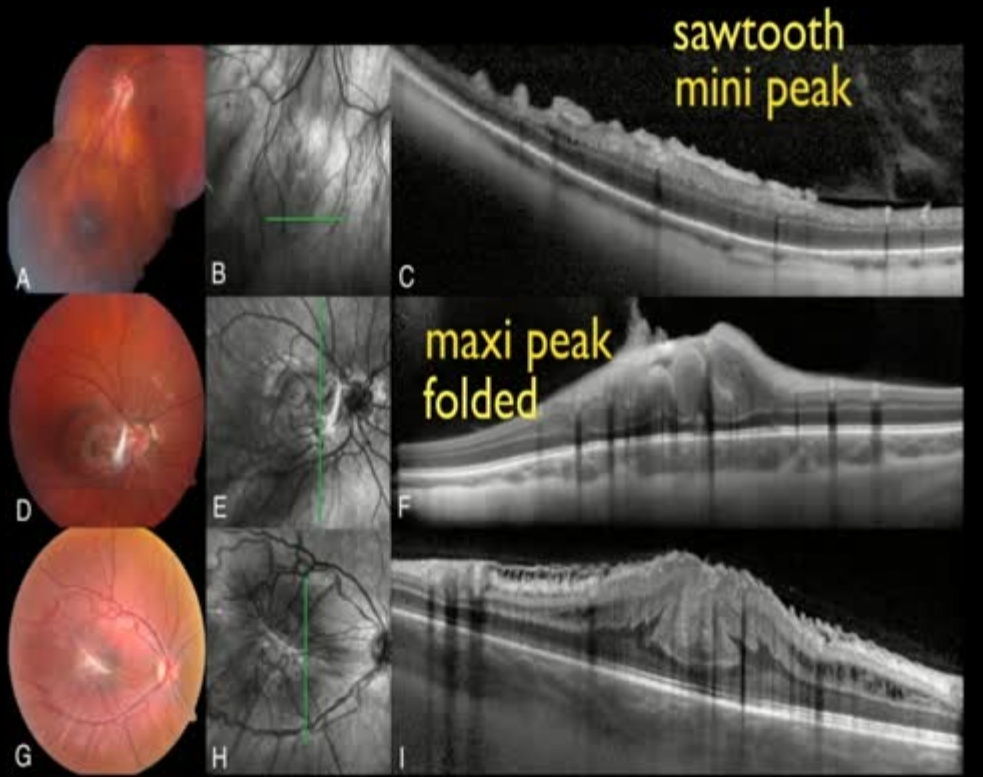

Retina RPE Combined Hamartoma

Like a mountain

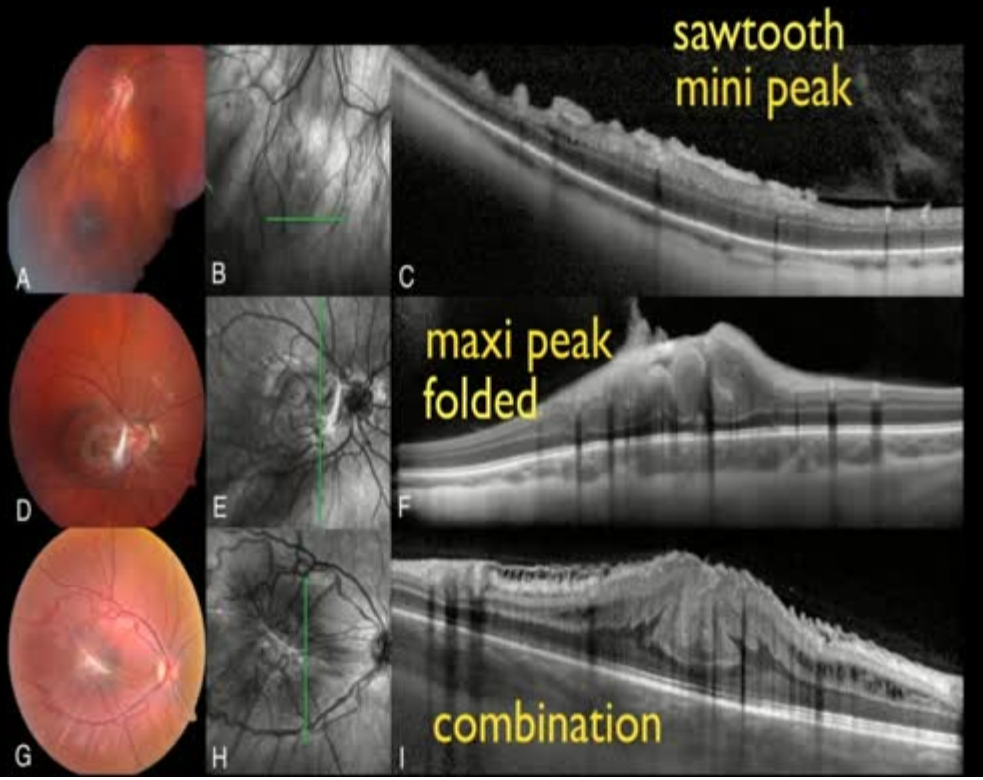

EPIRETINAL MEMBRANES INDICATE A SEVERE PHENOTYPE OF NEUROFIBROMATOSIS TYPE 2

ROBERT A. SISK, MD,* AUDINA M. BERROCAL, MD,*
AMY C. SCHEFLER, MD,* SANDER R. DUBOVY, MD,*
MISLEN S. BAUER, MD, FACMG†

Purpose: The purpose of this study was to describe a subset of severely affected patients with neurofibromatosis type 2 (NF2), multiple central nervous system tumors, and characteristic retinal lesions.

Methods: This is a retrospective observational case series of 4 patients with NF2. The time domain-optical coherence tomography findings of three patients have previously been described in another series.

Results: Ophthalmic signs were identified at a mean age of 6 years, and NF2 was diagnosed at a mean age of 11 years. Patients presented with diminished visual acuity in one or both eyes and epiretinal membranes in the absence of posterior vitreous detachment. The biomicroscopic and optical coherence tomography features were distinct from secondary epiretinal membranes or combined hamartomas of the retina and retinal pigment epithelium and pathognomonic for NF2. The ophthalmic manifestations were recognized before neurologic signs and led to the diagnosis of NF2 in 3 of the 4 patients. Each patient had ≥2 central nervous system tumors at the time of diagnosis, and 3 of 4 eventually required neurosurgical interventions for symptomatic, compressive lesions at a mean age of 12 years.

Conclusion: Recognition of epiretinal membranes with a characteristic optical coherence tomography appearance may permit early diagnosis in neurologically asymptomatic children with a severe phenotype of NF2.

RETINA 30:S51–S58, 2010


RAH
RA
RB
RCH
RRH
RCH
VPT
SCRAP
CHRPE
CHRRPE
CSHRPE
TM
ARPE

EPIRETINAL MEMBRANES INDICATE A SEVERE PHENOTYPE OF NEUROFIBROMATOSIS TYPE 2

ROBERT A. SISK, MD,* AUDINA M. BERROCAL, MD,*
AMY C. SCHEFLER, MD,* SANDER R. DUBOVY, MD,*
MISLEN S. BAUER, MD, FACMG†

Purpose: The purpose of this study was to describe a subset of severely affected patients with neurofibromatosis type 2 (NF2), multiple central nervous system tumors, and characteristic retinal lesions.

Methods: This is a retrospective observational case series of 4 patients with NF2. The time doma
been descr

Results:
diagnosed
one or bot
ment. The
secondary
ment epit
nized befo
patient had ≥2 central nervous system tumors at the time of diagnosis, and 3 of 4 eventually required neurosurgical interventions for symptomatic, compressive lesions at a mean age of 12 years.

Conclusion: Recognition of epiretinal membranes with a characteristic optical coherence tomography appearance may permit early diagnosis in neurologically asymptomatic children with a severe phenotype of NF2.

RETINA 30:S51–S58, 2010

Epiretinal membrane implies more severe CNS disease in NF2

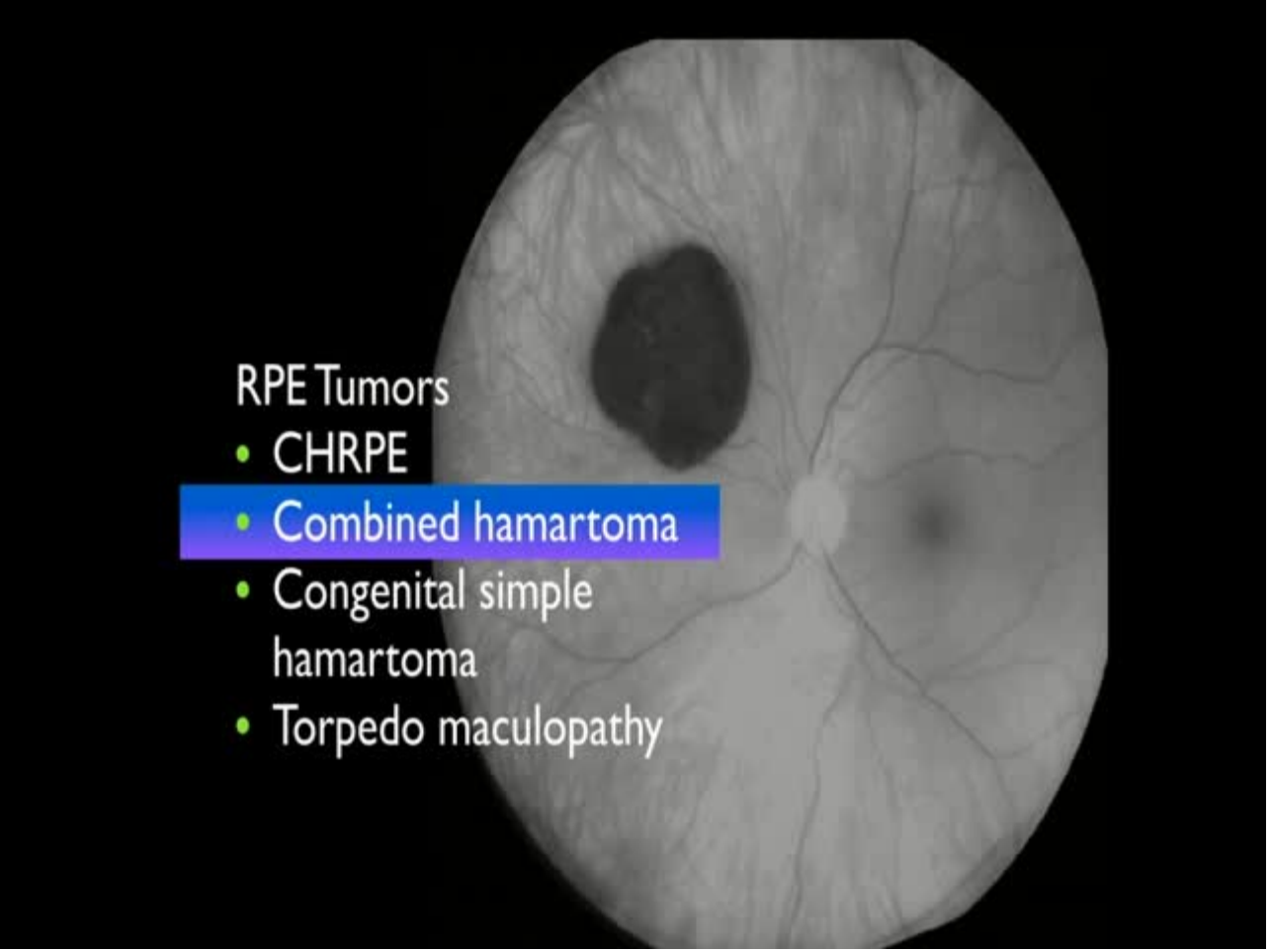
RPE Tumors
• CHRPE
• Combined hamartoma
• Congenital simple hamartoma
• Torpedo maculopathy

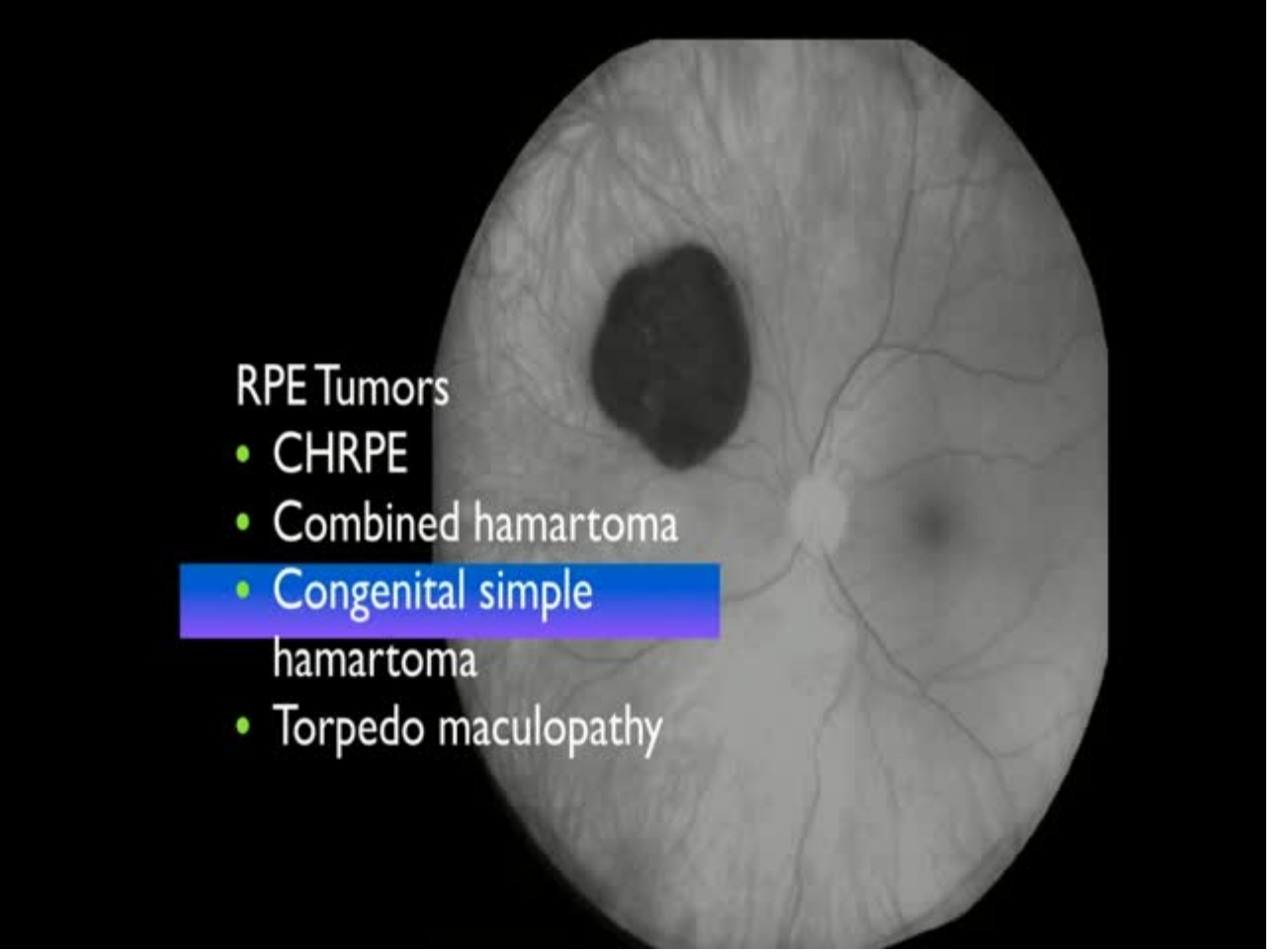
RPE Tumors
• CHRPE
• Combined hamartoma
• Congenital simple hamartoma
• Torpedo maculopathy

Congenital simple hamartoma RPE

Despite proximity to foveola, vision minimally affected

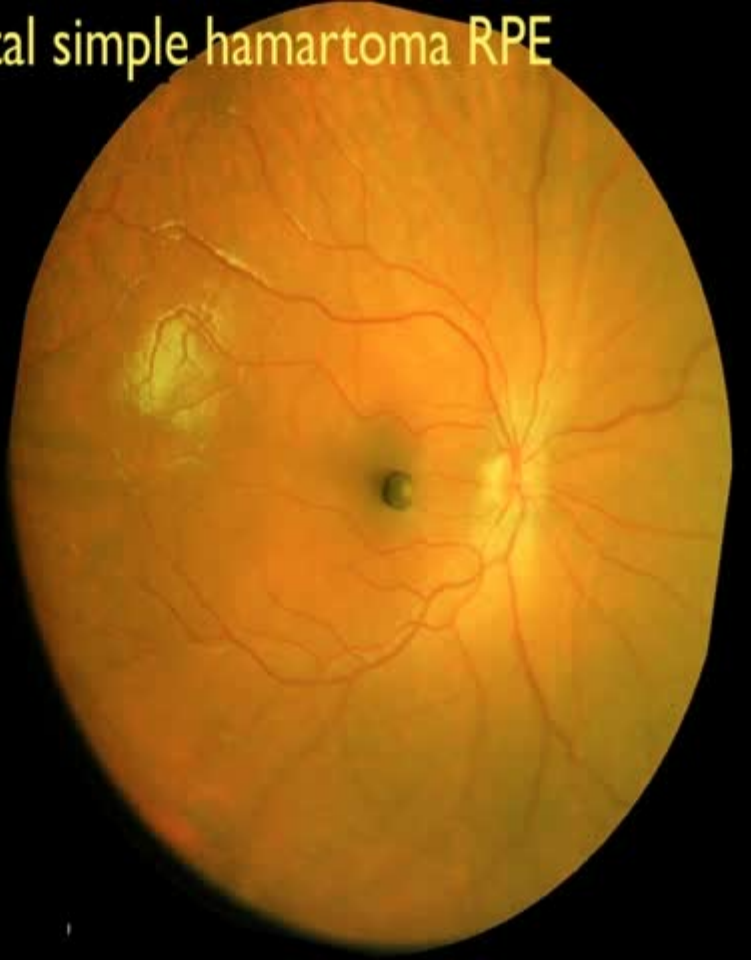

Congenital simple hamartoma RPE

Despite proximity to foveola, vision minimally affected

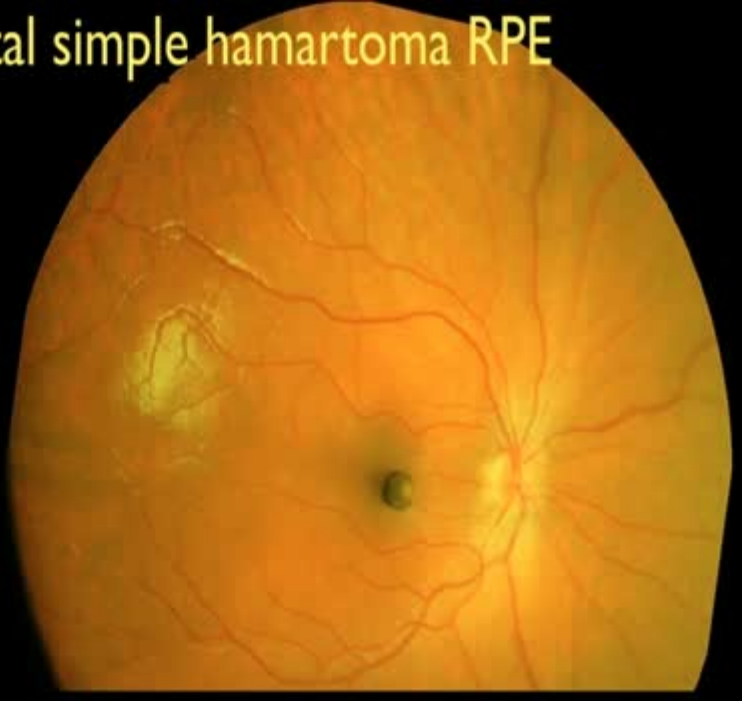

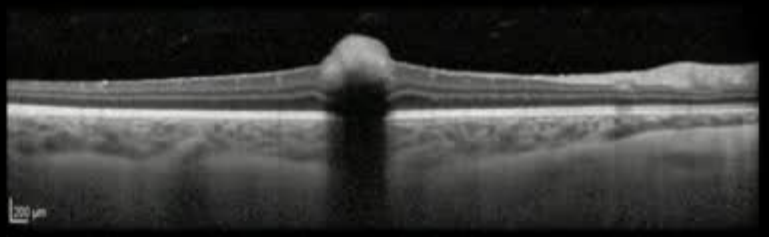

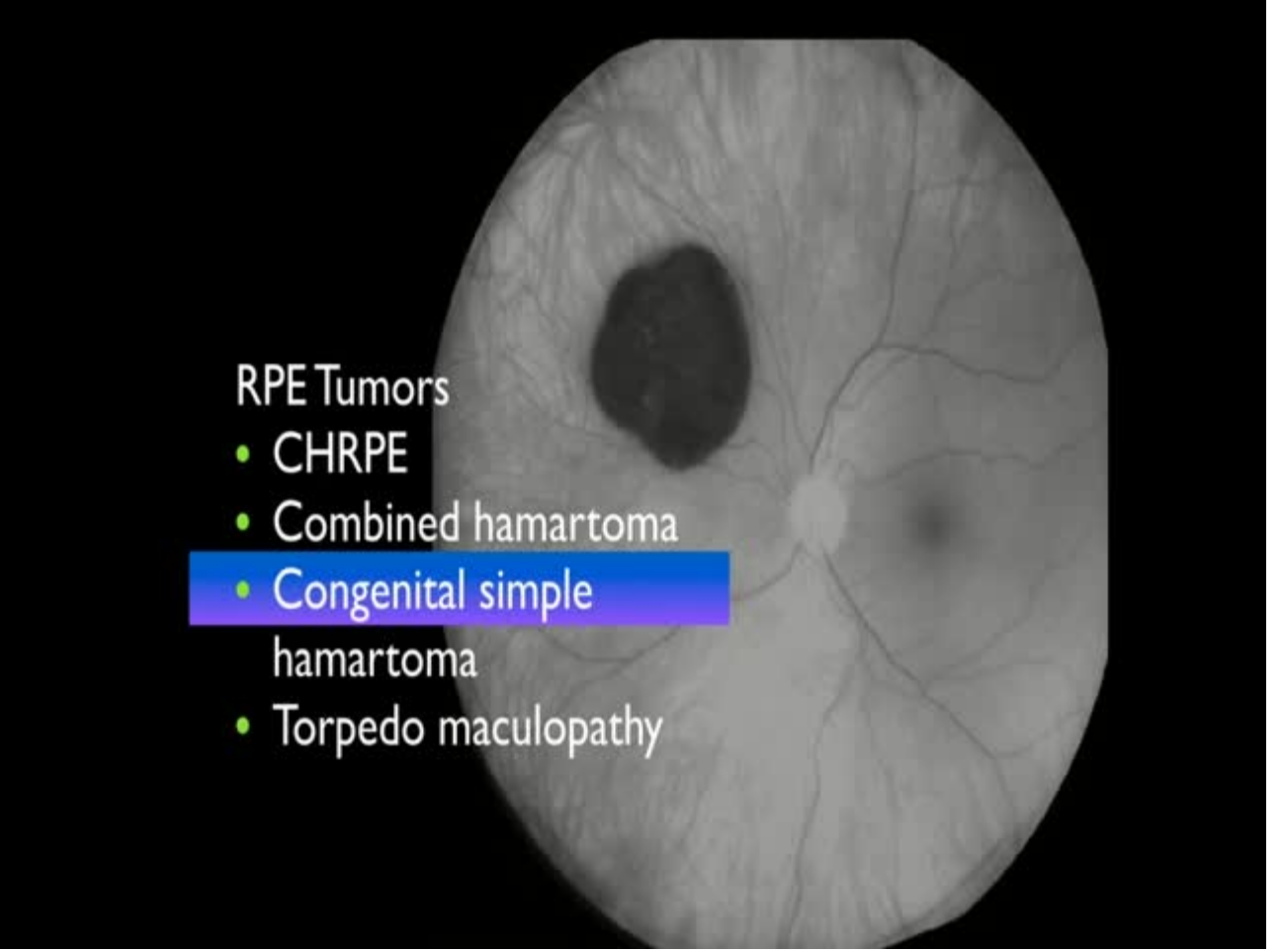
RPE Tumors
• CHRPE
• Combined hamartoma
• Congenital simple hamartoma
• Torpedo maculopathy

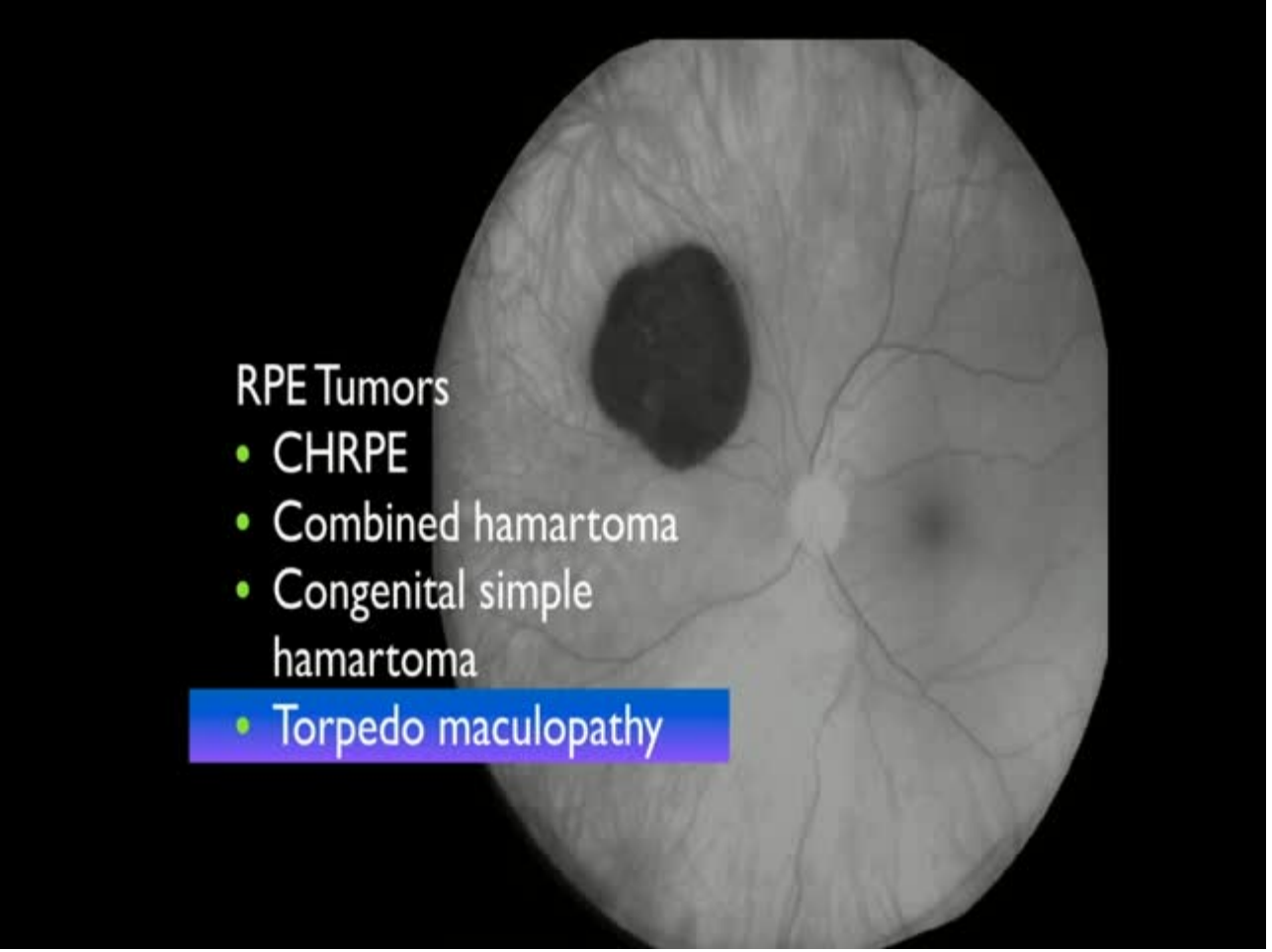
RPE Tumors
• CHRPE
• Combined hamartoma
• Congenital simple hamartoma
• Torpedo maculopathy

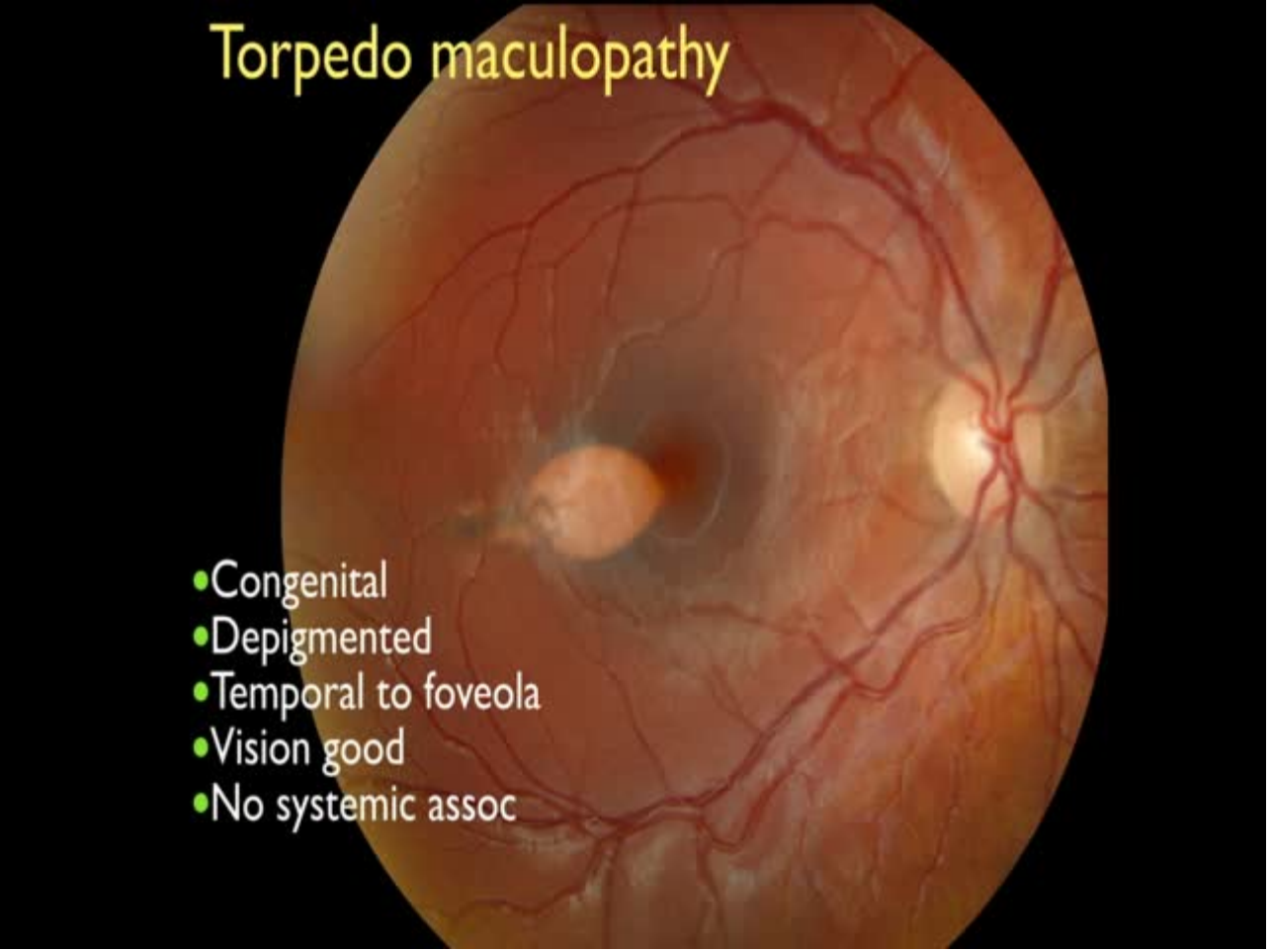
Torpedo maculopathy
•Congenital
•Depigmented
•Temporal to foveola
•Vision good
•No systemic assoc

SUTON FISHER M, RICHARD GRIFFIN MD

Torpedo Maculopathy at the Site of the Fetal "Bulge"

Torpedo maculopathy was discovered in 2 children as a pointed oval retinal pigment epithelial (RPE) defect in the temporal macula. This congenital finding could be related to the fetal temporal macular "bulge" that normally occurs at 5 to 6 months' gestation at the same site.

There are several congenital anomalies of the RPE, including congenital hypertrophy of the RPE (CHRPE), combined hamartoma of the retina and RPE, congenital simple hamartoma of the RPE, RPE hyperplasia associated with familial adenomatous polyposis, and torpedo maculopathy.[1-3] In 1992, Rosenman and Gass[4] described the lesions of "hypopigmented nevus of the retinal pigment epithelium," which was later called torpedo maculopathy.[5] This asymptomatic, torpedo-shaped defect in the RPE occurs in the temporal macular region with a pointed, torpedo-like tip directed toward the foveola. This defect closely resembles solitary CHRPE but differs in its nonrandom macular location and pointed torpedo shape.[5,6] In the few reported cases, there have been no systemic associations. Herein, we describe 2 cases of torpedo maculopathy and speculate as to its embryogenesis.

Report of Cases. Case 1. On routine eye examination, a 3-year-old girl with fix-and-follow visual acuity was discovered to have a temporal macular RPE defect with a pointed oval shape directed toward the foveola and hyperpigmented "frayed tail" appearance directed toward the ora serrata. The flat, nonpigmented lesion measured 2 mm horizontally and 1 mm vertically and was located 3.7 mm temporal to the optic disc (**Figure 1**). Observation was advised.

Case 2. An 11-year-old girl with uncorrected 20/20 visual acuity was discovered on routine eye examination to have a temporal macular RPE defect with a pointed oval shape toward the foveola and hyperpigmented rounded temporal margin. The flat, nonpigmented lesion measured 2 mm horizontally and 1 mm vertically and was located 4 mm temporal to the optic disc (**Figure 2**). Fundoplasmonic fitter results were negative. Observation was advised.

Comment. In 1985, Rosenman and Gass[7] described a 12-year-old boy with a small, flat, circumscribed, oval RPE lesion in the temporal macula. Additional reports confirmed the consistent pointed oval configuration and macular location of this condition (**Table**).[1-3,8] Bigorni and associates[1] reported 3 cases of asymptomatic torpedo maculopathy in a child and 2 adults. Other articles have displayed images of similar lesions dimensions measuring 2 to 3 mm horizontally and 1 mm vertically.[3,8]

Congenital hypertrophy of the RPE is a flat congenital RPE lesion that appears pigmented or nonpigmented and characteristically has rounded or scalloped margins.[1] Solitary CHRPE is located most often in the equatorial or peripheral fundus, randomly in various quadrants and rarely in the macula (7%).[1] Both CHRPE and torpedo macu-

Figure 1. Case 1. A 3-year-old girl with torpedo maculopathy in the temporal macular region of the right eye, with a pointed oval shape toward the foveola and hyperpigmented "frayed tail" temporally.

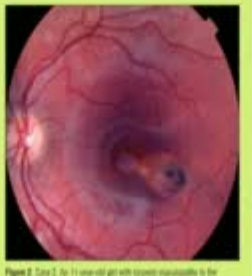

Figure 2. Case 2. An 11-year-old girl with torpedo maculopathy in the temporal macular region of the left eye with a pointed oval shape toward the foveola and hyperpigmented, rounded margin temporally.

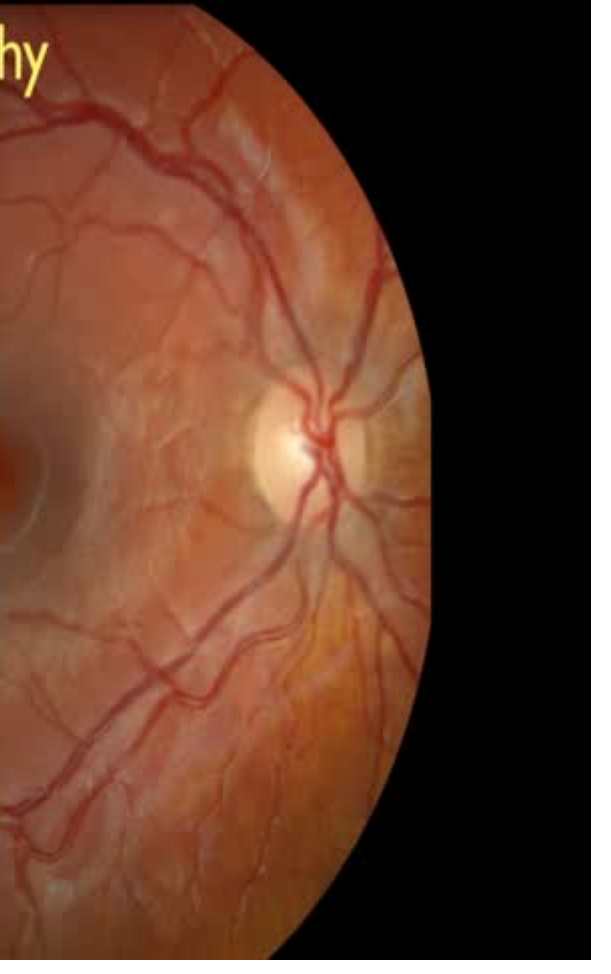

Torpedo maculopathy

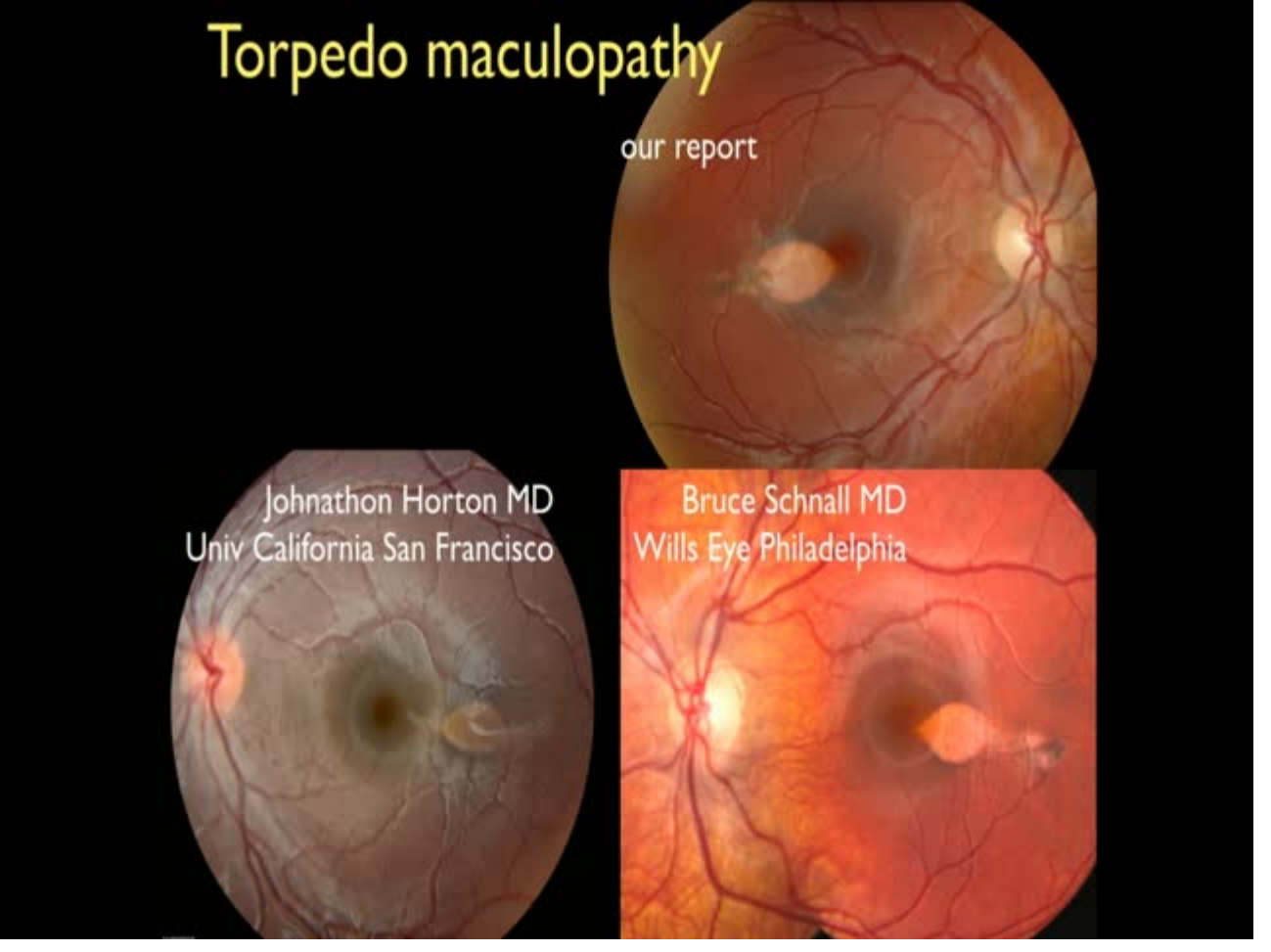


RAH Astrocytic hamartoma
RA Astrocytoma
RB Retinoblastoma
RCH Capillary hemangioma
RRH Racemose hemangioma
RCH Cavernous hemangioma
VPT Vasoproliferative tumor
SCRAP Solitary circ ret astrocyt prol
CHRPE Congenital hypertrophy RPE
CHRRPE Combined hamartoma RPE
CSHRPE Simple hamartoma RPE
TM Torpedo maculopathy
ARPE Adenoma/Ca RPE

Torpedo maculopathy

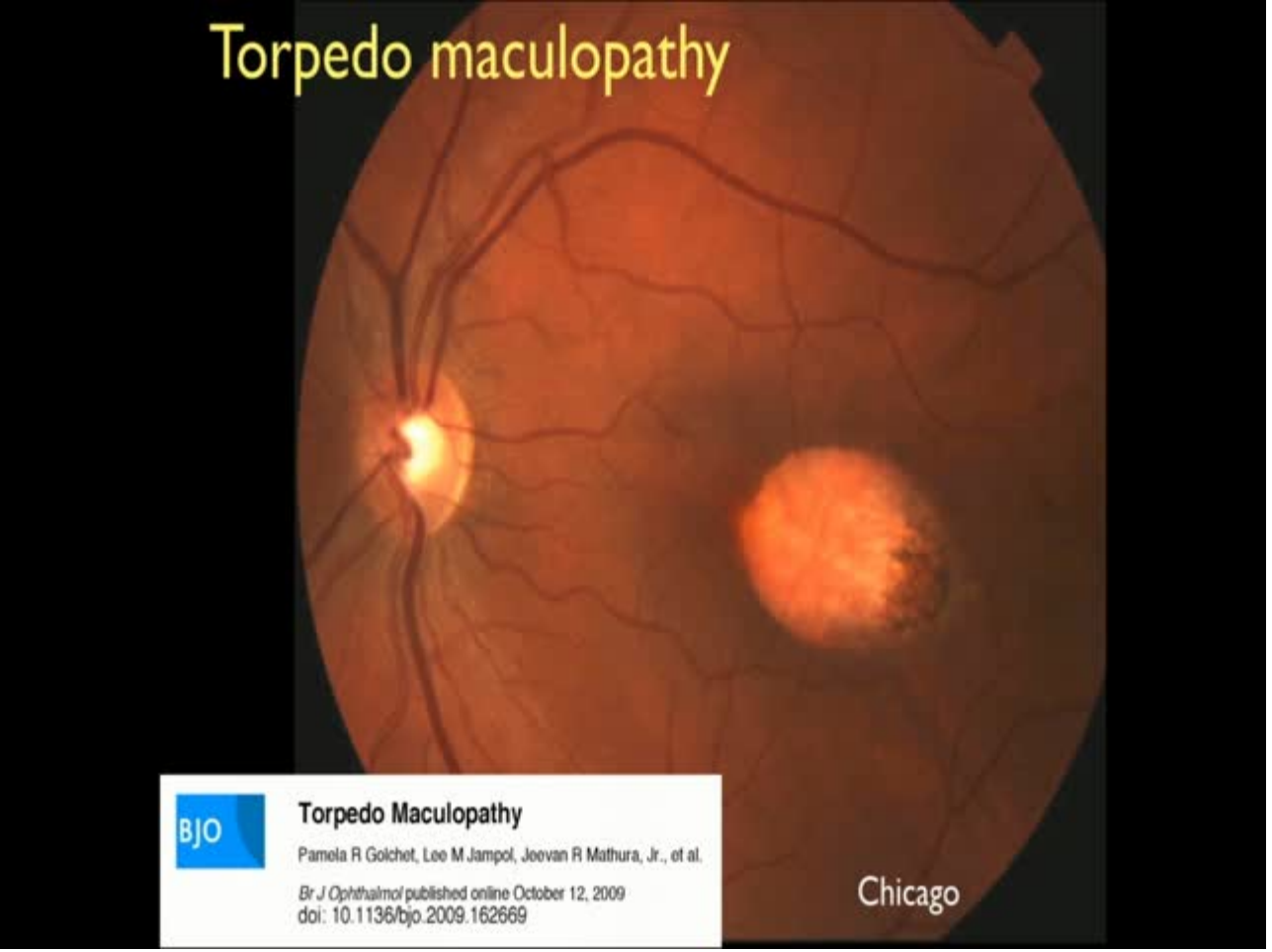

Torpedo maculopathy

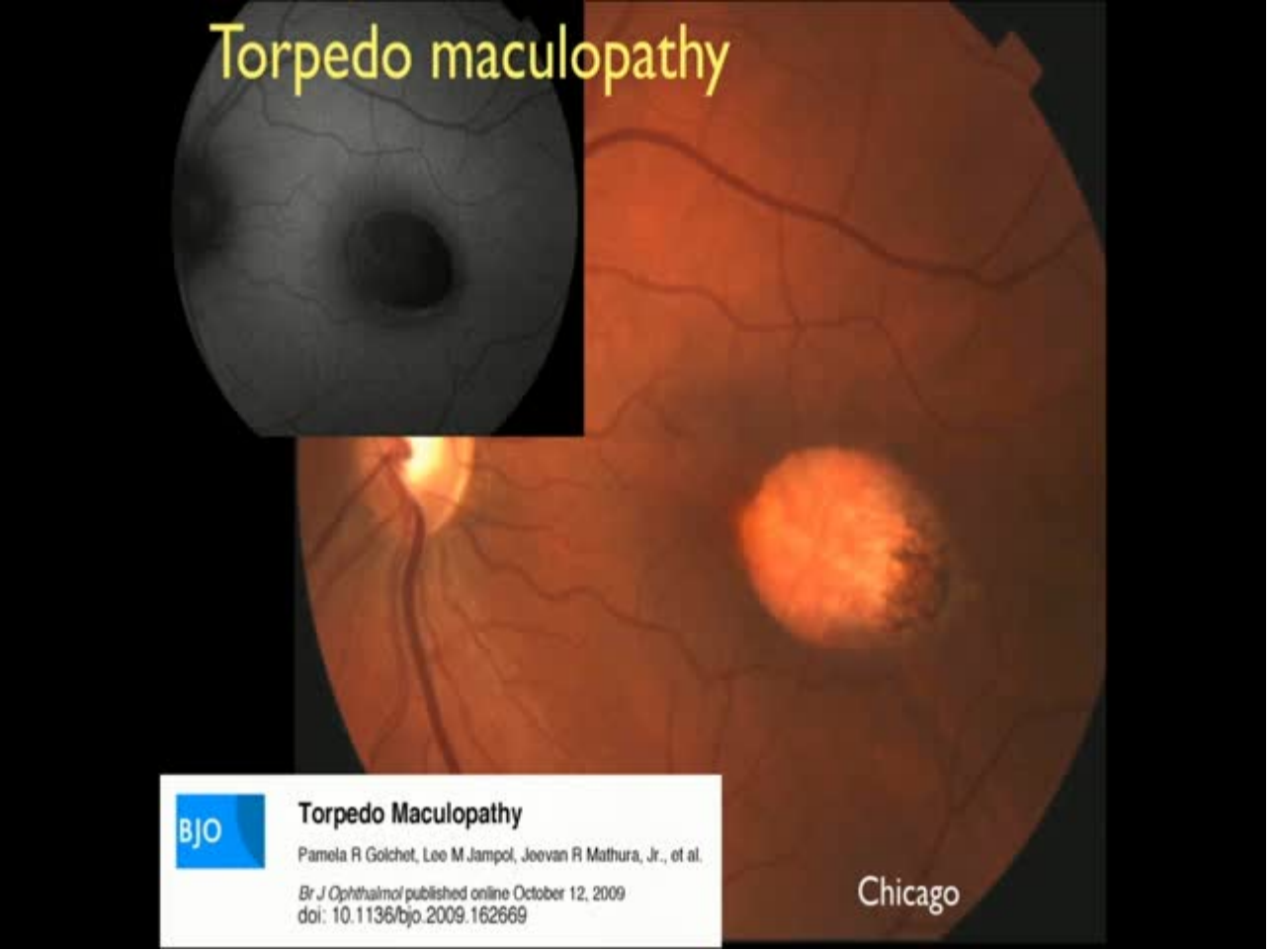

Torpedo maculopathy

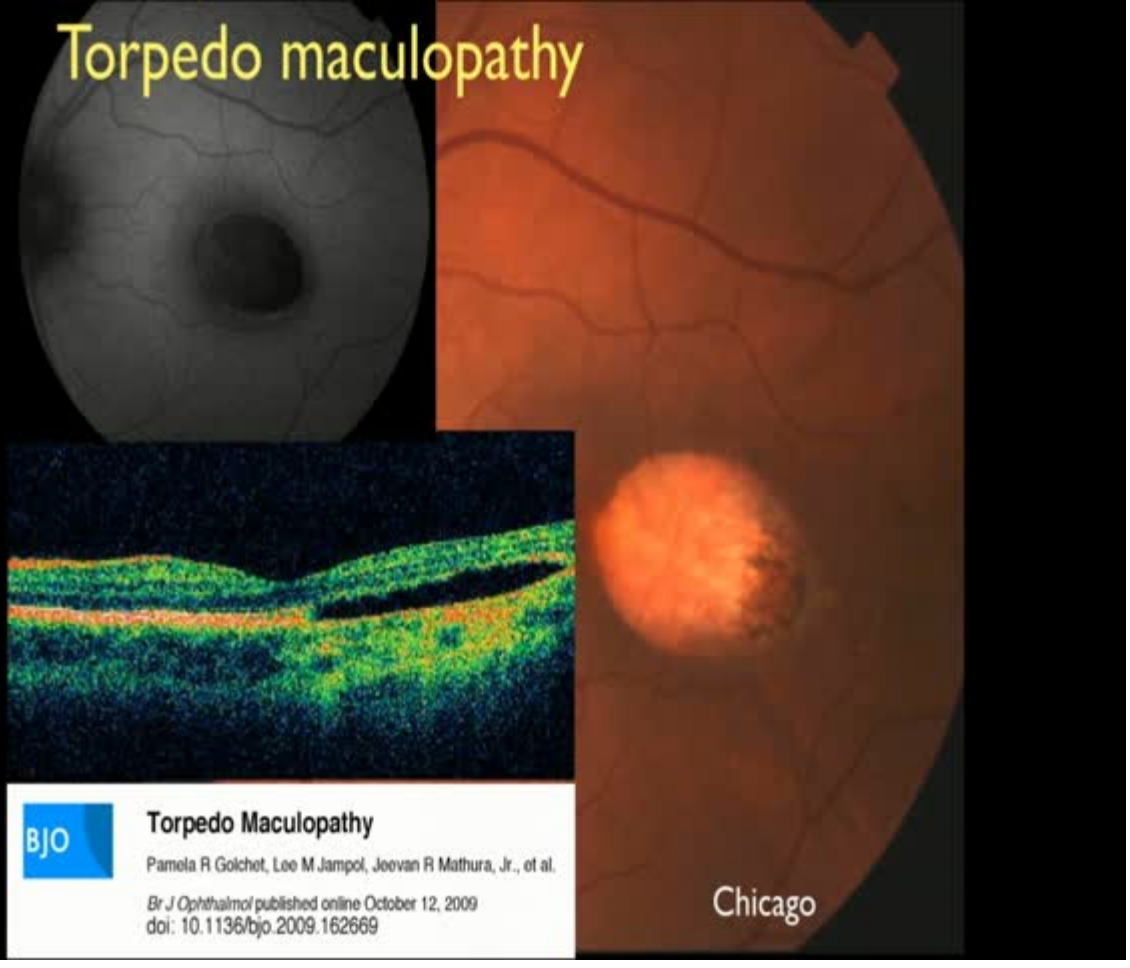

Torpedo maculopathy

subretinal cleft
- torpedo maculopathy
- CHRPE
- choroidal nevus

BJO

Torpedo Maculopathy

Pamela R Golchet, Lee M Jampol, Jeevan R Mathura, Jr., et al.

Br J Ophthalmol published online October 12, 2009
doi: 10.1136/bjo.2009.162669

Chicago

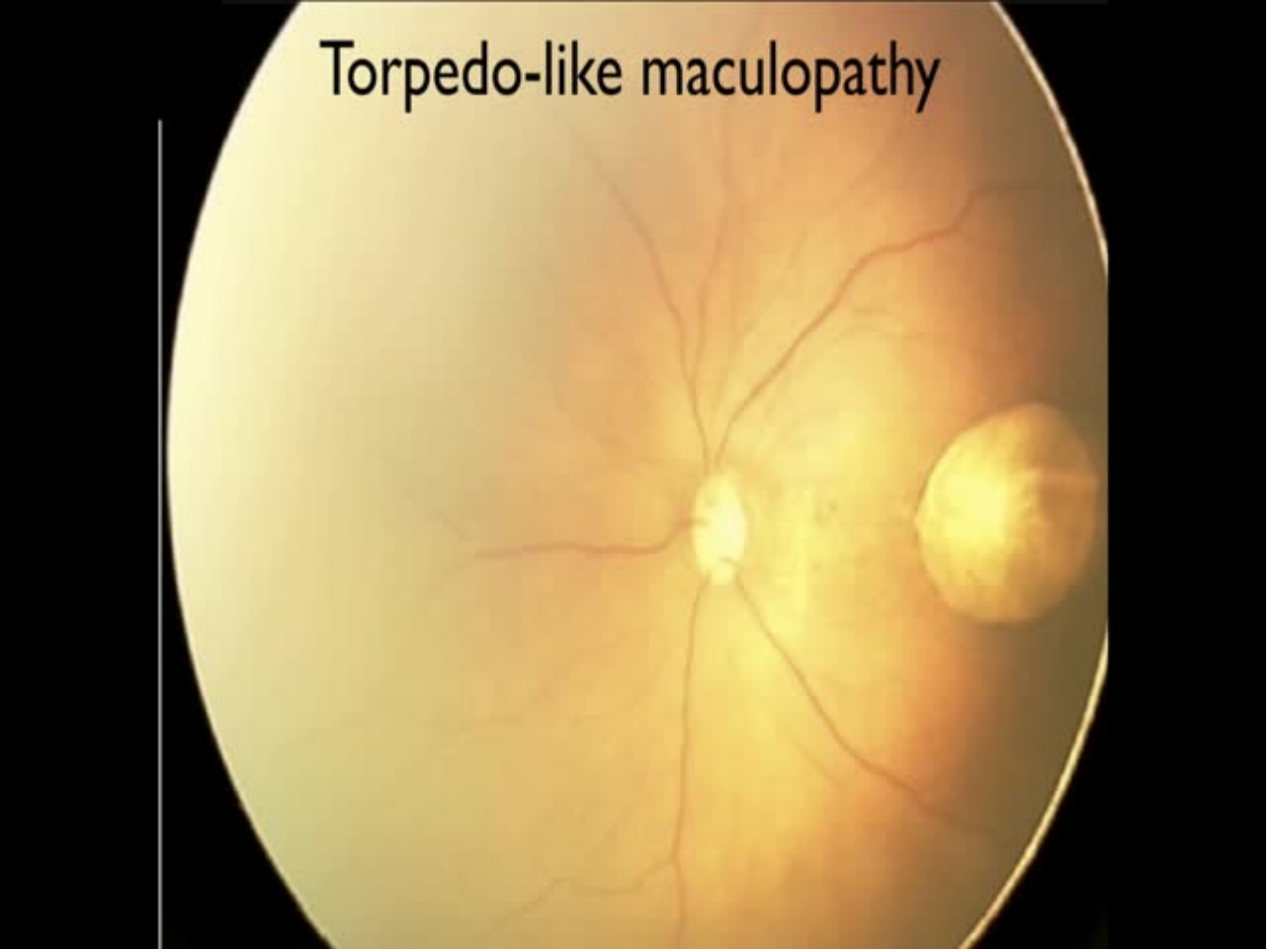
Torpedo-like maculopathy

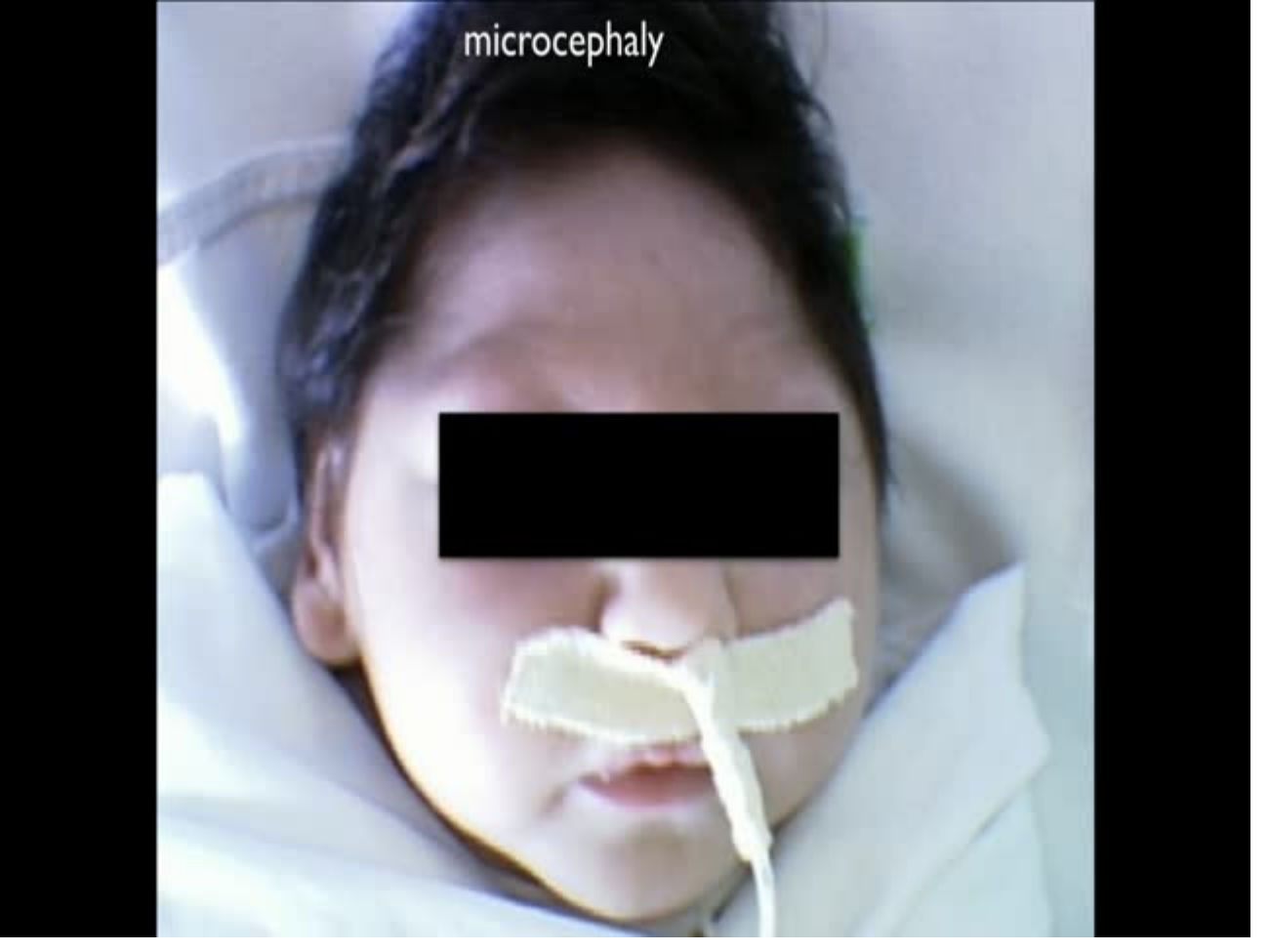
microcephaly

Expanded Spectrum of Congenital Ocular Findings in Microcephaly with Presumed Zika Infection

Homero Augusto de Miranda II, MD,[1] Marcelo Cavalcante Costa, MD,[1] Maria Auxiliadora Monteiro Frazão, MD,[1] Natália Simão, MD,[2] Sandra Franchischini, MD,[3] Darius M. Moshfeghi, MD[4]

Purpose: To describe the ocular findings of 3 cases of suspected congenital Zika viral infection with microcephaly and maculopathy.

Design: Retrospective, consecutive case series.

Participants: Three male infants born in northern Brazil whose mothers demonstrated a viral syndrome during the first trimester and who subsequently were born with microcephaly.

Methods: Observational report of macular findings.

Main Outcome Measures: Continued observation.

Results: Three male infants were born with microcephaly to mothers who had a viral syndrome during the first trimester of gestation in an area that subsequently has demonstrated epidemic Zika infection, a flavivirus related to Dengue. Ocular examination was performed. All 6 eyes demonstrated a pigmentary maculopathy ranging from mild to pronounced. In 4 eyes, well-delineated macular chorioretinal atrophy with a hyperpigmented ring developed. Three eyes demonstrated vascular tortuosity and 2 eyes demonstrated a pronounced early termination of the retinal vasculature on photographic evaluation. Two eyes demonstrated a washed out peripheral retina with a hypolucent spot. One eye had scattered subretinal hemorrhages external to the macula. Finally, 1 eye demonstrated peripheral pigmentary changes and clustered atrophic lesions resembling grouped congenital albinotic spots (polar bear tracks).

Conclusions: Zika virus has been linked to microcephaly in children of mothers with a viral syndrome during the first trimester of pregnancy. Ocular findings previously described a pigmentary retinopathy and atrophy that now can be expanded to include torpedo maculopathy, vascular changes, and hemorrhagic retinopathy. Ophthalmologic screening guidelines need to be defined to determine which children would benefit from newborn screening in affected regions. *Ophthalmology 2016;■:1–7 © 2016 by the American Academy of Ophthalmology.*

Expanded Spectrum of Congenital Ocular Findings in Microcephaly with Presumed Zika Infection

Homero Augusto de Miranda II, MD,[1] Marcelo Cavalcante Costa, MD,[1] Maria Auxiliadora Monteiro Frazão, MD,[1] Natália Simão, MD,[2] Sandra Franchischini, MD,[3] Darius M. Moshfeghi, MD[4]

Purpose: To describe the ocular findings of 3 cases of suspected congenital Zika viral infection with microcephaly and maculopathy.

Design: Retrospective, consecutive case series.

Participants: Three male infants born in northern Brazil whose mothers demonstrated a viral syndrome during the first trimester and who subsequently were born with microcephaly.

Methods: Observational report of macular findings.

Main Outcome Measures: Continued observation.

Results: Three male infants were born with microcephaly to mothers who had a viral syndrome during the first trimester of gestation in an area that subsequently has demonstrated epidemic Zika infection, a flavivirus related to Dengue. Ocular examination was performed. All 6 eyes demonstrated a pigmentary maculopathy ranging from mild to pronounced. In 4 eyes, well-delineated macular chorioretinal atrophy with a hyperpigmented ring developed. Three eyes demonstrated vascular tortuosity and 2 eyes demonstrated a pronounced early termination of the retinal vasculature on photographic evaluation. Two eyes demonstrated a washed out peripheral retina with a hypolucent spot. One eye had scattered subretinal hemorrhages external to the macula. Finally, 1 eye demonstrated peripheral pigmentary changes and clustered atrophic lesions resembling grouped

Conclusions: Zika virus has been linked to microcephaly in children of mothers with a viral syndrome during the first trimester of pregnancy. Ocular findings previously described a pigmentary retinopathy and atrophy that now can be expanded to include torpedo maculopathy, vascular changes, and hemorrhagic retinopathy. Ophthalmologic screening guidelines need to be defined to determine which children would benefit from newborn screening in affected regions. *Ophthalmology 2016;■:1–7 © 2016 by the American Academy of Ophthalmology.*

Expanded Spectrum of Congenital Ocular Findings in Microcephaly with Presumed Zika

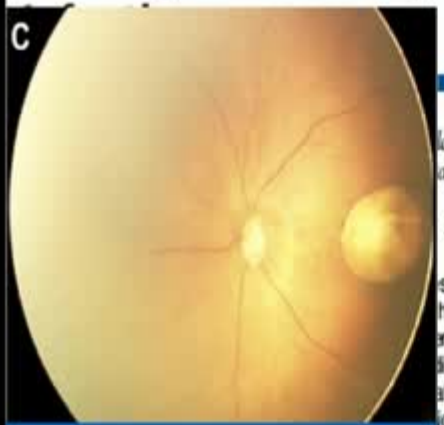

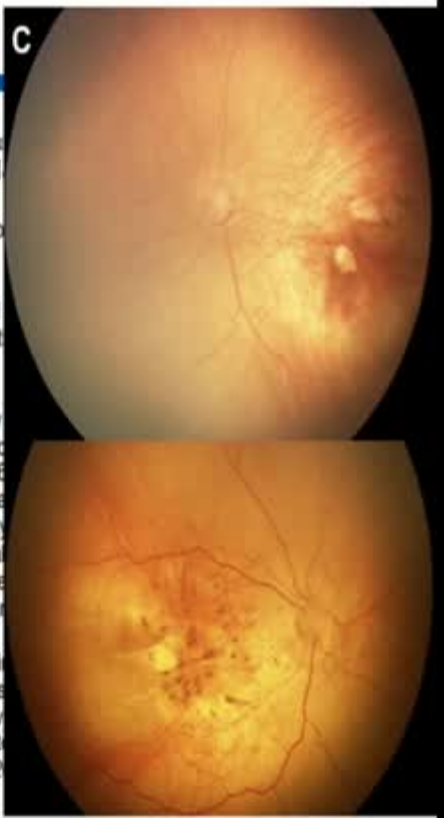

torpedo-like RPE defects in 4/6eyes along with disseminated RPE defects


RAH Astrocytic hamartoma
RA Astrocytoma
RB Retinoblastoma
RCH Capillary hemangioma
RRH Racemose hemangioma
RCH Cavernous hemangioma
VPT Vasoproliferative tumor
SCRAP Solitary circ ret astrocyt prol
CHRPE Congenital hypertrophy RPE
CHRRPE Combined hamartoma RPE
CSHRPE Simple hamartoma RPE
TM Torpedo maculopathy
ARPE Adenoma/Ca RPE

RAH	Astrocytic hamartoma
RA	Astrocytoma
RB	Retinoblastoma
RCH	Capillary hemangioma
RRH	Racemose hemangioma
RCH	Cavernous hemangioma
VPT	Vasoproliferative tumor
SCRAP	Solitary circ ret astrocyt prol
CHRPE	Congenital hypertrophy RPE
CHRRPE	Combined hamartoma RPE
CSHRPE	Simple hamartoma RPE
TM	Torpedo maculopathy
ARPE	Adenoma/Ca RPE


… back to alphabet soup


… back to alphabet soup


LEARN

Retinal Tumors in 2016

Alphabet Soup

Carol Shields
Ocular Oncology Service
Wills Eye Hospital
Philadlephia PA USA

Retinal Tumors in 2016

Thanks to our Founders

Gerald Bovino MD

Roy Levit MD

Allen Verne MD

RAH	Astrocytic hamartoma
RA	Astrocytoma
RB	Retinoblastoma
RCH	Capillary hemangioma
RRH	Racemose hemangioma
RCH	Cavernous hemangioma
VPT	Vasoproliferative tumor
SCRAP	Solitary circ ret astrocyt prol
CHRPE	Congenital hypertrophy RPE
CHRRPE	Combined hamartoma RPE
CSHRPE	Simple hamartoma RPE
TM	Torpedo maculopathy
ARPE	Adenoma/Ca RPE

RAH	Astrocytic hamartoma
RA	Astrocytoma
RB	Retinoblastoma
RCH	Capillary hemangioma
RRH	Racemose hemangioma
RCH	Cavernous hemangioma
VPT	Vasoproliferative tumor
SCRAP	Solitary circ ret astrocyt prol
CHRPE	Congenital hypertrophy RPE
CHRRPE	Combined hamartoma RPE
CSHRPE	Simple hamartoma RPE
TM	Torpedo maculopathy
ARPE	Adenoma/Ca RPE

RAH	Astrocytic hamartoma
RA	Astrocytoma
RB	Retinoblastoma
RCH	Capillary hemangioma
RRH	Racemose hemangioma
RCH	Cavernous hemangioma
VPT	Vasoproliferative tumor
SCRAP	Solitary circ ret astrocyt prol
CHRPE	Congenital hypertrophy RPE
CHRRPE	Combined hamartoma RPE
CSHRPE	Simple hamartoma RPE
TM	Torpedo maculopathy
ARPE	Adenoma/Ca RPE


RAH Astrocytic hamartoma
RA Astrocytoma
RB Retinoblastoma
RCH Capillary hemangioma
RRH Racemose hemangioma
RCH Cavernous hemangioma
VPT Vasoproliferative tumor
SCRAP Solitary circ ret astrocyt prol
CHRPE Congenital hypertrophy RPE
CHRRPE Combined hamartoma RPE
CSHRPE Simple hamartoma RPE
TM Torpedo maculopathy
ARPE Adenoma/Ca RPE

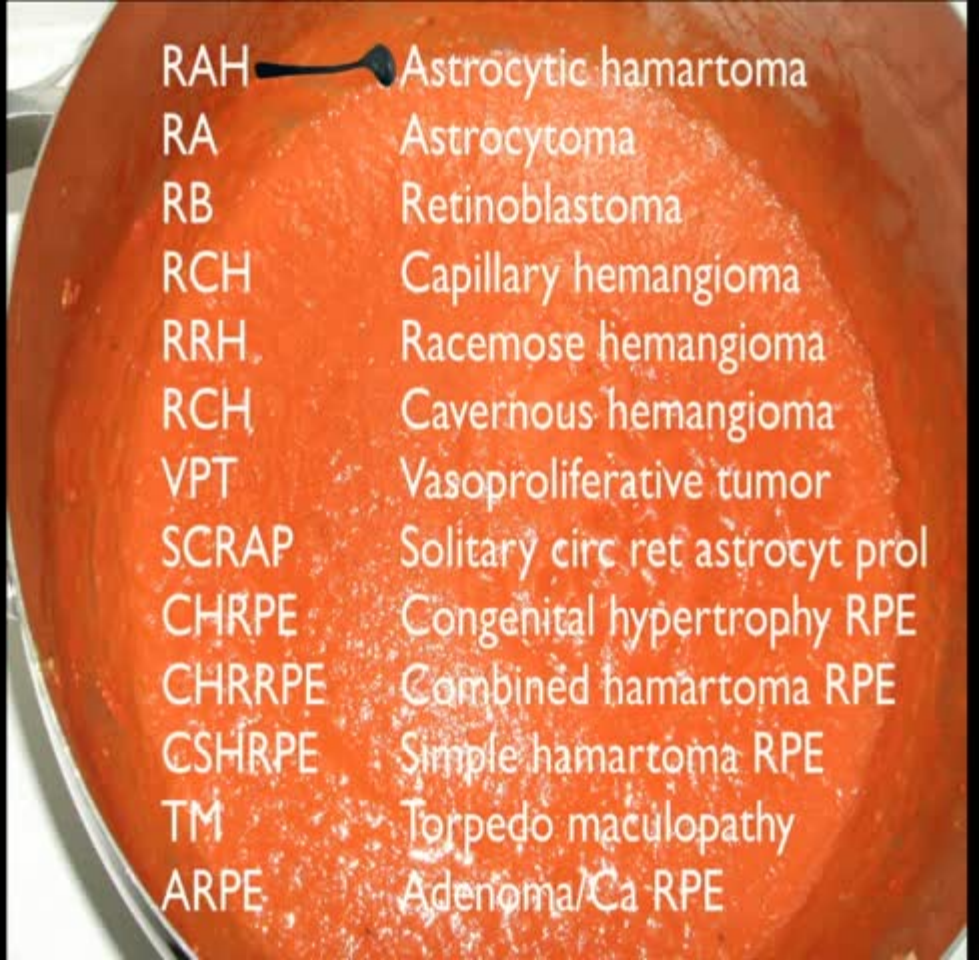
RAH Astrocytic hamartoma
RA Astrocytoma
RB Retinoblastoma
RCH Capillary hemangioma
RRH Racemose hemangioma
RCH Cavernous hemangioma
VPT Vasoproliferative tumor
SCRAP Solitary circ ret astrocyt prol
CHRPE Congenital hypertrophy RPE
CHRRPE Combined hamartoma RPE
CSHRPE Simple hamartoma RPE
TM Torpedo maculopathy
ARPE Adenoma/Ca RPE

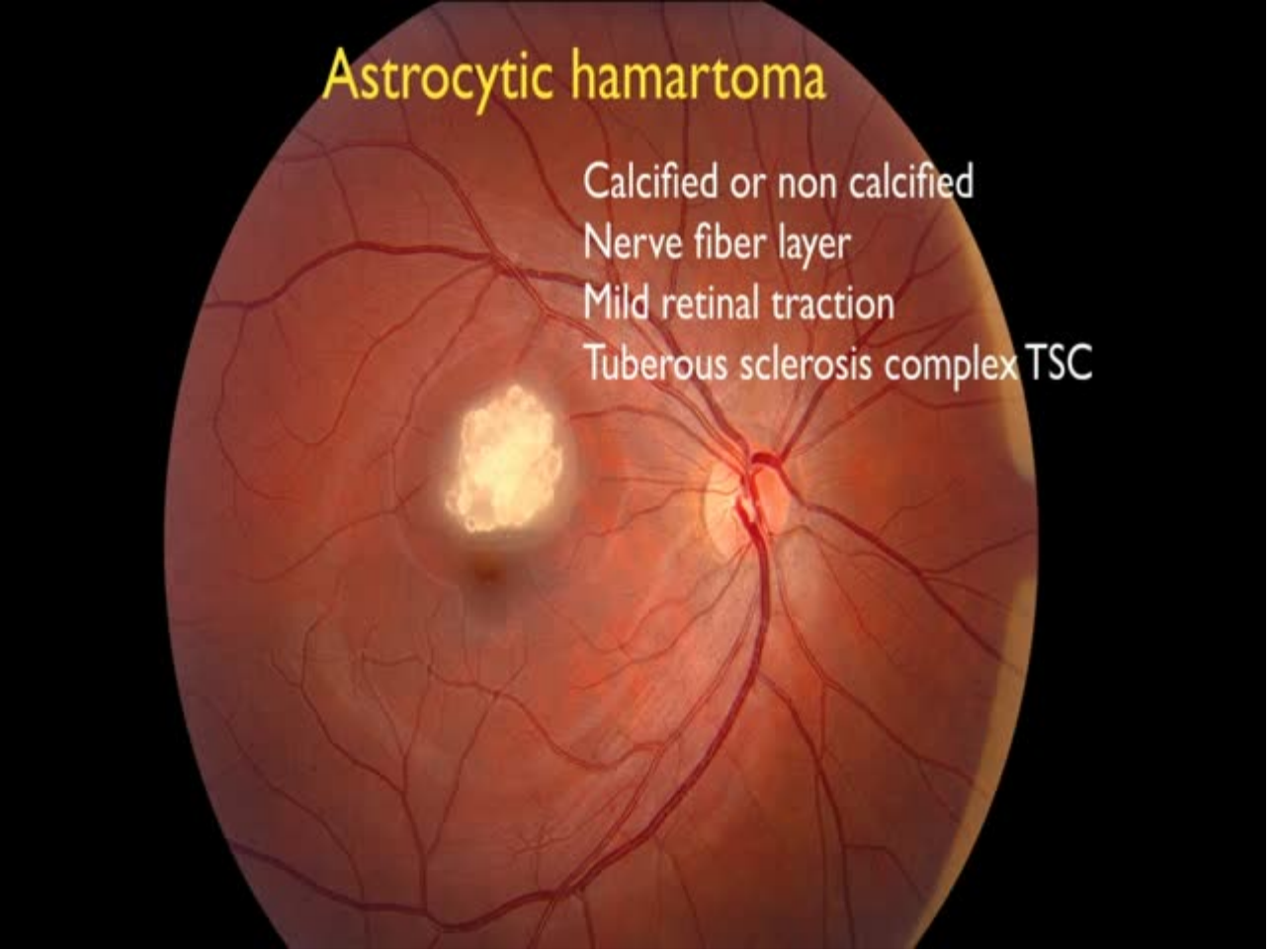
Astrocytic hamartoma
Calcified or non calcified
Nerve fiber layer
Mild retinal traction
Tuberous sclerosis complex TSC

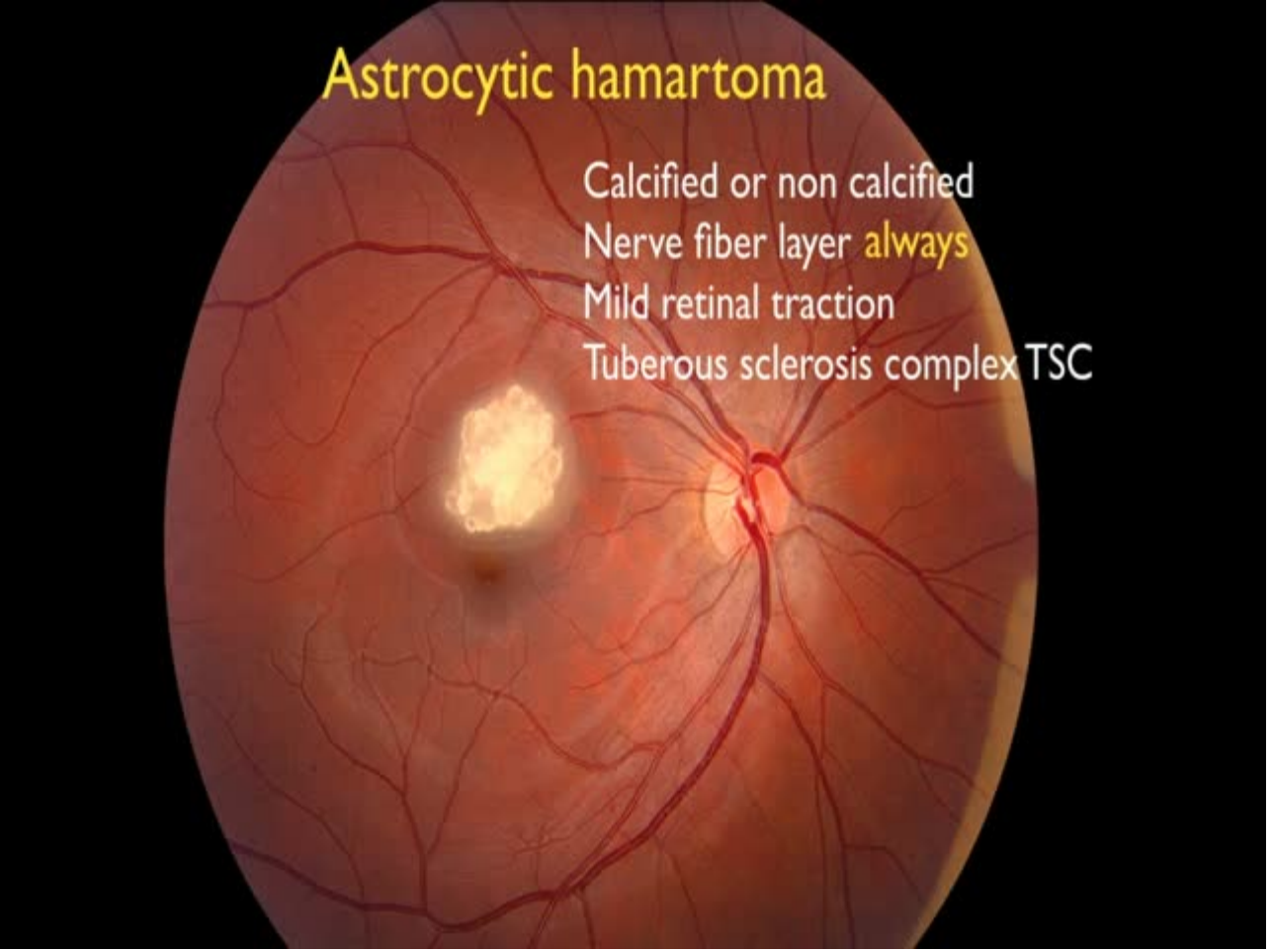
Astrocytic hamartoma
Calcified or non calcified
Nerve fiber layer always
Mild retinal traction
Tuberous sclerosis complex TSC

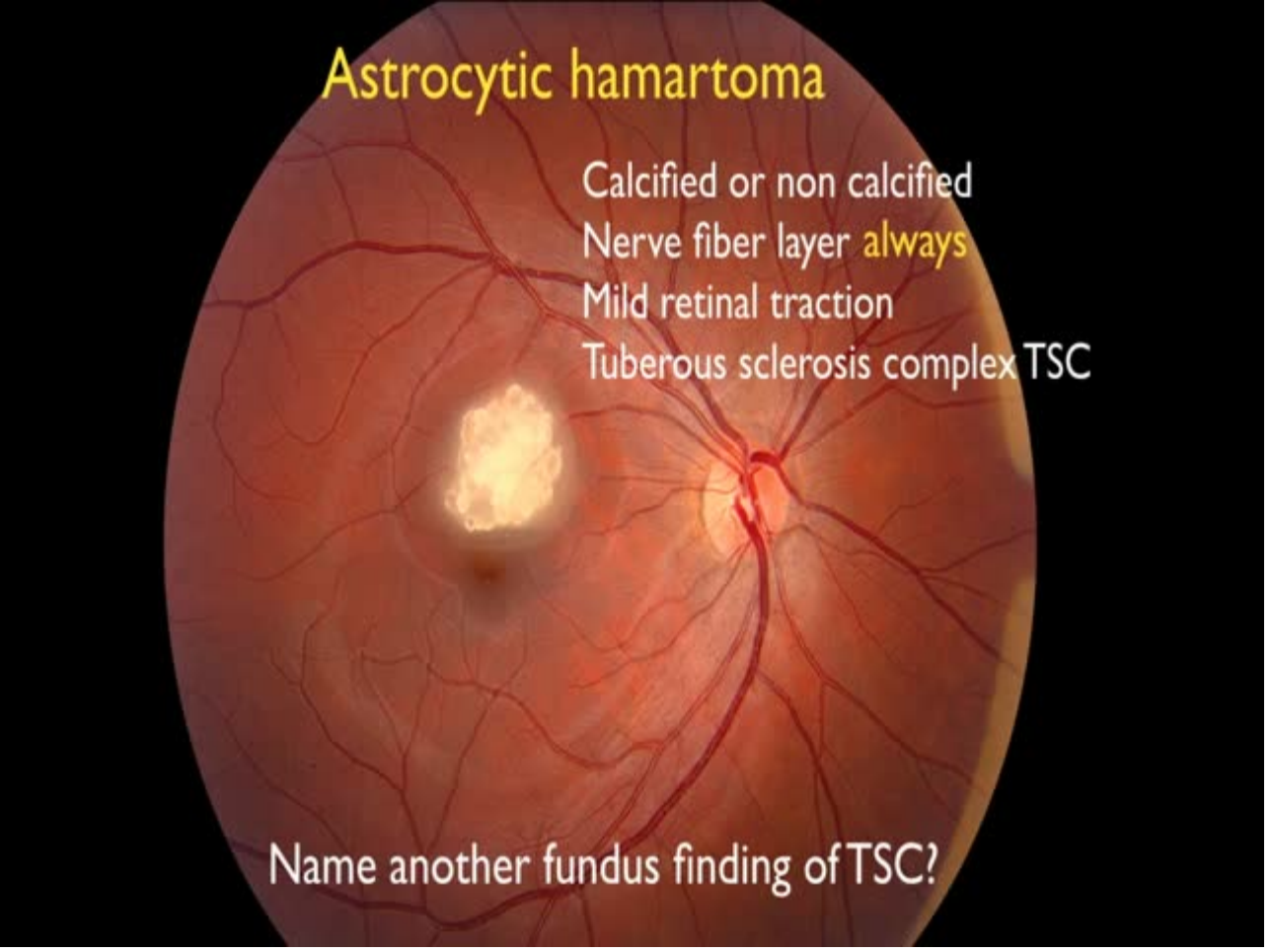
Astrocytic hamartoma
Calcified or non calcified
Nerve fiber layer always
Mild retinal traction
Tuberous sclerosis complex TSC
Name another fundus finding of TSC?

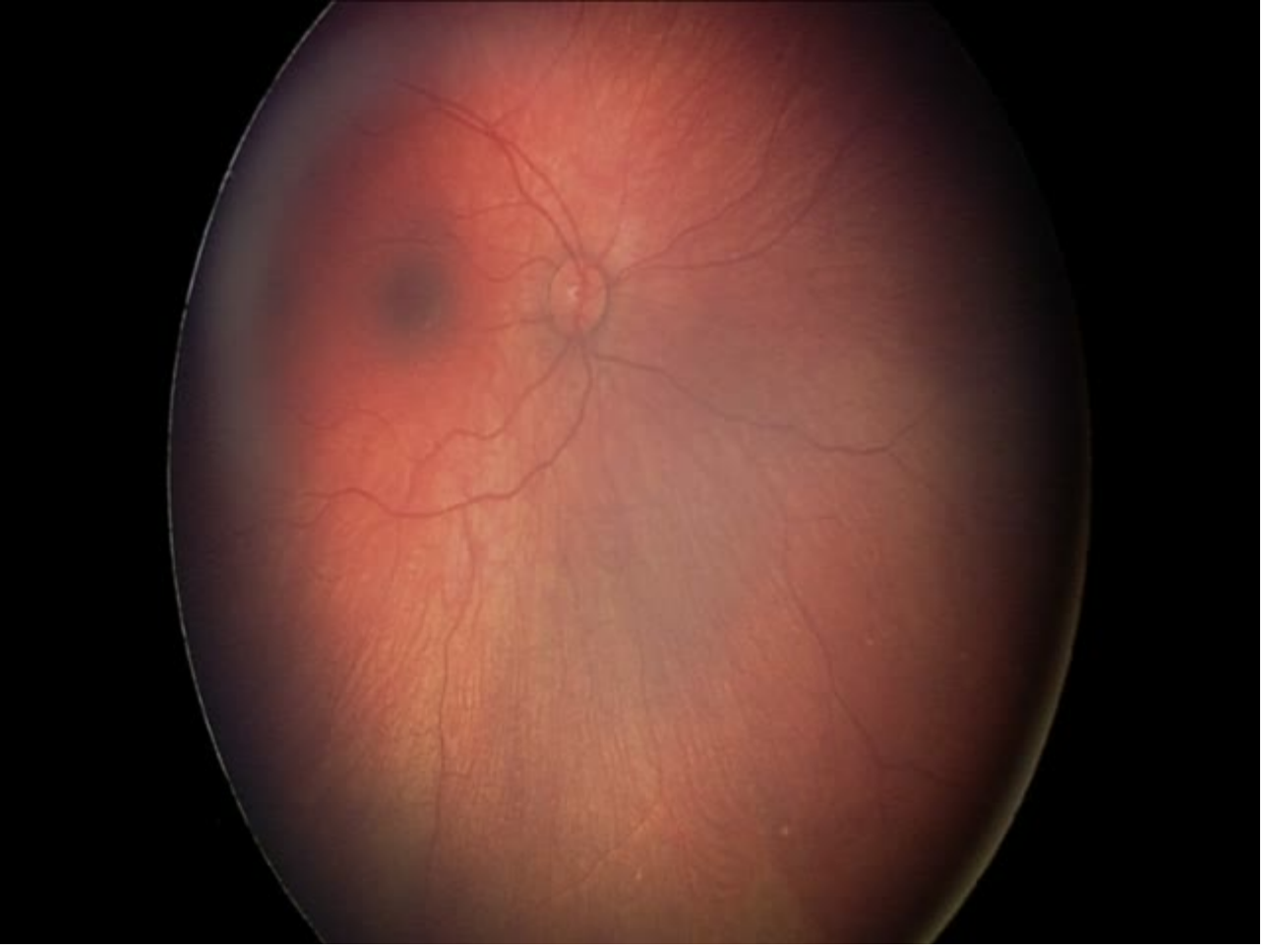

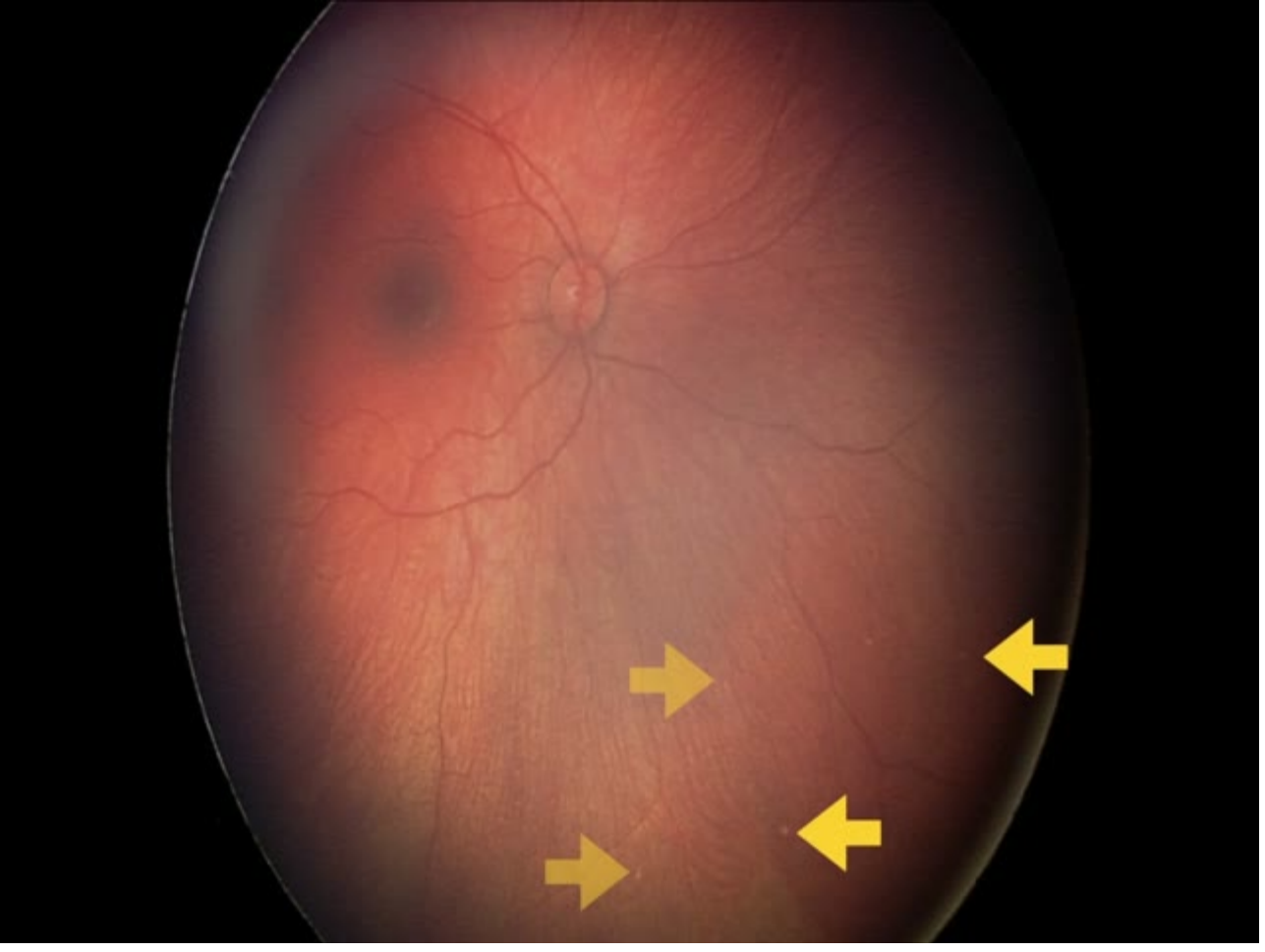

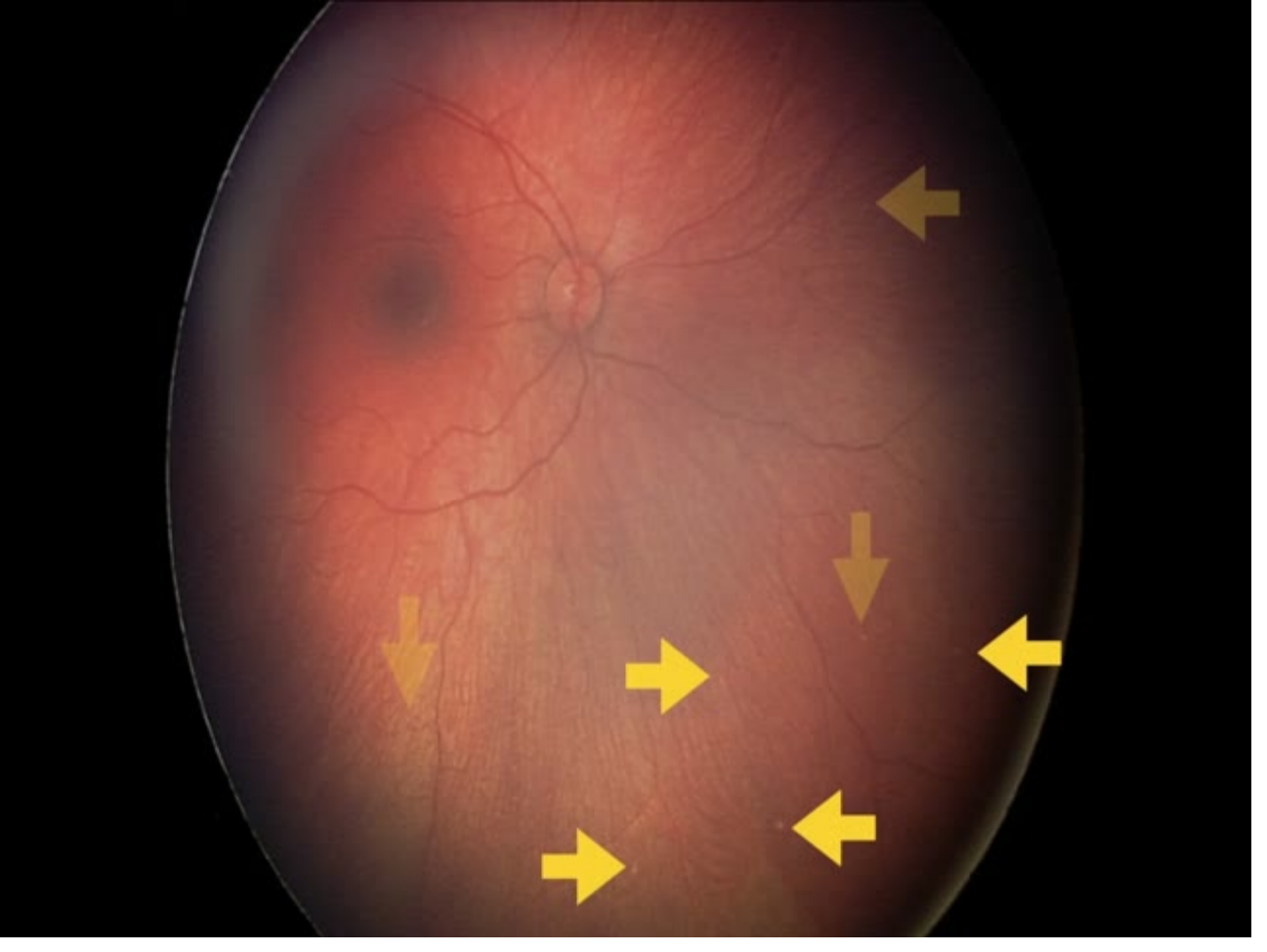

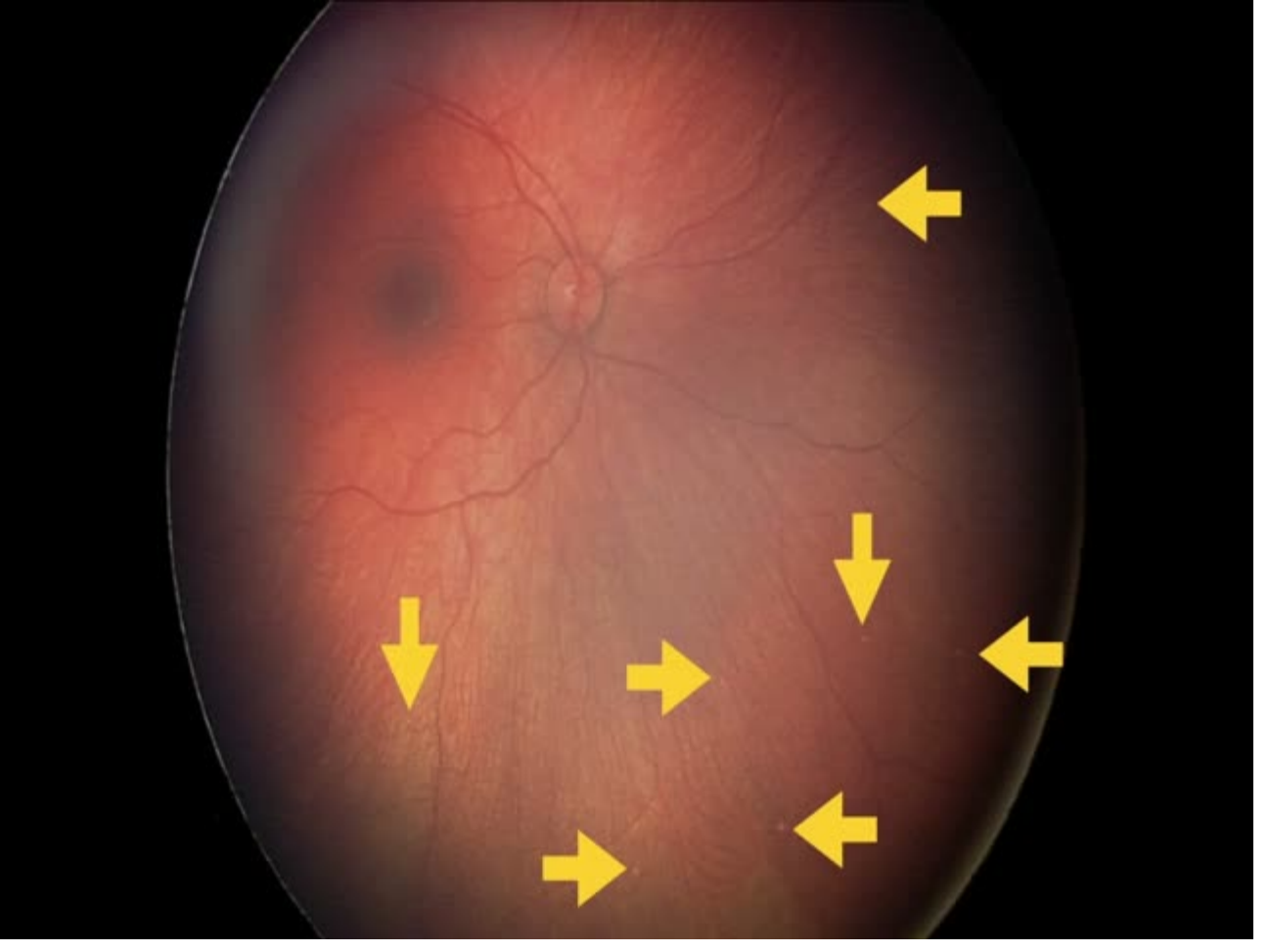

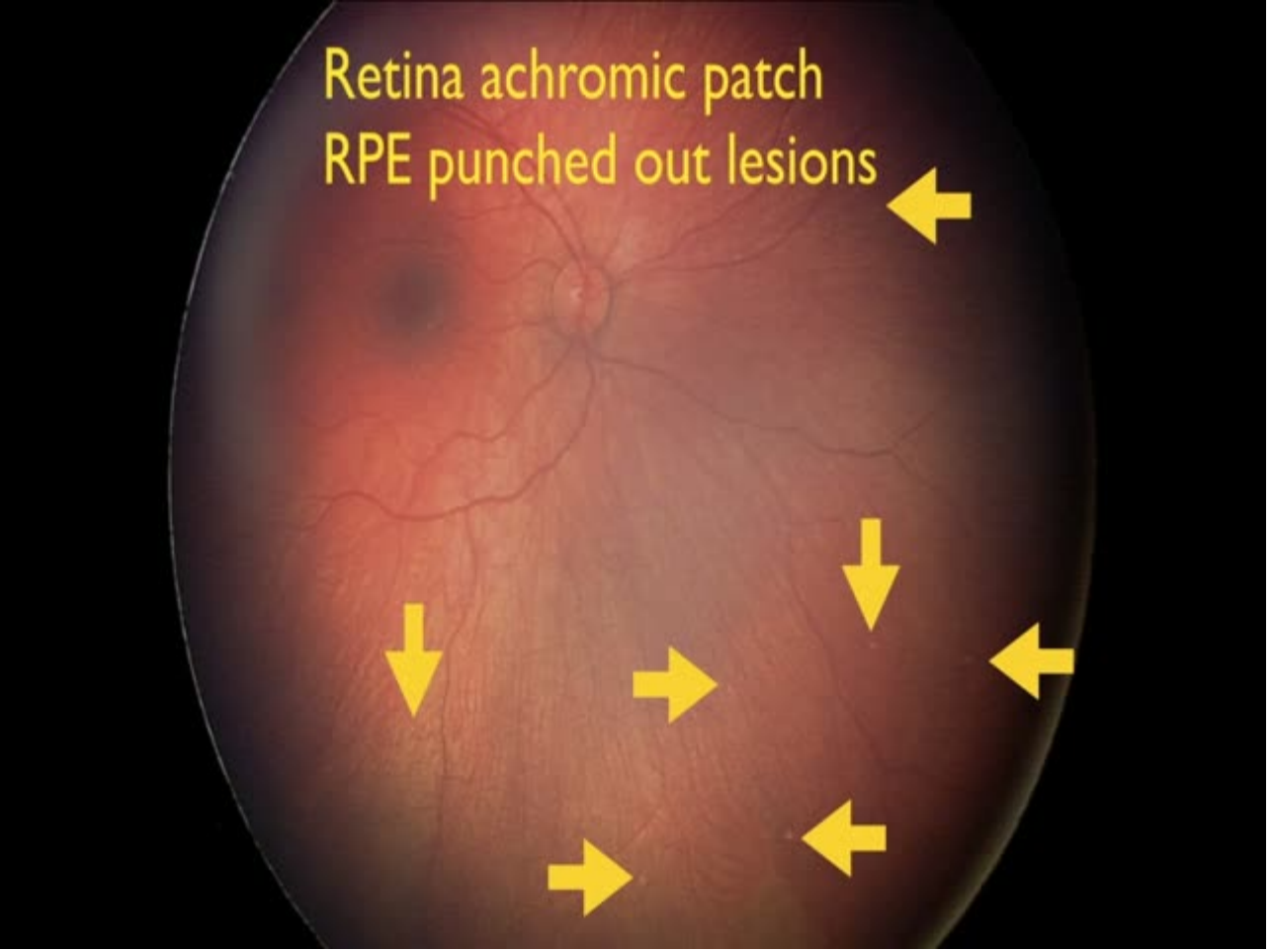
Retina achromic patch
RPE punched out lesions

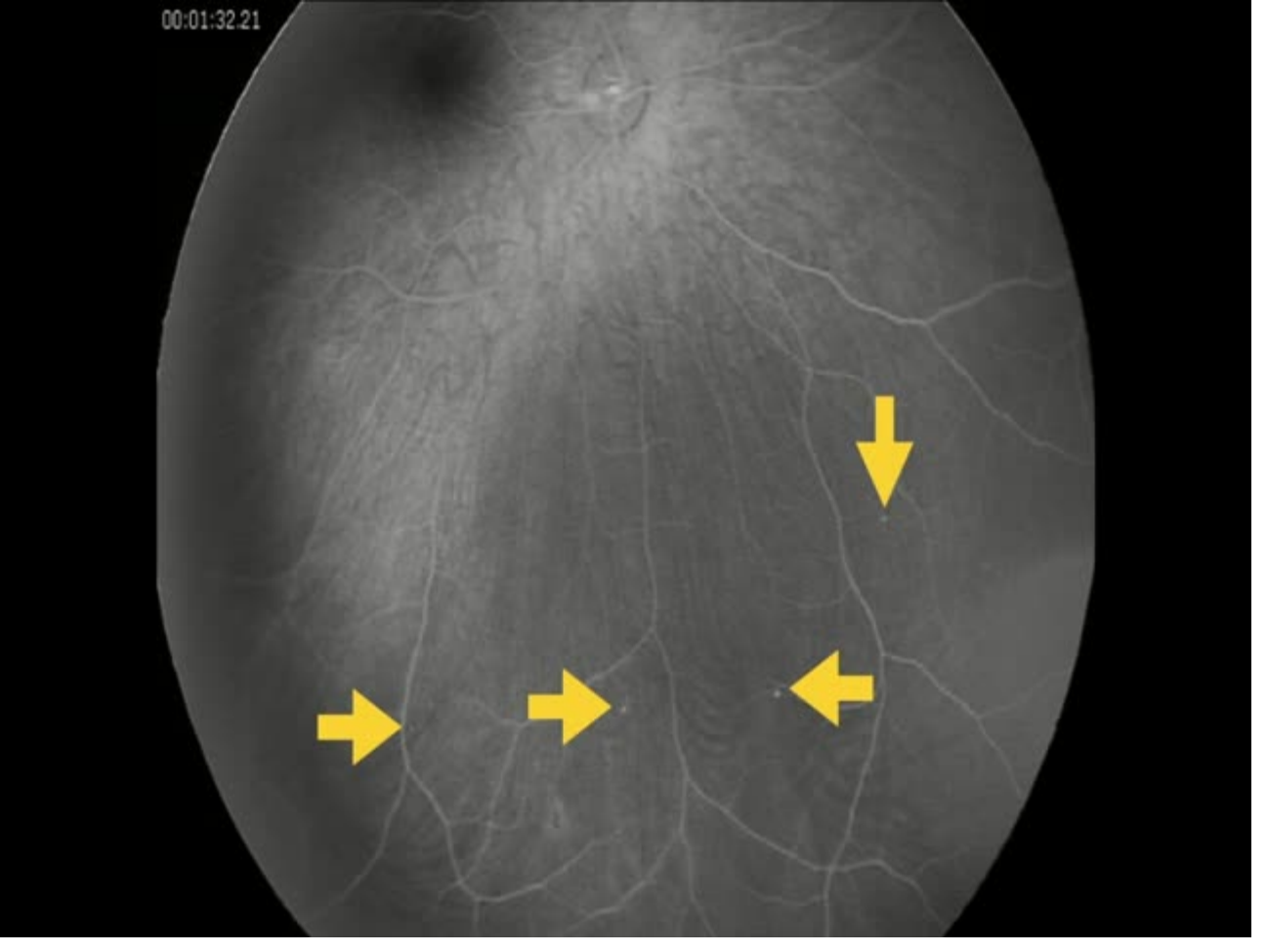
00:01:32.21

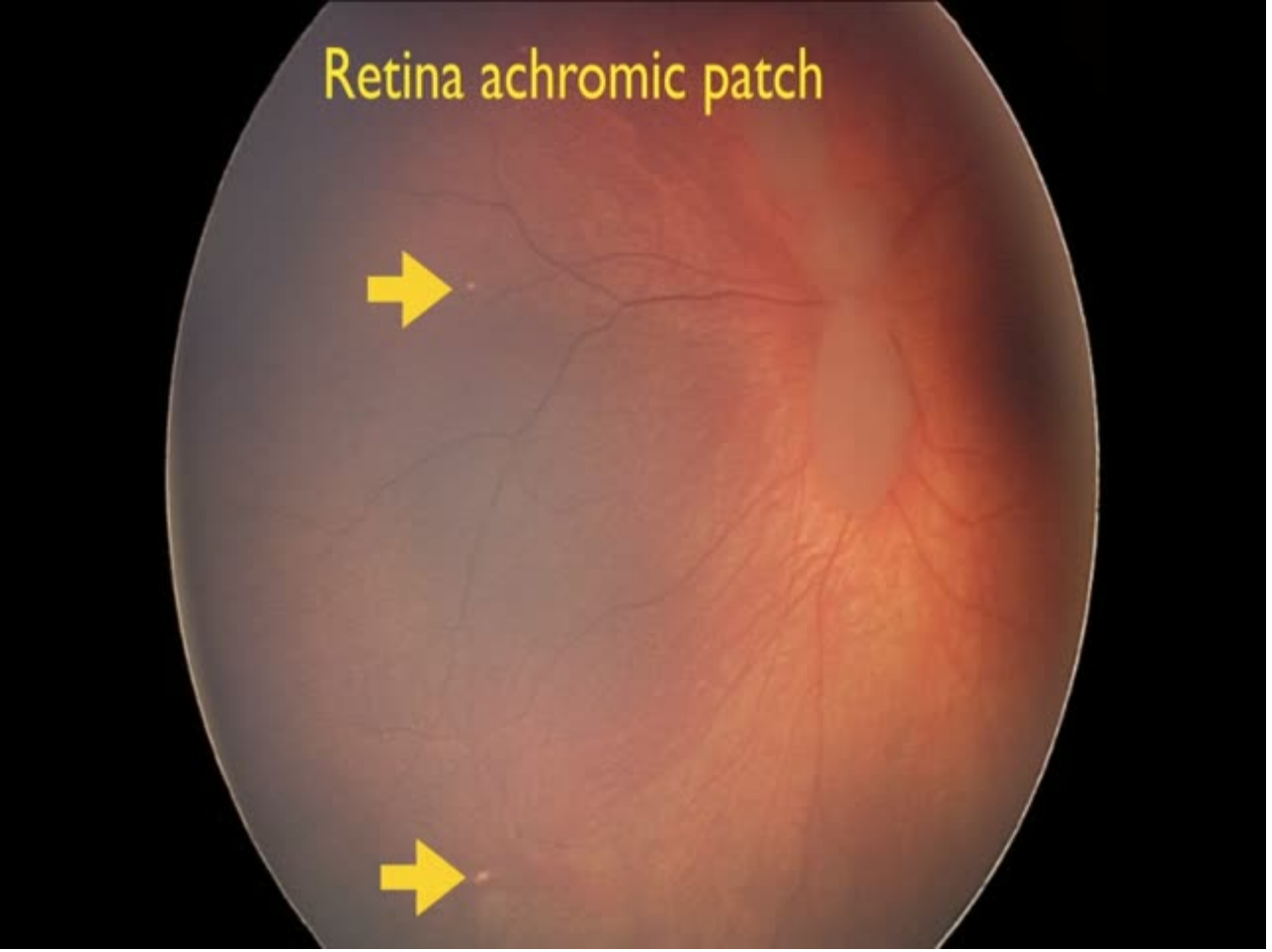
Retina achromic patch

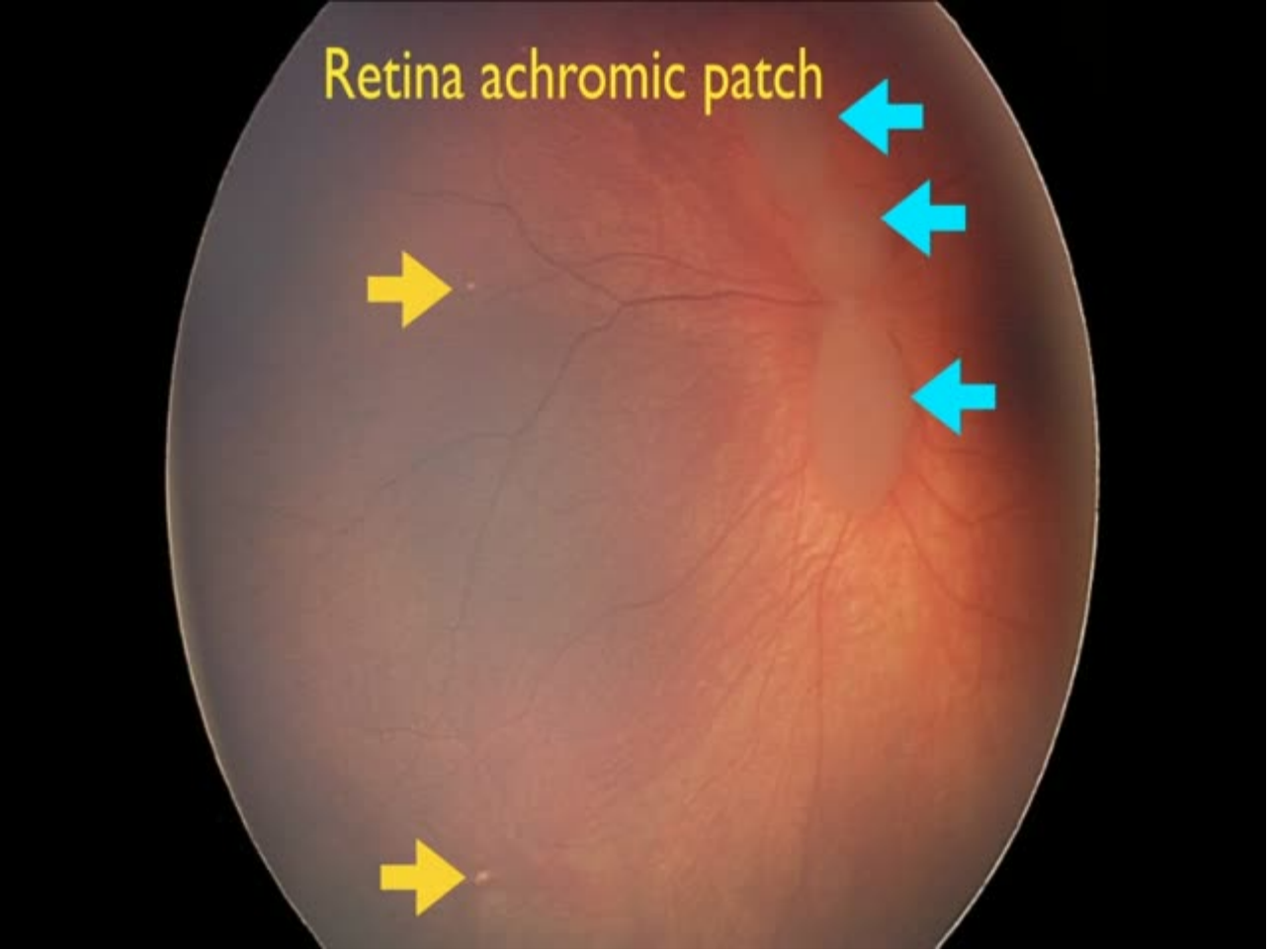
Retina achromic patch

Retinal Pigment Epithelial Depigmented Lesions Associated With Tuberous Sclerosis Complex

Carol L. Shields, MD
David A. Reichstein, MD
Carlos Bianciotto, MD
Jerry A. Shields, MD

Tuberous sclerosis complex (TSC) is a multisystem hamartomatous disorder that can occur in nearly every tissue in the body but primarily affects the skin, brain, and eye. Major and minor diagnostic criteria for TSC have been established by the Tuberous Sclerosis Consensus Conference in 1998[1] (eTable 1; http://www.archophthalmol.com). A diagnosis of definite TSC is established by the presence of 2 major features or 1

Retinal Pigment Epithelial Depigmented Lesions Associated With Tuberous Sclerosis Complex

Tuberous sclerosis
is a multisystem h
disorder that can
every tissue in the b
ily affects the skin,
Major and minor di
for TSC have been
the Tuberous Scler
Conference in 1998[1]
www.archophthalm
nosis of definite TSC
the presence of 2 ma

The most common eye finding of tuberous sclerosis is the retinal astrocytic hamartoma.[2] Other features include eyelid angiofibroma, iris atrophy, uveal coloboma, and retinal achromatic patch. The retinal achromatic patch is not clearly described, and this could represent a flat astrocytic hamartoma or retinal pigment epithelial (RPE) "punched-out" depigmentation.

Retinal Pigment Epithelial Depigmented Lesions Associated With Tuberous Sclerosis Complex

Tuberous sclerosis
is a multisystem h
disorder that can o
every tissue in the b
ily affects the skin,
Major and minor di
for TSC have been
the Tuberous Scler
Conference in 1998[1]
www.archophthalm
nosis of definite TSC
the presence of 2 ma

The most common eye finding of tuberous sclerosis is the retinal astrocytic hamartoma.[2] Other features include eyelid angiofibroma, iris atrophy, uveal coloboma, and retinal achromatic patch. The retinal achromatic patch is not clearly described, and this could represent a flat astrocytic hamartoma or retinal pigment epithelial (RPE) "punched-out" depigmentation.

Retinal Pigment Epithelial Depigmented Lesions Associated With Tuberous Sclerosis Complex

Tuberou
is a mu
disorde
every ti
ily affec
Major a
for TSC
the Tub
Confere
www.ar
nosis of
the presence of 2 major features or 1

Tuberous Sclerosis Complex [n=56]
retinal achromic patch in 12 (21%)
Related to ($p<0.05$)

- increased # retinal astrocytic hamartomas
- peripheral location RAH
- cognitive impairment
- seizures

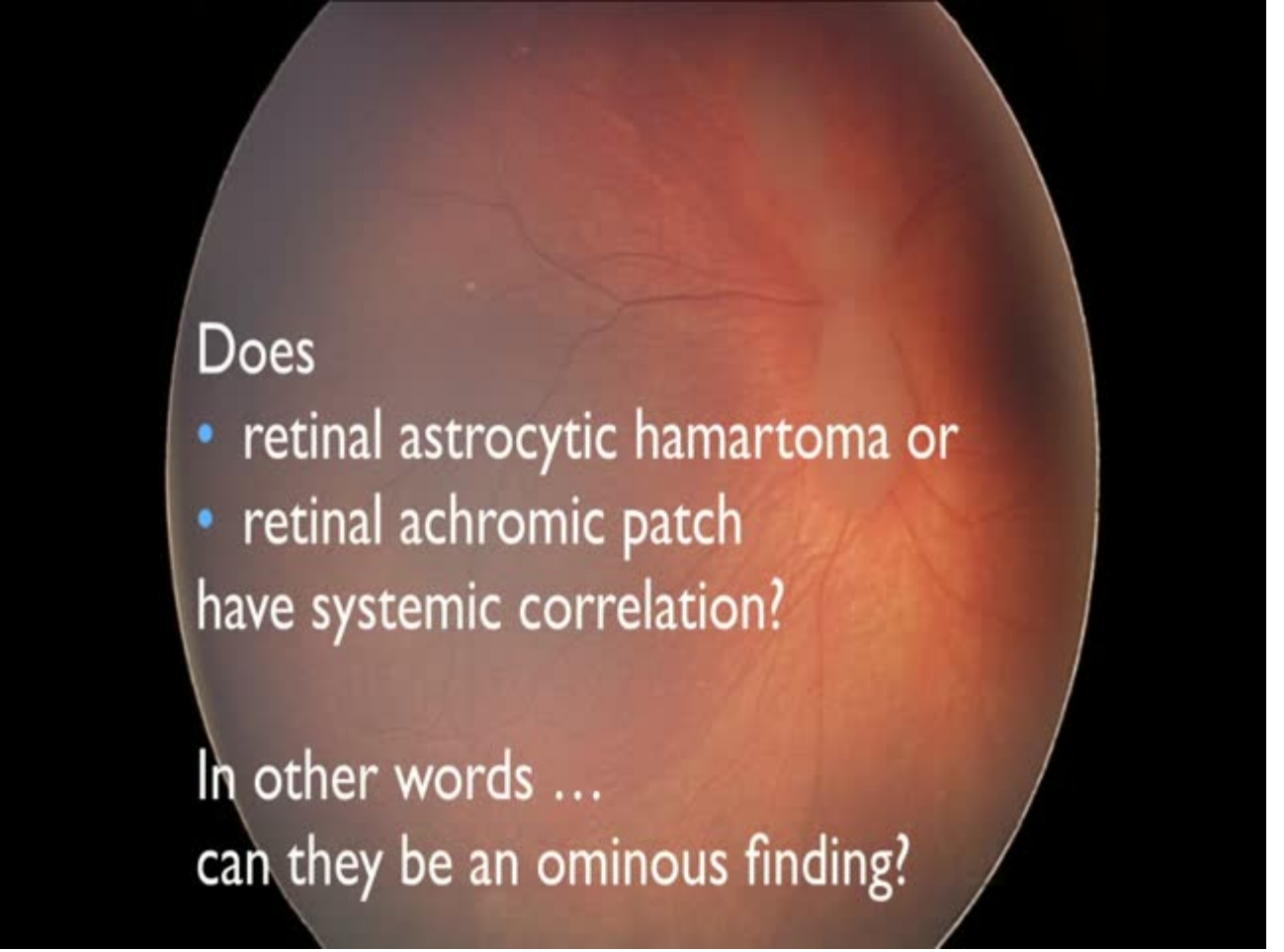
Does
• retinal astrocytic hamartoma or
• retinal achromic patch
have systemic correlation?
In other words …
can they be an ominous finding?

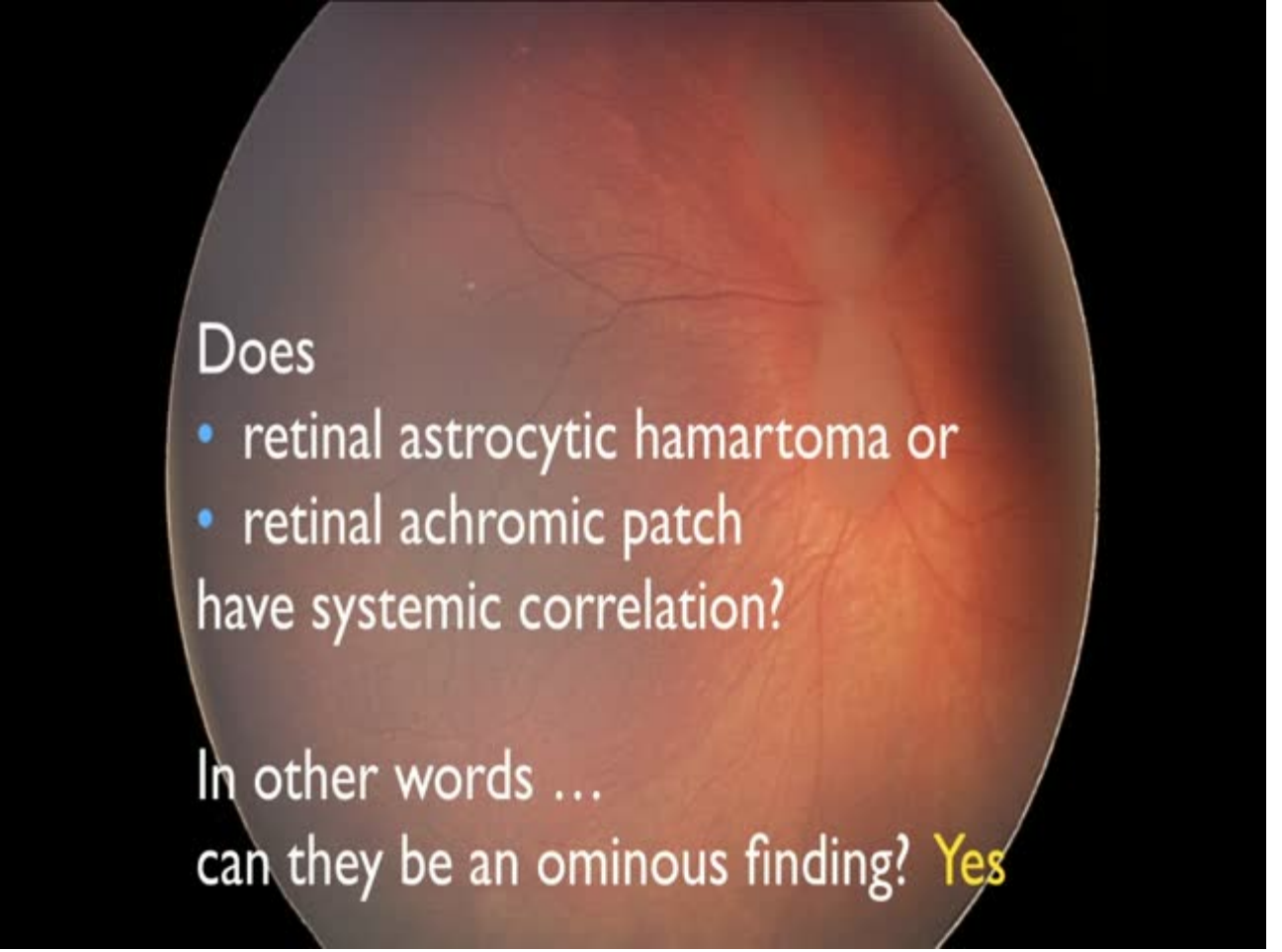
Does
• retinal astrocytic hamartoma or
• retinal achromic patch
have systemic correlation?
In other words …
can they be an ominous finding? Yes

Tuberous Sclerosis Complex: Genotype/Phenotype Correlation of Retinal Findings

Mary E. Aronow, MD,[1] Jo Anne Nakagawa, BS,[2,3] Ajay Gupta, MD,[2,4] Elias I. Traboulsi, MD,[1] Arun D. Singh, MD[1]

Objective: To evaluate genotype/phenotype correlations in individuals with astrocytic hamartoma (AH) and retinal achromic patch (AP) in the setting of tuberous sclerosis complex (TSC).

Design: Retrospective consecutive case series.

Participants: A total of 132 patients enrolled in the Cleveland Clinic Foundation Tuberous Sclerosis Program (CCF-TSCP) and 907 patients from the Tuberous Sclerosis Alliance (TSC-A).

Methods: Patient gender, age at TSC diagnosis, presence of *TSC1* or *TSC2* mutations, detailed ophthalmic examination findings, systemic manifestations, and whether or not the patient had a diagnosis of epilepsy or cognitive impairment were analyzed.

Main Outcome Measures: Genotype/phenotype correlation of retinal findings and systemic disease manifestations.

Results: No significant difference was found in the prevalence of AH or AP in the CCF-TSCP (36.1%) and TSC-A (34.1%) groups ($P = 0.743$). Astrocytic hamartomas were bilateral in 43.3% and 18.1% ($P = 0.009$) and multiple in 40.0% and 15.3% ($P = 0.008$) in the CCF-TSCP and TSC-A groups, respectively. In the CCF-TSCP group, the average number of AH was 4 (range, 2–7). Average tumor size was 1.0 disc diameter (range, 0.5–2.5 disc diameters). The most common location was along the arcades (41.5%), adjacent to the optic nerve (29.2%), and in the retinal periphery (27.7%). In the CCF-TSCP group, AP was observed in 12.0% of patients (40.0% bilateral, 50.0% multiple). The presence of retinal features was associated with giant cell astrocytoma (37.1% vs. 14.6%; $P = 0.018$), renal angiomyolipoma (60.0% vs. 27.1%; $P = 0.003$), cognitive impairment (77.1% vs. 43.8%; $P = 0.002$), and epilepsy (91.4% vs. 70.8% ($P = 0.022$) in those with and without retinal findings, respectively. In patients with retinal findings in both the CCF-TSCP and TSC-A groups, mutations in *TSC2* were more frequent than in *TSC1*, 3.3 times and 5.8 times, respectively; in those without retinal findings, the relative rates were 0.67 times and 2.3 times, respectively.

Conclusions: Individuals with retinal findings are more likely to have concomitant subependymal giant cell astrocytomas, renal angiomyolipomas, cognitive impairment, and epilepsy. *TSC2* mutations are more frequent in patients with retinal findings than in those without retinal findings.

Financial Disclosure(s): The author(s) have no proprietary or commercial interest in any materials discussed in this article. *Ophthalmology 2012;xx:xxx*

Tuberous Sclerosis Complex: Genotype/Phenotype Correlation of Retinal Findings

Tuberous Sclerosis Alliance n=907
Cleveland Clinic TSC program n=132
Astrocytic hamartoma 35%
Achromic patch 12%
If either lesion, pt at risk for
- subependymal giant cell astrocytoma
- renal angiomyolipoma
- cognitive impairment
- seizure

Conclusions: Individuals with retinal findings are more likely to have concomitant subependymal giant cell astrocytomas, renal angiomyolipomas, cognitive impairment, and epilepsy. *TSC2* mutations are more frequent in patients with retinal findings than in those without retinal findings.

Financial Disclosure(s): The author(s) have no proprietary or commercial interest in any materials discussed in this article. *Ophthalmology 2012;xx:xxx © 2012 by the American Academy of Ophthalmology.*

Tuberous Sclerosis Complex: Genotype/Phenotype Correlation of Retinal Findings

Tuberous Sclerosis Alliance n=907
Cleveland Clinic TSC program n=132
Astrocytic hamartoma 35%
Achromic patch 12%
If either lesion, pt at risk for
- subependymal giant cell astrocytoma
- renal angiomyolipoma
- co
- se

… so retinal findings imply greater risk for brain and kidney problems

RETINAL ASTROCYTIC HAMARTOMA

Optical Coherence Tomography Classification and Correlation With Tuberous Sclerosis Complex

FRANCESCO PICHI, MD,* DOMENICO MASSARO, MD,* MASSIMILIANO SERAFINO, MD,*
PAOLA CARRAI, MD,* GIAN P. GIULIARI, MD,†‡ CAROL L. SHIELDS, MD,§
CHIARA VERONESE, MD,¶ ANTONIO P. CIARDELLA, MD,¶ PAOLO NUCCI, MD*

Purpose: To propose a classification of retinal astrocytic hamartoma based on spectral domain optical coherence tomography and correlate each class with systemic manifestations of tuberous sclerosis complex.

Methods: Retrospective chart review conducted at four international referral medical retina centers. There were 43 consecutive patients with an established diagnosis of tuberous sclerosis complex based on presence of at least 2 major or 1 major and 2 minor features of the diagnostic criteria. Clinical and spectral domain optical coherence tomography features regarding retinal astrocytic hamartoma were documented.

Results: The mean patient age at presentation was 16.2 years. The retinal astrocytic hamartoma was classified as Type I (n = 41), Type II (n = 25), Type III (n = 20), or Type IV (n = 12). Patients with Type II showed greater number of cutaneous fibrous plaques (odds ratio = 64.8; 92% confidence interval: 64.2–65; $P < 0.001$); those with Type III displayed higher incidence of subependymal giant-cell astrocytomas (odds ratio = 43.2; 95% confidence interval: 43.0–43.3; $P < 0.001$); and those with Type IV showed higher incidence of pulmonary lymphangiomyomatosis (odds ratio = 126; 95% confidence interval: 122–128; $P < 0.001$).

Conclusion: Retinal astrocytic hamartoma can be classified into four morphologic groups, based on spectral domain optical coherence tomography. There are important systemic tuberous sclerosis complex correlations with each class.

RETINA 0:1–10, 2015

RETINAL ASTROCYTIC HAMARTOMA

Optical Coherence Tomography Classification and Correlation With Tuberous Sclerosis Complex

FRANCESCO PICHI, MD,* DOMENICO MASSARO, MD,* MASSIMILIANO SERAFINO, MD,*
PAOLA CARRAI, MD,* GIAN P. GIULIARI, MD,†‡ CAROL L. SHIELDS, MD,§
CHIARA VERONESE, MD,¶ ANTONIO P. CIARDELLA, MD,¶ PAOLO NUCCI, MD*

Purpose: To propose a classification of retinal astrocytic hamartoma based on spectral domain optical coherence tomography and correlate each class with systemic manifestations of tuberous sclerosis complex.

Methods: Retrospective chart review conducted at four international referral medical retina centers. There were 43 consecutive patients with an established diagnosis of tuberous sclerosis complex based on presence of at least 2 major or 1 major and 2 minor features of the diagnostic criteria. Clinical and spectral domain optical coherence tomography features regarding retinal astrocytic hamartoma were documented.

Results: The mean patient age at presentation was 16.2 years. The retinal astrocytic hamartoma was classified as Type I (n = 41), Type II (n = 25), Type III (n = 20), or Type IV (n = 12). Patients with Type II showed greater number of cutaneous fibrous plaques (odds ratio = 64.8; 92% confidence interval: 64.2–65; $P < 0.001$); those with Type III displayed higher incidence of subependymal giant-cell astrocytomas (odds ratio = 43.2; 95% confidence interval: 43.0–43.3; $P < 0.001$); and those with Type IV showed higher incidence of pulmonary lymphangiomyomatosis (odds ratio = 126; 95% confidence interval: 122–128; $P < 0.001$).

Conclusion: Retinal astrocytic hamartoma can be classified into four morphologic groups, based on spectral domain optical coherence tomography. There are important systemic tuberous sclerosis complex correlations with each class.

RETINA 0:1–10, 2015

RETINAL ASTROCYTIC HAMARTOMA

Optical Coherence Tomography Classification and Correlation With Tuberous Sclerosis Complex

FRANCESCO PICHI, MD,* DOMENICO MASSARO, MD,* MASSIMILIANO SERAFINO, MD,*
PAOLA CARRAI, MD,* GIAN P. GIULIARI, MD,†‡ CAROL L. SHIELDS, MD,§
CHIARA VERONESE, MD,¶ ANTONIO P. CIARDELLA, MD,¶ PAOLO NUCCI, MD*

Purpose: To propose a classification of retinal astrocytic hamartoma based on spectral domain optical
tations of tuber
Methods: R
retina centers.
tuberous sclero
features of the
tomography fe
Results: Th
hamartoma wa
12). Patients wi
64.8; 92% confidence interval: 64.2–65; $P < 0.001$); those with Type III displayed higher incidence of subependymal giant-cell astrocytomas (odds ratio = 43.2; 95% confidence interval: 43.0–43.3; $P < 0.001$); and those with Type IV showed higher incidence of pulmonary lymphangiomyomatosis (odds ratio = 126; 95% confidence interval: 122–128; $P < 0.001$).

Conclusion: Retinal astrocytic hamartoma can be classified into four morphologic groups, based on spectral domain optical coherence tomography. There are important systemic tuberous sclerosis complex correlations with each class.

RETINA 0:1–10, 2015

n=43 cases
proposed classification based on spectral domain OCT

AMERICAN ACADEMY™
OF OPHTHALMOLOGY

Retinal Astrocytic Hamartoma Arises in Nerve Fiber Layer and Shows "Moth-Eaten" Optically Empty Spaces on Optical Coherence Tomography

Q1

Q2 Carol L. Shields, MD, Emil A.T. Say, MD, Timothy Fuller, MD, Saurabh Arora, MD, Wasim A. Samara, MD, Jerry A. Shields, MD

Q3 ***Purpose:*** To evaluate the specific spectral-domain (SD) optical coherence tomography (OCT) features of retinal astrocytic hamartoma (RAH) and the relationship of these features with tumor size and location.

Design: Retrospective case series.

Participants: Forty-seven eyes of 42 patients with RAH.

Methods: All patients with clinically confirmed RAH were imaged with fundus photography and SD OCT.

Main Outcome Measures: Precise OCT retinal location of RAH features and the relationship of patient age, visual acuity, tumor size, and tumor location to presence and size of intralesional optically empty spaces (OESs), appearing as so-called moth-eaten spaces.

Results: Of 42 patients with RAH, 36 (86%) had unilateral disease and 6 (14%) had bilateral disease. Systemic tuberous sclerosis complex was present in 8 patients (19%). The largest tumor (per eye) demonstrated mean basal diameter of 3.0 mm (median, 2.0 mm) and mean thickness of 1.9 mm (median, 1.8 mm). The mean tumor proximity to the foveola was 3.0 mm and that to the optic disc was 1.8 mm. Related features included subretinal fluid (n = 9; 19%), cystoid retinal edema (n = 6; 13%), retinal traction (n = 11; 23%), intralesional cavities (n = 28; 60%), and intralesional calcification (n = 29; 62%). On SD OCT, the tumor epicenter was in the nerve fiber layer (n = 47; 100%), with all other retinal layers appearing thinned or compressed. The tumor showed OES (n = 43; 91%), representing intralesional calcification or cavitation, and each OES showed a mean diameter of 327 μm (median, 200 μm). When comparing number of OESs per SD OCT cut through the mass, we found no relationship with patient age, tumor diameter and thickness, distance

AMERICAN ACADEMY™
OF OPHTHALMOLOGY

100% cases

91% mass

Retinal Astrocytic Hamartoma Arises in Nerve Fiber Layer and Shows "Moth-Eaten" Optically Empty Spaces on Optical Coherence Tomography

Q1

Q2 Carol L. Shields, MD, Emil A.T. Say, MD, Timothy Fuller, MD, Saurabh Arora, MD, Wasim A. Samara, MD, Jerry A. Shields, MD

Q3 ***Purpose:*** To evaluate the specific spectral-domain (SD) optical coherence tomography (OCT) features of retinal astrocytic hamartoma (RAH) and the relationship of these features with tumor size and location.

Design: Retrospective case series.

Participants: Forty-seven eyes of 42 patients with RAH.

Methods: All patients with clinically confirmed RAH were imaged with fundus photography and SD OCT.

Main Outcome Measures: Precise OCT retinal location of RAH features and the relationship of patient age, visual acuity, tumor size, and tumor location to presence and size of intralesional optically empty spaces (OESs), appearing as so-called moth-eaten spaces.

Results: Of 42 patients with RAH, 36 (86%) had unilateral disease and 6 (14%) had bilateral disease. Systemic tuberous sclerosis complex was present in 8 patients (19%). The largest tumor (per eye) demonstrated mean basal diameter of 3.0 mm (median, 2.0 mm) and mean thickness of 1.9 mm (median, 1.8 mm). The mean tumor proximity to the foveola was 3.0 mm and that to the optic disc was 1.8 mm. Related features included subretinal fluid (n = 9; 19%), cystoid retinal edema (n = 6; 13%), retinal traction (n = 11; 23%), intralesional cavities (n = 28; 60%), and intralesional calcification (n = 29; 62%). On SD OCT, the tumor epicenter was in the nerve fiber layer (n = 47; 100%), with all other retinal layers appearing thinned or compressed. The tumor showed OES (n = 43; 91%), representing intralesional calcification or cavitation, and each OES showed a mean diameter of 327 μm (median, 200 μm). When comparing number of OESs per SD OCT cut through the mass, we found no relationship with patient age, tumor diameter and thickness, distance

AMERICAN ACADEMY™
OF OPHTHALMOLOGY

100% cases

91% cases

Retinal Astrocytic Hamartoma Arises in Nerve Fiber Layer and Shows "Moth-Eaten" Optically Empty Spaces on Optical Coherence Tomography

Carol L. Shields, MD, Emil A.T. Say, MD, Timothy Fuller, MD, Saurabh Arora, MD, Wasim A. Samara, MD, Jerry A. Shields, MD

Purpose: To evaluate the specific spectral-domain (SD) optical coherence tomography (OCT) features of retinal astrocytic hamartoma (RAH) and the relationship of these features with tumor size and location.

Design: Retrospective case series.

Participants: Forty-seven eyes of 42 patients with RAH.

Methods: All patients with clinically confirmed RAH were imaged with fundus photography and SD OCT.

Main Outcome Measures: Precise OCT retinal location of RAH features and the relationship of patient age, visual acuity, tumor size, and tumor location to presence and size of intralesional optically empty spaces (OESs), appearing as so-called moth-eaten spaces.

Results: Of 42 patients with RAH, 36 (86%) had unilateral disease and 6 (14%) had bilateral disease. Systemic tuberous sclerosis complex was present in 8 patients (19%). The largest tumor (per eye) demonstrated mean basal diameter of 3.0 mm (median, 2.0 mm) and mean thickness of 1.9 mm (median, 1.8 mm). The mean tumor proximity to the foveola was 3.0 mm and that to the optic disc was 1.8 mm. Related features included subretinal fluid (n = 9; 19%), cystoid retinal edema (n = 6; 13%), retinal traction (n = 11; 23%), intralesional cavities (n = 28; 60%), and intralesional calcification (n = 29; 62%). On SD OCT, the tumor epicenter was in the nerve fiber layer (n = 47; 100%), with all other retinal layers appearing thinned or compressed. The tumor showed OES (n = 43; 91%), representing intralesional calcification or cavitation, and each OES showed a mean diameter of 327 μm (median, 200 μm). When comparing number of OESs per SD OCT cut through the mass, we found no relationship with patient age, tumor diameter and thickness, distance

AMERICAN ACADEMY™ OF OPHTHALMOLOGY

100% cases

91% cases

Retinal Astrocytic Hamartoma Arises in Nerve Fiber Layer and Shows "Moth-Eaten" Optically Empty Spaces on Optical Coherence Tomography

Q1

Q9 Carol L. Shields, MD, Emil A.T. Say, MD, Timothy Fuller, MD, Saurabh Arora, MD, Wasim A. Samara, MD, Jerry A. Shields, MD

Q3 ***Purpose:*** To evaluate the specific spectral-domain (SD) optical coherence tomography (OCT) features of retinal astrocytic hamartoma (RAH) and the relationship of these features with tumor size and location.

Design: Retrospective case series.

Participants: Forty-seven eyes of 42 patients with RAH.

Methods: All patients with clinically confirmed RAH were imaged with fundus photography and SD OCT.

Main Outcome Measures: Precise OCT r age, visual acuity, tumor size, and tumor location to ESs), appearing as so-called moth-eaten spaces.

Results: Of 42 patients with RAH, 36 (8 ase. Systemic tuberous sclerosis complex was p non- strated mean basal diameter of 3.0 mm (mec mm). The mean tumor proximity to the foveola was tures included subretinal fluid (n = 9; 19%), cyst 3%), intralesional cavities (n = 28; 60%), and in mor epicenter was in the nerve fiber layer (n = d or compressed. The tumor showed OES (n = 43; [redacted] and each OES showed a mean diameter of 327 μm (median, 200 μm). When comparing number of OESs per SD OCT cut through the mass, we found no relationship with patient age, tumor diameter and thickness, distance

n=47 eyes

retinal layer of origin

moth-eaten spaces

Retina astrocytic hamartoma

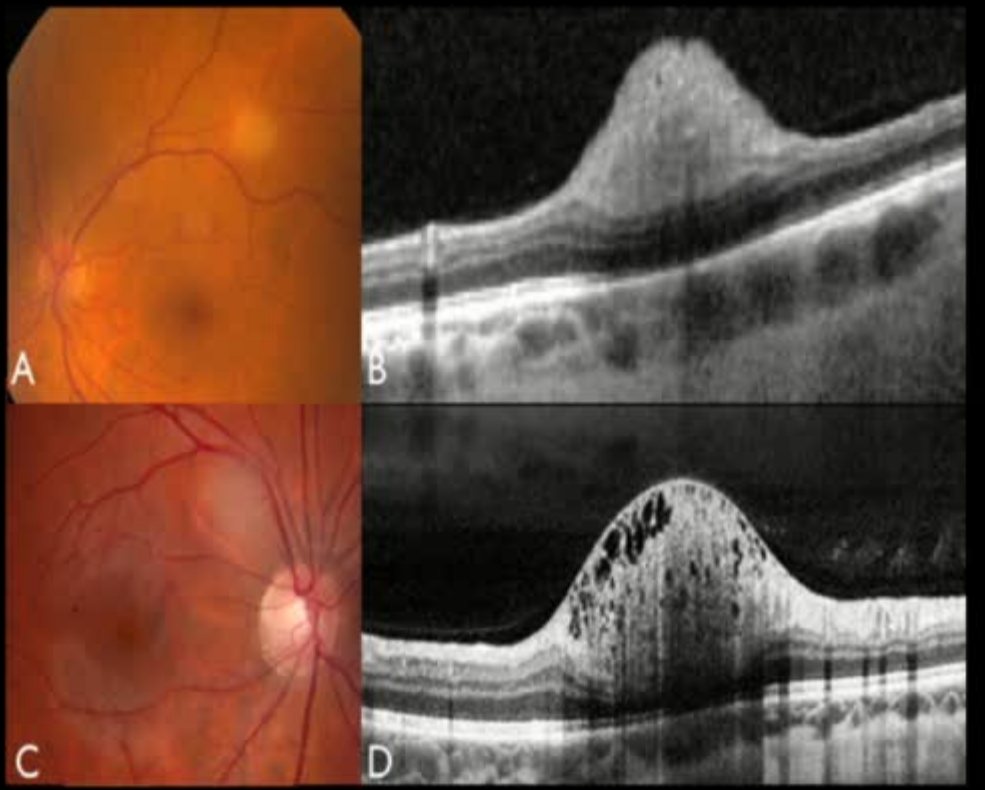

Retina astrocytic hamartoma

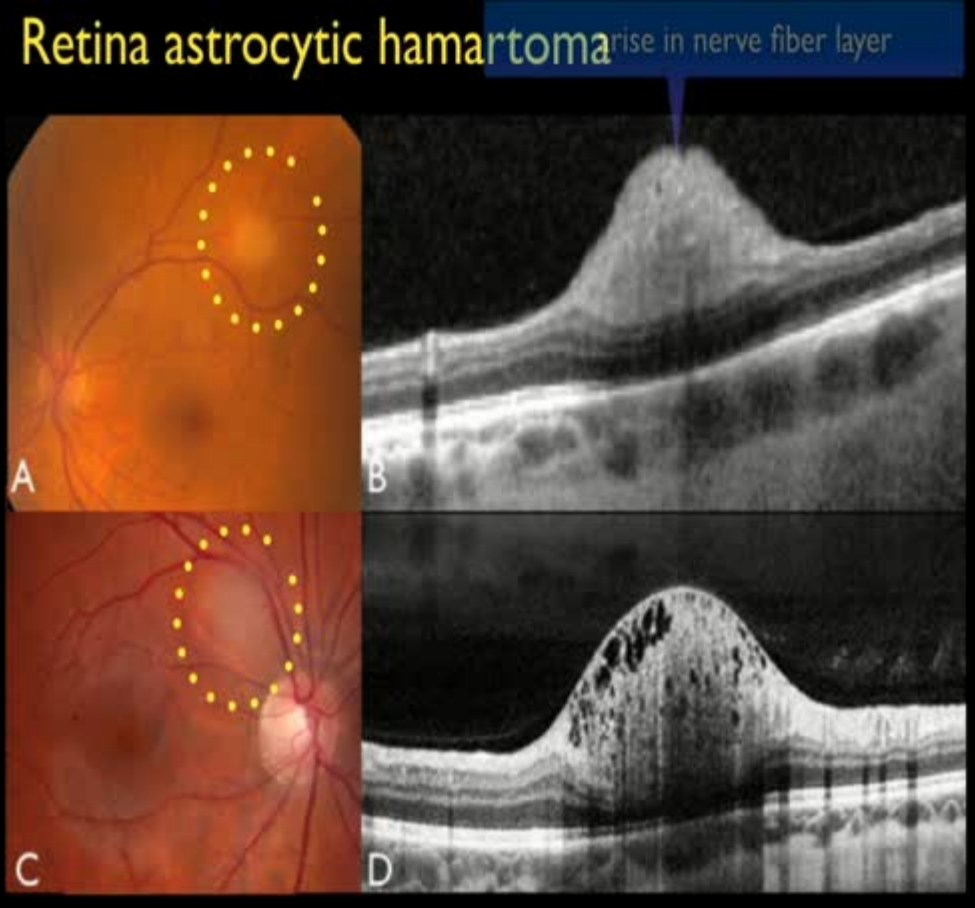

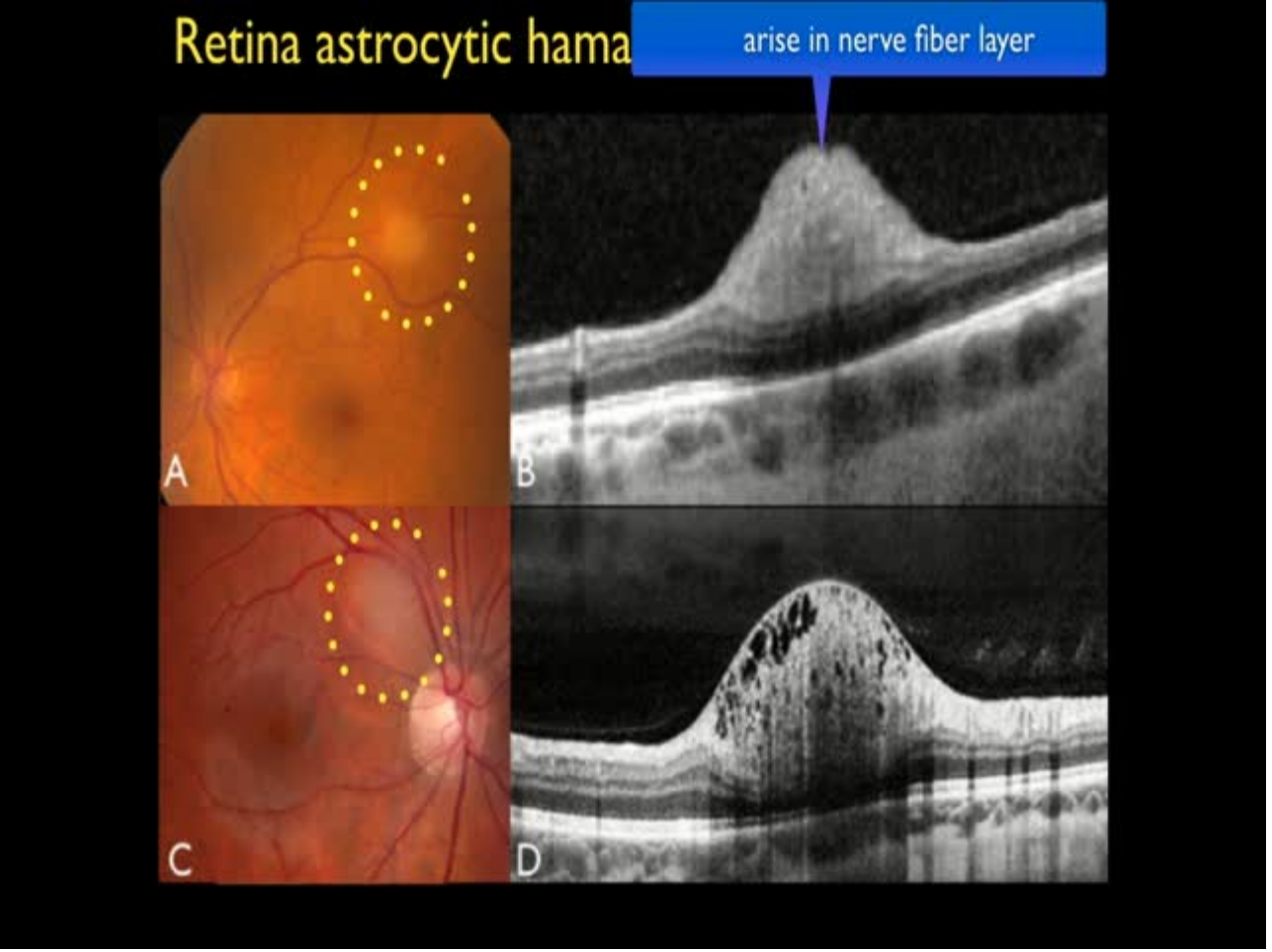
Retina astrocytic hama
arise in nerve fiber layer
A
B
C
D

Retina astrocytic hama

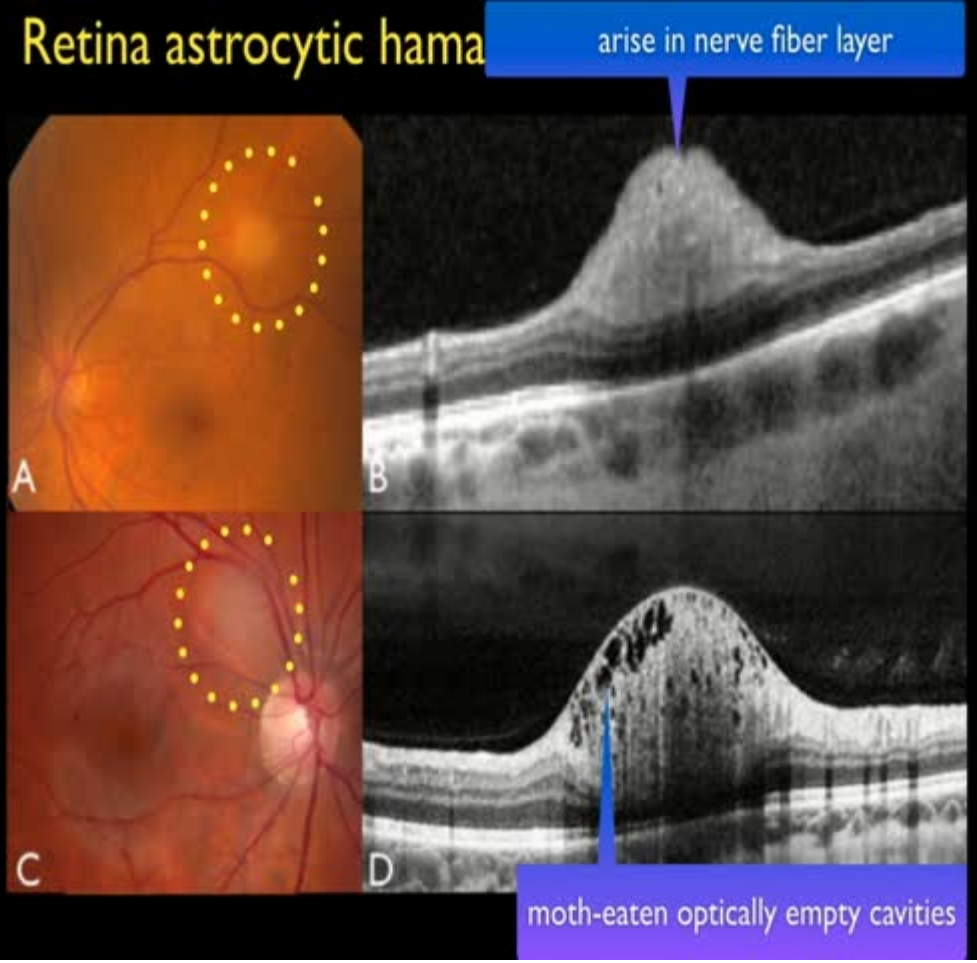

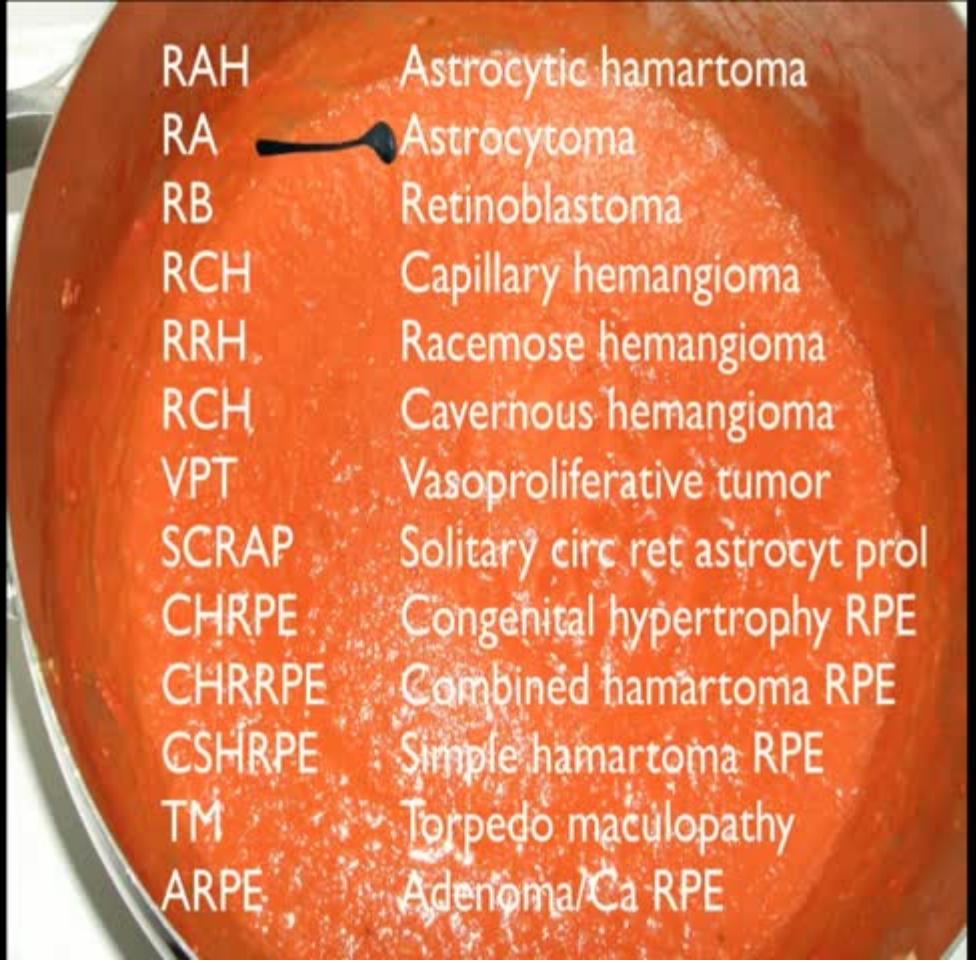
RAH Astrocytic hamartoma
RA Astrocytoma
RB Retinoblastoma
RCH Capillary hemangioma
RRH Racemose hemangioma
RCH Cavernous hemangioma
VPT Vasoproliferative tumor
SCRAP Solitary circ ret astrocyt prol
CHRPE Congenital hypertrophy RPE
CHRRPE Combined hamartoma RPE
CSHRPE Simple hamartoma RPE
TM Torpedo maculopathy
ARPE Adenoma/Ca RPE

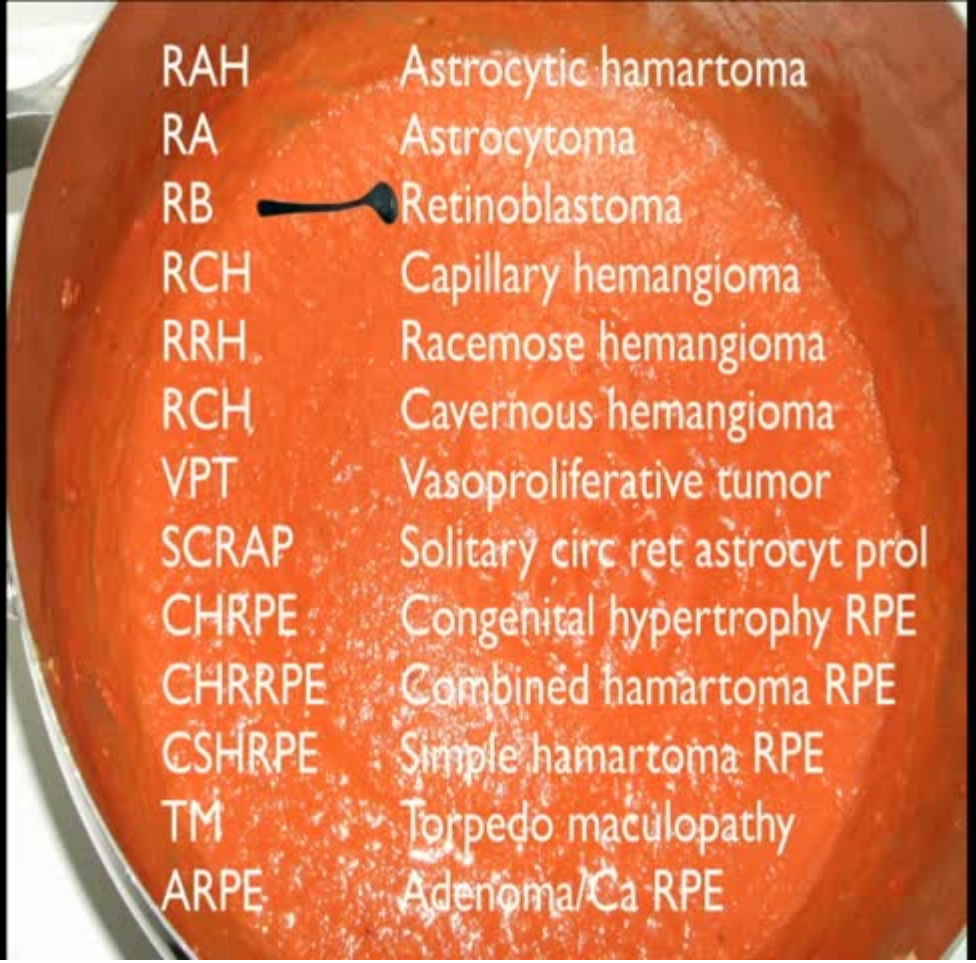
RAH Astrocytic hamartoma
RA Astrocytoma
RB Retinoblastoma
RCH Capillary hemangioma
RRH Racemose hemangioma
RCH Cavernous hemangioma
VPT Vasoproliferative tumor
SCRAP Solitary circ ret astrocyt prol
CHRPE Congenital hypertrophy RPE
CHRRPE Combined hamartoma RPE
CSHRPE Simple hamartoma RPE
TM Torpedo maculopathy
ARPE Adenoma/Ca RPE

Treatment of Retinoblastoma in 2015
Agreement and Disagreement

David H. Abramson, MD; Carol L. Shields, MD; Francis L. Munier, MD; Guillermo L. Chantada, MD, PhD

The management of intraocular retinoblastoma is rapidly changing, and even recent reviews on the subject are behind existing practices. The 4 authors of this report collectively represent their management strategies with an emphasis on areas of agreement and disagreement. Ophthalmic artery chemosurgery and intravitreous chemotherapy have completely replaced external beam radiotherapy, reduced the use of systemic chemotherapy, and diminished enucleations by 90% without evidence of compromising patient survival.

JAMA Ophthalmol. doi:10.1001/jamaophthalmol.2015.3108
Published online September 17, 2015.

Treatment of Retinoblastoma in 2015
Agreement and Disagreement

David H. Abramson, MD; Carol L. Shields, MD; Francis L. Munier, MD; Guillermo L. Chantada, MD, PhD

Buenos Aries

The management of intraocular retinoblastoma is rapidly changing, and even recent reviews on the subject are behind existing practices. The 4 authors of this report collectively represent their management strategies with an emphasis on areas of agreement and disagreement. Ophthalmic artery chemosurgery and intravitreous chemotherapy have completely replaced external beam radiotherapy, reduced the use of systemic chemotherapy, and diminished enucleations by 90% without evidence of compromising patient survival.

JAMA Ophthalmol. doi:10.1001/jamaophthalmol.2015.3108
Published online September 17, 2015.

Treatment of Retinoblastoma in 2015
Agreement and Disagreement

David H. Abramson, MD; Carol L. Shields, MD; Francis L. Munier, MD; Guillermo L. Chantada, MD, PhD

Brotherly LOVE Lausanne Buenos Aries

The management of intraocular retinoblastoma is rapidly changing, and even recent reviews on the subject are behind existing practices. The 4 authors of this report collectively represent their management strategies with an emphasis on areas of agreement and disagreement. Ophthalmic artery chemosurgery and intravitreous chemotherapy have completely replaced external beam radiotherapy, reduced the use of systemic chemotherapy, and diminished enucleations by 90% without evidence of compromising patient survival.

JAMA Ophthalmol. doi:10.1001/jamaophthalmol.2015.3108
Published online September 17, 2015.

Treatment of Retinoblastoma in 2015
Agreement and Disagreement

David H. Abramson, MD; Carol L. Shields, MD; Francis L. Munier, MD; Guillermo L. Chantada, MD, PhD

Big Apple | Brotherly LOVE | Lausanne | Buenos Aries

The management of intraocular retinoblastoma is rapidly changing, and even recent reviews on the subject are behind existing practices. The 4 authors of this report collectively represent their management strategies with an emphasis on areas of agreement and disagreement. Ophthalmic artery chemosurgery and intravitreous chemotherapy have completely replaced external beam radiotherapy, reduced the use of systemic chemotherapy, and diminished enucleations by 90% without evidence of compromising patient survival.

JAMA Ophthalmol. doi:10.1001/jamaophthalmol.2015.3108
Published online September 17, 2015.

Treatment of Retinoblastoma in 2015
Agreement and Disagreement

David H. Abramson, MD; Carol L. Shields, MD; Francis L. Munier, MD; Guillermo L. Chantada, MD, PhD

Big Apple | Brotherly LOVE | Lausanne | Buenos Aries

The management of intraocular retinoblastoma is rapidly changing, and even recent reviews on the subject are behind existing practices. The 4 authors of this report collectively represent their management strategies with an emphasis on areas of agreement and disagreement. Ophthalmic artery chemosurgery and intravitreous chemotherapy have completely replaced external beam radiotherapy, reduced the use of systemic chemotherapy, and diminished enucleations by 90% without evidence of compromising patient survival.

JAMA Ophthalmol. doi:10.1001/jamaophthalmol.2015.3108
Published online September 17, 2015.

Treatment of Retinoblastoma in 2015
Agreement and Disagreement

David H. Abramson, MD; Carol L. Shields, MD; Francis L. Munier, MD; Guillermo L. Chantada, MD, PhD

Big Apple | Brotherly LOVE | Lausanne | Buenos Aries

The management of intraocular retinoblastoma is rapidly changing, and even recent reviews on the subject are behind existing practices. The 4 authors of this report collectively

Agreement and Disagreement
Huge progress
Most successfully treated pediatric cancer

erapy,
al.

JAMA Ophthalmol. doi:10.1001/jamaophthalmol.2015.3108
Published online September 17, 2015.

Treatment of Retinoblastoma in 2015
Agreement and Disagreement

David H. Abramson, MD; Carol L. Shields, MD; Francis L. Munier, MD; Guillermo L. Chantada, MD, PhD

Targeted retinoblastoma management: when to use intravenous, intra-arterial, periocular, and intravitreal chemotherapy

Carol L. Shields[a], Sara E. Lally[a], Ann M. Leahey[b], Pascal M. Jabbour[c], Emi H. Caywood[d], Rachel Schwendeman[a], and Jerry A. Shields[a]

Purpose of review

The management of retinoblastoma is complex and involves strategically chosen methods of enucleation, radiotherapy, chemotherapy, laser photocoagulation, thermotherapy, and cryotherapy. Chemotherapy has become the most common eye-sparing modality. There are four routes of delivery of chemotherapy for retinoblastoma, including intravenous, intra-arterial, periocular, and intravitreal techniques. The purpose of this review is to discuss the current rationale for each method and the anticipated outcomes.

Recent findings

The diagnosis of retinoblastoma should be clinically established prior to embarking on a chemotherapy

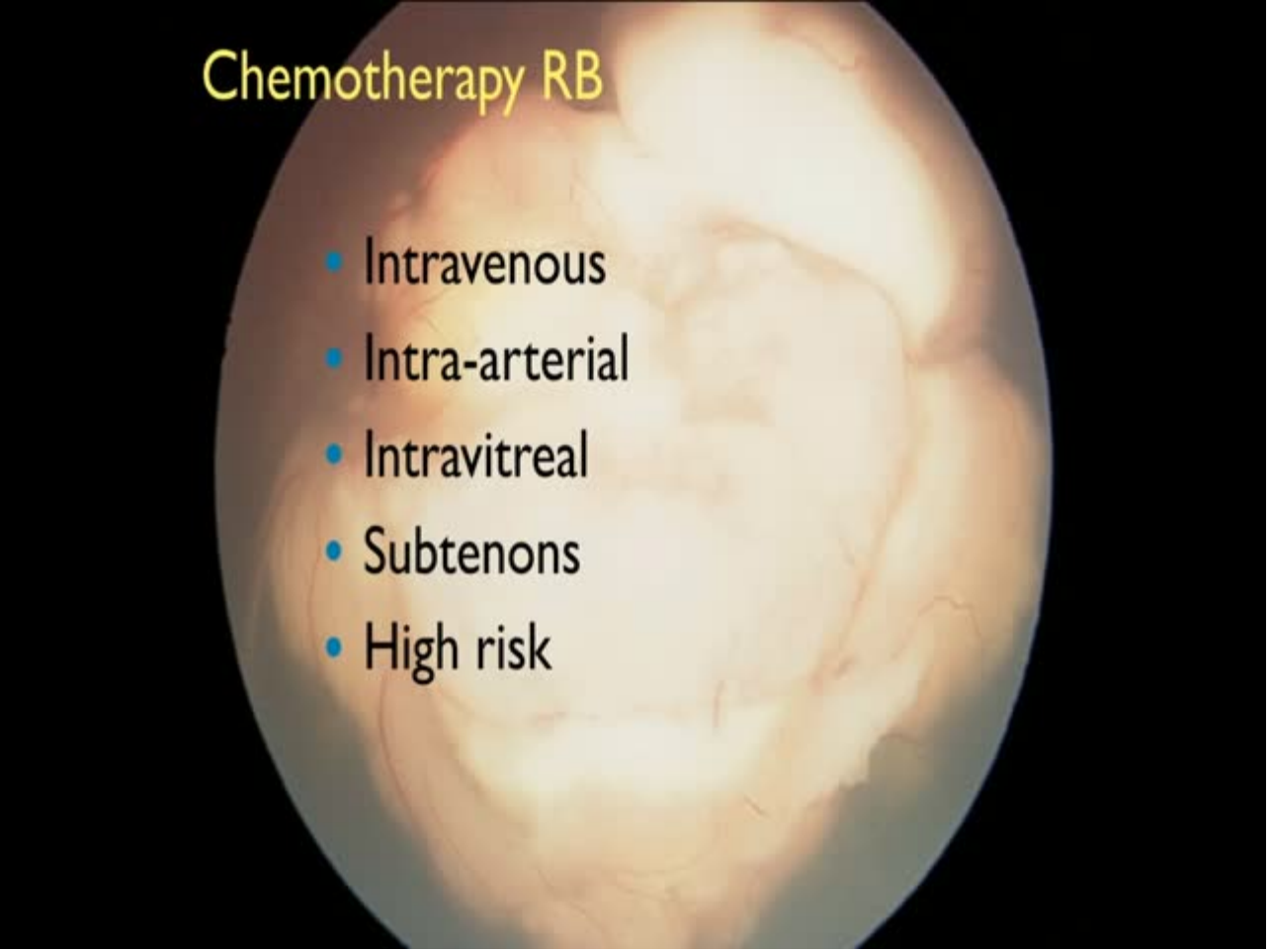
Chemotherapy RB
• Intravenous
• Intra-arterial
• Intravitreal
• Subtenons
• High risk

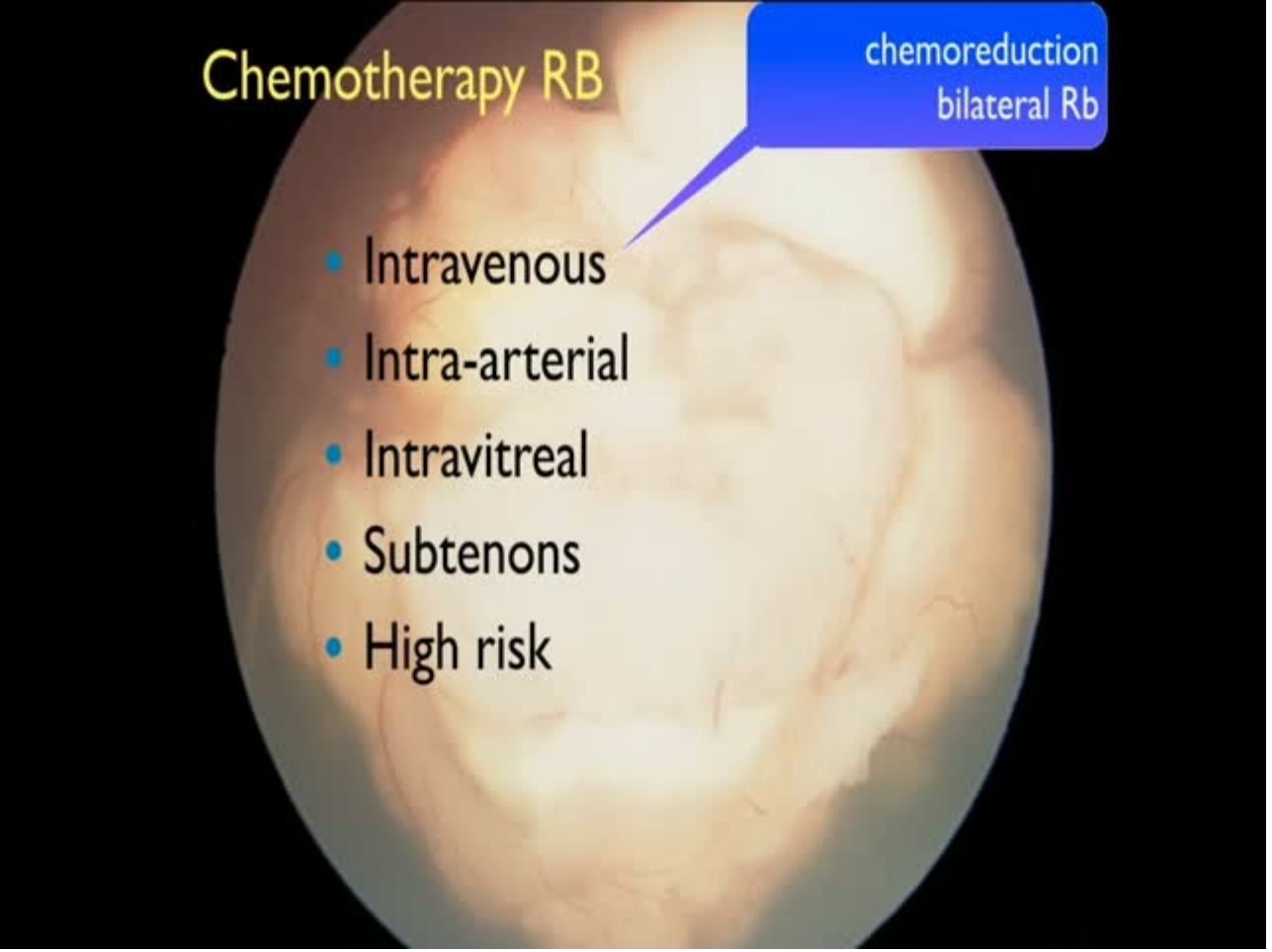
Chemotherapy RB
chemoreduction
bilateral Rb
• Intravenous
• Intra-arterial
• Intravitreal
• Subtenons
• High risk

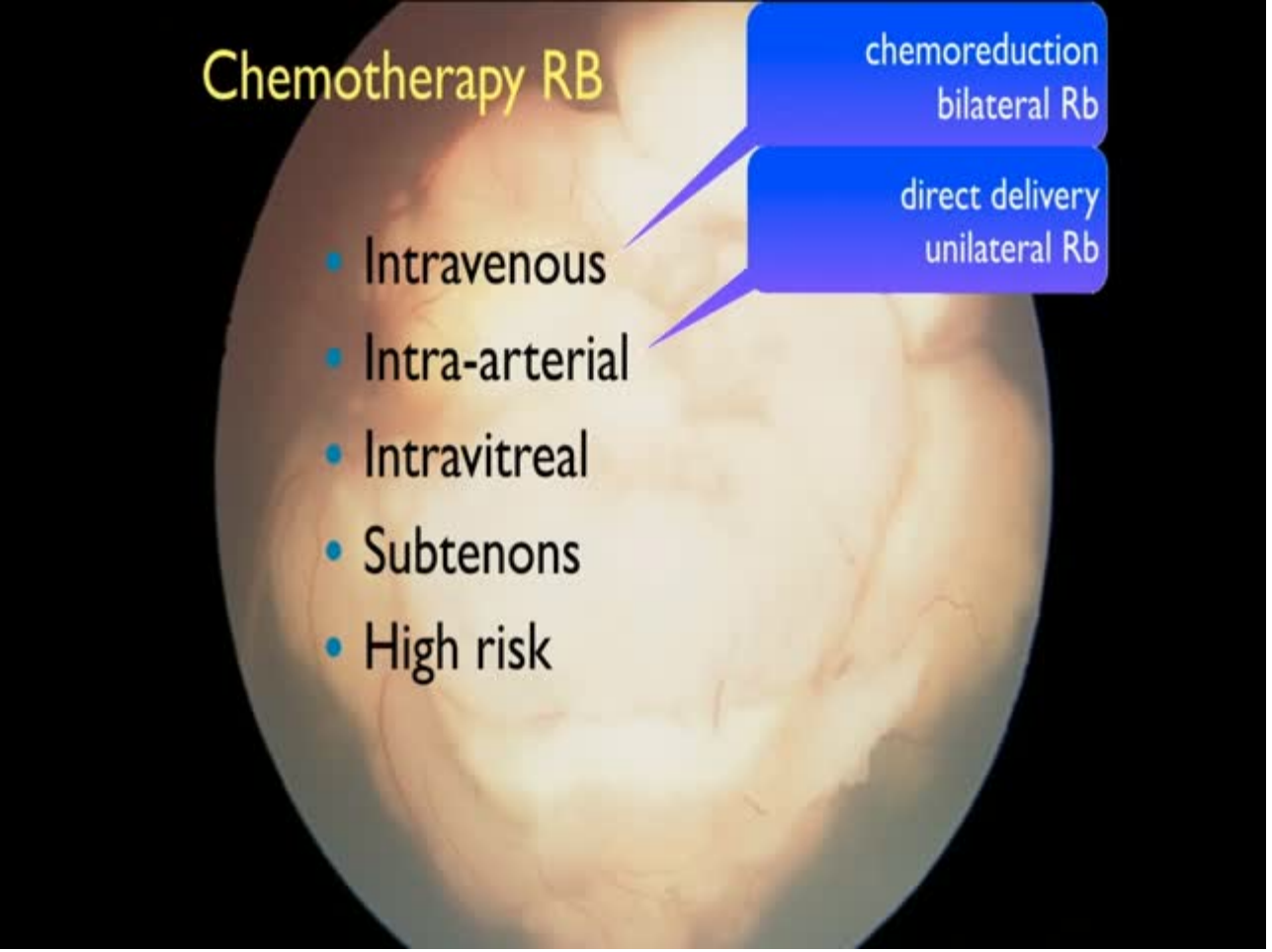
Chemotherapy RB
chemoreduction
bilateral Rb
direct delivery
unilateral Rb
• Intravenous
• Intra-arterial
• Intravitreal
• Subtenons
• High risk

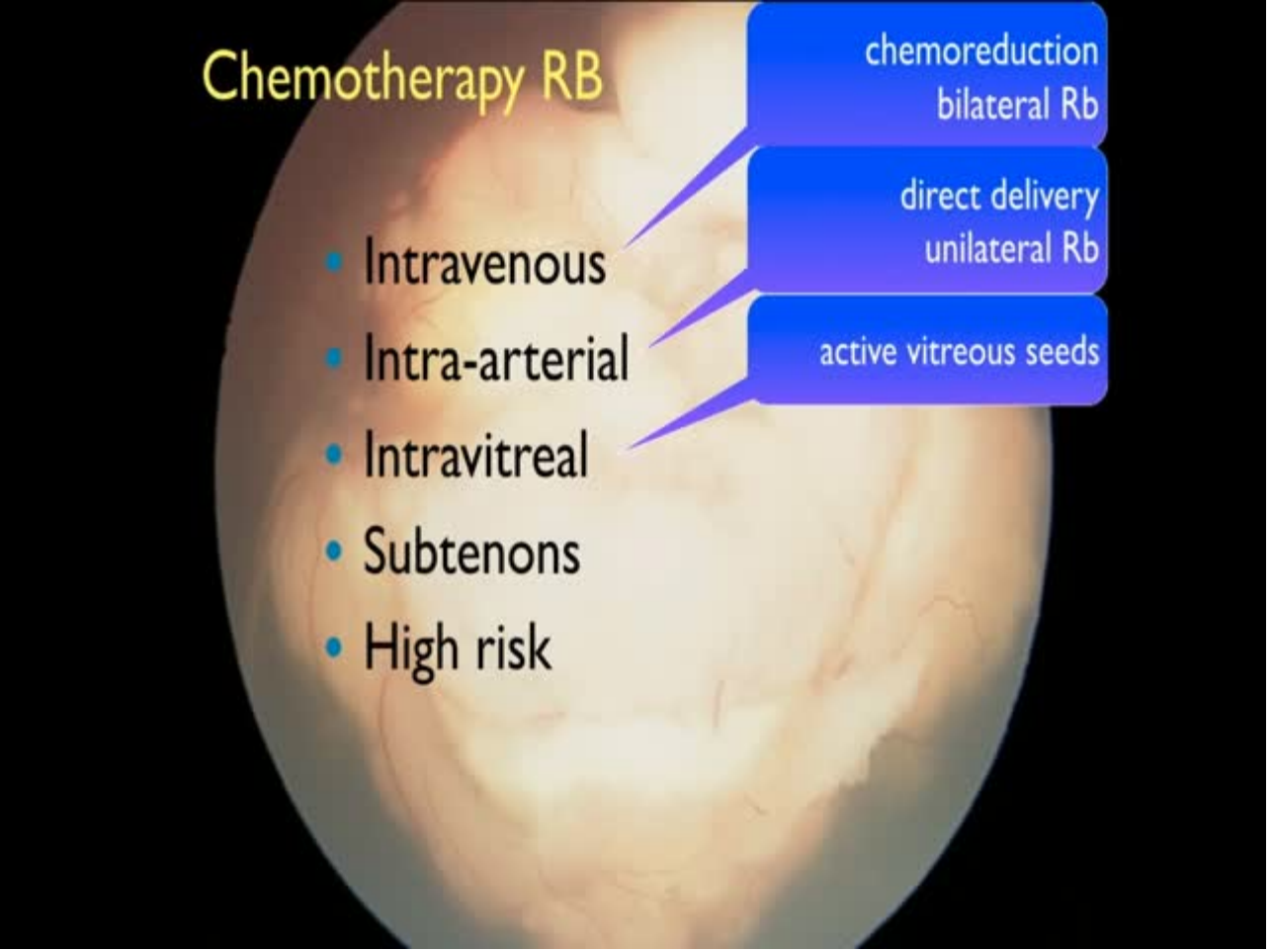
Chemotherapy RB
Intravenous
Intra-arterial
Intravitreal
Subtenons
High risk
chemoreduction
bilateral Rb
direct delivery
unilateral Rb
active vitreous seeds

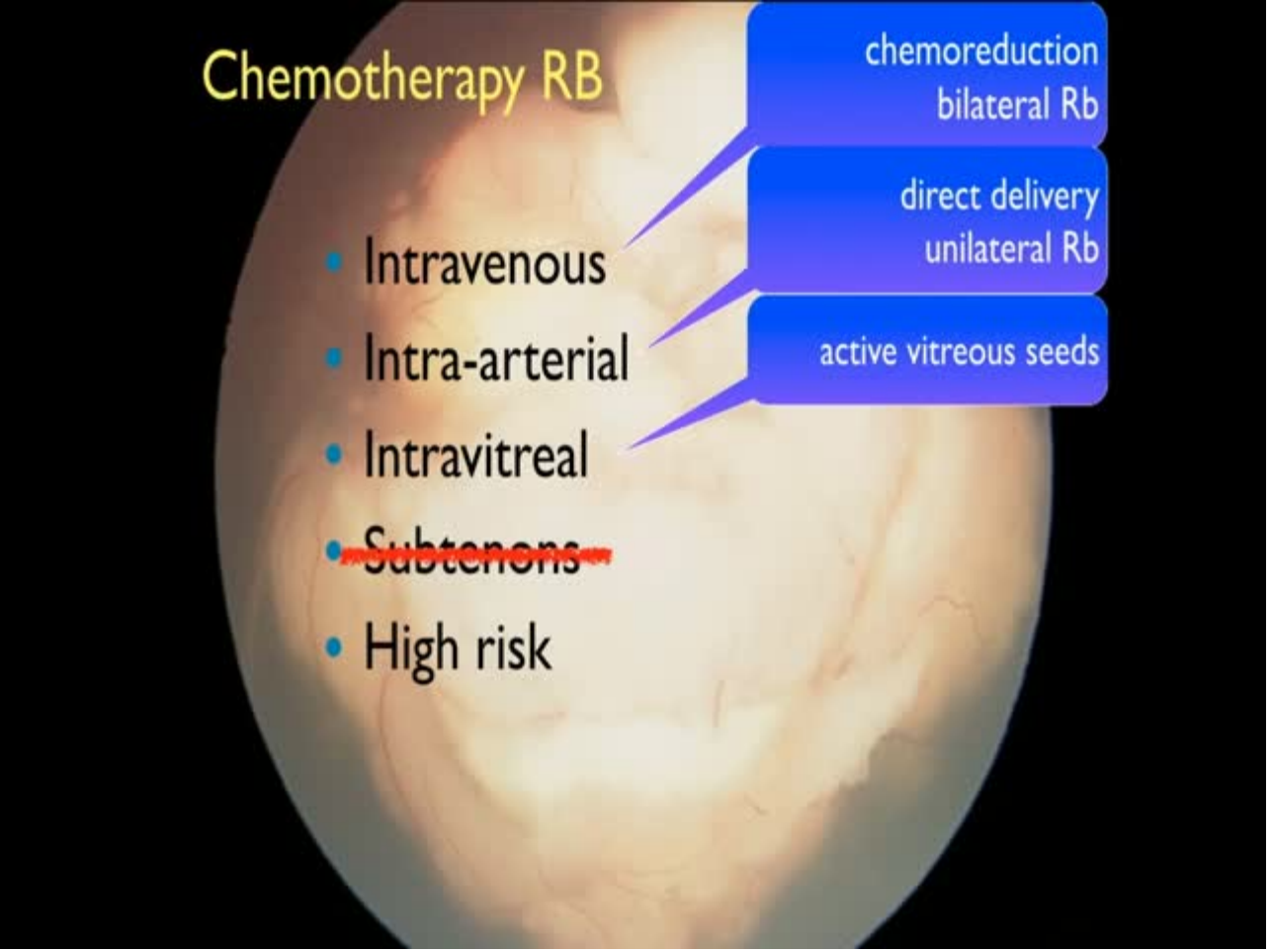
Chemotherapy RB
Intravenous
Intra-arterial
Intravitreal
~~Subtenons~~
High risk
chemoreduction
bilateral Rb
direct delivery
unilateral Rb
active vitreous seeds

Chemotherapy RB

- Intravenous
- Intra-arterial
- Intravitreal
- ~~Subtenons~~
- High risk

chemoreduction
bilateral Rb

direct delivery
unilateral Rb

active vitreous seeds

prevent metastasis

Chemotherapy RB

- Intravenous
- Intra-arterial
- Intravitreal
- ~~Subtenons~~
- High risk

chemoreduction
bilateral Rb

direct delivery
unilateral Rb

active vitreous seeds

prevent metastasis

Art and science, not a recipe

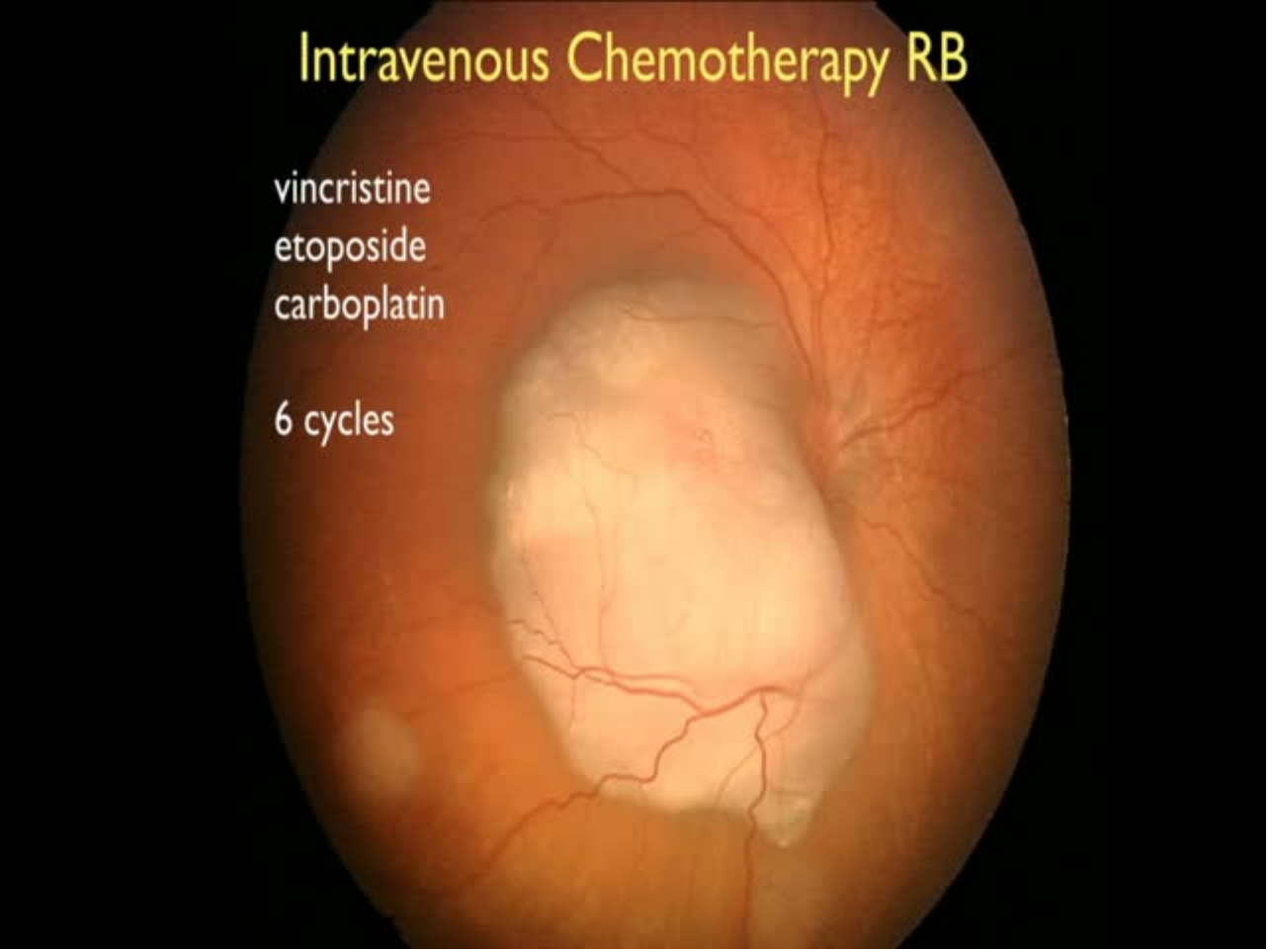
Intravenous Chemotherapy RB
vincristine
etoposide
carboplatin
6 cycles

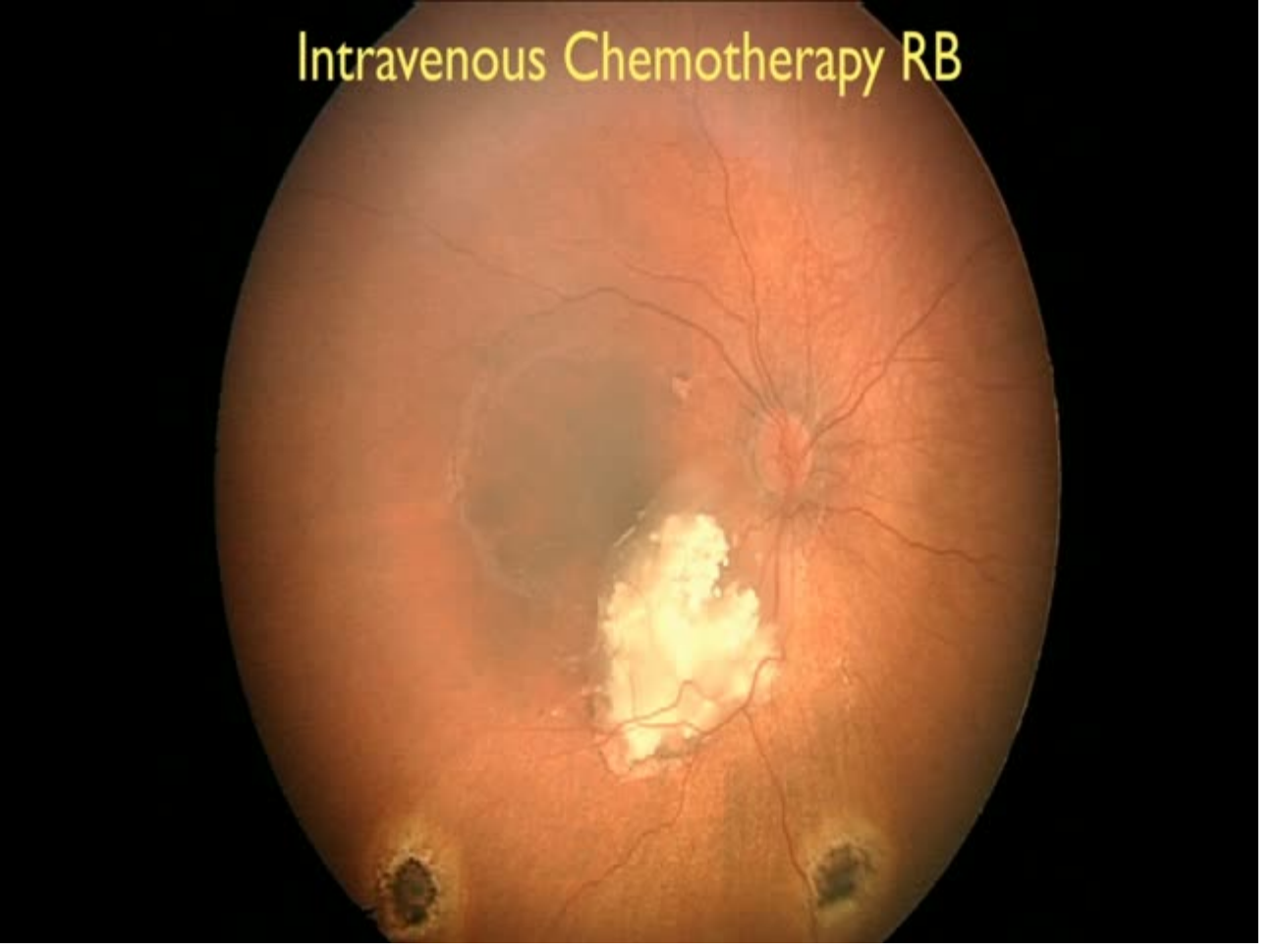
Intravenous Chemotherapy RB


Intra-arterial Chemotherapy RB
T1

Intra-arterial Chemotherapy RB

Intra-arterial Chemotherapy RB

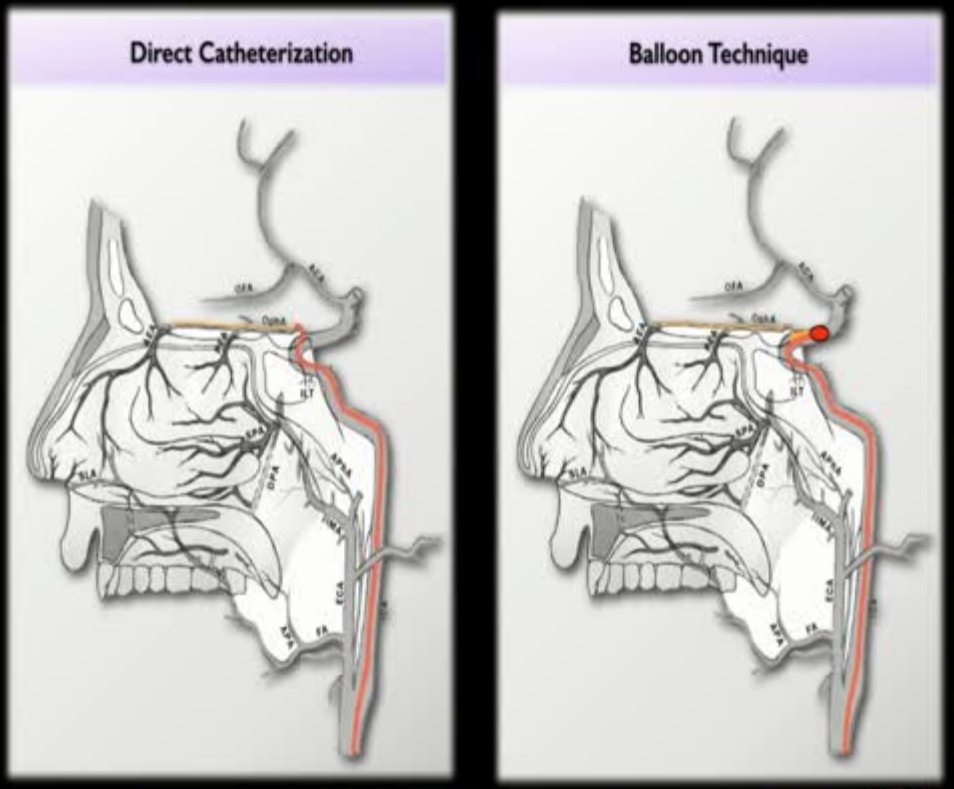

Intra-arterial Chemotherapy RB


Head to Head
Comparison


Head to Head
Comparison
IVC vs IAC for
Unilateral Rb

Asia Pac J Ophthalmol 2016

Unilateral Retinoblastoma Managed With Intravenous Chemotherapy Versus Intra-Arterial Chemotherapy. Outcomes Based on the International Classification of Retinoblastoma

Carol L. Shields, MD, Rodrigo Jorge, MD, PhD,*† Emil Anthony T. Say, MD,* George Magrath, MD,* Adel Alset, MD,* Emi Caywood, MD,‡ Ann M. Leahey, MD,§ Pascal Jabbour, MD,¶ and Jerry A. Shields, MD**

Purpose: The objective of this study was to compare outcomes after intravenous chemotherapy (IVC) versus intra-arterial chemotherapy (IAC) for unilateral retinoblastoma.

Design: A retrospective comparative interventional case series.

Methods: Patients with unilateral retinoblastoma managed with either IVC using vincristine, etoposide, and carboplatin or IAC using melphalan with or without topotecan with a minimum of 1-year follow-up were compared. The primary outcome measure was globe salvage.

Results: Of 91 patients with unilateral retinoblastoma, IVC was employed in 42 (46%) cases and IAC in 49 (54%). By comparison (IVC vs IAC), patients in the IAC group had greater mean tumor diameter (14 vs 18 mm, $P < 0.001$) and thickness (7 vs 10 mm, $P = 0.001$), greater percentage with active vitreous seeds (29% vs 55%, $P = 0.01$), and greater total retinal detachment (10% vs 43%, $P < 0.001$). There were no cases of group A in either treatment arm. Globe salvage was not significantly different in groups B, C, or E, but there was significantly improved globe salvage with IAC for group D (48% vs 91%, $P = 0.004$). Control was significantly better with IAC for solid tumor (62% vs 92%, $P = 0.002$), subretinal seeds (31% vs 86%, $P = 0.006$), and vitreous seeds (25% vs 74%, $P = 0.006$). There were no patients with pinealoblastoma, second cancer, metastasis, or death in either group.

Conclusions: For unilateral retinoblastoma, IAC provided significantly superior globe salvage compared with IVC for group D eyes. In addition, IAC provided significantly superior control for solid tumor, subretinal seeds, and vitreous seeds.

Key Words: retinoblastoma, intravenous chemotherapy, intra-arterial chemotherapy, chemoreduction

(*Asia Pac J Ophthalmol* 2016;00: 00-00)

Over the past 20 years, retinoblastoma management has witnessed a major shift in conservative therapy from radiotherapy to chemotherapy.[1-3] In the mid-1990s, intravenous chemotherapy (IVC, chemoreduction) was introduced with an unexpectedly high tumor control and globe salvage rate of more than 90% in eyes with minimal to moderate tumor [International Classification of Retinoblastoma (ICRB) groups A, B, and C] and approximately 50% for those with more advanced tumor (group D).[4-10] Enucleation has remained an important treatment for the most extreme retinoblastoma (group E) with massive intraocular disease, vitreous hemorrhage, secondary glaucoma, or eyes at risk for metastatic disease.[7,11] In the mid to late 2000s, superselective intra-arterial chemotherapy (IAC) was introduced for retinoblastoma management.[12-15] This modality was immediately found capable of controlling eyes with relatively advanced tumor that previously might have required enucleation.[16,17]

For the past 22 years we have employed IVC, and in the past 8 years we have used IAC in the management of retinoblastoma. There remains debate on which therapy is most suitable for unilateral and bilateral retinoblastoma.[18] Herein, we analyze our single-institution experience, comparing IVC versus IAC as primary therapy for unilateral retinoblastoma based on the ICRB.

MATERIALS AND METHODS

Patient Data

The medical records of all patients diagnosed with unilateral retinoblastoma and treated at the Ocular Oncology Service of Wills Eye Hospital, Thomas Jefferson University, from January

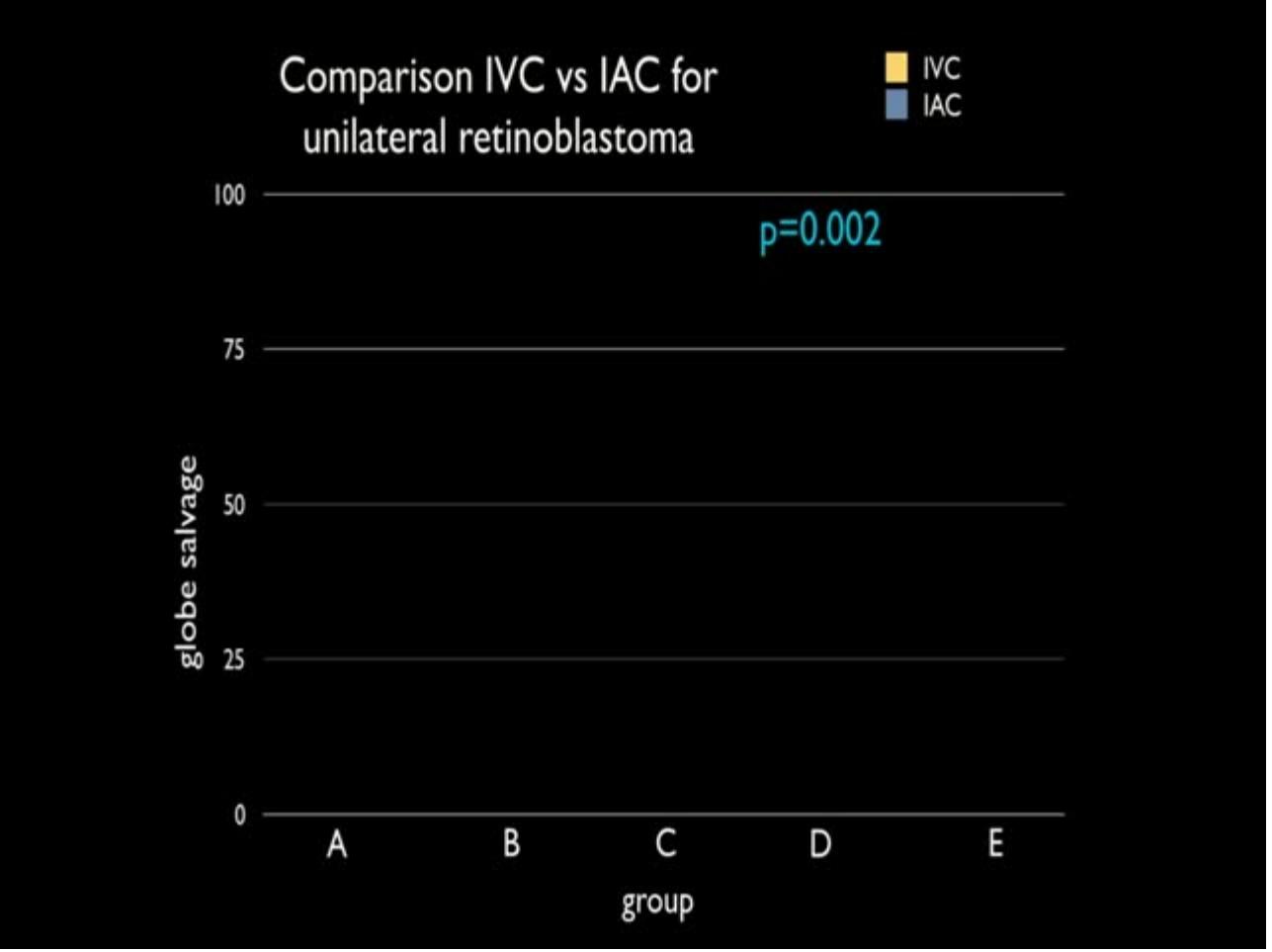
Comparison IVC vs IAC for
unilateral retinoblastoma
IVC
IAC
p=0.002
100
75
50
25
0
globe salvage
A
B
C
D
E
group

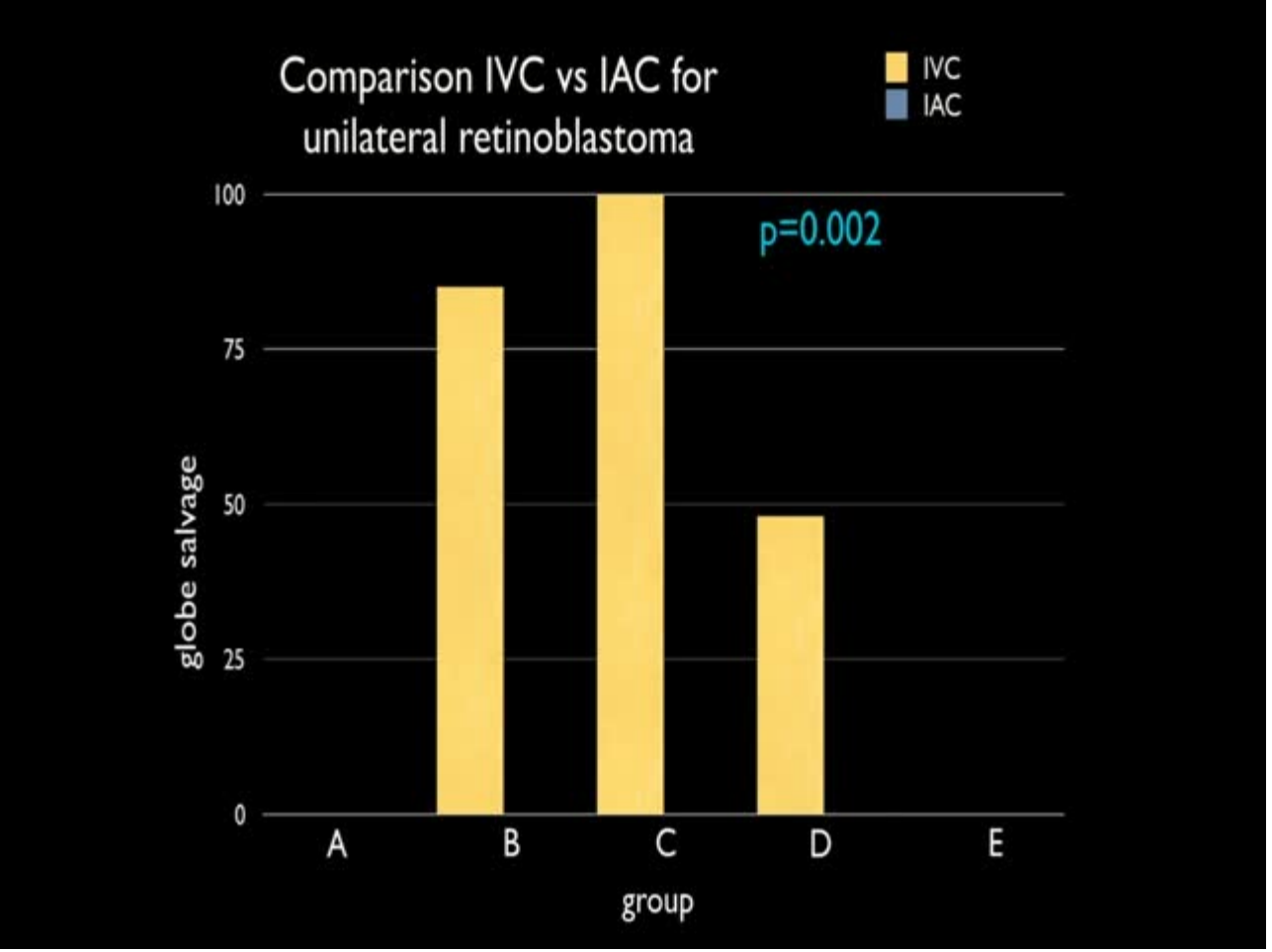
Comparison IVC vs IAC for
unilateral retinoblastoma
IVC
IAC
p=0.002
100
75
50
25
0
globe salvage
A
B
C
D
E
group

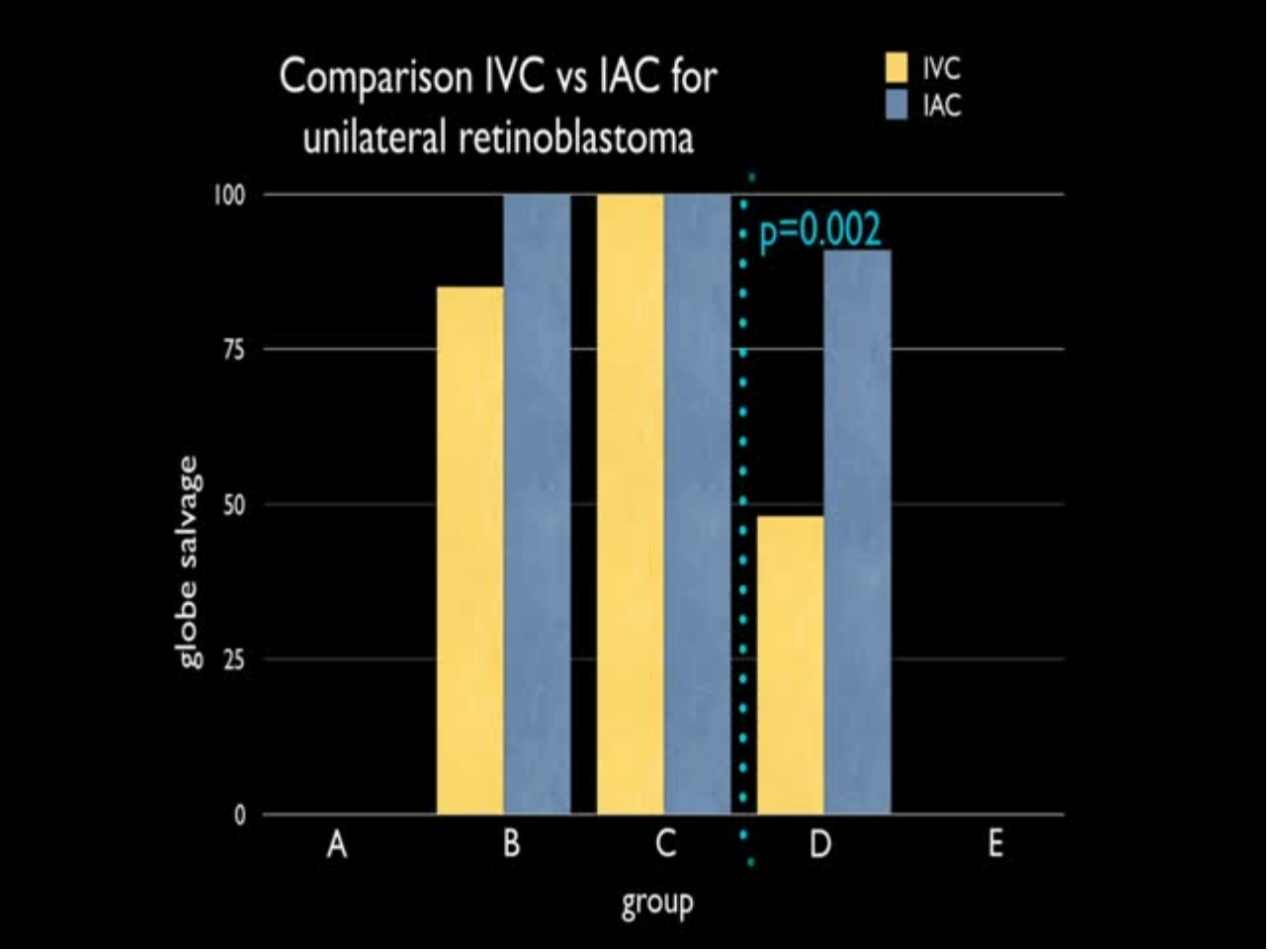
Comparison IVC vs IAC for
unilateral retinoblastoma
IVC
IAC
p=0.002
100
75
50
25
0
globe salvage
A
B
C
D
E
group

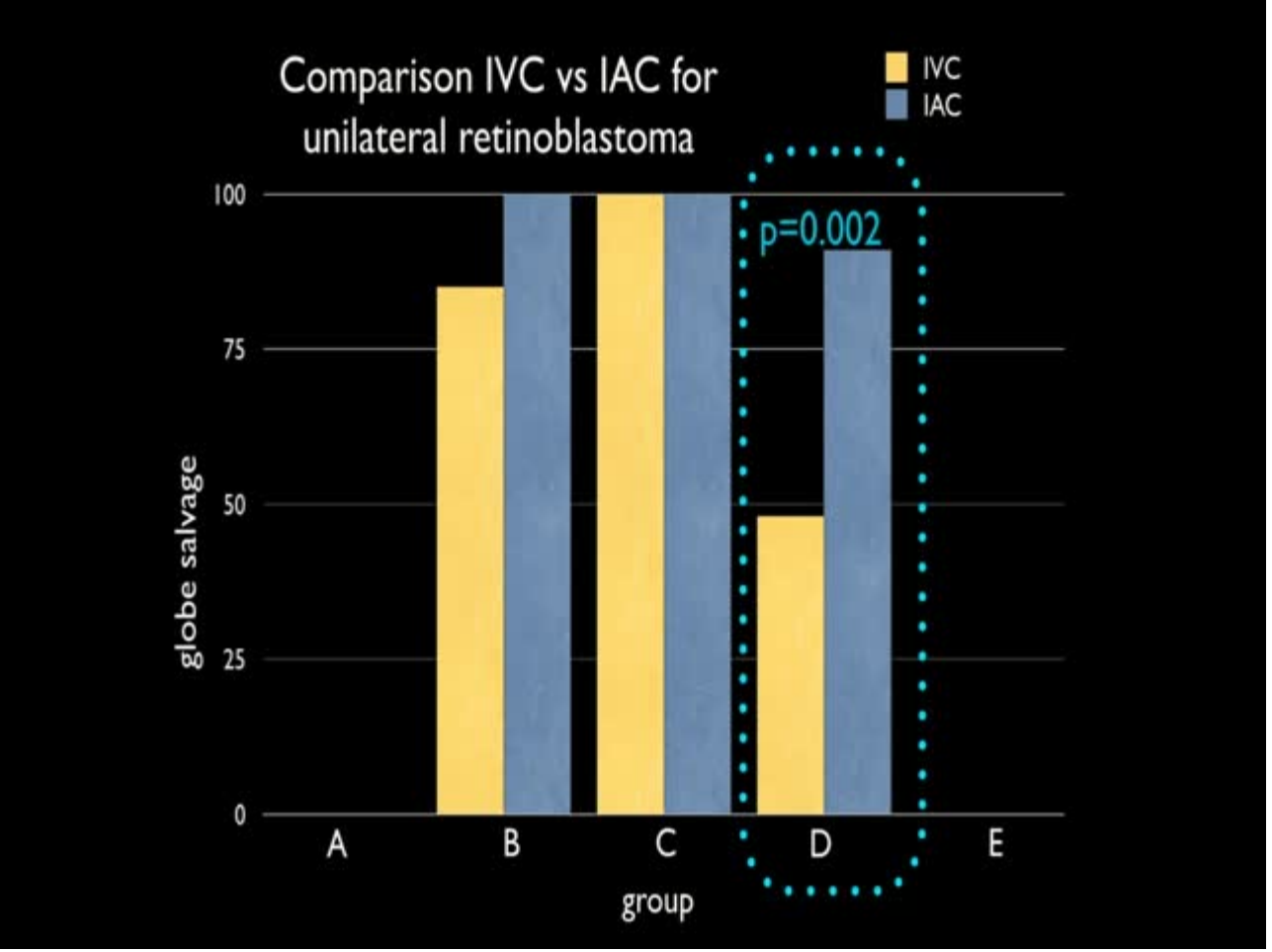
Comparison IVC vs IAC for
unilateral retinoblastoma
IVC
IAC
p=0.002
100
75
50
25
0
globe salvage
A
B
C
D
E
group

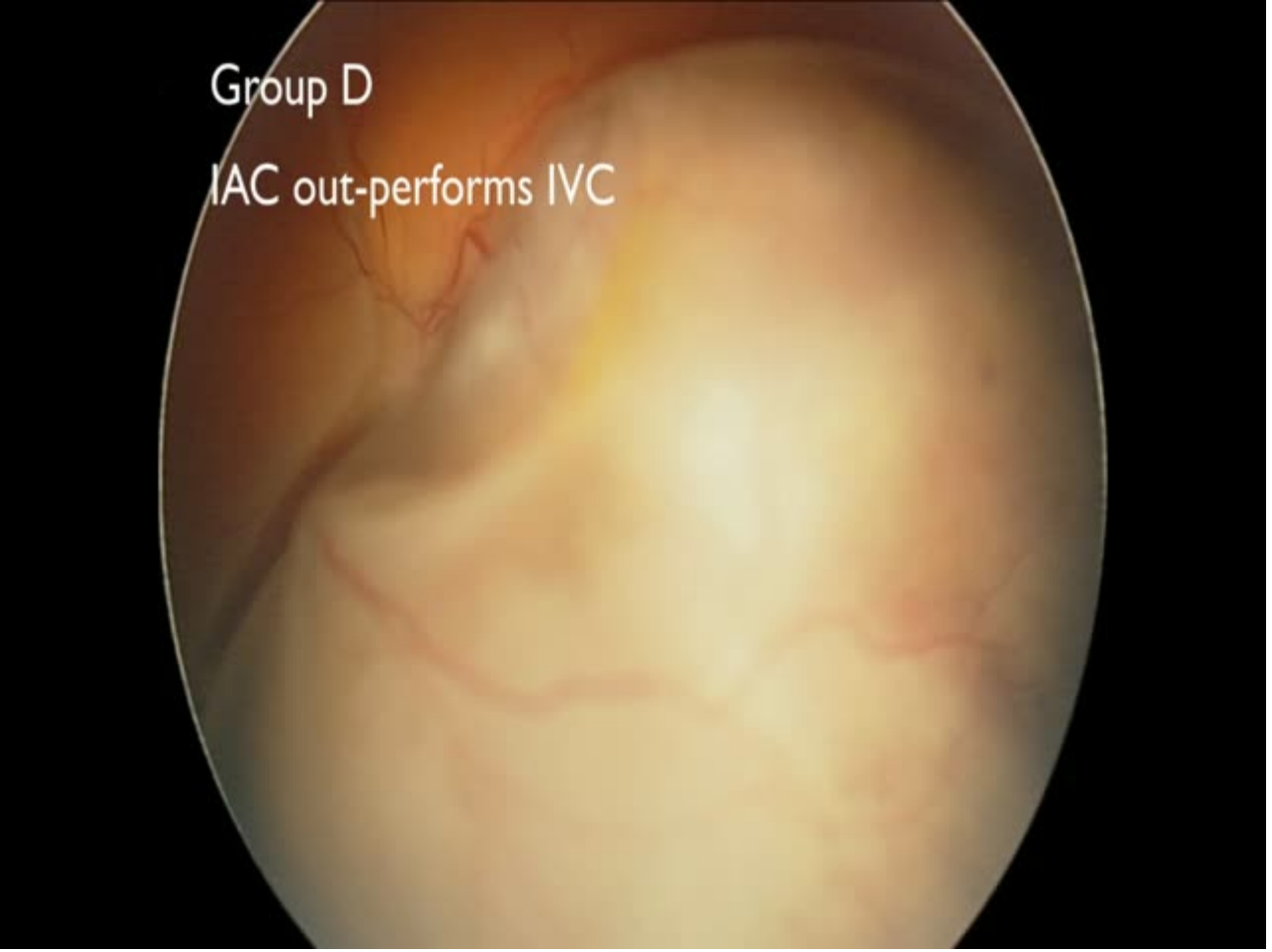
Group D
IAC out-performs IVC

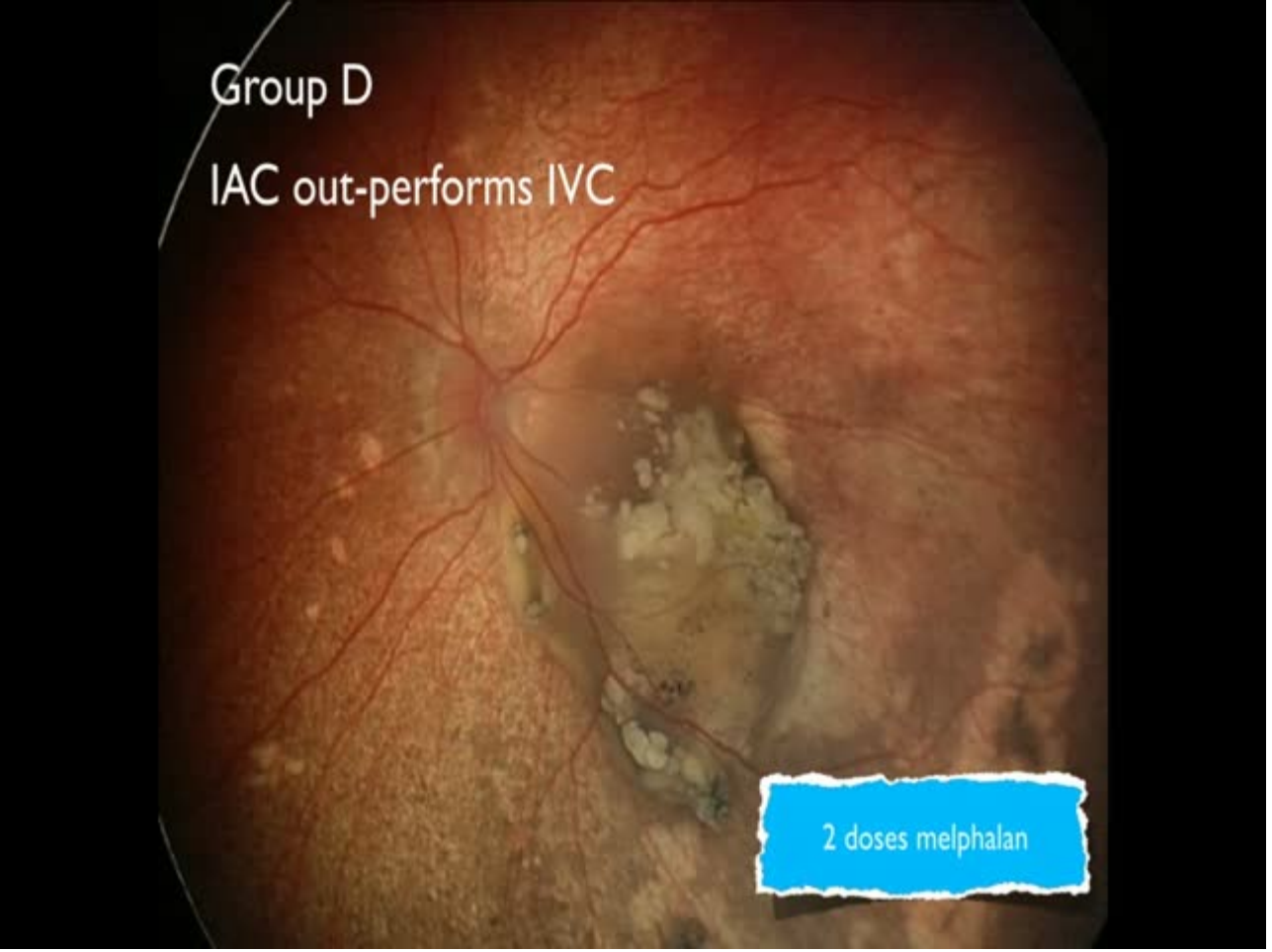
Group D
IAC out-performs IVC
2 doses melphalan

Intraarterial chemotherapy for retinoblastoma in a 2-month-old infant

Intraarterial chemotherapy for retinoblastoma in a 2-month-old infant

Intraarterial chemotherapy for retinoblastoma in a 2-month-old infant

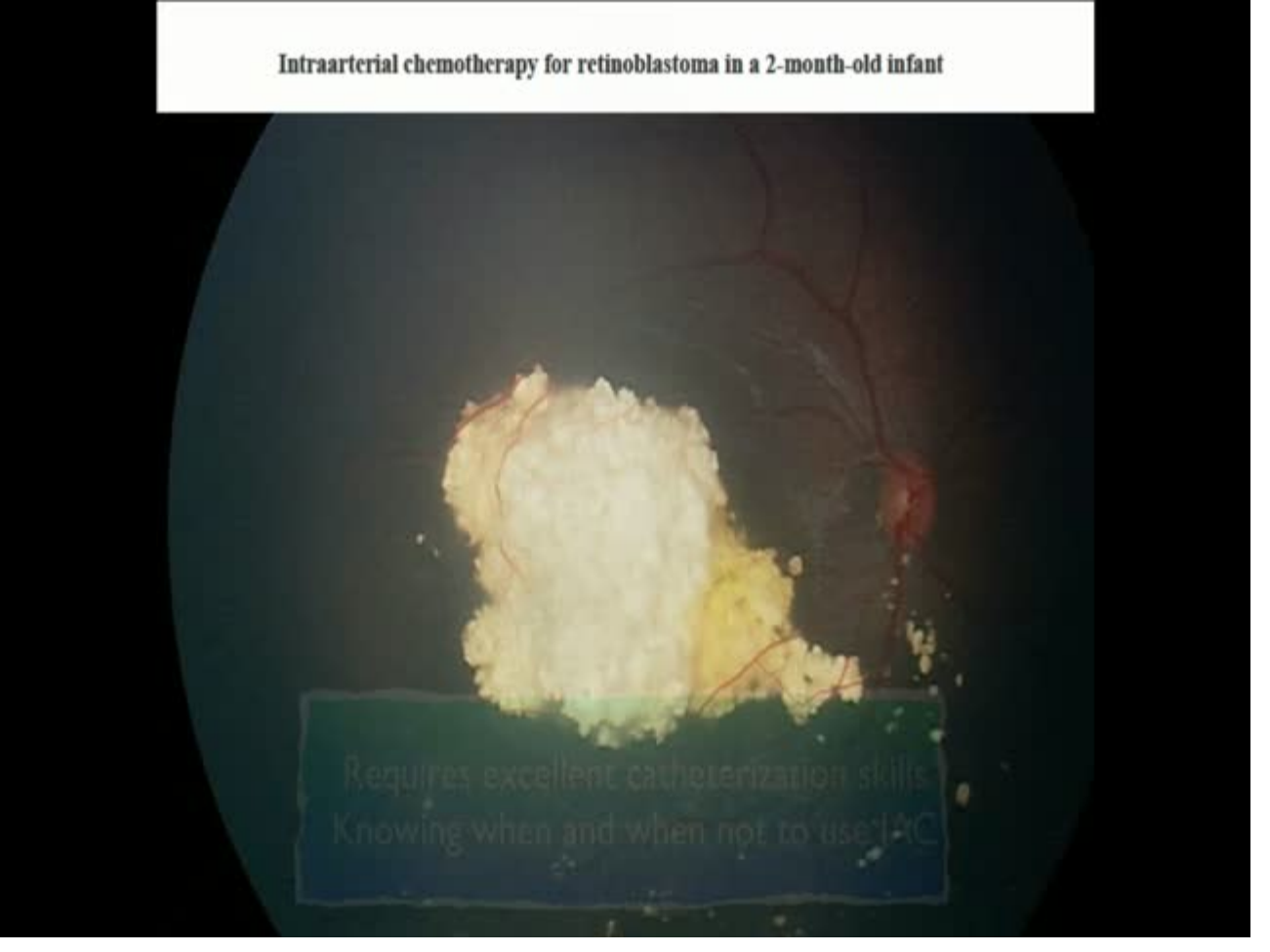

Intraarterial chemotherapy for retinoblastoma in a 2-month-old infant

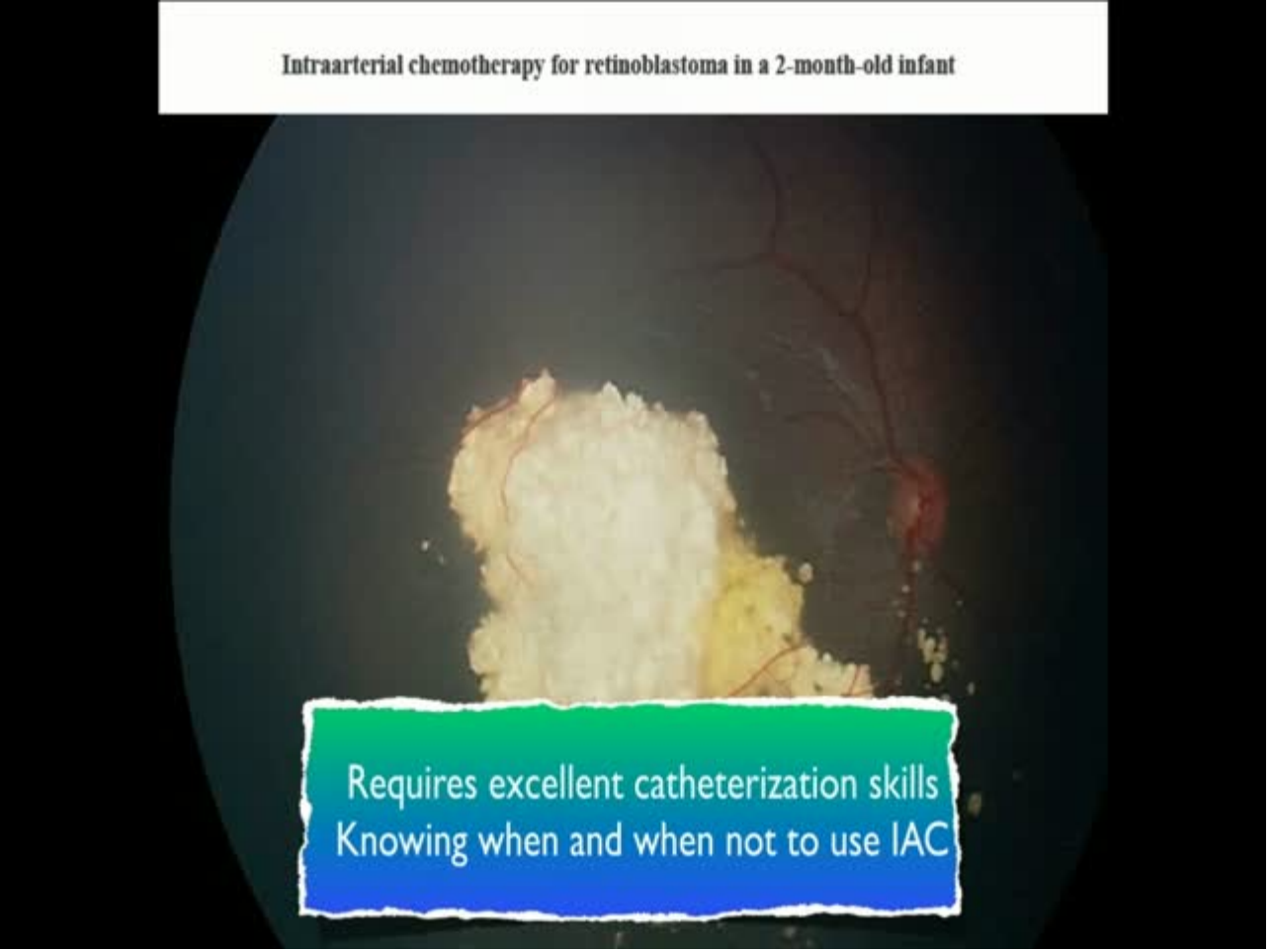

Intraarterial chemotherapy for adult onset retinoblastoma in a 32 year-old man

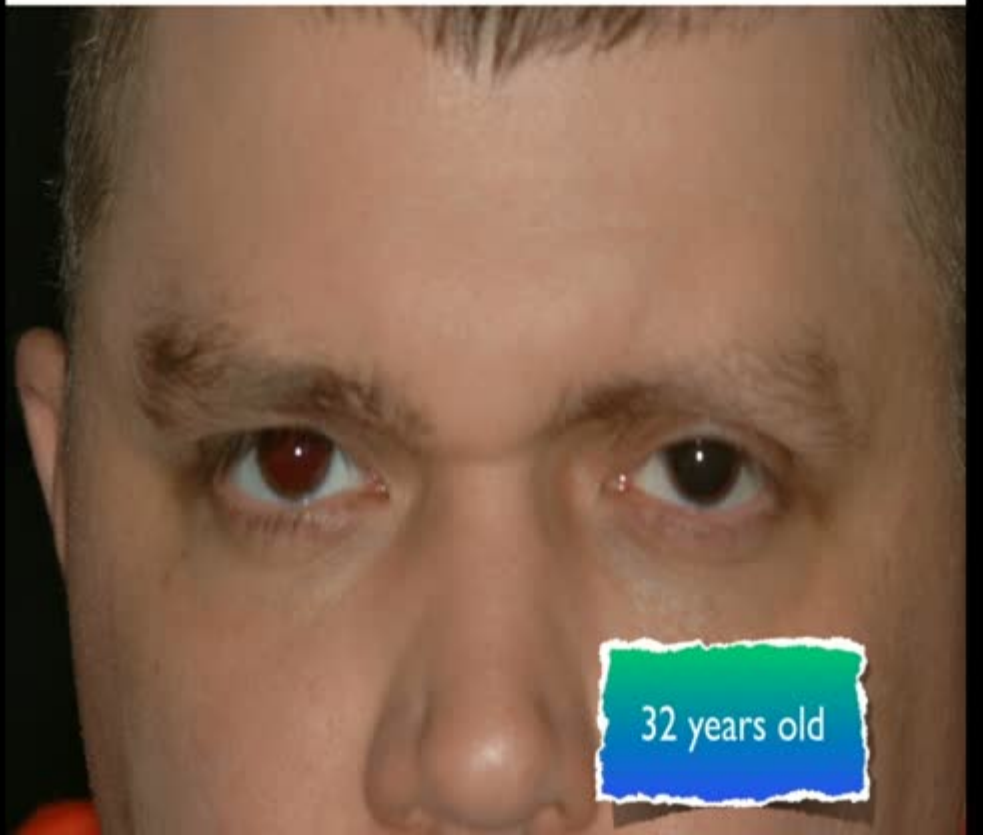

Intraarterial chemotherapy for adult onset retinoblastoma in a 32 year-old man

Intraarterial chemotherapy for adult onset retinoblastoma in a 32 year-old man

… required more than IAC
needed plaque radiotherapy + intravitreal chemotherapy

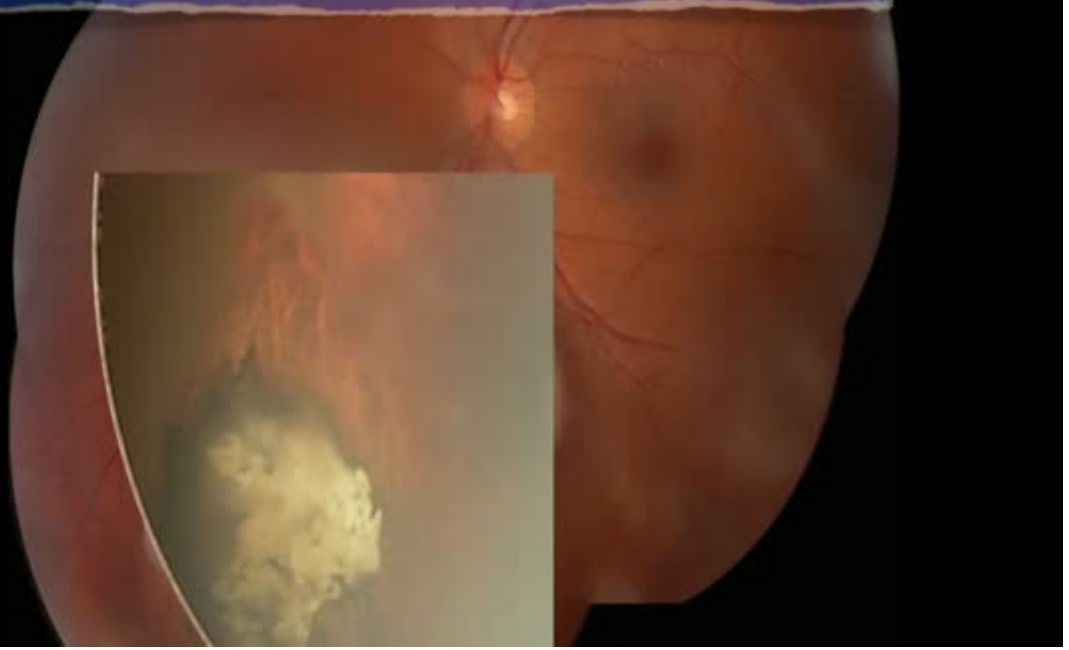

Intraarterial chemotherapy for adult onset retinoblastoma in a 32 year-old man

… required more than IAC
needed plaque radiotherapy + intravitreal chemotherapy

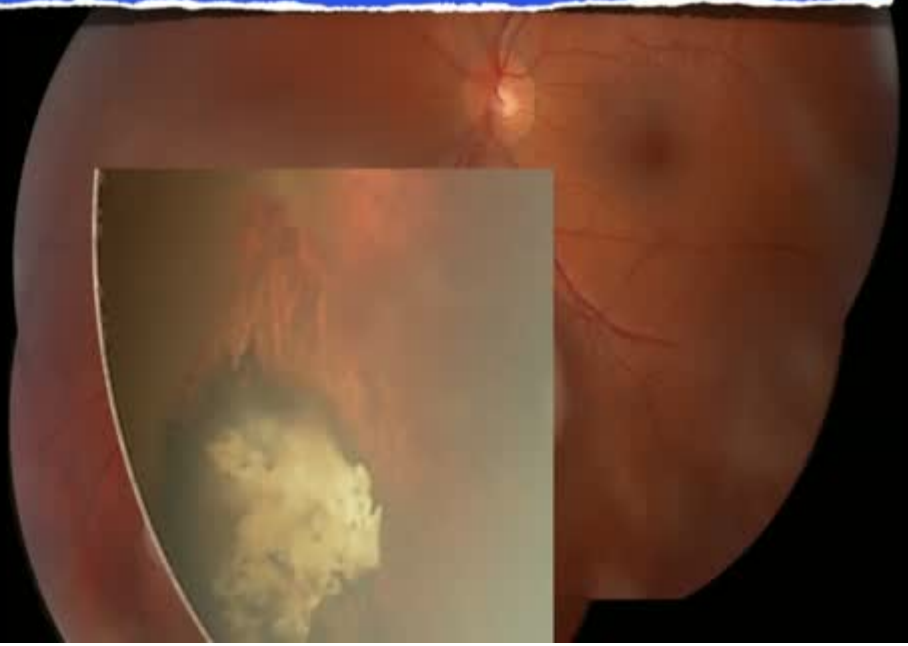

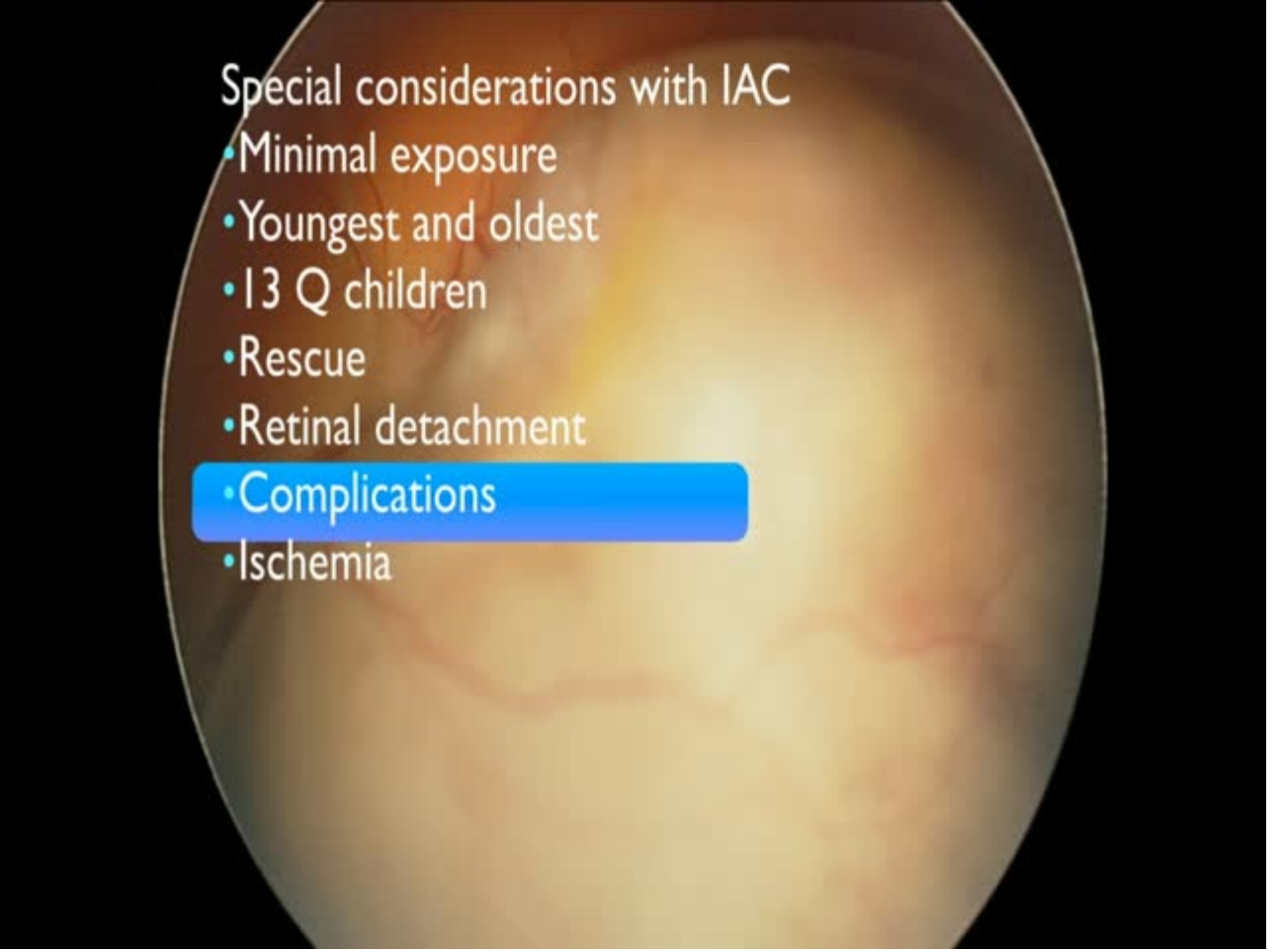
Special considerations with IAC
•Minimal exposure
•Youngest and oldest
•13 Q children
•Rescue
•Retinal detachment
•Complications
•Ischemia

Melphalan

nitrogen mustard alkylating agent

- pancytopenia
- leukemogenic
- male infertility

> 7 cycles could induce male infertility depending on the dose

Rhegmatogenous Retinal Detachment after Intra-Arterial Chemotherapy for Retinoblastoma.

The 2016 Founders Award Lecture

Carol L. Shields, M.D.

Emil Anthony T. Say, M.D.

Maria Pefkianaki, M.D., M.Sc., Ph.D.

Carl D. Regillo, M.D.

Emi H. Caywood, M.D.

Pascal M. Jabbour, M.D.

Jerry A. Shields, M.D.

From the Ocular Oncology Service (CLS, EATS, MP, JAS) and the Retina Service (CDR), Wills Eye